RL-TR-95-164, Vol III (of five)
Final Technical Report
September 1995

HIGH-LEVEL ADAPTIVE SIGNAL PROCESSING ARCHITECTURE WITH APPLICATIONS TO RADAR NON-GAUSSIAN CLUTTER, Spherically Invariant Random Processes for Radar Clutter Modeling, Simulation, and Distribution Identification

University of Massachusetts at Amherst

Muralidhar Rangaswamy (Syracuse University)

APPROVED FOR PUBLIC RELEASE; DISTRIBUTION UNLIMITED.

Rome Laboratory
Air Force Materiel Command
Griffiss Air Force Base, New York

This report has been reviewed by the Rome Laboratory Public Affairs Office (PA) and is releasable to the National Technical Information Service (NTIS). At NTIS it will be releasable to the general public, including foreign nations.

RL-TR-95-164, Vol III (of five), has been reviewed and is approved for publication.

APPROVED: Vincent C. Vannicola

DR. VINCENT C. VANNICOLA
Project Engineer

FOR THE COMMANDER: Donald W Hanson

DONALD W. HANSON
Director of Surveillance & Photonics

If your address has changed or if you wish to be removed from the Rome Laboratory mailing list, or if the addressee is no longer employed by your organization, please notify RL (OCSS) Griffiss AFB NY 13441. This will assist us in maintaining a current mailing list.

Do not return copies of this report unless contractual obligations or notices on a specific document require that it be returned.

REPORT DOCUMENTATION PAGE

Form Approved
OMB No. 0704-0188

1. AGENCY USE ONLY (Leave Blank)	2. REPORT DATE	3. REPORT TYPE AND DATES COVERED
	September 1995	Final Apr 91 - Jun 94

4. TITLE AND SUBTITLE
HIGH-LEVEL ADAPTIVE SIGNAL PROCESSING ARCHITECTURE WITH APPLICATIONS TO RADAR NON-GAUSSIAN CLUTTER, Spherically Invariant Random Processes for Radar Clutter (see reverse)

5. FUNDING NUMBERS
C - F30602-91-C-0038
PE - 62702F
PR - 4506
TA - 11
WU - 1B

6. AUTHOR(S)
Muralidhar Rangaswamy (Syracuse University)

7. PERFORMING ORGANIZATION NAME(S) AND ADDRESS(ES)
University of Massachusetts at Amherst
Department of Computer Science
Lederle Graduate Research Center
Amherst MA 01003

8. PERFORMING ORGANIZATION REPORT NUMBER
N/A

9. SPONSORING/MONITORING AGENCY NAME(S) AND ADDRESS(ES)
Rome Laboratory (OCSS)
26 Electronic Pky
Griffiss AFB NY 13441-4514

10. SPONSORING/MONITORING AGENCY REPORT NUMBER
RL-TR-95-164, Vol III (of five)

11. SUPPLEMENTARY NOTES
Rome Laboratory Project Engineer: Dr. Vincent C. Vannicola/OCSS/(315) 330-2861

12a. DISTRIBUTION/AVAILABILITY STATEMENT
Approved for public release; distribution unlimited.

12b. DISTRIBUTION CODE

13. ABSTRACT (Maximum 200 words)
We describe the accomplishments of a collaborative effort carried out by a team of researchers from the University of Massachusetts at Amherst (headed by V. Lesser), Boston University (headed by H. Nawab), and Syracuse University (headed by D. Weiner) on the development of a high-level signal processing architecture called IPUS (Integrated Processing and Understanding of Signals). Based on the IPUS generic testbed architecture and "radar and sound understanding" (RESUN) architectures, we have been able to transfer IPUS technology from a LISP environment to a C++ environment for use in an IPUS Radar Clutter Analysis Testbed. Though not as well-developed as the sound understanding application because of its newness, this radar testbed has still clearly demonstrated the potential of IPUS-like technologies for CFAR processing of radar returns. There has also been significant development of knowledge for weak signal detection. This knowledge has involved the application of the Ozturk algorithm to hypothesize the distribution of data in a clutter patch based on a small amount of data. Also, techniques have been developed for partitioning the radar surveillance volume into background noise and clutter patches, for weak signal detection in K-distributed clutter, and the efficient use of Rejection Theorem for Weibull clutter generation. Though the effort on the application of IPUS to communications was given less priority, we still did some interesting theoretical work on (see reverse)

14. SUBJECT TERMS	15. NUMBER OF PAGES
Radar, Signal processing, Artificial intelligence detection. Clutter, Non-Gaussian	188
	16. PRICE CODE

17. SECURITY CLASSIFICATION OF REPORT	18. SECURITY CLASSIFICATION OF THIS PAGE	19. SECURITY CLASSIFICATION OF ABSTRACT	20. LIMITATION OF ABSTRACT
UNCLASSIFIED	UNCLASSIFIED	UNCLASSIFIED	UL

4. (Cont'd)

Modeling, Simulation, and Distribution Identification

13. (Cont'd)

weak signal detection in communication systems subject to spherically invariant random processes (SIRP) interference.

Abstract

This investigation is motivated by the problem of detection of weak signals in a strong radar clutter background. The fundamental issues that need to be addressed in the weak signal detection problem are radar clutter modeling, simulation and distribution approximation. These issues are easily addressed when the clutter is a correlated Gaussian random process. However, these issues have not received much attention when the clutter is a correlated non-Gaussian random process.

This thesis addresses the problem of modeling, simulation and distribution approximation of correlated non-Gaussian radar clutter. The theory of spherically invariant random processes is used for statistical characterization of non-Gaussian radar clutter. Several examples of multivariate probability density functions arising from spherically invariant random processes are presented. A new result which uniquely characterizes the multivariate probability density functions arising from spherically invariant random processes is obtained. Two new canonical computer simulation procedures are developed in order to simulate radar clutter that can be described by spherically invariant random processes. Finally, a new algorithm is used to address the problem of distribution identification of the clutter using relatively small sample sizes. This technique makes use of the result which uniquely characterizes the multivariate probability density functions arising from spherically invariant random processes and reduces the multivariate distribution approximation problem to an equivalent univariate distribution approximation problem resulting in a major simplification of processing.

Contents

List of Figures

List of Tables

Chapter 1

Introduction

The problem of weak signal detection in non-Gaussian noise is of interest to engineers in many disciplines such as radar, sonar, digital communications and radio astronomy. In this research, we are interested in the detection of weak radar targets in a strong clutter background. When a signal is transmitted by a radar, the resulting received signal consists of returns from a target (desired signal) and returns from such objects as buildings, trees, water, land and weather, depending on the environment. Any return other than that from the target is an unwanted signal and is defined as **radar clutter.**

The fundamental issues that need to be addressed are:

(1) Specification of suitable statistical models for the clutter background.

(2) Development of efficient computer simulation procedures for generating samples characterized by the various statistical models.

(3) Development of an identification procedure for fitting one or more statistical models to a set of experimental data.

With respect to item (1), a complete statistical clutter model should provide us with a closed form analytical expression for the probability density function (PDF) of the clutter. This should include information about the correlation of the clutter, thereby enabling us to take advantage of this correlation in order to cancel the clutter. We are interested in processing either N complex samples or $2N$ quadrature components obtained by sampling a complex random process which has a non-Rayleigh envelope

PDF and a phase that is uniformly distributed over the interval $(0, 2\pi)$. In addition, it is assumed that the envelope and the phase are statistically independent. We can think of a vector $\mathbf{Y} = [Y_{c1}, \ldots Y_{cN}, Y_{s1} \ldots Y_{sN}]^T$ to represent the collection of the complex samples that have been obtained by sampling the complex process. The subscripts c and s denote the inphase and out of phase quadrature components, respectively. The issue that we need to address is the specification of the joint PDF of the N complex samples or the $2N$ quadrature components. In other words, we need to specify the PDF of the vector $\mathbf{Y}$. We require that the multivariate probability density functions be specified in closed form to facilitate their use in the derivation of optimal radar signal processors.

For each PDF of $\mathbf{Y}$ that is developed, we need to obtain an efficient computer simulation scheme for generating random vectors having this PDF. Computer simulation is necessary because it is likely that it will not be possible to evaluate analytically the performance of optimal non-Gaussian radar receivers. In such cases, performance must be evaluated by computer simulation.

More often than not, the background clutter is not known a priori. Also, the parameters of the clutter are unknown. Therefore, we need to develop estimation procedures to approximate the clutter PDF and its parameters. We need to address the problem of distribution identification and parameter estimation. It is desirable to have available an extensive list of possible multivariate probability density functions so that a good fit can be found for a given environment. In practice, only a small number of samples may be available. Therefore, there is a need to develop efficient procedures to handle small sample sizes.

Because the clutter is apt to change in space and time, the radar signal processor must be adaptive to meet the changing conditions. The approach proposed here for the characterization, computer generation and distribution identification of the clutter based on the theory of spherically invariant random processes lends itself to adaptive receivers.

This dissertation addresses the above issues and is organized as follows. In Chapter 2 we present a review of the literature as it pertains to the modeling of radar clutter as a spherically invariant random process. Chapter 3 presents techniques for obtaining the joint PDF of N complex, non-Gaussian, random variables, assuming that the

clutter can be characterized as a spherically invariant random process. The need for a library of multivariate non-Gaussian PDFs is discussed. Several examples illustrating the various techniques for specifying the multivariate non-Gaussian PDF are provided. Finally, a key result useful for identifying the multivariate non-Gaussian PDFs arising from spherically invariant random processes is presented in Chapter 3.

Chapter 4 deals with the problem of computer generation of correlated non-Gaussian radar clutter that can be characterized as a spherically invariant random process. Two canonical simulation procedures are presented. A graphical goodness of fit test procedure is presented, to validate the simulation procedures.

In Chapter 5 we concern ourselves with the distribution identification of radar clutter characterized by spherically invariant random processes. A new graphical scheme based on a key result presented in Chapter 3 is used to address the distribution identification problem. This procedure reduces the multivariate distribution identification problem to an equivalent univariate distribution identification problem, resulting in considerable computational simplicity. Finally, a new technique for shape parameter estimation is suggested based on the identification procedure. The chief advantage of this scheme is that relatively few samples are needed for the distribution identification problem.

Conclusions and suggestions for future research are presented in Chapter 6.

Chapter 2

Background

2.1 Introduction

We present an overview of the literature as it pertains to the modeling of radar clutter by spherically invariant random processes. In addition, relevant mathematical preliminaries are presented in this chapter. When a radar transmits a signal, the received echo may consist of returns from one or more targets, buildings, trees, water, land and weather depending on the environment. The target returns contribute to the desired signal while the other returns contribute to the clutter. Many investigators [1, 2, 3, 4] have reported experimental measurements for which the clutter probability density function has an extended tail. The extended tail gives rise to relatively large probabilities of false alarm. The Gaussian model for the clutter fails to predict this behavior. Two approaches have been used to explain the non-Gaussian behavior. One of them is based on the fact that application of the central limit theorem (CLT) is not appropriate. The other approach is based on the nonstationary reflectivity properties of the scanned areas. In any event, non-Gaussian models for the univariate (marginal) clutter PDF have been proposed. Commonly reported marginal non-Gaussian PDFs for the clutter are Weibull [1], log-normal [5, 6] and K-distributions [3, 7, 2]. Second order statistics for these models have been reported in terms of autocorrelation functions or power spectral densities [8, 4].

The Weibull [1] and log-normal [2] models for radar clutter are primarily based on empirical studies, while the K-distribution has been shown to have physical significance [9, 2] in that the observed statistical properties can be related to the electromagnetic and geometric factors pertaining to the scattering surface. Computer

simulation schemes for Weibull and Log-normal clutter based on the univariate PDFs and correlation functions have been developed in [10] and [11], respectively. Extension of the Weibull and Log-normal and K-distributed clutter models for coherent radar processing have been developed in [12, 5, 13] respectively.

Statistical characterization of the clutter is necessary in order to obtain the optimal radar signal processor. Usually, radars process N pulses at a time. A complete statistical characterization of the clutter requires the specification of the joint probability density function (PDF) of the N samples. When the pulse returns are statistically independent, the joint PDF is simply the product of the marginal PDFs. However, the clutter can be highly correlated. In fact, the correlation between samples is useful in canceling the clutter. Consequently, it is desirable to include the correlation information in the multivariate PDF. For non-Gaussian processes this can be done in more than one way. The theory of spherically invariant random processes (SIRP) provides a powerful mechanism for obtaining the joint PDF of the N correlated non-Gaussian random variables. Applications for the theory of SIRPs can be found in the problem of random flights [14], signal detection and estimation problems in communication theory [15, 16], speech signal processing [17, 18], radar clutter modeling and simulation [19, 13, 20, 21, 22]. The following sections provide a brief overview of literature on the theory of SIRPs.

2.2 Definitions

In this section we present certain definitions and mathematical preliminaries pertaining to the theory of SIRPs. A random vector $\mathbf{Y} = [Y_1, Y_2, \ldots, Y_N]^T$, $N \geq 1$, is said to be a spherically invariant random vector (SIRV) if its PDF has the form

$$f_{\mathbf{Y}}(\mathbf{y}) = k|\mathbf{\Sigma}|^{-\frac{1}{2}} h_N[(\mathbf{y}-\mathbf{b})^T \mathbf{\Sigma}^{-1}(\mathbf{y}-\mathbf{b})] \tag{2.1}$$

where k is a normalization chosen so that the volume under the curve of the PDF is unity, $\mathbf{b}$ is a N by 1 vector, $\mathbf{\Sigma}$ is a N by N non-negative definite matrix, and $h_N(.)$ is a one dimensional, non-negative, real valued monotonically decreasing function. Note that the PDF of an SIRV is elliptically symmetric (i.e., constant contours of $f_{\mathbf{Y}}(\mathbf{y})$ are composed of ellipses). If every random vector obtained by sampling a random process $y(t)$ is a spherically invariant random vector, regardless of the sampling instants or

the number of samples, then the process $y(t)$ is defined to be a spherically invariant random process (SIRP).

Kingman [14] introduced the definition of spherically symmetric random vectors (SSRV). In particular, a random vector $\mathbf{X} = [X_1, X_2, \ldots X_N]^T$ is said to be spherically symmetric provided its PDF has the form

$$f_{\mathbf{X}}(\mathbf{x}) = kh_N[(x_1^2 + x_2^2 + \ldots + x_N^2)^{\frac{1}{2}}] = kh_N(\mathbf{x}^T\mathbf{x}) \tag{2.2}$$

where $h_N(.)$ is an arbitrary, non-negative, monotonically decreasing radial function of dimension N and k is a normalization constant chosen so that the volume under the curve of the PDF is unity. The subscript N is used to emphasize that we are dealing with N random variables. Throughout the manuscript, it is assumed that the PDF of a random vector is the joint PDF of its components. Equivalently, if $\omega = [\omega_1, \omega_2, \ldots, \omega_N]^T$, the characteristic function of the SSRV $\mathbf{X}$ defined by $\Phi_{\mathbf{X}}(\omega) = E[exp(j\omega^T\mathbf{X})]$, has the form

$$\Phi_{\mathbf{X}}(\omega) = g_N[(\omega_1^2 + \omega_2^2 + \ldots + \omega_N^2)^{\frac{1}{2}}] \tag{2.3}$$

where $g_N(.)$ is a non-negative conjugate symmetric function which is magnitude integrable. An SSRV is a special case of an SIRV, arising from eq (2.1) when $\mathbf{b} = 0$ and $\mathbf{\Sigma} = \mathbf{I}$ where $\mathbf{I}$ is the identity matrix. In Appendix A, we prove that the characteristic function of an SSRV is also spherically symmetric.

2.3 Characterization of SIRVs

In this section we present some important theorems that help us to characterize the PDF of a SIRV. The work of Yao [15], Kingman [23] and Wise [24] gave rise to a representation theorem for SSRVs. The representation theorem can be stated as follows.

Theorem 1 *A random vector $\mathbf{X} = [X_1, X_2, \ldots X_N]^T$ is an SSRV for any N, if and only if there exists a non-negative random variable T such that the random variables X_i, $(i = 1, 2, \ldots N)$ conditioned on $T = t$ are independent, identically distributed, Gaussian random variables with zero mean and variance equal to $2t$.*

Proof: Necessity: By definition, the characteristic function of $\mathbf{X}$ is

$$\begin{aligned}\Phi_{\mathbf{X}}(\omega) &= E[exp(j\omega^T\mathbf{X})] \\ &= \int_{-\infty}^{\infty}\ldots\int_{-\infty}^{\infty} exp(j\omega^T\mathbf{x}) f_{\mathbf{X}}(\mathbf{x})d\mathbf{x}.\end{aligned} \tag{2.4}$$

The PDF of the random variable T is introduced by noting that

$$\begin{aligned}f_{\mathbf{X}}(\mathbf{x}) &= \int_{-\infty}^{\infty} f_{\mathbf{X},T}(\mathbf{x},t)dt \\ &= \int_{-\infty}^{\infty} f_{\mathbf{X}|T}(\mathbf{x}|t) f_T(t)dt.\end{aligned} \tag{2.5}$$

Substituting into the expression for the characteristic function and interchanging the order of integration we obtain

$$\Phi_{\mathbf{X}}(\omega) = \int_{-\infty}^{\infty} \Phi_{\mathbf{X}|T}(\omega,t) f_T(t)dt \tag{2.6}$$

where

$$\Phi_{\mathbf{X}|T}(\omega,\, t) = \int_{-\infty}^{\infty}\ldots\int_{-\infty}^{\infty} exp(j\omega^T\mathbf{x}) f_{\mathbf{X}|T}(\mathbf{x}|t)d\mathbf{x}. \tag{2.7}$$

Since $\mathbf{X}$ is an SSRV for any N, its characteristic function has the form of eq (2.3). This requires that the functional form of $\Phi_{\mathbf{X}|T}(\omega,t)$ remain unchanged for all N. Furthermore, $\Phi_{\mathbf{X}|T}(\omega,t)$ must also be a function of $(\omega_1^2+\omega_2^2+\ldots+\omega_N^2)$ for any choice of N. The only characteristic function satisfying these conditions [23] is

$$\Phi_{\mathbf{X}|t}(\omega,t) = exp[-t(\omega_1^2+\omega_2^2+\ldots+\omega_N^2)] \tag{2.8}$$

where the conditional PDF of $\mathbf{X}$, given $T=t$, is recognized to be multivariate Gaussian, with X_i, $(i=1,\,2,\,\ldots,N)$ being statistically independent identically distributed, zero mean Gaussian random variables with variance $2t$. Because the variance equals $2t$, T must be a non-negative random variable. Necessity follows. Note that the theorem does not give any physical significance for T. Neither does it reveal how to determine $f_T(t)$.

Sufficeincy: To prove sufficiency, we need to show that every product of a Gaussian random vector $\mathbf{Z}$ having zero mean and identity covariance matrix and a random variable $S'=\sqrt{2T}$ with PDF $f_{S'}(s')$ results in a PDF of the form of eq (2.2).

In particular, consider the product $\mathbf{X} = \mathbf{Z}S'$. The PDF of $\mathbf{X}$ conditioned on S' is then given by

$$f_{\mathbf{X}|S'}(\mathbf{x}|s') = (2\pi)^{-\frac{N}{2}}|s'|^{-N}exp(-\frac{p'}{2|s'|^2}) \tag{2.9}$$

where $p' = \mathbf{x}^T\mathbf{x}$. From the theorem on total probability, the PDF of $\mathbf{X}$ can be written as

$$f_{\mathbf{X}}(\mathbf{x}) = (2\pi)^{-\frac{N}{2}}\int_{-\infty}^{\infty}|s'|^{-N}exp(-\frac{p'}{2|s'|^2})f_{S'}(s')ds'. \tag{2.10}$$

For convenience, we can write the PDF of S' as

$$f_{S'}(s') = f_1(s') + f_2(s') \tag{2.11}$$

where

$$f_1(s') = \begin{cases} f(s') & s' \geq 0 \\ 0 & \text{otherwise} \end{cases} \tag{2.12}$$

and

$$f_2(s') = \begin{cases} f(s') & s' \leq 0 \\ 0 & \text{otherwise} \end{cases} \tag{2.13}$$

Then, eq (2.10) can be expressed as

$$f_{\mathbf{X}}(\mathbf{x}) = (2\pi)^{-\frac{N}{2}}\int_{-\infty}^{0}|s'|^{-N}exp(-\frac{p'}{2|s'|^2})f_2(-s')ds' + (2\pi)^{-\frac{N}{2}}\int_{0}^{\infty}|s'|^{-N}exp(-\frac{p'}{2|s'|^2})f_1(s')ds'. \tag{2.14}$$

Making the change of variable $-s' = \zeta$ in the first integral of eq (2.14), we have

$$f_{\mathbf{X}}(\mathbf{x}) = (2\pi)^{-\frac{N}{2}}\int_{0}^{\infty}(s')^{-N}exp(-\frac{p'}{2(s')^2})f_{S'}(s')ds'. \tag{2.15}$$

Thus, it is clear that regardless of whether S' is positive or negative, the PDF of $\mathbf{X}$ has the form of eq (2.15). Henceforth, we always consider the product of $\mathbf{Z}$ and a non-negaitve random variable S in our analysis.

Comparing eqs (2.15) and (2.2), we can write $k = (2\pi)^{-\frac{N}{2}}$ and

$$h_N(p') = \int_{0}^{\infty}(s')^{-N}exp(-\frac{p'}{2(s')^2})f_{S'}(s')ds'. \tag{2.16}$$

Note that $h_N(p)$ given by eq (2.16) is a non-negative, monotonically decreasing function of p, for all N. Therefore, the PDF of eq (2.15) is entirely equivalent to that of eq (2.2). This establishes the theorem. Thus, it is clear that the PDF of an SSRV is uniquely determined by the specification of a Gaussian random vector having zero mean and identity covariance matrix and a first order PDF $f_S(s)$ called the characteristic PDF.

The following theorem in [25] states that a SIRV is related to an SSRV by a linear transformation.

Theorem 2 *If* $\mathbf{X}$ *is an SSRV, with characteristic PDF* $f_S(s)$*, then the deterministic linear transformation*

$$\mathbf{Y} = \mathbf{AX} + \mathbf{b} \tag{2.17}$$

results in $\mathbf{Y}$ *being an SIRV having the same characteristic PDF. It is required that* $\mathbf{A}$ *be a matrix such that* $\mathbf{AA}^T$ *is nonsingular and* $\mathbf{b}$ *be an N by 1 vector.*

Proof: Since $\mathbf{X}$ is an SSRV, we can express $\mathbf{X}$ as $\mathbf{X} = \mathbf{Z}S$, where $\mathbf{Z}$ is a Gaussian random vector having zero mean and identity covariance matrix and S is a non-negative random variable. Hence,

$$\mathbf{Y} = \mathbf{AZ}S + \mathbf{b}. \tag{2.18}$$

Conditioned on S, the PDF of $\mathbf{Y}$ is Gaussian, with mean vector equal to $\mathbf{b}$ and covariance matrix equal to $\mathbf{AA^T}s^2$. The PDF of $\mathbf{Y}$ conditioned on S is given by

$$f_{\mathbf{Y}|S}(\mathbf{y}|s) = (2\pi)^{-\frac{N}{2}}|\mathbf{\Sigma}|^{-\frac{1}{2}}s^{-N}exp(-\frac{p}{2s^2}) \tag{2.19}$$

where $p = (\mathbf{y}-\mathbf{b})^T\mathbf{\Sigma}^{-1}(\mathbf{y}-\mathbf{b})$ and $|\mathbf{\Sigma}|$ denotes the determinant of the covariance matrix $\mathbf{\Sigma} = \mathbf{AA^T}$. Implicit herein is the assumption that S has unit mean square value. Using the theorem on total probability, the PDF of $\mathbf{Y}$ can be written as

$$f_{\mathbf{Y}}(\mathbf{y}) = (2\pi)^{-\frac{N}{2}}|\mathbf{\Sigma}|^{-\frac{1}{2}}h_N(p) \tag{2.20}$$

where

$$h_N(p) = \int_0^\infty s^{-N}exp(-\frac{p}{2s^2})f_S(s)ds. \tag{2.21}$$

The PDF of $\mathbf{Y}$ is of the form of eq (2.1). Therefore, $\mathbf{Y}$ is an SIRV.

The PDF of an SIRV is uniquely determined by the specification of a mean vector, a covariance matrix and a first order PDF called the characteristic PDF. Theorem 1 for SSRVs generalizes for SIRVs in a straightforward manner. The only difference is that conditioned on the non-negative random variable T, the $\{Y_k : (k = 1, 2, \ldots N)\}$ are no longer statistically independent. Instead, the PDF of $\mathbf{Y}$ conditioned on T is a multivariate Gaussian PDF. By the same argument used for SSRVs, an SIRV can be written as a product of a Gaussian random vector and a non-negative random variable. The only difference is that the mean of the Gaussian random vector need not be zero and its covariance matrix is not the identity matrix. As a corollary of Theorem 2 [15], it can be readily shown that every linear transformation on an SIRV results in another SIRV having the same characteristic PDF. As a special case, when $f_S(s) = \delta(s-1)$ where $\delta(.)$ is the unit impulse function, $h_N(p) = exp(-\frac{p}{2})$ and the corresponding SIRV PDF given by eq (2.20) is the multivariate Gaussian PDF. Therefore, the multivariate Gaussian PDF is a special case of the SIRV PDF.

The following theorem from [16] provides an interesting property of SSRVs when represented in generalized spherical co-ordinates.

Theorem 3 *A random vector* $\mathbf{X} = [X_1 \ldots X_N]^T$ *is an SSRV if and only if there exist* N *random variables* $R \in (0, \infty)$, $\Theta \in (0, 2\pi)$ *and* $\Phi_k \in (0, \pi)$, $(k = 1, \ldots N-2)$ *such that when the components of* $\mathbf{X}$ *are expressed in the generalized spherical coordinates*

$$\begin{aligned} X_1 &= R\cos(\Phi_1) \\ X_k &= R\cos(\Phi_k)\textstyle\prod_{i=1}^{k-1}\sin(\Phi_i) \quad (1 < k \leq N-2) \\ X_{N-1} &= R\cos(\Theta)\textstyle\prod_{i=1}^{N-2}\sin(\Phi_i) \\ X_N &= R\sin(\Theta)\textstyle\prod_{i=1}^{N-2}\sin(\Phi_i) \end{aligned} \tag{2.22}$$

then the random variables R, Θ and Φ_k are mutually statistically independent and have PDFs of the form

$$\begin{aligned} f_R(r) &= \frac{r^{N-1}}{2^{\frac{N}{2}-1}\Gamma(\frac{N}{2})} h_N(r^2)u(r) \\ f_{\Phi_k}(\phi_k) &= \frac{\Gamma(\frac{N-k+1}{2})}{\sqrt{\pi}\Gamma(\frac{N-k}{2})} sin^{N-1-k}(\phi_k)[u(\phi_k) - u(\phi_k - \pi)] \\ f_\Theta(\theta) &= (2\pi)^{-1}[u(\theta) - u(\theta - 2\pi)] \end{aligned} \tag{2.23}$$

where $\Gamma(.)$ is the Eulero Gamma function and $u(.)$ is the unit step function.

Proof: Since the random vector $\mathbf{X}$ is an SSRV, its PDF is of the form of eq (2.2) with $h_N(p')$ being given by eq (2.16). The Jacobian of the transformation given by eq (2.22) is obtained in [26] as

$$J = (R^{N-1} \prod_{k=1}^{N-2} sin^{N-1-k}(\phi_k))^{-1}. \tag{2.24}$$

Using eq (2.2) and eq (2.24) and noting that $R^2 = \sum_{k=1}^{N} X_k^2$, the joint PDF of R, Θ and Φ_k $(k = 1, 2, \ldots N-2)$ becomes

$$f_{R,\Theta,\Phi_1 \ldots \Phi_{N-2}}(r, \theta, \phi_1 \ldots \phi_{N-2}) = \frac{r^{N-1}}{(2\pi)^{\frac{N}{2}}} h_N(r^2) \prod_{k=1}^{N-2} sin^{N-1-k}(\phi_k) \tag{2.25}$$

Since the joint PDF in eq (2.25), can be written as a product of the marginal PDFs given in eq (2.23), the variables R, Θ and Φ_k, are mutually statistically independent with the prescribed PDFs . In order to prove the sufficient part of the property, we start with the marginal PDFs of R, Θ and Φ_k given by eq (2.23) and, under the assumption of statistical independence, obtain the joint PDF of eq (2.25). Using the inverse Jacobian of that given by eq (2.24), results in the PDF of $\mathbf{X}$ being given by eq (2.2).

2.4 Determining the PDF of an SIRV

In this section we shall present schemes for determining the PDF of an SIRV. We recognize that the PDF of an SIRV is uniquely determined by the specification of a mean vector, a covariance matrix and a characteristic first order PDF and that the SIRV PDF has the form of eq (2.20). Several techniques are available in the literature for specifying $h_N(p)$. The simplest technique is to use eq (2.21). However,

this procedure requires the knowledge of the characteristic PDF $f_S(s)$. Therefore, when $f_S(s)$ is not known in closed form or it is difficult to evaluate the integral in eq (2.21), alternate methods for specifying $h_N(p)$ must be examined.

To study the behavior of $h_N(p)$, it is convenient to replace p, which is a quadratic form depending on N, by the dummy scalar variable q. We then write

$$h_N(q) = \int_0^\infty s^{-N} exp(-\frac{q}{2s^2}) f_S(s) ds. \tag{2.26}$$

When both sides of eq (2.26) are differentiated with respect to q, we obtain

$$\frac{dh_N(q)}{dq} = -\frac{1}{2}\int_0^\infty s^{-N-2} exp(-\frac{q}{2s^2}) f_S(s) ds. \tag{2.27}$$

The right hand side of eq (2.27) is related to $h_{N+2}(q)$ by the factor of $-\frac{1}{2}$. Thus, we have an interesting result pointed out in [19] that

$$h_{N+2}(q) = (-2)\frac{dh_N(q)}{dq}. \tag{2.28}$$

Because

$$f_{\mathbf{Y}}(\mathbf{y}) = (2\pi)^{-\frac{N+2}{2}} |\Sigma|^{-\frac{1}{2}} h_{N+2}(p) \tag{2.29}$$

when $\mathbf{Y}$ is of dimension $N+2$, it follows that $h_N(q)$ must be a monotonically decreasing function for all N. Eq (2.28) provides a mechanism for relating higher order PDFs with those of lower order, for a given SIRV. More precisely, starting with $N = 1$ and $N = 2$, and using eq (2.28) repeatedly, gives the following pair of recurrence relations.

$$\begin{aligned} h_{2N+1}(q) &= (-2)^N \frac{d^N h_1(q)}{dq^N} \\ h_{2N+2}(q) &= (-2)^N \frac{d^N h_2(q)}{dq^N}. \end{aligned} \tag{2.30}$$

Therefore, starting from $h_1(q)$ and $h_2(q)$ all PDFs of odd and even order respectively, can be generated by the use of eq (2.30). However, since $h_N(.)$ is defined to be a non-negative monotonically decreasing function for all N, $h_1(.)$ and $h_2(.)$ must belong to a class of functions that are non-negative and monotonically decreasing. Consequently, their successive derivatives will alternate between negative and positive functions that are monotonically increasing and decreasing, respectively. Given $h_N(q)$, the N^{th} order

SIRV PDF is given by

$$f_{\mathbf{Y}}(\mathbf{y}) = (2\pi)^{-\frac{N}{2}}|\Sigma|^{-\frac{1}{2}}h_N(p) \tag{2.31}$$

where $h_N(p)$ is nothing more than $h_N(q)$ with q replaced by p.

Another approach for specifying $h_N(p)$ that begins with the univariate characteristic function has been proposed in [27, 15, 16]. It is required that the univariate characteristic function be a real even function whose magnitude is integrable. Also, it is assumed that the components of the SIRV are identically distributed. Under these conditions, it has been shown that

$$h_N(p) = (\sqrt{p})^{1-\frac{N}{2}} \int_0^\infty \omega^{\frac{N}{2}} \phi(\omega) J_{\frac{N-2}{2}}(\omega\sqrt{p}) d\omega \tag{2.32}$$

where $\phi(\omega)$ is the univariate characteristic function and $J_\alpha(\eta)$ is the Bessel function of order α. Eq (2.32) has an elegant proof by induction which is presented here. From eq (2.20) it follows that $h_1(p)$ is related to the first order SIRV PDF of the i^{th} component. More explicitly, we can write

$$f_{Y_i}(y_i) = (\sqrt{2\pi}\sigma)^{-1} h_1(p_i) \quad (i = 1, 2, \ldots N) \tag{2.33}$$

where $p_i = \frac{y_i^2}{\sigma^2}$ and σ^2 is the common variance of the random variables Y_i ($i = 1, 2, \ldots N$). For convenience, assume that σ^2 is unity. The univariate characteristic function is then given by

$$\phi_i(\omega) = \int_{-\infty}^{\infty} f_{Y_i}(y_i) exp(j\omega y_i) dy_i \tag{2.34}$$

Using the inverse Fourier transform and noting that $y_i = \sqrt{p_i}$, $h_1(p_i)$ can be expressed in terms of the characteristic function as

$$h_1(p_i) = \frac{1}{\sqrt{2\pi}} \int_{-\infty}^{\infty} \phi_i(\omega) exp(-j\omega\sqrt{p}) d\omega. \tag{2.35}$$

Since $\phi_i(\omega)$ is the same for all i, the subscript i in eq (2.35) can be dropped. In addition, because $\phi(\omega)$ is an even function, we can rewrite eq (2.35) as

$$h_1(p) = \sqrt{\frac{2}{\pi}} \int_0^\infty \phi(\omega) cos(\omega\sqrt{p}) d\omega. \tag{2.36}$$

Recognizing that $cos(x) = \sqrt{\frac{\pi x}{2}} J_{-\frac{1}{2}}(x)$, and replacing p by the dummy variable q, we have

$$h_1(q) = (\sqrt{q})^{\frac{1}{2}} \int_0^\infty \omega^{\frac{1}{2}} \phi(\omega) J_{-\frac{1}{2}}(\omega\sqrt{q}) d\omega. \tag{2.37}$$

Since the derivation makes use of eq (2.28) it is necessary to consider odd and even values of N separately. For odd values of N, eq (2.32) can be written as

$$h_{2N-1}(q) = (\sqrt{q})^{\frac{3}{2}-N} \int_0^\infty \omega^{N-\frac{1}{2}} \phi(\omega) J_{\frac{2N-3}{2}}(\omega\sqrt{q}) d\omega \tag{2.38}$$

Equation (2.38) is now shown to hold for all N by means of induction. With $N = 1$, eq (2.38) reduces to eq (2.37). It remains to show that eq (2.38) is valid when N is replaced by $N+1$. Differentiating both sides of eq (2.38) with respect to q, we obtain

$$\frac{dh_{2N-1}(q)}{dq} = \int_0^\infty \omega^{N-\frac{1}{2}} \phi(\omega) \frac{d}{dq}[(\sqrt{q})^{\frac{3}{2}-N} J_{\frac{2N-3}{2}}(\omega\sqrt{q})] d\omega. \tag{2.39}$$

First, focus on the term $\frac{d}{dq}[(\sqrt{q})^{\frac{3}{2}-N} J_{\frac{2N-3}{2}}(\omega\sqrt{q})]$. Since this involves the derivative of a product, we can write

$$\frac{d}{dq}[(\sqrt{q})^{\frac{3}{2}-N} J_{\frac{2N-3}{2}}(\omega\sqrt{q})] = \frac{1}{2}(\frac{3}{2}-N)(\sqrt{q})^{-\frac{1}{2}-N} J_{\frac{2N-3}{2}}(\omega\sqrt{q}) + (\sqrt{q})^{\frac{3}{2}-N} \frac{d}{dq}[J_{\frac{2N-3}{2}}(\omega\sqrt{q}). \tag{2.40}$$

Using the identity [28]

$$\frac{dJ_\alpha(\eta)}{d\eta} = \frac{\alpha}{\eta} J_\alpha(\eta) - J_{\alpha+1}(\eta) \tag{2.41}$$

we have

$$\frac{d}{dq}[J_{\frac{2N-3}{2}}(\omega\sqrt{q})] = \frac{\omega}{2}(\sqrt{q})^{-1}[\frac{2N-3}{2\omega\sqrt{q}} J_{\frac{2N-3}{2}}(\omega\sqrt{q}) - J_{\frac{2N-1}{2}}(\omega\sqrt{q})]. \tag{2.42}$$

Substituting eq (2.42) in eq (2.40) gives

$$\frac{d}{dq}[(\sqrt{q})^{\frac{3}{2}-N} J_{\frac{2N-3}{2}}(\omega\sqrt{q})] = -\frac{\omega}{2}(\sqrt{q})^{\frac{1}{2}-N} J_{\frac{2N-1}{2}}(\omega\sqrt{q}) \tag{2.43}$$

Consequently, eq (2.39) reduces to

$$\frac{dh_{2N-1}(q)}{dq} = -\frac{1}{2}(\sqrt{q})^{\frac{1}{2}-N} \int_0^\infty \omega^{N+\frac{1}{2}} \phi(\omega) J_{\frac{2N-1}{2}}(\omega\sqrt{q}) d\omega. \tag{2.44}$$

However, from eq (2.28) we know that $h_{2N+1}(q) = (-2)\frac{dh_{2N-1}(q)}{dq}$. Hence, we have

from eq (2.44)

$$h_{2N+1}(q) = (\sqrt{q})^{\frac{1}{2}-N} \int_0^\infty \omega^{N+\frac{1}{2}} \phi(\omega) J_{\frac{2N-1}{2}}(\omega\sqrt{q}) d\omega. \tag{2.45}$$

Because eq (2.45) is identical to eq (2.38) with N replaced by $N+1$, it has been shown by induction that eq (2.38) is valid for all N. For ease of derivation, it was assumed that the components of $\mathbf{Y}$ have identical variances. However, since the functional form of $h_N(p)$ is invariant to the choice of p, it follows that eq (2.32)is valid for all odd values of N.

In a similar manner, starting with $h_2(p)$, it can be shown that

$$h_{2N+2}(p) = \sqrt{p}^{-N} \int_0^\infty \omega^{N+1} \phi(\omega) J_N(\omega\sqrt{p}) d\omega \tag{2.46}$$

for all N. Note that eq (2.46) is identical to eq (2.32) with N replaced by $2N+2$. The proof of this result is presented in Chapter 3. Thus, in general, for any N (odd or even), we can write $h_N(p)$ as in eq (2.32).

2.5 Properties of SIRVs

In this section we present certain important properties of SIRVs.

2.5.1 PDF Characterization

The multivariate PDF of an SIRV as given by eqs. (2.20) and (2.21) is uniquely determined by the specification of a mean vector $\mathbf{b}$, a covariance matrix $\mathbf{\Sigma}$ and a characteristic first order PDF $f_S(s)$. It is a non-negative, real valued monotonically decreasing function, $h_N(.)$, of a non-negative quadratic form multiplied by a constant. The type of SIRV is determined by the form of $h_N(.)$ or, equivalently, the choice of $f_S(s)$. Higher order PDFs can be obtained by the use of eq (2.32) whereas lower order PDFs can be obtained in the usual manner by integrating out the unwanted variables. We discuss this procedure in Appendix A. The PDFs of all orders are of the same type. The marginal PDFs are used to classify the type of SIRV.

2.5.2 Closure Under Linear Transformation

As shown in Theorem 2 of Section 2.3, every linear transformation of the form of eq (2.17) on an SIRV results in another SIRV having the same characteristic PDF. This feature is called the closure property of SIRVs [15, 16].

2.5.3 Minimum Mean Square Error Estimation

In minimum mean square error estimation (MMSE) problems, given a set of data, SIRVs are found to result in linear estimators [27, 15, 29]. An interesting proof of this property is presented here. Let $\mathbf{Y} = [\mathbf{Y_1}^T\ \mathbf{Y_2}^T]^T$ where $\mathbf{Y_1} = [Y_1, Y_2, \ldots Y_m]^T$ and $\mathbf{Y_2} = [Y_{m+1}, Y_{m+2}, \ldots Y_N]^T$ denote the partitions of $\mathbf{Y}$. It has been pointed out in [30] that the minimum mean square error estimate of the random vector $\mathbf{Y_2}$ given the observations from the random vector $\mathbf{Y_1}$, is given by

$$\hat{\mathbf{Y}}_2 = E[\mathbf{Y_2}|\mathbf{Y_1}] \tag{2.47}$$

where $E[\mathbf{Y_2}|\mathbf{Y_1}]$ denotes the conditional mean or the expected value of $\mathbf{Y_2}$ given $\mathbf{Y_1}$. Assume that $\mathbf{Y}$ is an SIRV of dimension N with characteristic PDF $f_S(s)$. Also, for convenience, it is assumed that the mean of $\mathbf{Y}$ is zero. The covariance matrix of $\mathbf{Y}$ denoted by $\mathbf{\Sigma}$ can be partitioned as

$$\mathbf{\Sigma} = \begin{bmatrix} \mathbf{C_{11}} & \mathbf{C_{12}} \\ \mathbf{C_{21}} & \mathbf{C_{22}} \end{bmatrix} \tag{2.48}$$

where $\mathbf{C_{11}}$ denotes the covariance matrix of $\mathbf{Y_1}$, $\mathbf{C_{12}}$ denotes the cross covariance matrix of the vectors $\mathbf{Y_1}$ and $\mathbf{Y_2}$, $\mathbf{C_{21}}$ is the transpose of $\mathbf{C_{12}}$, and $\mathbf{C_{22}}$ denotes the covariance matrix of the vector $\mathbf{Y_2}$. The PDF of $\mathbf{Y_2}$ given $\mathbf{Y_1}$ is expressed as

$$f_{\mathbf{Y_2}|\mathbf{Y_1}}(\mathbf{y_2}|\mathbf{y_1}) = \frac{f_{\mathbf{Y}}(\mathbf{y})}{f_{\mathbf{Y_1}}(\mathbf{y_1})}. \tag{2.49}$$

Recall from eqs. (2.20) and (2.21) that

$$f_{\mathbf{Y}}(\mathbf{y}) = (2\pi)^{-\frac{N}{2}} |\mathbf{\Sigma}|^{-\frac{1}{2}} h_N(p) \tag{2.50}$$

where

$$h_N(p) = \int_0^\infty s^{-N} exp(-\frac{p}{2s^2}) f_S(s) ds \tag{2.51}$$

and $p = \mathbf{y}^T \boldsymbol{\Sigma}^{-1} \mathbf{y}$. Note that the inverse covariance matrix can be partitioned as [26]

$$\boldsymbol{\Sigma}^{-1} = \begin{bmatrix} \mathbf{A} & \mathbf{B} \\ \mathbf{C} & \mathbf{D} \end{bmatrix} \tag{2.52}$$

where

$$\begin{aligned} \mathbf{A} &= (\mathbf{C}_{11} - \mathbf{C}_{12}\mathbf{C}_{22}^{-1}\mathbf{C}_{21})^{-1} \\ \mathbf{B} &= -\mathbf{A}\mathbf{C}_{12}\mathbf{C}_{22}^{-1} \\ \mathbf{C} &= -\mathbf{D}\mathbf{C}_{21}\mathbf{C}_{11}^{-1} \\ \mathbf{D} &= (\mathbf{C}_{22} - \mathbf{C}_{21}\mathbf{C}_{11}^{-1}\mathbf{C}_{12})^{-1}. \end{aligned} \tag{2.53}$$

Expanding the quadratic form, we have

$$p = \mathbf{y}_1^{\mathrm{T}}\mathbf{A}\mathbf{y}_1 + \mathbf{y}_1^{\mathrm{T}}\mathbf{B}\mathbf{y}_2 + \mathbf{y}_2^{\mathrm{T}}\mathbf{C}\mathbf{y}_1 + \mathbf{y}_2^{\mathrm{T}}\mathbf{D}\mathbf{y}_2. \tag{2.54}$$

Adding and subtracting $\mathbf{y}_1^{\mathrm{T}}\mathbf{C}_{11}^{-1}\mathbf{y}_1$ to the right hand side of eq (2.54) gives

$$p = \mathbf{y}_1^{\mathrm{T}}(\mathbf{A} - \mathbf{C}_{11}^{-1})\mathbf{y}_1 + \mathbf{y}_1^{\mathrm{T}}\mathbf{C}_{11}^{-1}\mathbf{y}_1 + \mathbf{y}_1^{\mathrm{T}}\mathbf{B}\mathbf{y}_2 + \mathbf{y}_2^{\mathrm{T}}\mathbf{C}\mathbf{y}_1 + \mathbf{y}_2^{\mathrm{T}}\mathbf{D}\mathbf{y}_2. \tag{2.55}$$

Note that

$$\mathbf{A} - \mathbf{C}_{11}^{-1} = -\mathbf{B}\mathbf{C}_{21}\mathbf{C}_{11}^{-1}. \tag{2.56}$$

Hence,

$$p = \mathbf{y}_1^{\mathrm{T}}\mathbf{C}_{11}^{-1}\mathbf{y}_1 - \mathbf{y}_1^{\mathrm{T}}\mathbf{B}\mathbf{C}_{21}\mathbf{C}_{11}^{-1}\mathbf{y}_1 + \mathbf{y}_1^{\mathrm{T}}\mathbf{B}\mathbf{y}_2 + \mathbf{y}_2^{\mathrm{T}}\mathbf{C}\mathbf{y}_1 + \mathbf{y}_2^{\mathrm{T}}\mathbf{D}\mathbf{y}_2. \tag{2.57}$$

However, it can be shown that

$$\begin{aligned} \mathbf{y}_2^{\mathrm{T}}\mathbf{C}\mathbf{y}_1 &= -\mathbf{y}_2^{\mathrm{T}}\mathbf{D}\mathbf{C}_{21}\mathbf{C}_{11}^{-1}\mathbf{y}_1 \\ \mathbf{y}_1^{\mathrm{T}}\mathbf{B}\mathbf{y}_2 &= -\mathbf{y}_1^{\mathrm{T}}\mathbf{C}_{11}^{-1}\mathbf{C}_{12}\mathbf{D}\mathbf{y}_2 \\ -\mathbf{y}_1^{\mathrm{T}}\mathbf{B}\mathbf{C}_{21}\mathbf{C}_{11}^{-1}\mathbf{y}_1 &= \mathbf{y}_1^{\mathrm{T}}\mathbf{C}_{11}^{-1}\mathbf{C}_{12}\mathbf{D}\mathbf{C}_{21}\mathbf{C}_{11}^{-1}\mathbf{y}_1 \end{aligned} \tag{2.58}$$

Making these substitutions in the expression for p, it follows that

$$p = \mathbf{y_1^T C_{11}^{-1} y_1 + y_2^T D y_2 - y_2^T D C_{21} C_{11}^{-1} y_1 - y_1^T C_{11}^{-1} C_{12} D y_2 + y_1^T C_{11}^{-1} C_{12} D C_{21} C_{11}^{-1} y_1}. \tag{2.59}$$

This can be rewritten as

$$p = \mathbf{y_1^T C_{11}^{-1} y_1} + (\mathbf{y_2 - C_{21} C_{11}^{-1} y_1})^T \mathbf{D}(\mathbf{y_2 - C_{21} C_{11}^{-1} y_1}) \tag{2.60}$$

For simplicity, we define

$$\begin{aligned} p_1 &= \mathbf{y_1^T C_{11}^{-1} y_1} \\ p_2 &= (\mathbf{y_2 - C_{21} C_{11}^{-1} y_1})^T \mathbf{D}(\mathbf{y_2 - C_{21} C_{11}^{-1} y_1}). \end{aligned} \tag{2.61}$$

Then,

$$p = p_1 + p_2. \tag{2.62}$$

From eqs (2.62) and (2.49)-(2.51), we have

$$f_{\mathbf{Y_2}|\mathbf{Y_1}}(\mathbf{y_2}|\mathbf{y_1}) = \frac{k}{f_{\mathbf{Y_1}}(\mathbf{y_1})} \int_0^\infty s^{-N} exp(-\frac{p_1 + p_2}{2s^2}) f_S(s) ds. \tag{2.63}$$

where $k = (2\pi)^{-\frac{N}{2}} |\mathbf{\Sigma}|^{-\frac{1}{2}}$. Next, consider

$$E[\mathbf{Y_2}|\mathbf{Y_1}] = \frac{k}{f_{\mathbf{Y_1}}(\mathbf{y_1})} \int_0^\infty s^{-N} exp(-\frac{p_1}{2s^2}) \int_{\mathbf{Y_2}} \mathbf{y_2} exp(-\frac{p_2}{2s^2}) d\mathbf{y_2} f_S(s) ds. \tag{2.64}$$

Noting that

$$\int_{\mathbf{Y_2}} \mathbf{y_2} exp(-\frac{p_2}{2s^2}) d\mathbf{y_2} = (2\pi)^{\frac{N-m}{2}} |\mathbf{D}|^{-\frac{1}{2}} s^{N-m} [\mathbf{C_{21} C_{11}^{-1} y_1}], \tag{2.65}$$

gives

$$E[\mathbf{Y_2}|\mathbf{Y_1}] = \frac{k_1}{f_{\mathbf{Y_1}}(\mathbf{y_1})} \int_0^\infty s^{-m} exp(-\frac{p_1}{2s^2}) f_S(s) ds \tag{2.66}$$

where $k_1 = (2\pi)^{-\frac{m}{2}} |\mathbf{\Sigma}|^{-\frac{1}{2}} |\mathbf{D}|^{-\frac{1}{2}} [\mathbf{C_{21} C_{11}^{-1} y_1}]$. When a matrix is partitioned as in eq (2.52), it is known that [31]

$$|\mathbf{\Sigma}| = |\mathbf{C_{11}}| |\mathbf{C_{22} - C_{21} C_{11}^{-1} C_{12}}|. \tag{2.67}$$

Since

$$\mathbf{D} = (\mathbf{C_{22}} - \mathbf{C_{21}}\mathbf{C_{11}^{-1}}\mathbf{C_{12}})^{-1}, \tag{2.68}$$

it follows that

$$|\mathbf{\Sigma}| = |\mathbf{C_{11}}||\mathbf{D^{-1}}| \tag{2.69}$$

Thus,

$$|\mathbf{\Sigma^{-1}}| = |\mathbf{C_{11}}|^{-1}|\mathbf{D}|. \tag{2.70}$$

Hence, $k_1 = (2\pi)^{-\frac{m}{2}}|\mathbf{C_{11}}|^{-\frac{1}{2}}[\mathbf{C_{21}}\mathbf{C_{11}^{-1}}\mathbf{y_1}]$. Finally, since

$$f_{\mathbf{Y_1}}(\mathbf{y_1}) = (2\pi)^{-\frac{m}{2}}|\mathbf{C_{11}}|^{-\frac{1}{2}}\int_0^\infty s^{-m}exp(-\frac{p_1}{2s^2})f_S(s)ds, \tag{2.71}$$

$$\hat{\mathbf{Y}}_2 = E[\mathbf{Y_2}|\mathbf{Y_1}] = [\mathbf{C_{21}}\mathbf{C_{11}^{-1}}\mathbf{y_1}] \tag{2.72}$$

It is seen that the MMSE estimate of $\mathbf{Y_2}$ given the data $\mathbf{Y_1}$ is a linear function of $\mathbf{Y_1}$.

If the random vectors $\mathbf{Y_1}$ and $\mathbf{Y_2}$ have non-zero means denoted by $\mathbf{b_1}$ and $\mathbf{b_2}$ respectively, then eq (2.72) takes the form

$$E[\mathbf{Y_2}|\mathbf{Y_1}] = \mathbf{b_2} + \mathbf{C_{21}}\mathbf{C_{11}^{-1}}(\mathbf{y_1} - \mathbf{b_1}). \tag{2.73}$$

As a consequence of this property, when the random vectors $\mathbf{Y_1}$ and $\mathbf{Y_2}$ are uncorrelated so that $\mathbf{C_{21}} = \mathbf{0}$, then we have

$$E[\mathbf{Y_2}|\mathbf{Y_1}] = \mathbf{b_2} = E[\mathbf{Y_2}]. \tag{2.74}$$

This property is referred to as semi independence in [27, 32, 15]. However, for all SIRVs except the Gaussian, this result does not imply that

$$f_{\mathbf{Y_2}|\mathbf{Y_1}}(\mathbf{y_2}|\mathbf{y_1}) \;=\; f_{\mathbf{Y_2}}(\mathbf{y_2}) \tag{2.75}$$

This emphasizes the property that although uncorrelatedness guarantees statistical independence for Gaussian random vectors, it is not a general property of SIRVs.

2.5.4 Distribution Of Sums of SIRVs

While it is true that the sum of two jointly Gaussian random vectors is also Gaussian, the same is not true for SIRVs in general. This result holds for two SIRVs, when

they are statistically independent, having zero mean and when the covariance matrix of the first is within a multiplicative constant of the covariance matrix of the second [15, 16]. More precisely, let $\mathbf{Y_1} = [Y_{11}, Y_{12}, \ldots Y_{1N}]^T$ and $Y_2 = [Y_{21}, Y_{22}, \ldots Y_{2N}]^T$ denote two independent zero mean SIRVs. The covariance matrix and characteristic PDF of $\mathbf{Y_1}$ are denoted by $\mathbf{\Sigma_1}$ and $f_{S_1}(s_1)$. The corresponding quantities for $\mathbf{Y_2}$ are denoted by $\mathbf{\Sigma_2}$ and $f_{S_2}(s_2)$. We are interested in obtaining the distribution of the sum given by

$$\mathbf{Y} = \mathbf{Y_1} + \mathbf{Y_2}. \tag{2.76}$$

The characteristic function of $\mathbf{Y}$ is given by

$$E[exp(j\omega^T\mathbf{Y})] = g_1(\omega^\mathbf{T}\mathbf{\Sigma_1}\omega)g_2(\omega^\mathbf{T}\mathbf{\Sigma_2}\omega) \tag{2.77}$$

where $g_1(.)$ and $g_2(.)$ are the characteristic functions of $\mathbf{Y_1}$ and $\mathbf{Y_2}$, respectively. If $\mathbf{Y}$ is a zero mean SIRV, then its characteristic function has the form

$$E[exp(j\omega^T\mathbf{Y})] = g(\omega^\mathbf{T}\mathbf{\Sigma}\omega). \tag{2.78}$$

In order to write eq (2.77) as a function of a single quadratic form, Σ_2 must be within a multiplicative constant of Σ_1.

2.5.5 Markov Property for SIRPs

An interesting property of SIRPs is that a zero mean wide sense stationary SIRP is Markov if and only if its autocorrelation function has the form

$$R(t_1, t_2) = exp(-a|(t_1 - t_2|) \tag{2.79}$$

This result is well known for the special case of a zero mean wide sense stationary Gaussian random process. To demonstrate the more general result we consider N samples from a zero mean wide sense stationary SIRP $y(t)$. Let $\mathbf{Y} = [Y_1, Y_2 \ldots, Y_N]^T$ denote the vector of successive samples obtained from the SIRP.

Given that $y(t)$ is a zero mean wide sense stationary Markov SIRP, we first show that its autocorrelation function must have the form of eq (2.79).Let Y_1, Y_2 and Y_3 denote the random variables obtained by sampling $y(t)$ at time instants t_1, t_2 and t_3 such that $t_1 \leq t_2 \leq t_3$. Since $y(t)$ is a Markov process, the joint PDF of Y_1, Y_2 and

Y_3 can be expressed as

$$f_{Y_1,Y_2,Y_3}(y_1,y_2,y_3) = f_{Y_1}(y_1) f_{Y_2|Y_1}(y_2|y_1) f_{Y_3|Y_2}(y_3|y_2). \tag{2.80}$$

The autocorrelation function $R(t_3,t_1) = E[Y_3Y_1]$ is given by

$$R(t_3,t_1) = \int_{-\infty}^{\infty}\int_{-\infty}^{\infty}\int_{-\infty}^{\infty} y_3 y_1 f_{Y_1,Y_2,Y_3}(y_1,y_2,y_3)dy_1dy_2dy_3. \tag{2.81}$$

Also,

$$R(t_2,t_2) = E[Y_2^2] = \int_{-\infty}^{\infty} y_2^2 f_{Y_2}(y_2)dy_2. \tag{2.82}$$

Hence,

$$R(t_3,t_1)R(t_2,t_2) = \int_{-\infty}^{\infty}\int_{-\infty}^{\infty}\int_{-\infty}^{\infty}\int_{-\infty}^{\infty} y_3 y_1 f_{Y_1,Y_2,Y_3}(y_1,y_2,y_3)dy_1dy_2dy_3y_2^2 f_{Y_2}(y_2)dy_2. \tag{2.83}$$

Using eq (2.80) we can rewrite the above equation as

$$R(t_3,t_1)R(t_2,t_2) = \int_{-\infty}^{\infty}\int_{-\infty}^{\infty} y_3 y_2 f_{Y_3,Y_2}(y_3,y_2)dy_3dy_2 \int_{-\infty}^{\infty}\int_{-\infty}^{\infty} y_2 y_1 f_{Y_2,Y_1}(y_2,y_1)dy_2dy_1. \tag{2.84}$$

Consequently,

$$R(t_3,t_1)R(t_2,t_2) = R(t_3,t_2)R(t_2,t_1) \tag{2.85}$$

The only non-trivial autocorrelation function satisfying this property is given by eq (2.79).

Since $y(t)$ is a zero mean SIRP, it follows that $E[\mathbf{Y}] = \mathbf{0}$. Letting $b = exp(-a)$, we can write the covariance matrix of $\mathbf{Y}$ as

$$\mathbf{\Sigma} = \begin{bmatrix} 1 & b & \dots & b^{N-1} \\ b & 1 & \dots & b^{N-2} \\ b^2 & b & \dots & b^{N-3} \\ \dots & \dots & \dots & \dots \\ b^{N-1} & b^{N-2} & \dots & 1 \end{bmatrix} \tag{2.86}$$

under the assumption that $t_1, t_2, \dots, t_N = 1, 2, \dots, N$. We then make use of eq (2.73)

to obtain

$$E[Y_N|Y_{N-1},\, Y_{N-2}\ldots,Y_1] = [b^{N-1}\, b^{N-2}\ldots b]\Sigma_{\mathbf{y}'}{}^{-1}\mathbf{Y}' \tag{2.87}$$

where $\mathbf{Y}' = [Y_1,\, Y_2,\, \ldots,Y_{N-1}]^T$ and

$$\Sigma_{\mathbf{y}'} = \begin{bmatrix} 1 & b & \ldots & b^{N-2} \\ b & 1 & \ldots & b^{N-3} \\ \ldots & \ldots & \ldots & \ldots \\ b^{N-2} & b^{N-3} & \ldots & 1 \end{bmatrix} \tag{2.88}$$

Recognizing that

$$\Sigma_{\mathbf{y}'}{}^{-1} = \frac{1}{1-b^2}\begin{bmatrix} 1 & -b & 0\ldots & \ldots & 0 & \\ -b & 1+b^2 & -b & 0 & \ldots & 0 \\ 0 & -b & 1+b^2 & \ldots & \ldots & 0 \\ \ldots & \ldots & \ldots & \ldots & \ldots & \ldots \\ 0 & \ldots & \ldots & -b & 1+b^2 & -b \\ 0 & \ldots & \ldots & \ldots & -b & 1 \end{bmatrix}. \tag{2.89}$$

Therefore, we can rewrite eq (2.87) as

$$E[Y_N|Y_{N-1},\, Y_{N-2}\ldots,Y_1] = bY_{N-1}. \tag{2.90}$$

From eq (2.73), we also obtain

$$E[Y_N|Y_{N-1}] = bY_{N-1}. \tag{2.91}$$

Clearly $E[Y_N|Y_{N-1}] = E[Y_N|Y_{N-1},\, Y_{N-2}\ldots,Y_1]$. Since this must be true for all choices of $Y_1,\, Y_2,\, \ldots,Y_{N-1}$, it follows that $f_{Y_N|Y_{N-1},Y_{N-2}\ldots,Y_1}(y_N|y_{N-1},\, y_{N-2}\ldots,y_1) = f_{y_N|y_{N-1}}(y_N|y_{N-1})$. Hence, $y(t)$ is Markov.

2.5.6 Kalman Filter for SIRPs

It has been shown by Chu in [29] that the Kalman filter for SIRPs is identical to the corresponding filter for a Gaussian random process. The model considered in [29] is given by

$$\begin{aligned} \mathbf{x_{k+1}} &= \mathbf{F_k x_k} + \mathbf{G_k w_k} \ \ (k = 0, 1, \ldots, N-1) \\ \mathbf{y_k} &= \mathbf{H_k x_k} + \mathbf{v_k} \ \ (k = 0, 1, \ldots, N-1) \end{aligned} \tag{2.92}$$

where $\mathbf{x_k}$ denotes the state vector of the underlying process, $\mathbf{w_k}$ is its excitation vector, $\mathbf{y_k}$ denotes the observation vector and $\mathbf{v_k}$ is the measurement noise. It is assumed that $\mathbf{x_k}$, $\mathbf{w_k}$ and $\mathbf{v_k}$ are jointly SIRP with a common characteristic PDF $f_S(s)$. Also, let

$$\begin{gathered} E[\mathbf{x_k}] = \overline{\mathbf{x_k}} \ \ (k = 0, 1, \ldots, N-1) \\ E[(\mathbf{x_k} - \overline{\mathbf{x_k}})(\mathbf{x_k} - \overline{\mathbf{x_k}})^{\mathrm{T}}] = \mathbf{M_k} \\ E[\mathbf{w_k}] = E[\mathbf{v_k}] = 0 \\ E[(\mathbf{x_k} - \overline{\mathbf{x_k}})\mathbf{w_k}^T] = E[(\mathbf{x_k} - \overline{\mathbf{x_k}})\mathbf{v_k}^T] = E[\mathbf{w_k v_k^T}] = 0 \\ E[\mathbf{w_{kl} w_{km}}] = \mathbf{Q_k}\delta_{l,m} \\ E[\mathbf{v_{kl} v_{km}}] = \mathbf{R_k}\delta_{l,m} \end{gathered} \tag{2.93}$$

where $\mathbf{w_{km}}$ and $\mathbf{v_{km}}$ are the m^{th} components of $\mathbf{w_k}$ and $\mathbf{v_k}$ respectively, and $\delta_{l,m}$ is the Kronecker delta function. Hence, $\mathbf{x_k}$, $\mathbf{w_k}$ and $\mathbf{v_k}$ are mutually uncorrelated while $\mathbf{w_k}$ and $\mathbf{v_k}$ are each white with zero mean.

The innovations vectors is defined as

$$\check{\mathbf{y}}_{\mathbf{k|k-1}} = \mathbf{y_k} - \mathbf{H_k}\hat{\mathbf{x}}_{\mathbf{k|k-1}} \tag{2.94}$$

where $\hat{\mathbf{x}}_{\mathbf{k|k-1}}$ is the MMSE estimate of $\mathbf{x_k}$ given the observation vectors up to $k-1$. The covariance matrix of the innovations can be shown to be

$$Cov(\check{\mathbf{y}}_{\mathbf{k|k-1}}) = \mathbf{S_{k|k-1}} = (\mathbf{H_k M_k H_k^T} + \mathbf{R_k}). \tag{2.95}$$

It can be readily shown that $\mathbf{x_k}$ and $\mathbf{y_k}$ are jointly SIRP. Therefore, the MMSE

estimate of $\mathbf{x_k}$ given the observation vectors up to $k-1$ is a linear function of $\mathbf{y_m}$ $m = 1, 2, \ldots, k-1$, as shown by eq (2.73). Hence, the Kalman filter equations for SIRPs are identical to those for the Gaussian case. The Kalman gain denoted by $\mathbf{K_{k|k}}$ is expressed as

$$\mathbf{K_{k|k}} = \mathbf{M_k H_k^T S_{k|k-1}^{-1}}. \tag{2.96}$$

The measurement update $\hat{\mathbf{x}}_{\mathbf{k|k}}$ is given by

$$\hat{\mathbf{x}}_{\mathbf{k|k}} = \hat{\mathbf{x}}_{\mathbf{k|k-1}} + \mathbf{K_{k|k}}\tilde{\mathbf{y}}_{\mathbf{k|k-1}} = (\mathbf{I} - \mathbf{K_{k|k}})\hat{\mathbf{x}}_{\mathbf{k|k-1}} + \mathbf{K_{k|k}}\mathbf{y}_k. \tag{2.97}$$

The covariance matrix of the error in the update can be written as

$$\mathbf{C}_k = \mathbf{M_k} - \mathbf{M_k H_k^T}(\mathbf{H_k M_k H_k^T} + \mathbf{R_k})^{-1}\mathbf{H_k M_k}. \tag{2.98}$$

The prediction is then given by

$$\hat{\mathbf{x}}_{\mathbf{k+1|k}} = \mathbf{F_k}\hat{\mathbf{x}}_{\mathbf{k|k}}. \tag{2.99}$$

Finally, the covariance matrix of the prediction is expressed as

$$\mathbf{M_{k+1}} = \mathbf{F_k C_k F_k^T} + \mathbf{G_k Q_k G_k^T} \tag{2.100}$$

When systems driven by non-Gaussian noise are encountered in practice, under the assumption of joint SIRP, these equations provide an efficient computation formula for the Kalman filter.

2.5.7 Statistical Independence

We point out that the only case for which the components of an SSRV are statistically independent occurs when the SSRV is Gaussian. This property is proved in Appendix A.

2.5.8 Ergodicity of SIRPs

It has been pointed out in [27] that an ergodic SIRP is necessarily Gaussian. The proof of the non-ergodicity of SIRPs (except Gaussian) can be easily obtained using the representation theorem [15] for SIRPs which states that an SIRP is a univariate randomization of the Gaussian random process. More precisely, if $y(t)$ is an SIRP, then it can be expressed as $y(t) = Sz(t)$, where S is a non-negative random variable

and $z(t)$ is a Gaussian random process. Clearly, if $z(t)$ is stationary, then $y(t)$ will also be stationary. However, different realizations of S result in different scale factors for the sample functions of $y(t)$. Therefore, time averages will differ from one sample function to another and, in general, will not equal the corresponding ensemble average. Consequently, $y(t)$ cannot be ergodic. When S is a non-random constant, $y(t)$ is a Gaussian random process. Then $y(t)$ will be ergodic provided $z(t)$ is also ergodic. It is concluded that only Gaussian SIRPs can be ergodic.

2.6 Conclusion

In this chapter, we have presented an overview of the literature on the modeling of radar clutter and the theory of SIRPs. It is clear from this chapter that the PDF of an SIRV is uniquely determined by the specification of a mean vector, a covariance matrix and a characteristic first order PDF. It is also seen that many interesting properties of Gaussian random processes extend readily to SIRPs. A major difference with non-Gaussian SIRPs is their non-ergodic behavior. Consequently, time averages do not result in corresponding ensemble averages. However, if ensemble averages are used instead of time averages, then non-ergodicity is not a serious problem. In the following chapters, we shall present the application of SIRPs for non-Gaussian radar clutter modeling, simulation and distribution identification.

Chapter 3

Radar Clutter Modeling Using Spherically Invariant Random Processes

3.1 Introduction

In this chapter we consider the use of the theory of spherically invariant random processes (SIRP) for modeling correlated non-Gaussian radar clutter. It has been pointed out in chapter 2 that radar clutter can be non-Gaussian and that radars process N pulses at a time. Furthermore, the clutter can be highly correlated. Therefore, by clutter modeling we mean the specification of the joint probability density function (PDF) of the N correlated clutter samples. Since we are dealing with correlated clutter, the joint PDF cannot be constructed by simply taking the product of the marginal PDFs. This chapter presents a mathematically elegant and tractable approach for specifying the joint PDF of N clutter samples. In addition, we discuss the characterization of Gaussian and non-Gaussian correlated random vectors, the need for a library of multivariate PDFs for modeling correlated non-Gaussian clutter, several techniques for establishing this library and, finally, a key result for the distribution identification of multivariate correlated non-Gaussian random vectors.

Specifically, the problem of modeling a random vector obtained by sampling a stochastic process $y(t)$ at N time instants is of interest to us. The stochastic process may be real or complex. In addition, there is no restriction on the number of samples obtained or the sampling time instants. In order to completely characterize the

random vector we need to specify the joint probability density function of the N samples (real or complex) or, equivalently, specify the joint characteristic function. This problem is very well treated when the underlying stochastic process is Gaussian. The joint PDF in this case can be written as $(2\pi)^{-\frac{N}{2}}|\Sigma|^{-\frac{1}{2}}exp(-\frac{p}{2})$, where p is a non-negative quadratic form given by $p = [\mathbf{y} - \mu]^{\mathbf{T}}\Sigma^{-1}[\mathbf{y} - \mu]$. Here μ and Σ denote the mean vector and covariance matrix of the Gaussian random vector $\mathbf{Y}$ whose components are the N samples of $y(t)$. However, if $y(t)$ is not a Gaussian random process, there is no unique specification for the joint PDF of the N samples except when the samples are statistically independent.

When processing real world data, neither the Gaussian nature of the underlying stochastic process nor the statistical independence of the samples is guaranteed. In fact, it is likely that the samples may be correlated. Hence, we need to obtain multivariate non-Gaussian PDFs which can model the correlation between samples. In practice, radar clutter can vary from one application to another. Therefore, we need to have available a library of possible multivariate non-Gaussian PDFs so that an appropriate PDF can be chosen to approximate the data for each clutter scenario.

The theory of **Spherically Invariant Random Processes** (SIRP) provides us with elegant and mathematically tractable techniques to construct multivariate non-Gaussian PDFs. Spherically invariant random processes are generalizations of the familiar Gaussian random process. The PDF of every random vector obtained by sampling a SIRP is uniquely determined by the specification of a mean vector, a covariance matrix and a characteristic first order PDF. In addition, the PDF of a random vector obtained by sampling a SIRP is a function of a non-negative quadratic form. However, the PDF does not necessarily involve an exponential dependence on the quadratic form, as in the Gaussian case. Such a random vector is called a **Spherically Invariant Random Vector** (SIRV).

There are two kinds of models for non-Gaussian radar clutter. One is called the endogenous model, where the desired non-Gaussian process with prescribed envelope PDF and correlation function is realized by using a zero memory non- linear transformation on a Gaussian process having a prespecified correlation function. In this approach it is not possible to independently control the envelope PDF and the correlation properties of the non-Gaussian process. In addition, not all nonlinearities

give rise to a non-negative definite covariance matrix at their outputs [33, 34]. The second model is called an exogenous product model [13]. In this model, the desired non-Gaussian clutter is generated by the product of a Gaussian random process and an independent non-Gaussian process which can be highly correlated. In this scheme, the desired envelope PDF and the correlation properties can be controlled independently. The exogenous model can be thought of as a slowly time variant non-Gaussian process modulating a Gaussian random process. The SIRP is a special case of the exogenous model, arising when the modulating process does not change rapidly during the observation interval and can be approximated as a random variable. This is due to the fact that the representation theorem for SIRPs allows us to explicitly write the non-Gaussian process as a product of a Gaussian process and a non-negative random variable. By assuming statistical independence between the modulating random variable and the Gaussian process, it is possible to independently control the non-Gaussian envelope PDF and its correlation properties. The SIRP is the only known case of the exogenous multiplicative model which allows the specification of the N^{th} order PDF.

Section 3.2 outlines the problem of interest. In Section 3.3 we present several techniques to obtain SIRVs. Examples based on various techniques described in Section 3.3 are used to obtain a library of SIRV PDFs in Section 3.4. Finally, in Section 3.5, we present a key result which characterizes SIRVs by using the quadratic form appearing in their PDFs.

3.2 Problem Statement

We assume we are dealing with coherent radar clutter. By coherent radar clutter, we mean that the clutter is processed in terms of its in-phase and out -of-phase quadrature components. Pre-detection radar clutter, being a bandpass random process, admits a representation of the form

$$y(t) = Re\{\tilde{y}(t)exp(j\omega_0 t)\} \tag{3.1}$$

where $\tilde{y}(t) = y_c(t) + jy_s(t)$ denotes the complex envelope of the clutter process, ω_0 is a known carrier frequency, $y_c(t)$ and $y_s(t)$ denote the in-phase and out-of-phase quadrature components of the complex process $\tilde{y}(t)$. Equation (3.1) can be rewritten

as

$$y(t) = y_c(t)cos(\omega_0 t) - y_s(t)sin(\omega_0 t). \tag{3.2}$$

We are interested in specifying the joint PDF of N samples obtained by sampling the process $y(t)$. Since it is always more convenient to work with the associated low pass process, we consider the equivalent problem of specifying the PDF of N complex samples obtained from the complex process $\tilde{y}(t)$. The PDF of a complex random variable is defined to be the joint PDF of its in-phase and out-of-phase quadrature components. Therefore, it follows that the joint PDF of N complex random variables is the joint PDF of the $2N$ in-phase and out-of-phase quadrature components. While dealing with complex random variables, it is sometimes more convenient to work with their envelope and phase. The envelope R_i and phase Θ_i of a complex random variable $\tilde{Y}_i = Y_{ci} + jY_{si}$ are defined by

$$\begin{aligned} R_i &= \sqrt{Y_{ci}^2 + Y_{si}^2} \\ \Theta_i &= \arctan(\tfrac{Y_{si}}{Y_{ci}}). \end{aligned} \tag{3.3}$$

We consider the problem of specifying the PDF of a random vector $\mathbf{Y}^T = [\mathbf{Y_c}^T : \mathbf{Y_s}^T]$ obtained by sampling the random process $\tilde{y}(t)$, where $\mathbf{Y_c} = [Y_{c1}, Y_{c2}, \ldots, Y_{cN}]^T$ and $\mathbf{Y_s} = [Y_{s1}, Y_{s2}, \ldots, Y_{sN}]^T$. The subscripts c and s denote the in phase and out of phase quadrature components, respectively. We assume that the process $y(t)$ is a wide sense stationary random process. The necessary and sufficient conditions for $y(t)$ to be a wide sense stationary random process [30] are:

(A) The quadrature components have zero mean.

(B) The envelope of the pairwise quadrature components is statistically independent of the phase and the phase is uniformly distributed over the interval $(0, 2\pi)$. This results in the pair wise quadrature components being identically distributed and their joint PDF being circularly symmetric. This also results in the orthogonality of the pairwise quadrature components at each sampling instant.

(C) The autocovariance function and crosscovariance function of the

quadrature processes of the complex process $\tilde{y}(t) = y_c(t) + jy_s(t)$ satisfy the conditions given by

$$\begin{aligned} K_{cc}(\tau) &= K_{ss}(\tau) \\ K_{cs}(\tau) &= -K_{sc}(\tau) \end{aligned} \tag{3.4}$$

where

$$\begin{aligned} K_{cc}(\tau) &= E\{X_c(t)X_c(t-\tau)\} \\ K_{ss}(\tau) &= E\{X_s(t)X_s(t-\tau)\} \\ K_{cs}(\tau) &= E\{X_c(t)X_s(t-\tau)\} \\ K_{sc}(\tau) &= E\{X_s(t)X_c(t-\tau)\}. \end{aligned} \tag{3.5}$$

Any choice of autocovariance and crosscovariance functions is allowed as long as requirement (C) is satisfied and the resulting covariance matrix of $\mathbf{Y}$ is nonnegative definite.

Due to requirement (A), $E\{\mathbf{Y_c}\} = E\{\mathbf{Y_s}\} = 0$. It follows that $E\{\mathbf{Y}\} = \mathbf{0}$. As a consequence of requirements (B) and (C), the covariance matrix of $\mathbf{Y}$, given by

$$\mathbf{\Sigma} = \begin{bmatrix} \mathbf{\Sigma_{cc}} & | & \mathbf{\Sigma_{cs}} \\ - & | & - \\ \mathbf{\Sigma_{sc}} & | & \mathbf{\Sigma_{ss}} \end{bmatrix}, \tag{3.6}$$

must satisfy the conditions:

$$\begin{aligned} \mathbf{\Sigma_{cc}} &= \mathbf{\Sigma_{ss}} \\ \mathbf{\Sigma_{cs}} &= -\mathbf{\Sigma_{sc}} \end{aligned} \tag{3.7}$$

with the elements of the main diagonal of the matrices $\mathbf{\Sigma_{cs}}$ and $\mathbf{\Sigma_{sc}}$ being equal to zero. Note that $\mathbf{\Sigma_{cc}} = E\{\mathbf{Y_c}\mathbf{Y_c^T}\}$, $\mathbf{\Sigma_{cs}} = E\{\mathbf{Y_c}\mathbf{Y_s^T}\}$, $\mathbf{\Sigma_{sc}} = E\{\mathbf{Y_s}\mathbf{Y_c^T}\}$ and $\mathbf{\Sigma_{ss}} = E\{\mathbf{Y_s}\mathbf{Y_s^T}\}$. Finally, we point out, regardless of the value of N, we always have an even order PDF when dealing with quadrature components. We are now in a position to proceed with the characterization of $\mathbf{Y}$ as an SIRV.

For an SIRV, it is pointed out that the PDF of a given order automatically implies all lower order PDFs. For example, if N random variables are jointly Gaussian, it is well known that the i^{th} order PDF, $i = 1, 2, \ldots, N-1$ is Gaussian. This property of SIRVs is called internal consistency. The requirements (A)-(C) arising from the wide sense stationarity requirements of the process $y(t)$ are called external consistency conditions. Requirements (A)-(C) are not inherent to the SIRP and do not hold when the SIRP is not wide sense stationary.

3.3 Techniques for Determining the SIRV PDF

In this section, several techniques are presented for obtaining $h_{2N}(p)$. For convenience, temporal wide sense stationarity of the underlying bandpass process is assumed. However, the functional form of $h_{2N}(.)$ is unaffected whether or not the random process is temporally wide sense stationary. Hence, it is allowable to let $p = (\mathbf{y} - \mathbf{b})^T \boldsymbol{\Sigma}^{-1} (\mathbf{y} - \mathbf{b})$ in the final result, in general, where $\mathbf{b}$ is any mean non-zero vector and $\boldsymbol{\Sigma}$ is any non-negative definite matrix.

Recall from Chapter 2 that the PDF of an SIRV $\mathbf{Y}^T = [\mathbf{Y_c}^T : \mathbf{Y_s}^T]$ with $\mathbf{Y_c}$ and $\mathbf{Y_s}$ defined in Section 3.2 is given by

$$f_{\mathbf{Y}}(\mathbf{y}) = (2\pi)^{-N} |\boldsymbol{\Sigma}|^{-\frac{1}{2}} h_{2N}(p) \tag{3.8}$$

Assuming temporal wide sense stationarity, $p = \mathbf{y}^T \boldsymbol{\Sigma}^{-1} \mathbf{y}$ where $\boldsymbol{\Sigma}$ is given by eq (3.6). The mean vector of $\mathbf{Y}$ is zero due to requirement (A) in Section 3.2. The covariance matrix $\boldsymbol{\Sigma}$ having the form of eq (3.6) and satisfying the requirements of eq (3.7) is readily determined when the autocorrelation function of the process is specified. Given $\boldsymbol{\Sigma}$, several techniques for obtaining $h_{2N}(p)$ are presented in this section.

The representation theorem for SIRVs allows us to express $\mathbf{Y}$ as a product of a Gaussian random vector $\mathbf{Z}$, having the same dimensions as $\mathbf{Y}$ and a non-negative random variable S. For the problem of radar clutter modeling, since it is desirable to control the non-Gaussian nature of $\mathbf{Y}$ and its correlation properties independently, we assume that the random variable S is statistically independent of $\mathbf{Z}$. In addition, the covariance matrix of the SIRV can be made equal to the covariance matrix of the Gaussian random vector by requiring $E(S^2)$ to be unity. Finally, it is pointed out that the mean of $\mathbf{Z}$ is necessarily zero.

A physical interpretation can be given to $\mathbf{Z}$ and S. Consider a surveillance volume subdivided into contiguous range-Doppler-azimuth cells. Assuming a large enough cell size such that many scatterers are located in each cell, the N pulse returns from a given cell can be modeled as the Gaussian vector $\mathbf{Z}$ due to the central limit theorem. Also assume that the average clutter power remains constant over the N pulse returns in a coherent processing interval. However, the average clutter power is allowed to vary independently from cell to cell since different sets of scatterers are located in each cell. The variation of the average clutter power from cell to cell is modeled by the square of the non-negative random variable S.

3.3.1 SIRVs with Known Characteristic PDF

We consider specification of the PDF of the SIRV $\mathbf{Y}$ when its characteristic PDF is known in closed form. We have pointed out in the previous section that the mean vector of $\mathbf{Y}$ is zero. Also, we have discussed the specification of the covariance matrix of $\mathbf{Y}$. Now, we shall focus on the specification of $h_{2N}(p)$. As a consequence of the representation theorem, we can write

$$h_{2N}(p) = \int_0^\infty s^{-2N} exp(-\frac{p}{2s^2}) f_S(s) ds. \tag{3.9}$$

Equation (3.9) enables us to specify $h_{2N}(p)$ when the characteristic PDF $f_S(s)$ is known in closed form. However, in some cases, even though an analytical expression is known for the characteristic PDF, it may be difficult to evaluate the integral in eq (3.9) in closed form. In such instances, an alternate method for specifying $h_{2N}(p)$ must be examined. The method presented in the next section is useful for these cases.

3.3.2 SIRVs with Unknown Characteristic PDFs

When the characteristic PDF of the SIRV is unknown or when the integral in eq (3.9) is difficult to evaluate, we propose an alternate method to obtain $h_{2N}(p)$. Recall that we are dealing with an even order PDF. Therefore, we can use eq (2.30) starting with $h_2(q)$ to obtain $h_{2N}(q)$. It is worthwhile pointing out that $h_2(.)$ is related to the first order envelope PDF. From requirement (B) of Section 3.2, the joint PDF of the i^{th} in phase and out of phase quadrature components can be expressed as

$$f_{Y_{ci},Y_{si}}(y_{ci}, y_{si}) = (2\pi)^{-1}\sigma^{-2}h_2(p) \quad (i = 1, 2, \ldots, N) \tag{3.10}$$

where $p = \frac{(y_{ci}^2+y_{si}^2)}{\sigma^2}$ and σ^2 denotes the common variance of the in phase and out of phase quadrature components. The envelope and phase corresponding to the i^{th} quadrature components is given by

$$\begin{aligned} R_i &= \sqrt{Y_{ci}^2 + Y_{si}^2} \\ \Theta_i &= \arctan \frac{Y_{si}}{Y_{ci}}. \end{aligned} \tag{3.11}$$

Due to the assumption of wide sense stationarity, we can drop the subscript i in eq (3.11). The Jacobian of the transformation given by eq (3.11) is $J = R^{-1}$, where J denotes the Jacobian. Using the Jacobian in eq (3.10) results in the joint PDF of R and Θ being given by

$$f_{R,\Theta}(r, \theta) = \frac{r}{2\pi\sigma^2} h_2(\frac{r^2}{\sigma^2}). \tag{3.12}$$

Clearly, the joint PDF in eq (3.12) can be factored as a product of the marginal PDFs of the random variables R and Θ. Consequently, the random variables R and Θ are statistically independent with PDFs given by

$$\begin{aligned} f_R(r) &= \frac{r}{\sigma^2} h_2(\frac{r^2}{\sigma^2}) \quad (0 \leq r \leq \infty) \\ f_\Theta(\theta) &= (2\pi)^{-1} \quad (0 \leq \theta \leq 2\pi). \end{aligned} \tag{3.13}$$

Equation (3.13) relates the envelope PDF to $h_2(.)$. Hence, we can write

$$h_2(\frac{r^2}{\sigma^2}) = \frac{\sigma^2}{r} f_R(r). \tag{3.14}$$

Thus, eq (3.14) provides a mechanism to obtain $h_2(q)$. Starting from $h_2(q)$, we then use eq (2.30) to obtain $h_{2N}(q)$. Since not all non-Gaussian envelope PDFs are admissible for characterization as SIRVs, we must check that $h_2(q)$ and its derivatives satisfy the monotonicity conditions stated in Chapter 2. Finally, $h_{2N}(p)$ is obtained by simply replacing q by $p = (\mathbf{y} - \mathbf{b})^T \mathbf{\Sigma}^{-1} (\mathbf{y} - \mathbf{b})$ in $h_{2N}(q)$.

3.3.3 Hankel Transform Approach

In this section we present an approach based on the Hankel transform for specifying $h_{2N}(p)$. Recall that the joint PDF of the i^{th} in-phase and out-of-phase quadrature components of $\mathbf{Y}$ is given by eq (3.10). For convenience, it is assumed that σ^2 is

unity. Dropping the subscript i from eq (3.10), the joint characteristic function of Y_{ci} and Y_{si} is expressed as

$$\phi_{Y_c,Y_s}(\omega_1, \omega_2) = (2\pi)^{-1} \int_{-\infty}^{\infty} \int_{-\infty}^{\infty} exp(j\omega_1 y_c + j\omega_2 y_s) h_2(y_c^2 + y_s^2) dy_c dy_s. \tag{3.15}$$

Introducing the transformations

$$\begin{aligned} R &= \sqrt{Y_c^2 + Y_s^2} \\ \Theta &= \arctan \tfrac{Y_s}{Y_c} \\ \omega &= \sqrt{\omega_1^2 + \omega_2^2} \\ \alpha &= \arctan \tfrac{\omega_2}{\omega_1} \end{aligned} \tag{3.16}$$

we can rewrite eq (3.15) as

$$\phi_{Y_c,Y_s}(\omega_1, \omega_2) = (2\pi)^{-1} \int_0^{\infty} \int_0^{2\pi} exp[j\omega r\{cos(\theta)cos(\alpha) + sin(\theta)sin(\alpha)\}] r h_2(r^2) dr\, d\theta. \tag{3.17}$$

Noting that $cos(A - B) = cos(A)cos(B) + sin(A)sin(B)$, we can rewrite eq (3.17) as

$$\phi_{Y_c,Y_s}(\omega_1, \omega_2) = (2\pi)^{-1} \int_0^{\infty} \int_0^{2\pi} exp[j\omega r cos(\theta - \alpha)] r h_2(r^2) dr\, d\theta. \tag{3.18}$$

Interchanging the order of integration in eq (3.18), and recognizing that [35]

$$J_0(x) = \frac{1}{2\pi} \int_0^{2\pi} exp[jx cos(\beta - \gamma)] d\beta, \tag{3.19}$$

where $J_0(x)$ is the Bessel function of order zero, we have

$$\phi_{Y_c,Y_s}(\omega_1, \omega_2) = \int_0^{\infty} r h_2(r^2) J_0(\omega r) dr. \tag{3.20}$$

From eq (3.20), it is clear that the joint characteristic function of Y_c and Y_s is a function of $\omega = \sqrt{\omega_1^2 + \omega_2^2}$. Hence, it is a circularly symmetric characteristic function. Denoting this function by $\Psi(\omega)$, we can write

$$\Psi(\omega) = \int_0^{\infty} r h_2(r^2) J_0(\omega r) dr. \tag{3.21}$$

Equation (3.21) is recognized as the Hankel transform of order zero of $h_2(r^2)$. Using the inverse Hankel transform, we obtain

$$h_2(r^2) = \int_0^\infty \omega \Psi(\omega) J_0(\omega r) d\omega. \tag{3.22}$$

Introducing the dummy variable w, we can write

$$h_2(q) = \int_0^\infty \omega \Psi(\omega) J_0(\omega \sqrt{q}) d\omega. \tag{3.23}$$

We then use eq (2.30) to obtain $h_{2N}(q)$. More explicitly, we can write

$$h_{2N}(q) = (-2)^{N-1} \int_0^\infty \omega \Psi(\omega) \frac{d^{N-1}}{dq^{N-1}} [J_0(\omega \sqrt{q})] d\omega. \tag{3.24}$$

Using the identity [35]

$$\frac{dJ_0(\eta)}{d\eta} = -J_1(\eta) \tag{3.25}$$

we have

$$\frac{dJ_0(\omega\sqrt{q})}{dq} = -\frac{\omega}{2} w^{-\frac{1}{2}} J_1(\omega\sqrt{q}). \tag{3.26}$$

Use of the recurrence relation [35]

$$\frac{d}{d\eta}[\eta^{-\alpha} J_\alpha(\eta)] = -\eta^{-\alpha} J_{\alpha+1}(\eta) \tag{3.27}$$

results in

$$\frac{d^2}{dq^2}[J_0(\omega\sqrt{q})] = \frac{\omega^2}{4} (\sqrt{q})^{-2} J_2(\omega\sqrt{q}). \tag{3.28}$$

Repeated use of eq (3.27) gives

$$\frac{d^{N-1}}{dq^{N-1}}[J_0(\omega\sqrt{q})] = (-1)^{N-1} \frac{\omega^{N-1}}{2^{N-1}} (\sqrt{q})^{-N+1} J_{N-1}(\omega\sqrt{q}). \tag{3.29}$$

Substituting eq (3.29) in eq (3.24) gives

$$h_{2N}(q) = (\sqrt{q})^{1-N} \int_0^\infty \omega^N \Psi(\omega) J_{N-1}(\omega\sqrt{q}) d\omega. \tag{3.30}$$

Finally, $h_{2N}(p)$ is obtained from eq (3.30) by replacing q by $p = (\mathbf{y} - \mathbf{b})^T \boldsymbol{\Sigma}^{-1} (\mathbf{y} - \mathbf{b})$. This completes the proof of eq (2.32) for even values of N which had been previously deferred. The integral in eq (3.30) is recognized as the Hankel transform of order

$N-1$ of $\Psi(\omega)$. A number of Hankel transforms have been provided in [36] and these will be made use of in the examples presented in Section 3.4.

3.4 Examples of Complex SIRVs

This section presents examples based on the approaches discussed in Section 3.3 and is divided into three parts. In section 3.4.1, we present examples that assume the knowledge of the characteristic PDF. In Section 3.4.2, the marginal envelope PDF is assumed to be known whereas in Section 3.4.3, knowledge of the marginal characteristic function is assumed. Finally, at the end of Section 3.4.3 we point out some univariate PDFs that cannot be generalized to SIRV characterization. We consider the problem of determining the PDF of the random vector $\mathbf{Y}^T = [\mathbf{Y_c}^T : \mathbf{Y_s}^T]$ specified in Section 3.2. It is assumed that the mean vector of $\mathbf{Y}$ and its covariance matrix $\mathbf{\Sigma}$ are known. Consequently, specification of the PDF of $\mathbf{Y}$ of the form of eq (3.8) reduces to determination of $h_{2N}(p)$.

3.4.1 Examples Based on the Characteristic PDF

3.4.1.1 Gaussian Distribution

The Gaussian marginal PDF for the quadrature components having mean b_k and variance σ_k^2 is

$$f_{Y_k}(y_k) = \frac{1}{\sqrt{(2\pi)}\sigma_k} exp(-\frac{(y_k - b_k)^2}{2\sigma_k^2}) \quad (-\infty \leq y_k \leq \infty). \tag{3.31}$$

The characteristic PDF for this example is given by

$$f_S(s) = \delta(s-1) \tag{3.32}$$

where $\delta(.)$ is the unit impulse function. Using eq (2.21), it is seen that the resulting $h_N(p)$ is given by

$$h_N(p) = exp(-\frac{p}{2}). \tag{3.33}$$

where $p = (\mathbf{y}-\mathbf{b})^{\mathbf{T}}\mathbf{\Sigma}^{-1}(\mathbf{y}-\mathbf{b})$. The corresponding PDF for any N is given by eq (2.20). For $N = 1$, this result reduces to eq (3.31). When $\mathbf{Y}$ is made up of quadrature components, we obtain the the corresponding $h_{2N}(p)$ by simply replacing N by $2N$ in eq (3.33). Whenever a characteristic PDF can be made to approach a unit impulse function displaced to the right of the origin by appropriate choice of its parameters, it follows that the corresponding SIRV PDF will approach the Gaussian

PDF.

3.4.1.2 K-Distribution

The K-distributed envelope PDF, by definition, is given by

$$f_R(r) = \frac{2b}{\Gamma(\alpha)}(\frac{br}{2})^{\alpha} K_{\alpha-1}(br)u(r) \tag{3.34}$$

where α is the shape parameter of the distribution, b denotes the scale parameter of the distribution, $K_N(t)$ is the N^{th} order modified Bessel function of the second kind and $u(r)$ is the unit step function. The K-distributed envelope PDF is commonly used for modeling radar clutter PDFs that have extended tails [19, 20] and [2, 9]. In particular, the PDF becomes heavy tailed as α approaches zero. Plots of eq (3.34) for several values of α are shown in Figures 3.1-3.4.

The K-distributed envelope PDF arises when we consider the product of a Rayleigh distributed random variable R' and an independent Chi-distributed random variable V. More precisely, we consider the product $R = R'V$, with R' and V being statistically independent. Their PDFs are given by

$$f_{R'}(r') = r' exp(-\frac{[r']^2}{2}) \quad 0 \leq r' \leq \infty \tag{3.35}$$

and

$$f_V(v) = \frac{2b}{\Gamma(\alpha)2^{\alpha}}(bv)^{2\alpha-1} exp(-\frac{b^2v^2}{2}) \;\; 0 \leq v < \infty, \tag{3.36}$$

respectively. Consequently, the PDF of R is given by

$$\begin{aligned} f_R(r) &= \int_0^{\infty} f_{R|V}(r|v) f_V(v) dv \\ &= \int_0^{\infty} \frac{r}{v^2} exp(-\frac{r^2}{2v^2}) \frac{2b}{\Gamma(\alpha)2^{\alpha}}(bv)^{2\alpha-1} exp(-\frac{b^2v^2}{2}). \end{aligned} \tag{3.37}$$

From [35], we have

$$K_{\nu}(xz) = \frac{z^{\nu}}{2}\int_0^{\infty} exp[-\frac{x}{2}(t + \frac{z^2}{t})]t^{-\nu-1}dt \quad [|argz| < \frac{\pi}{4}], \;\; z > 0. \tag{3.38}$$

Letting $v^2 = t$ in eq (3.37) and using the result of eq (3.38), the PDF of eq (3.34) follows.

The quadrature components corresponding to the Rayleigh envelope PDF are independent identically distributed zero mean Gaussian random variables having unit

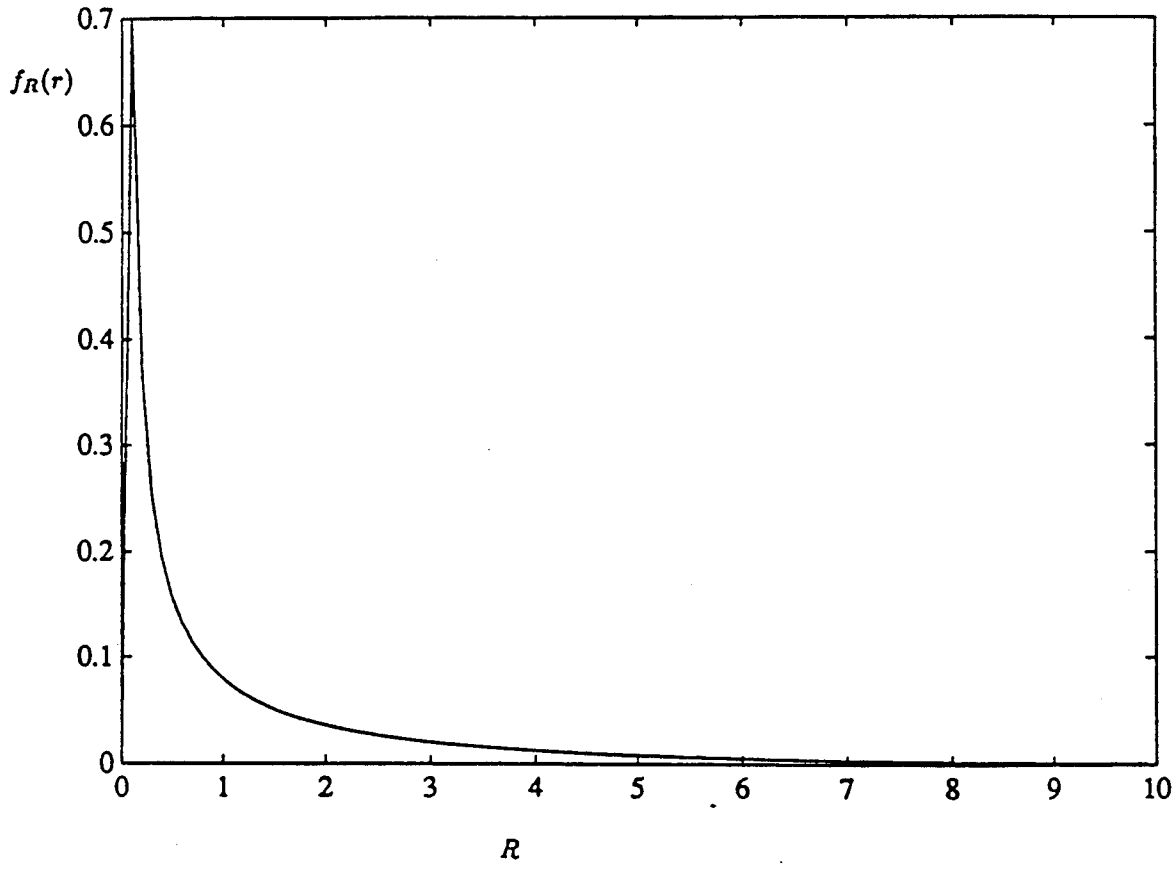

Figure 3.1: K-distribution, $b = 0.31$, $\alpha = 0.05$

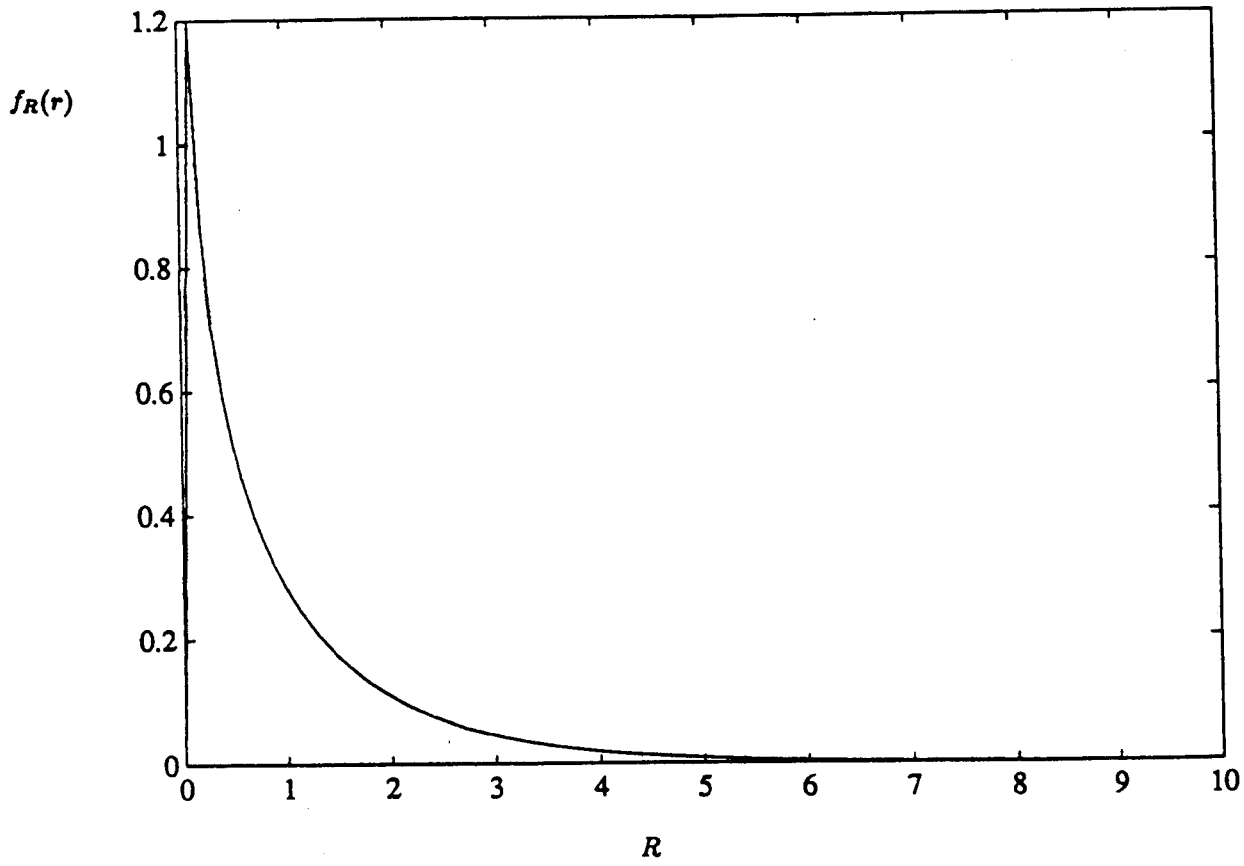

Figure 3.2: K-distribution, $b = 0.77$, $\alpha = 0.3$

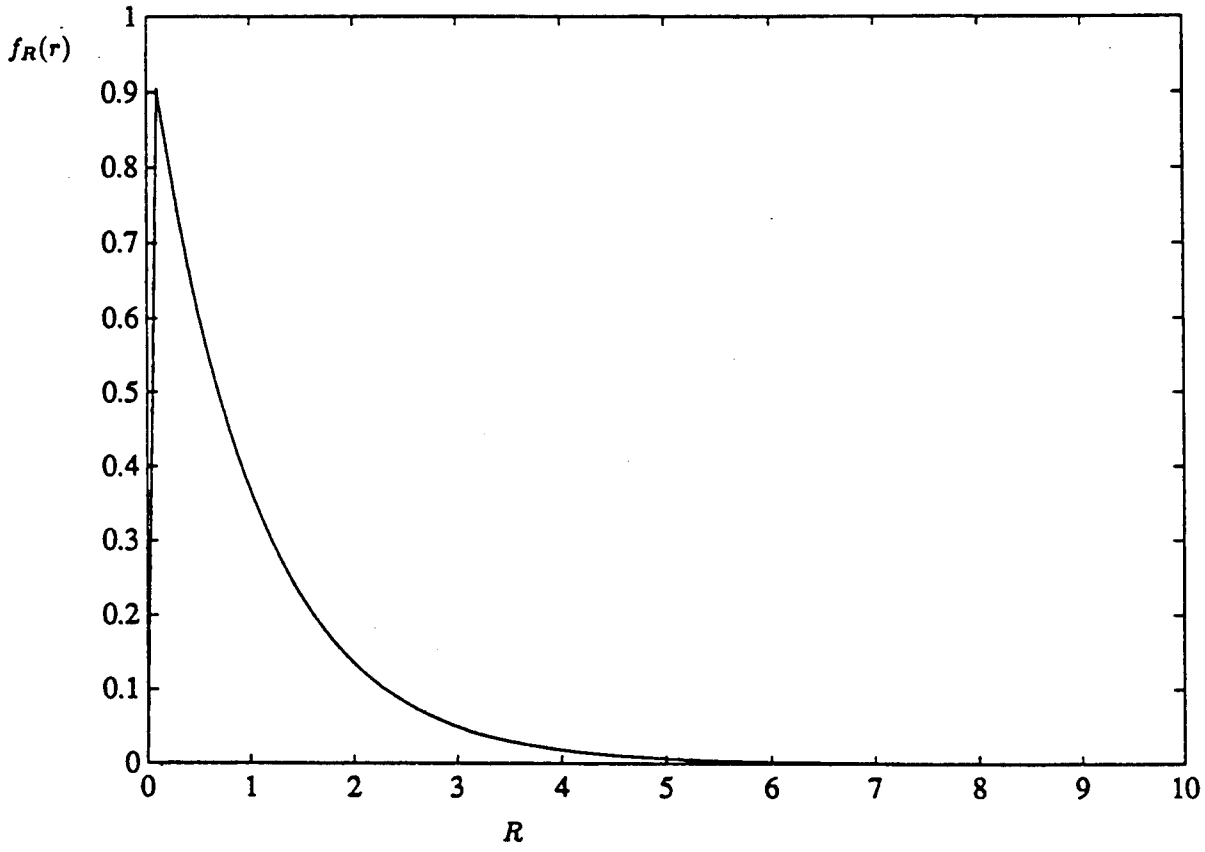

Figure 3.3: K-distribution, $b = 1$, $\alpha = 0.5$

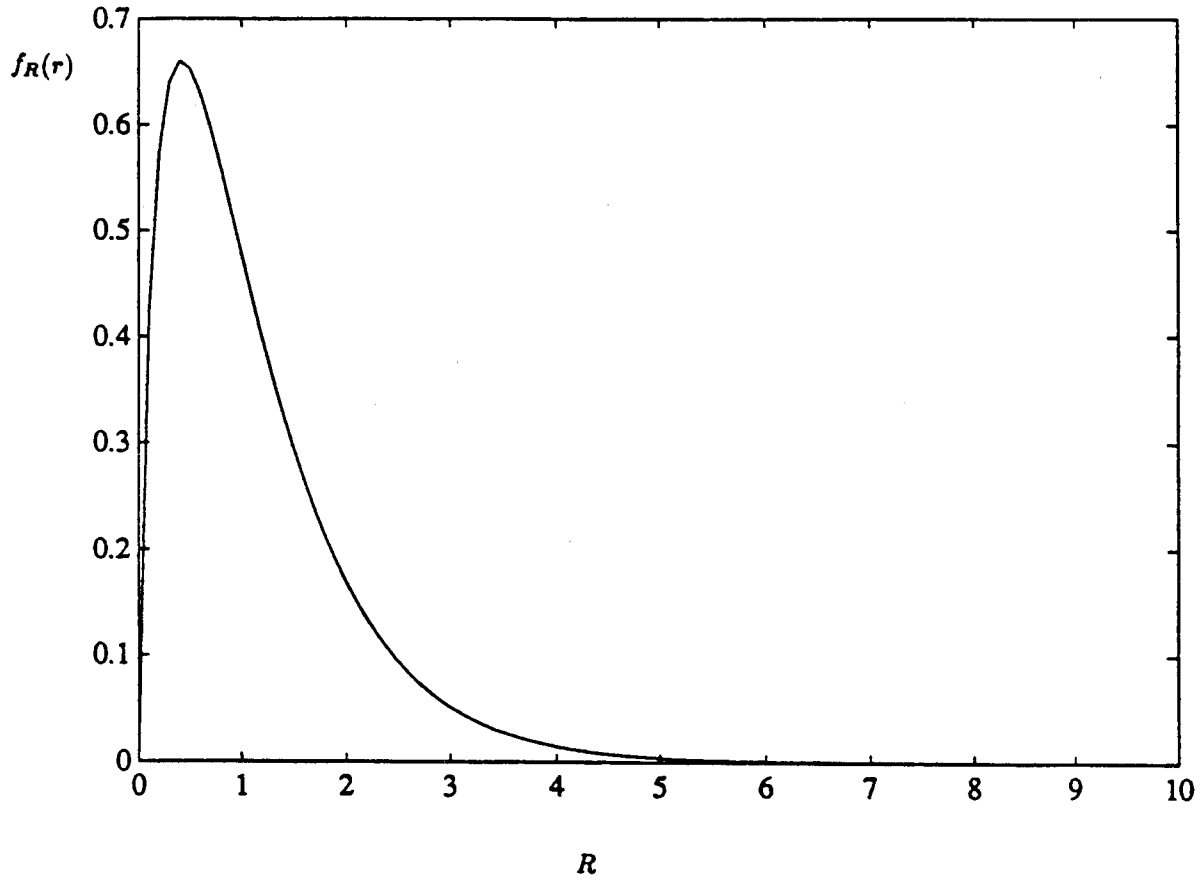

Figure 3.4: K-distribution, $b = 1.4$, $\alpha = 0.99$

variance. The PDF of the quadrature components corresponding to R' is expressed as

$$f_{Z_c}(z) = f_{Z_s}(z) = (2\pi)^{-\frac{1}{2}} exp(-\frac{z^2}{2}) \tag{3.39}$$

where Z_c and Z_s denote the in phase and out of phase quadrature components. The quadrature components arising from the K-distributed envelope PDF, denoted by Y_c and Y_s, respectively, can be expressed as

$$\begin{aligned} Y_c &= Z_c V \\ Y_s &= Z_s V. \end{aligned} \tag{3.40}$$

Note that $|\tilde{Y}| = |\tilde{Z}|V$ and $\Theta_{\tilde{Y}} = \Theta_{\tilde{Z}}$. Consequently, the PDF of Y_c is given by

$$f_{Y_c}(y_c) = \frac{b^{2\alpha}}{\sqrt{2\pi}\Gamma(\alpha)2^{\alpha-1}} \int_0^\infty v^{2\alpha-2} exp[-\frac{1}{2}(\frac{y_c^2}{v^2} + b^2v^2)]dv. \tag{3.41}$$

Making the change of variables $t = b^2v^2$ and $z^2 = b^2y_c^2$, and using eq (3.38), the PDF of Y_c is expressed as

$$f_{Y_c}(y_c) = \frac{2b}{\Gamma(\alpha)\sqrt{2\pi}2^\alpha} |by_c|^{\alpha-\frac{1}{2}} K_{\frac{1}{2}-\alpha}(b|y_c|) \quad -\infty < y_c < \infty \tag{3.42}$$

where the absolute value denoted by $|.|$ is used on account of the requirement that $z > 0$. In a similar manner, it can be shown that the PDF of Y_s has the same functional form as eq (3.42). The PDF of eq (3.42) is called the Generalized Laplace PDF [16].

The characteristic PDF for the K-distributed SIRV is

$$f_S(s) = \frac{2b}{\Gamma(\alpha)2^\alpha}(bs)^{2\alpha-1} exp(-\frac{b^2s^2}{2})u(s). \tag{3.43}$$

Using eqs (2.21) and (3.38),

$$h_N(p) = \int_0^\infty s^{-N} exp(-\frac{p}{2s^2}) \frac{2b}{\Gamma(\alpha)2^\alpha}(bs)^{2\alpha-1} exp(-\frac{b^2s^2}{2})ds. \tag{3.44}$$

Making the change of variables $t = b^2 s^2$ and $z^2 = b^2 p$, the resulting $h_N(p)$ is given by

$$h_N(p) = \frac{b^N}{\Gamma(\alpha)} \frac{(b\sqrt{p})^{\alpha - \frac{N}{2}}}{2^{\alpha-1}} K_{\frac{N}{2}-\alpha}(b\sqrt{p}). \tag{3.45}$$

The corresponding SIRV PDF for any N is given by using eq (2.20). For the case when $N = 1$, this reduces to eq (3.42). When dealing with quadrature components, we use eq (3.45) with N replaced by $2N$

3.4.1.3 Student-t Distribution

The Student-t distribution for the quadrature components is given by

$$f_{Y_k}(y_k) = \frac{\Gamma(\nu + \frac{1}{2})}{b\sqrt{\pi}\Gamma(\nu)} (1 + \frac{y_k^2}{b^2})^{-\nu - \frac{1}{2}} \ (-\infty < y_k < \infty), \ \nu > 0 \tag{3.46}$$

where b is the scale parameter, ν is the shape parameter $\Gamma(\nu)$ is the Eulero-Gamma function and $k = c, s$. Plots of the Student-t distribution are shown for several values of ν in Figures 3.5-3.7. The characteristic PDF for this example is

$$f_S(s) = \frac{2}{\Gamma(\nu)} (\frac{1}{2})^{\nu} b^{2\nu-1} (s^{-1})^{2\nu+1} exp(-\frac{b^2}{2s^2}) u(s). \tag{3.47}$$

Use of eq (2.21) results in $h_N(p)$ being given by

$$h_N(p) = \frac{2^{\frac{N}{2}} b^{2\nu} \Gamma(\nu + \frac{N}{2})}{\Gamma(\nu)(b^2 + p)^{\frac{N}{2}+\nu}}. \tag{3.48}$$

The corresponding SIRV PDF for any N is given by eq (2.20). For $N = 1$, this result reduces to eq (3.46). When dealing with quadrature components, we make use of eq (3.48) with N replaced by $2N$.

3.4.1.4 Mixture of Gaussian PDFs

An interesting non-Gaussian marginal PDF that is admissible as an SIRV is the mixture of Gaussian PDFs. We consider the PDF given by

$$f_{Y_k}(y_k) = \sum a_i (2\pi k_i^2)^{-\frac{1}{2}} exp(-\frac{(y_k - b_k)^2}{2k_i^2}) \tag{3.49}$$

for the quadrature components of $\mathbf{Y}$. The characteristic PDF for this example is given by

$$f_S(s) = \sum a_i \delta(s - k_i). \tag{3.50}$$

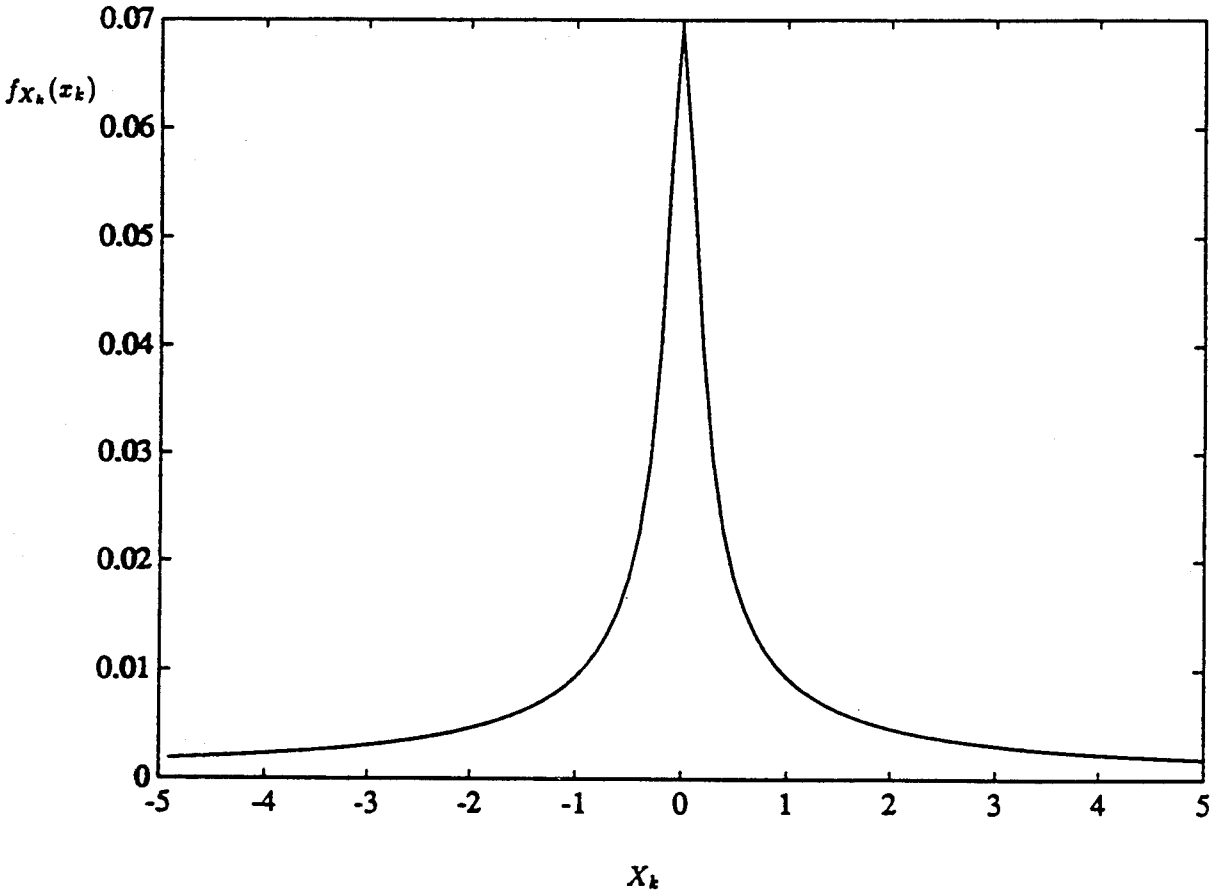

Figure 3.5: Student-t distribution, $b = 0.14$, $\nu = 0.01$

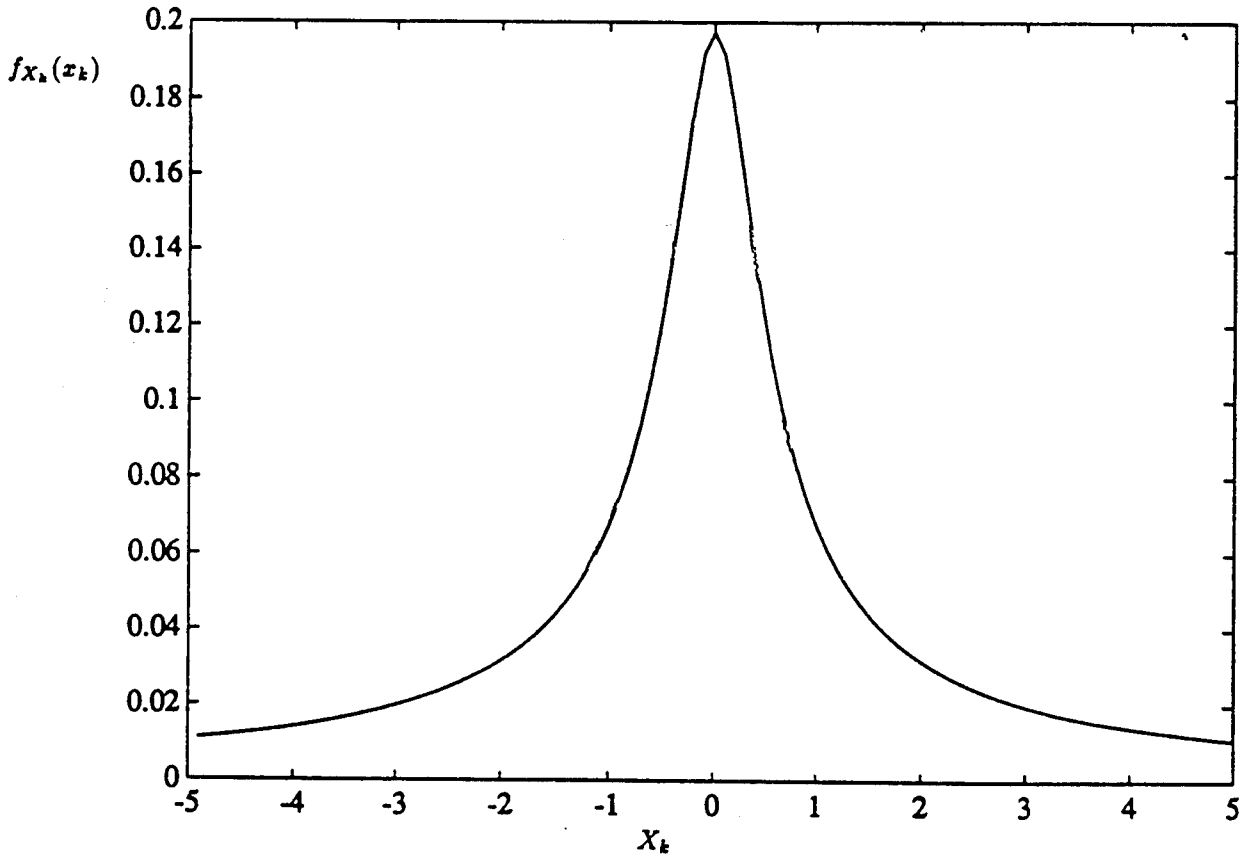

Figure 3.6: Student-t distribution, $b = 0.45$, $\nu = 0.1$

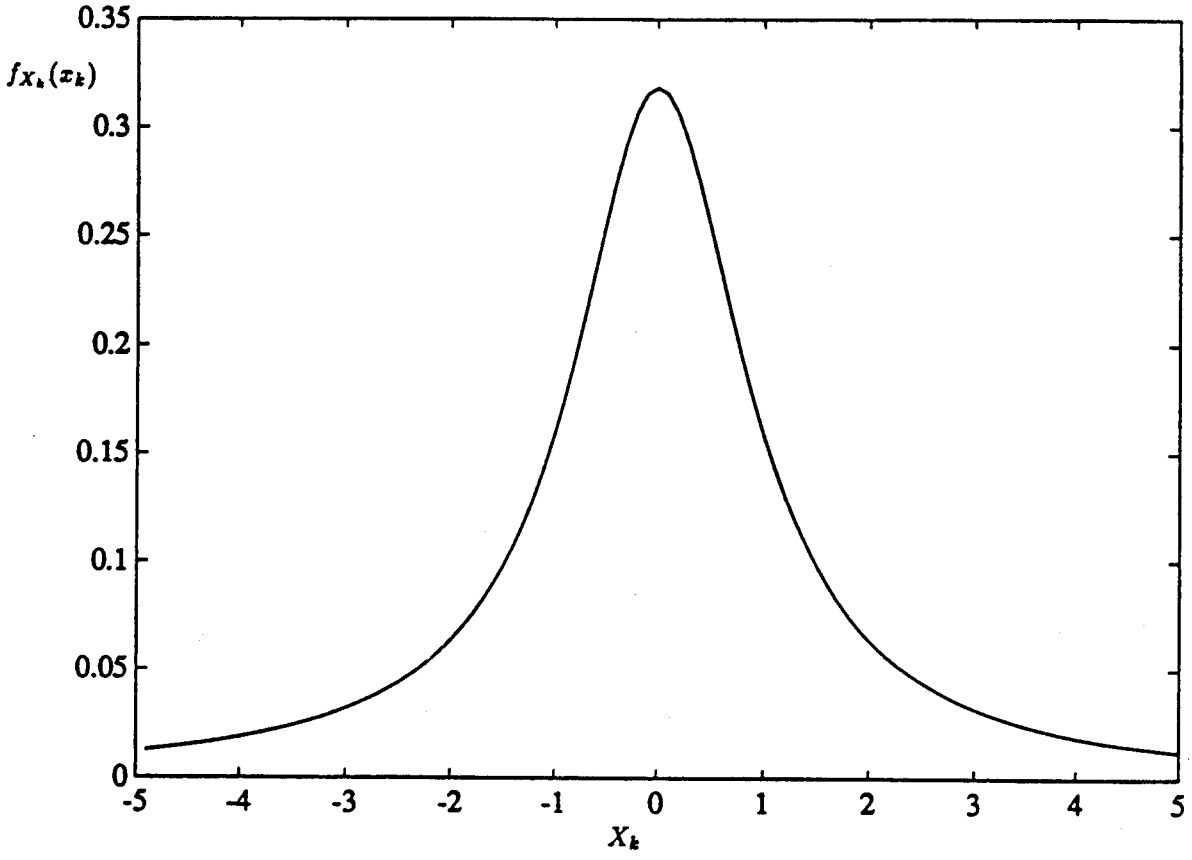

Figure 3.7: Student-t distribution, $b = 1$, $\nu = 0.5$

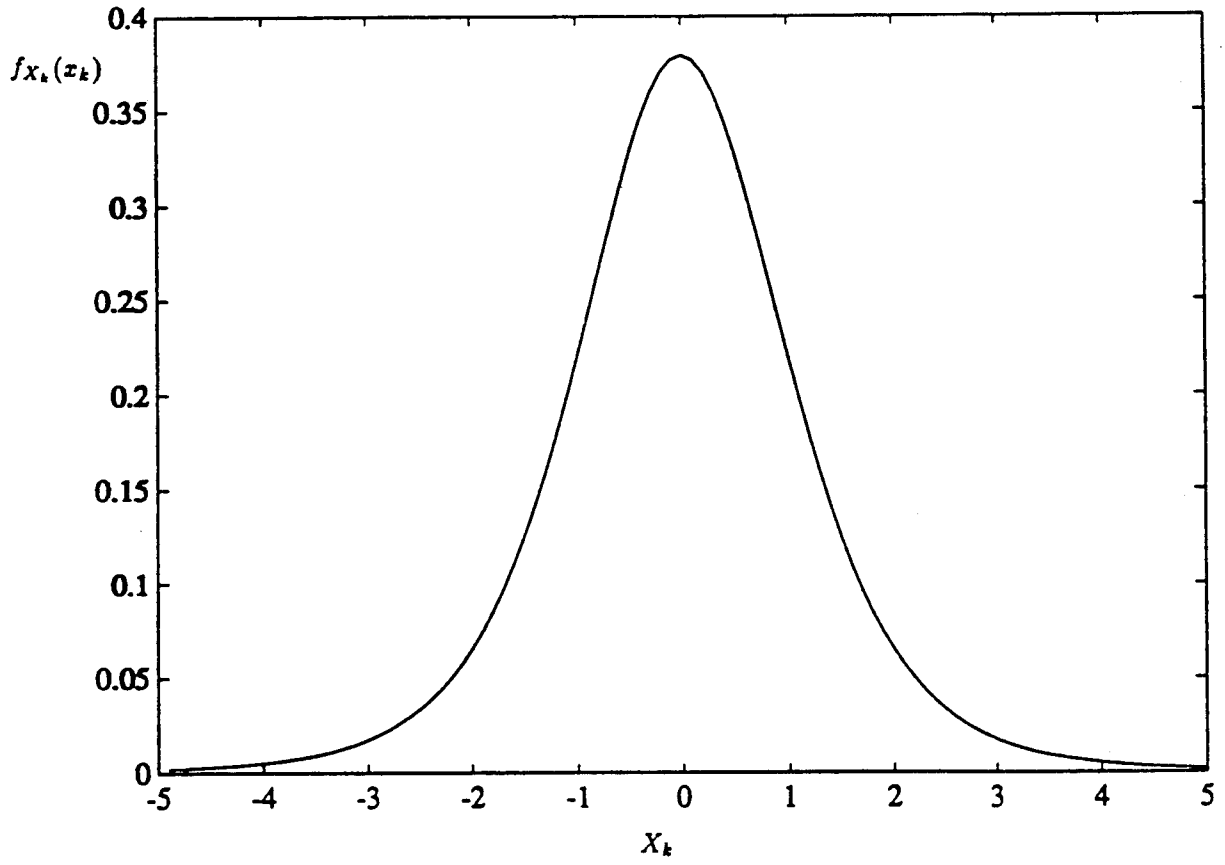

Figure 3.8: Student-t distribution, $b = 2.23$, $\nu = 2.5$

Note that S is a discrete random variable, with a_i denoting the probability $P(S = k_i)$. Also, it is required that

$$\begin{aligned} a_i &\geq 0 \quad i = 1, 2, \ldots \\ \textstyle\sum_i a_i &= 1. \end{aligned} \tag{3.51}$$

Using eq (2.21), it is seen that

$$h_N(p) = \sum_i k_i^{-N} a_i exp(-\frac{p}{2k_i^2}). \tag{3.52}$$

The corresponding SIRV PDF for any N is given by eq (2.20). For $N = 1$, this result reduces to eq (3.49). When dealing with quadrature components, we make use of the result of eq (3.52) with N replaced by $2N$. Note that the a_i's can be assigned any desired discrete distribution.

3.4.2 Examples Based on Marginal Envelope PDF

We shall report here on some new SIRV PDFs obtained starting from the marginal envelope PDF. Note in general, that the characteristic PDF for all the examples considered here are not available in closed form. Since σ^2 is the common variance of the in phase and out of phase quadrature components, σ^2 is equal to $\frac{1}{2}E(R^2)$. In addition, recall that the binomial coefficient is defined by

$$\binom{l}{i} = \frac{l!}{i!(l-i)!}. \tag{3.53}$$

In all the examples in this section, we start with $h_2(q)$ and obtain $h_{2N}(q)$ by the process of successive differentiation. The corresponding $h_{2N}(p)$ for each example is obtained by replacing q by p in $h_{2N}(q)$. In all the examples presented in this section, note that the envelope PDFs reduce to the Rayleigh envelope PDF for appropriately chosen parameters.

3.4.2.1 Chi Envelope PDF

We consider the Chi distributed envelope PDF given by

$$f_R(r) = \frac{2b}{\Gamma(\nu)}(br)^{2\nu-1} exp(-b^2r^2) \quad (0 \leq r \leq \infty) \tag{3.54}$$

where b denotes the scale parameter and ν denotes the shape parameter. Plots of the Chi envelope PDF are shown in Figures 3.8-3.10 for several values of ν. Using eq(3.14), we can write

$$h_2(q) = \frac{2}{\Gamma(\nu)}(b\sigma)^{2\nu} q^{\nu-1} exp(-b^2\sigma^2 q). \tag{3.55}$$

Using eq(2.30), we have

$$\begin{aligned} h_{2N}(q) &= (-2)^{N-1} \tfrac{d^{N-1}h_2(q)}{dq^{N-1}} \\ &= \tfrac{(-2)^{N-1}}{\Gamma(\nu)} 2(b\sigma)^{2\nu} \tfrac{d^{N-1}}{dq^{N-1}}[q^{\nu-1} exp(-b^2\sigma^2 q)]. \end{aligned} \tag{3.56}$$

Recall Leibnitz's theorem for the n^{th} derivative of a product [35], which states that

$$\frac{d^n(uv)}{dx^n} = \sum_{k=0}^{n} \begin{pmatrix} n \\ k \end{pmatrix} \frac{d^k u}{dx^k} \frac{d^{n-k} v}{dx^{n-k}} \tag{3.57}$$

where u and v are functions of x. Noting that

$$\frac{d^k(q^{\nu-1})}{dq^k} = \frac{\Gamma(\nu)}{\Gamma(\nu-k)} q^{\nu-k-1}, \tag{3.58}$$

it follows that

$$h_{2N}(q) = (-2)^{N-1} A \sum_{k=1}^{N} G_k q^{\nu-k} exp(-Bq) \tag{3.59}$$

where

$$\begin{aligned} G_k &= \begin{pmatrix} N-1 \\ k-1 \end{pmatrix} (-1)^{N-k} B^{N-k} \frac{\Gamma(\nu)}{\Gamma(\nu-k+1)} \\ A &= \frac{2}{\Gamma(\nu)}(b\sigma)^{2\nu} \\ B &= b^2\sigma^2. \end{aligned} \tag{3.60}$$

An important condition that must be pointed out is that the SIRV PDF is valid only for $\nu \leq 1$. This is due to the fact that $h_2(p)$ and its derivatives are monotonically decreasing functions only in the range of values of ν mentioned above. Finally, for

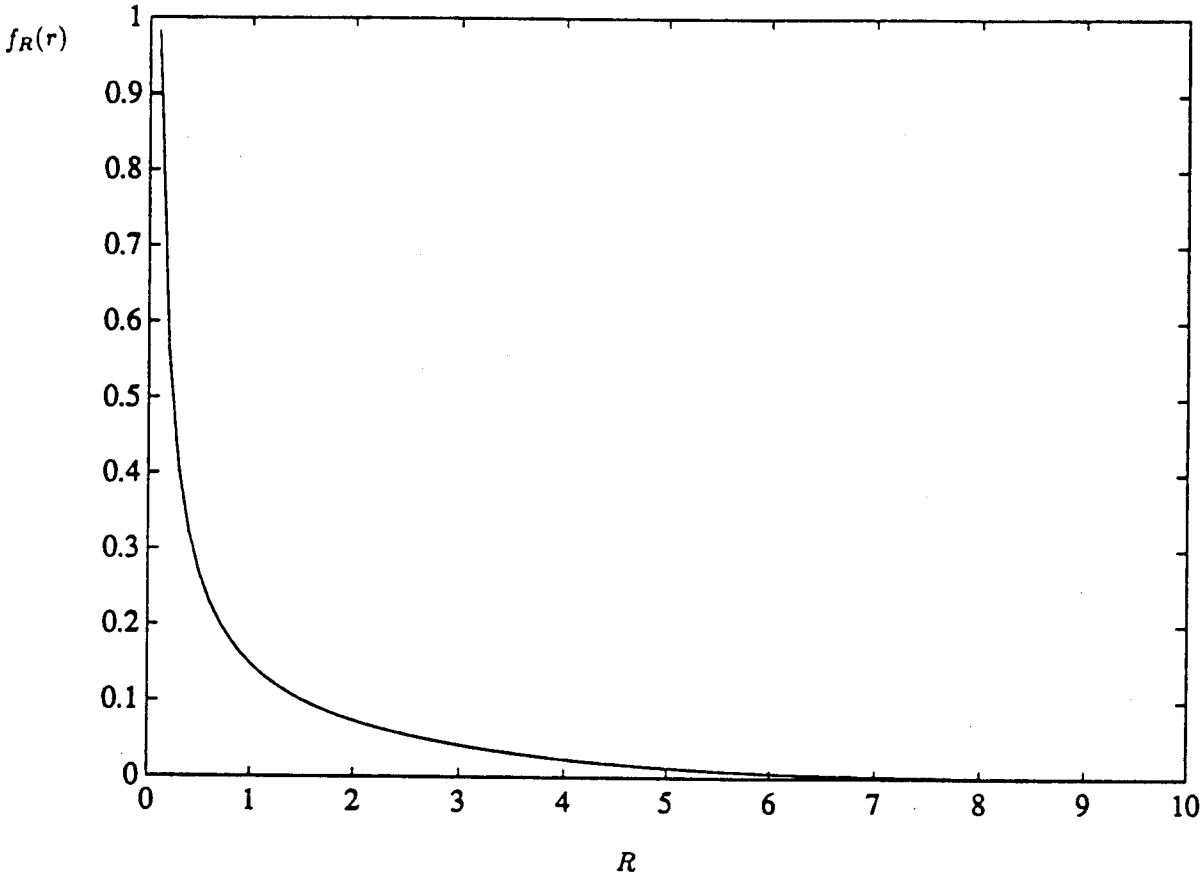

Figure 3.9: Chi Envelope PDF, $b = 0.22$, $\nu = 0.1$

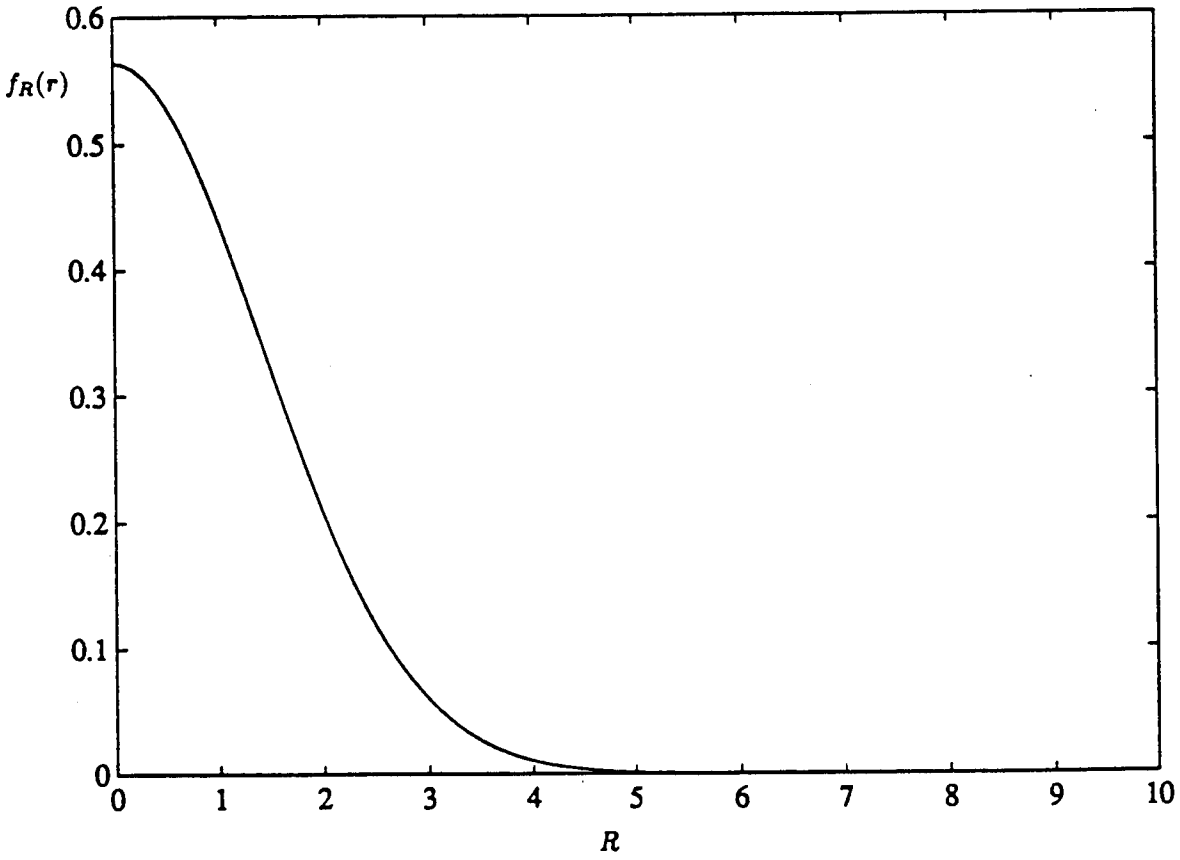

Figure 3.10: Chi Envelope PDF, $b = 0.5$, $\nu = 0.5$

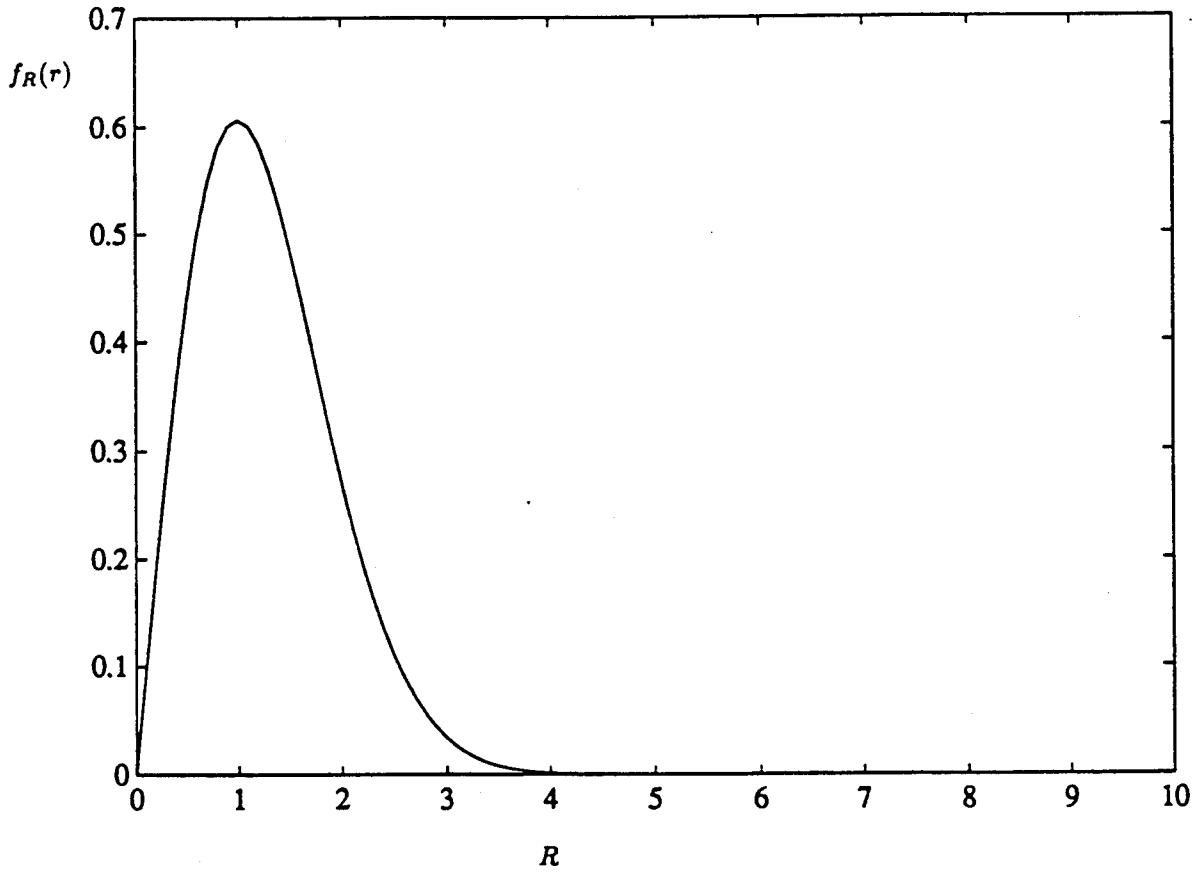

Figure 3.11: Chi Envelope PDF, $b = 0.70$, $\nu = 1.0$

$\nu = 1$, note that the Chi envelope PDF reduces to the Rayleigh envelope PDF. The corresponding SIRV PDF then becomes Gaussian.

3.4.2.2 Weibull Envelope PDF

The Weibull distributed envelope PDF is given by

$$f_R(r) = abr^{b-1}exp(-ar^b) \qquad (0 \leq r \leq \infty). \tag{3.61}$$

where a is the scale parameter and b is the shape parameter. Plots of the Weibull distribution for several values of b are shown in Figures 3.11-3.13. Using eq (3.14), we have

$$h_2(q) = ab\sigma^b q^{\frac{b}{2}-1}exp(-a\sigma^b q^{\frac{b}{2}}) = (-2)\frac{d}{dq}[exp(-Aq^{\frac{b}{2}})] \tag{3.62}$$

where $A = a\sigma^b$. From eq (2.30), we have

$$h_{2N}(q) = (-2)^N \frac{d^N}{dq^N}[exp(-Aq^{\frac{b}{2}})]. \tag{3.63}$$

The rule for obtaining the N^{th} derivative of a composite function is [35]: If $f(x) = F(y)$ and $y = \varphi(x)$, then

$$\frac{d^N}{dx^N}\{f(x)\} = \sum_{k=1}^{N} \frac{U_k}{k!}\frac{d^k}{dy^k}[F(y)] \tag{3.64}$$

where

$$U_k = \sum_{m=1}^{k}(-1)^{k-m}\begin{pmatrix} k \\ m \end{pmatrix} y^{k-m}\frac{d^N y^m}{dx^N}. \tag{3.65}$$

Making the association $x = q$ and $y = -Aq^{\frac{b}{2}}$, we have

$$h_{2N}(q) = \sum_{k=1}^{N} C_k q^{\frac{kb}{2}-N}exp(-Aq^{\frac{b}{2}}) \tag{3.66}$$

where

$$C_k = \sum_{m=1}^{k}(-1)^{m+N}2^N\frac{A^k}{k!}\begin{pmatrix} k \\ m \end{pmatrix}\frac{\Gamma(1+\frac{mb}{2})}{\Gamma(1+\frac{mb}{2}-N)}. \tag{3.67}$$

The Weibull envelope PDF is admissible for characterization as an SIRV for values of b less than or equal to 2. This is due to the fact that $h_2(q)$ and its derivatives

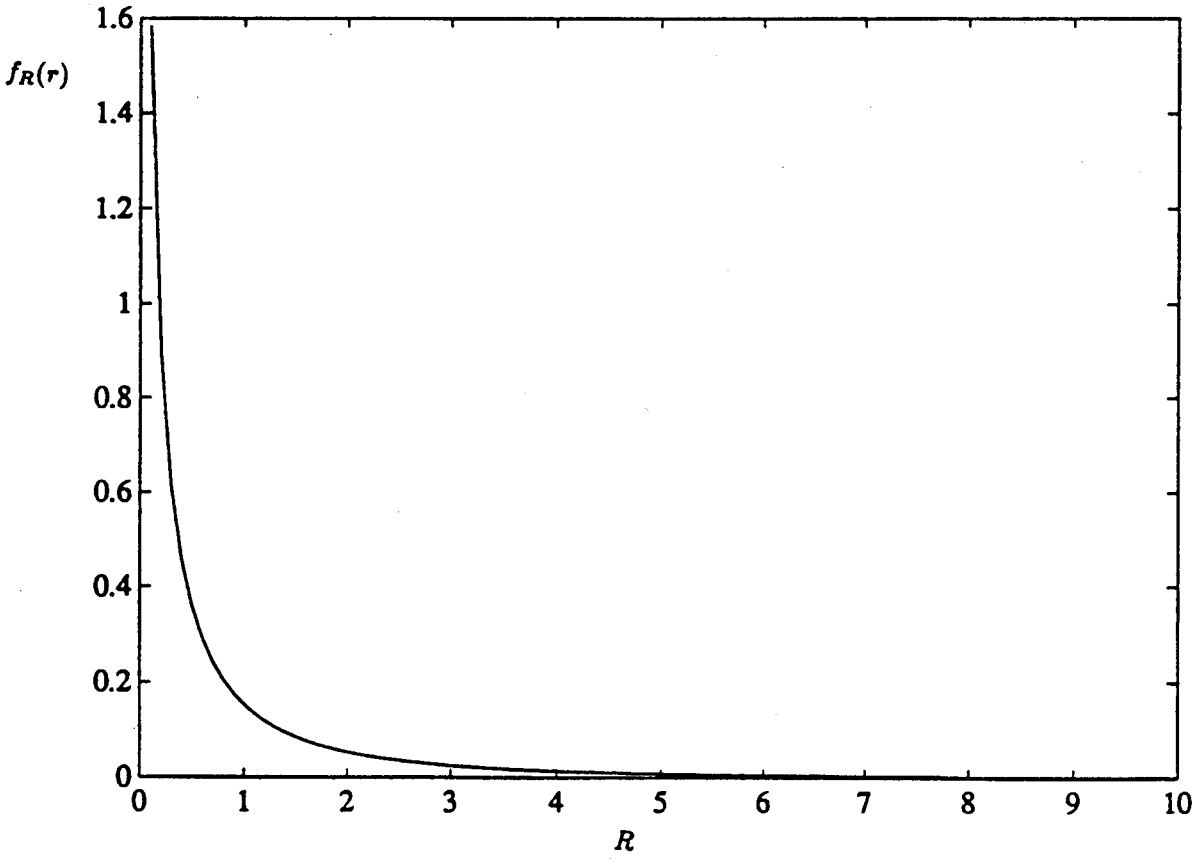

Figure 3.12: Weibull distributed Envelope PDF, $b = 0.5$, $a = 1.86$

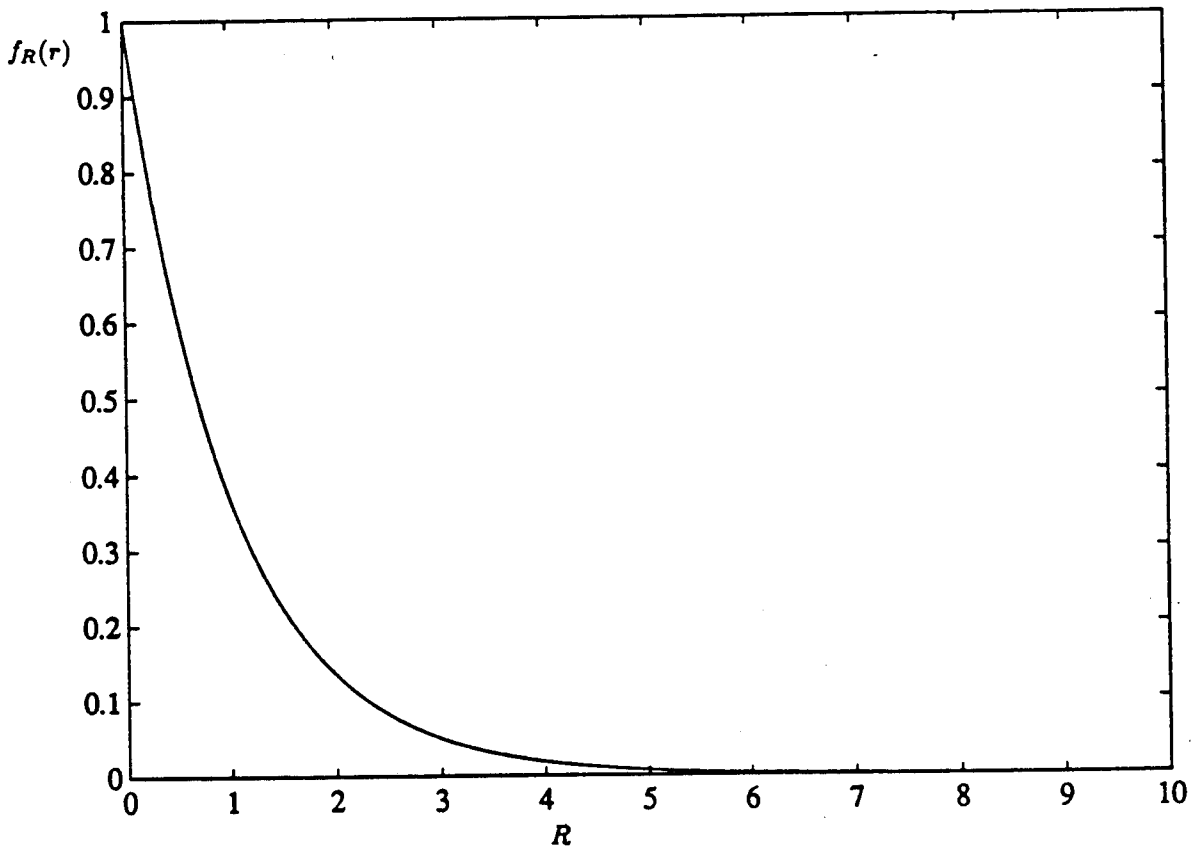

Figure 3.13: Weibull distributed, $b = 1$, $a = 1$

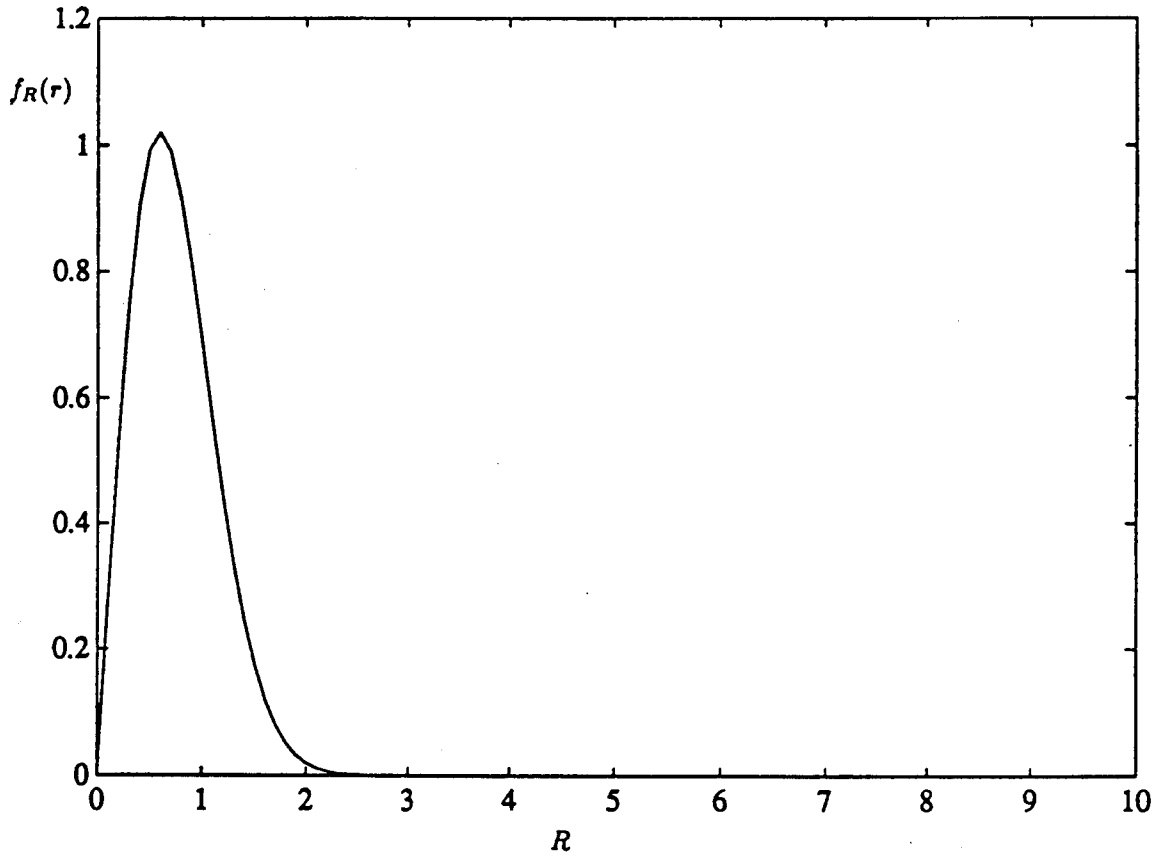

Figure 3.14: Weibull distributed, $b = 2$, $a = 0.5$

fail to satisfy the monotonicity condition for other values of b. However, this is not a serious restriction for the point of view of radar clutter modeling because the Weibull envelope PDF is of interest in modeling large tailed clutter. Such a situation arises only when $0 < b \leq 2$. The Weibull envelope PDF reduces to the Rayleigh envelope PDF when $b = 2$. The corresponding SIRV PDF then becomes Gaussian. Another case of interest arises when $b = 1$. In this case the Weibull envelope PDF corresponds to the Exponential envelope PDF.

3.4.2.3 Generalized Rayleigh Envelope PDF

The next PDF considered is for the Generalized Rayleigh envelope which is given by

$$f_R(r) = \frac{\alpha r}{\beta^2 \Gamma(\frac{2}{\alpha})} exp[-(\frac{r}{\beta})^\alpha] \ \ (0 \leq r \leq \infty) \tag{3.68}$$

where α is the shape parameter and β is the scale parameter. Plots of the Generalized Rayleigh distribution are shown for several values of α in Figures 3.15-3.17.

Proceeding as in the previous example, we find that

$$h_2(q) = Aexp(-Bq^{\frac{a}{2}}) \tag{3.69}$$

where

$$\begin{aligned} A &= \frac{\sigma^2 \alpha}{\beta^2 \Gamma(\frac{2}{\alpha})} \\ B &= \beta^{-\alpha} \sigma^\alpha \end{aligned} \tag{3.70}$$

Using eqs (1.25), (2.63) and (2.64), we have

$$h_{2N}(q) = \sum_{k=1}^{N-1} D_k q^{\frac{k\alpha}{2} - N + 1} exp(-Bq^{\frac{a}{2}}) \tag{3.71}$$

where

$$D_k = \sum_{m=1}^{k} (-1)^{m+N-1} 2^{N-1} \frac{B^k}{k!} \begin{pmatrix} k \\ m \end{pmatrix} \frac{\Gamma(1 + \frac{m\alpha}{2})}{\Gamma(2 + \frac{m\alpha}{2} - N)} \tag{3.72}$$

Note that the SIRV PDF is valid only in the range $(0 \leq \alpha \leq 2)$. This is because of the fact that the monotonicity conditions for the derivatives of $h_2(p)$ are satisfied only for the specified range of α. The Generalized Rayleigh envelope PDF reduces to the Rayleigh envelope PDF when $\alpha = 2$.

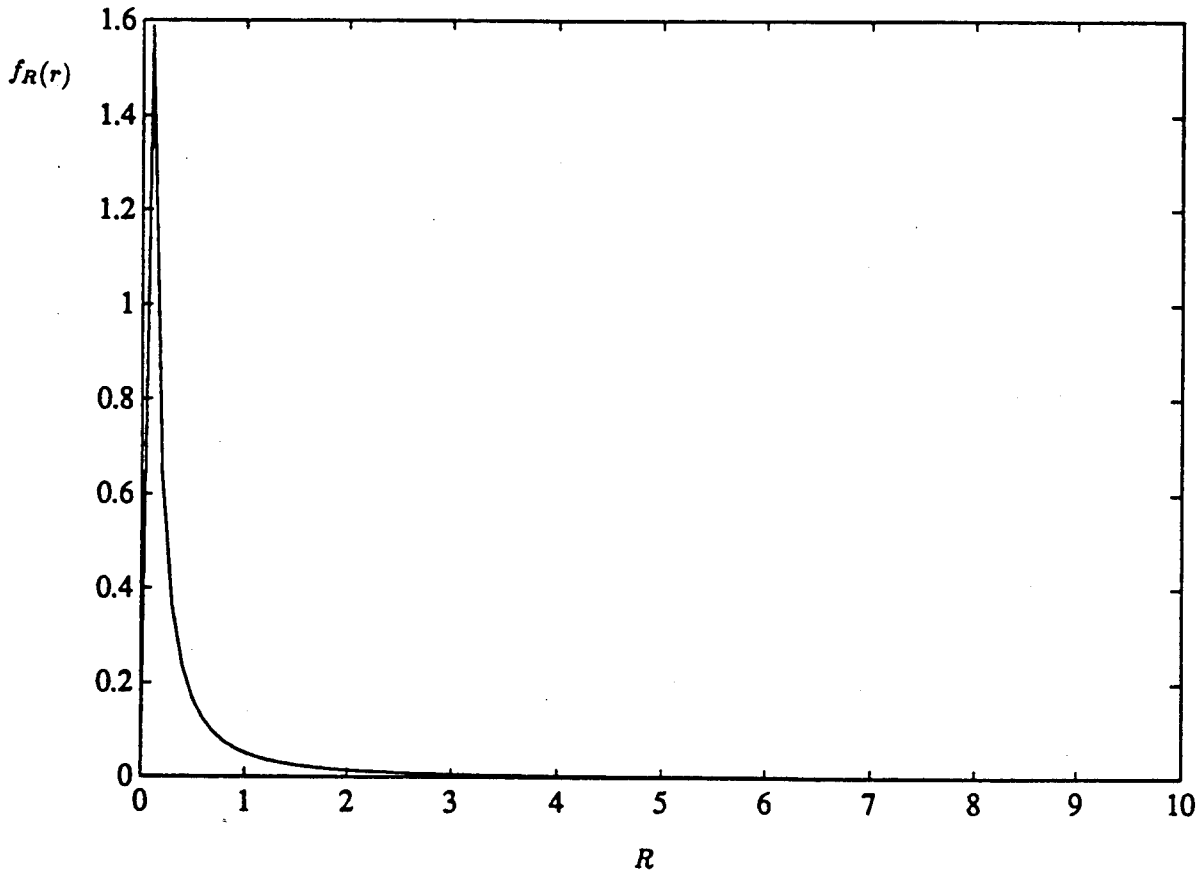

Figure 3.15: Generalized Rayleigh distributed Envelope PDF, $\alpha = 0.1$, $\beta = 3.45 \times 10^{-15}$

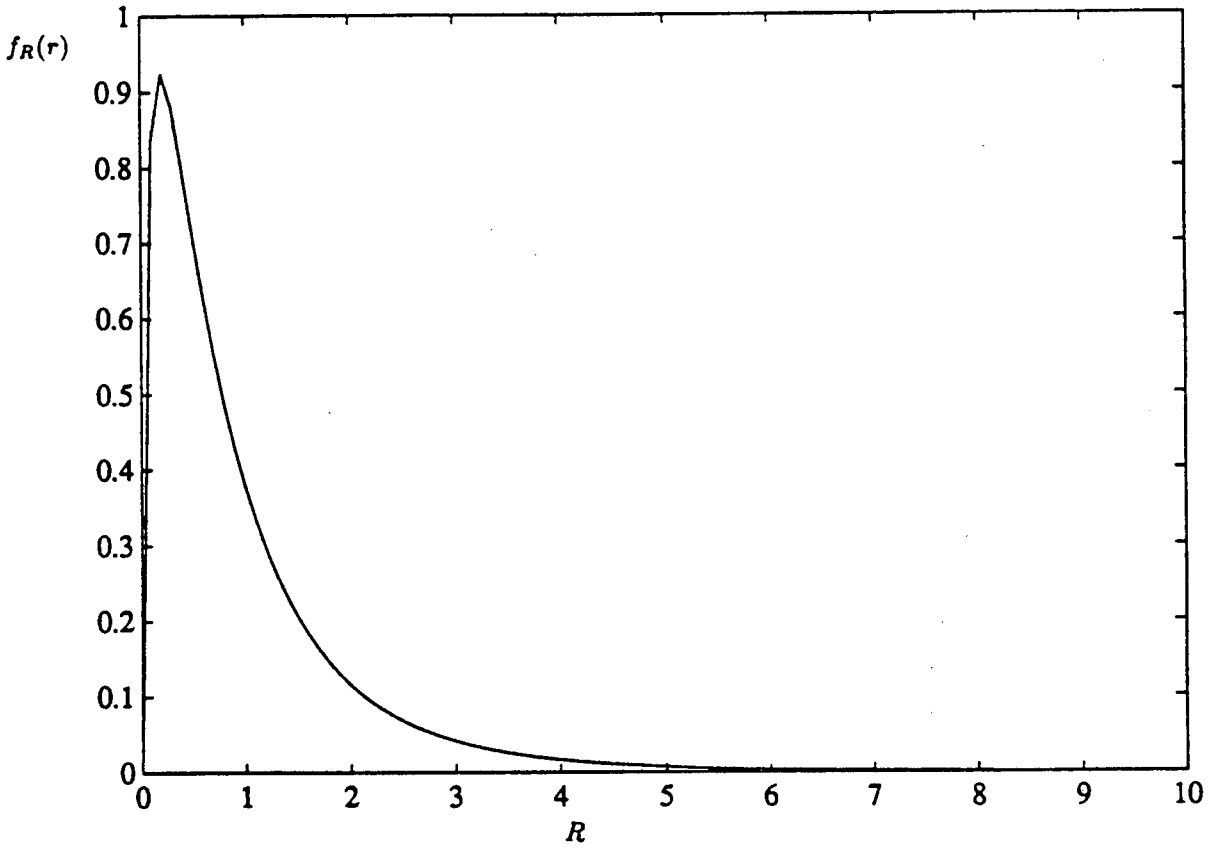

Figure 3.16: Generalized Rayleigh distributed Envelope PDF, $\alpha = 0.5$, $\beta = 0.048$

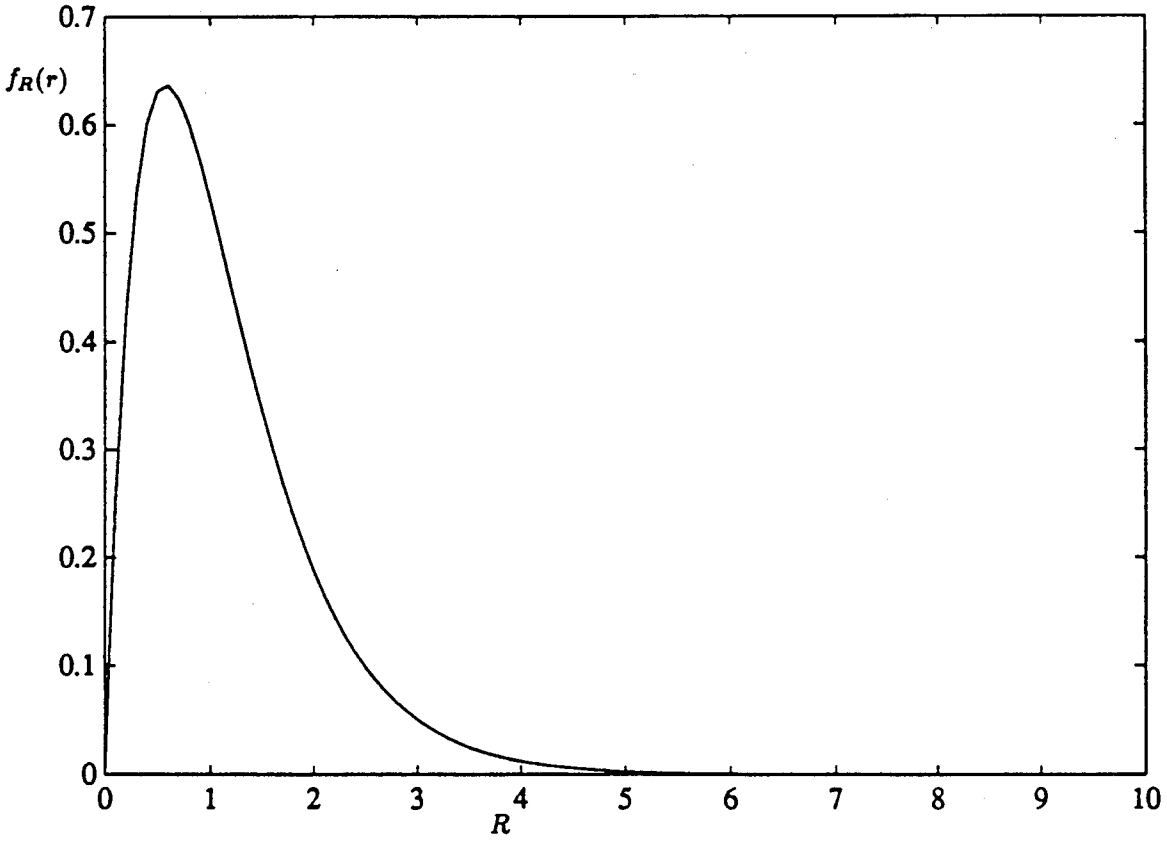

Figure 3.17: Generalized Rayleigh distributed Envelope PDF, $\alpha = 1$, $\beta = 0.577$

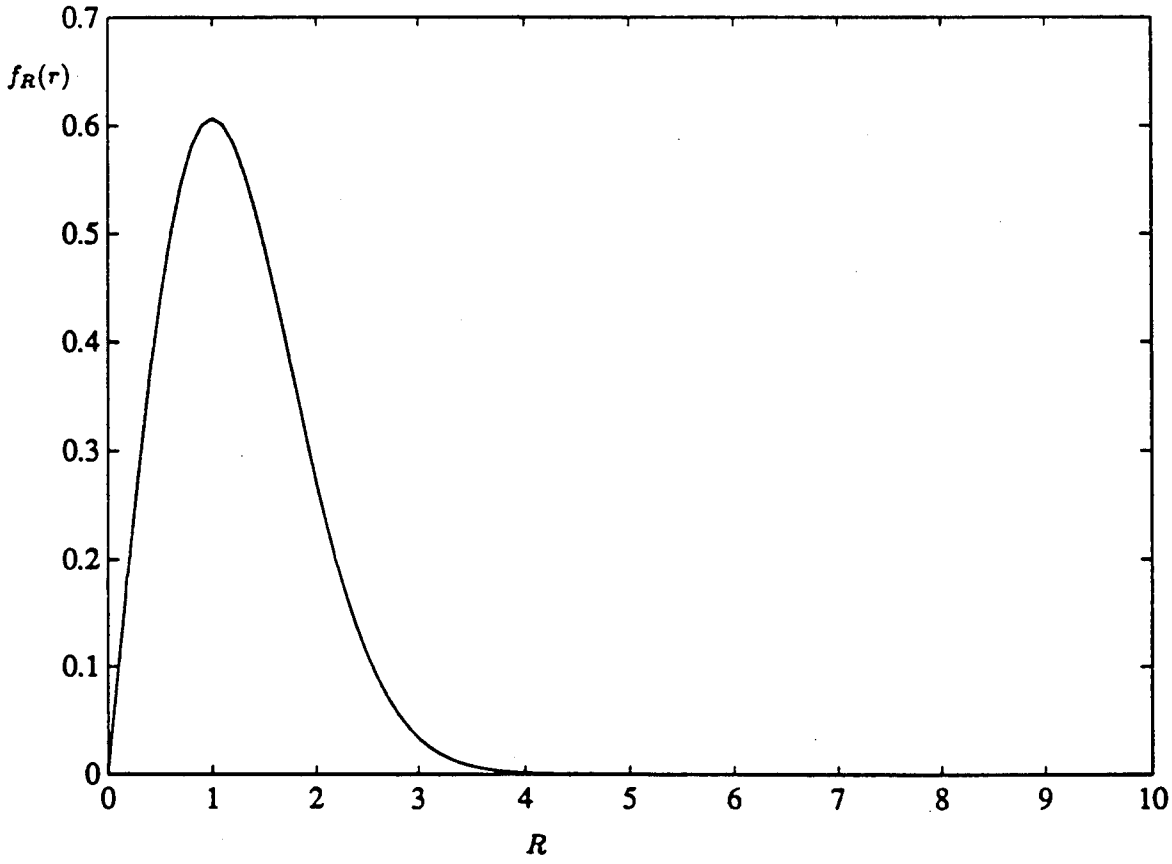

Figure 3.18: Generalized Rayleigh distributed Envelope PDF, $\alpha = 2$, $\beta = 1.414$

3.4.2.4 Rician Envelope PDF

There are two possible ways in which the Rician envelope PDF occurs. One possibility arises through a complex zero mean random process with correlated quadrature components that are Gaussian. The other is through a non-zero mean complex Gaussian process. The former case is considered here, since the SIRV PDF can be obtained by differentiation of $h_2(q)$. For this case, the envelope PDF is given by

$$f_R(r) = \frac{r}{\sqrt{1-\rho^2}} exp[-\frac{r^2}{2(1-\rho^2)}] I_0[\frac{\rho r^2}{2(1-\rho^2)}] \qquad (3.73)$$
$$(0 \leq r \leq \infty)$$
$$(0 < \rho \leq 1)$$

where $I_0(x)$ is the modified Bessel's function of the first kind of order zero. Plots of the Rician envelope PDF for several values of ρ are shown in Figures 3.19-3.21. Let

$$A = \frac{\sigma^2}{2(1-\rho^2)}. \qquad (3.74)$$

Using eq (3.14) we have

$$h_2(q) = \frac{\sigma^2}{\sqrt{1-\rho^2}} exp(-Aq) I_0(\rho Aq). \qquad (3.75)$$

From eq (2.30)

$$h_{2N}(q) = (-2)^{N-1} \frac{d^{N-1} h_2(q)}{dq^{N-1}}. \qquad (3.76)$$

We then use eq (3.57) and the identities [35]

$$I_n(x) = \frac{1}{2\pi} \int_0^{2\pi} cos(n\theta) exp[x cos(\theta)] d\theta$$
$$cos^k(\theta) = \frac{1}{2^k} \sum_{m=0}^{k} \binom{k}{m} cos[(k-2m)\theta] \qquad (3.77)$$

to obtain

$$h_{2N}(q) = \frac{\sigma^{2N}}{(1-\rho^2)^{N-\frac{1}{2}}} \sum_{k=0}^{N-1} \binom{N-1}{k} (-1)^k (\frac{\rho}{2})^k \xi_k exp(-Aq) \qquad (3.78)$$

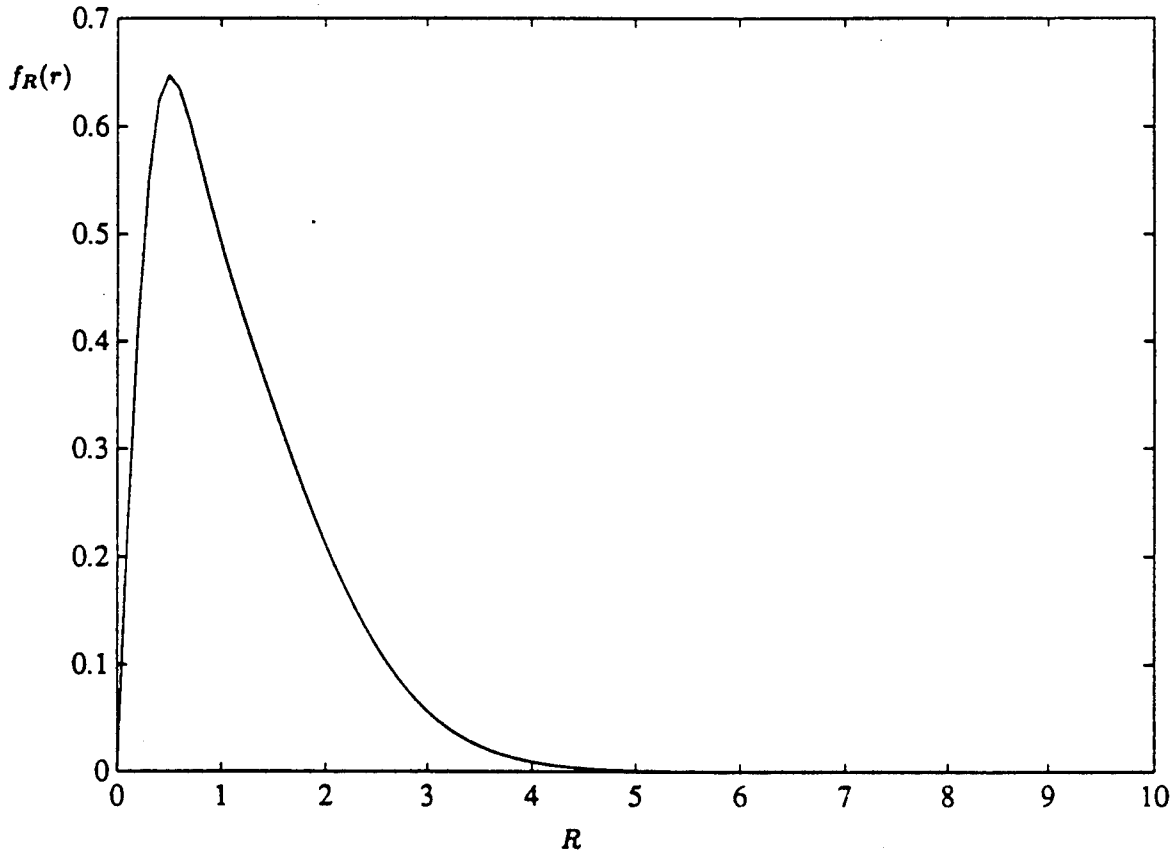

Figure 3.19: Rician Envelope PDF, $\rho = 0.25$

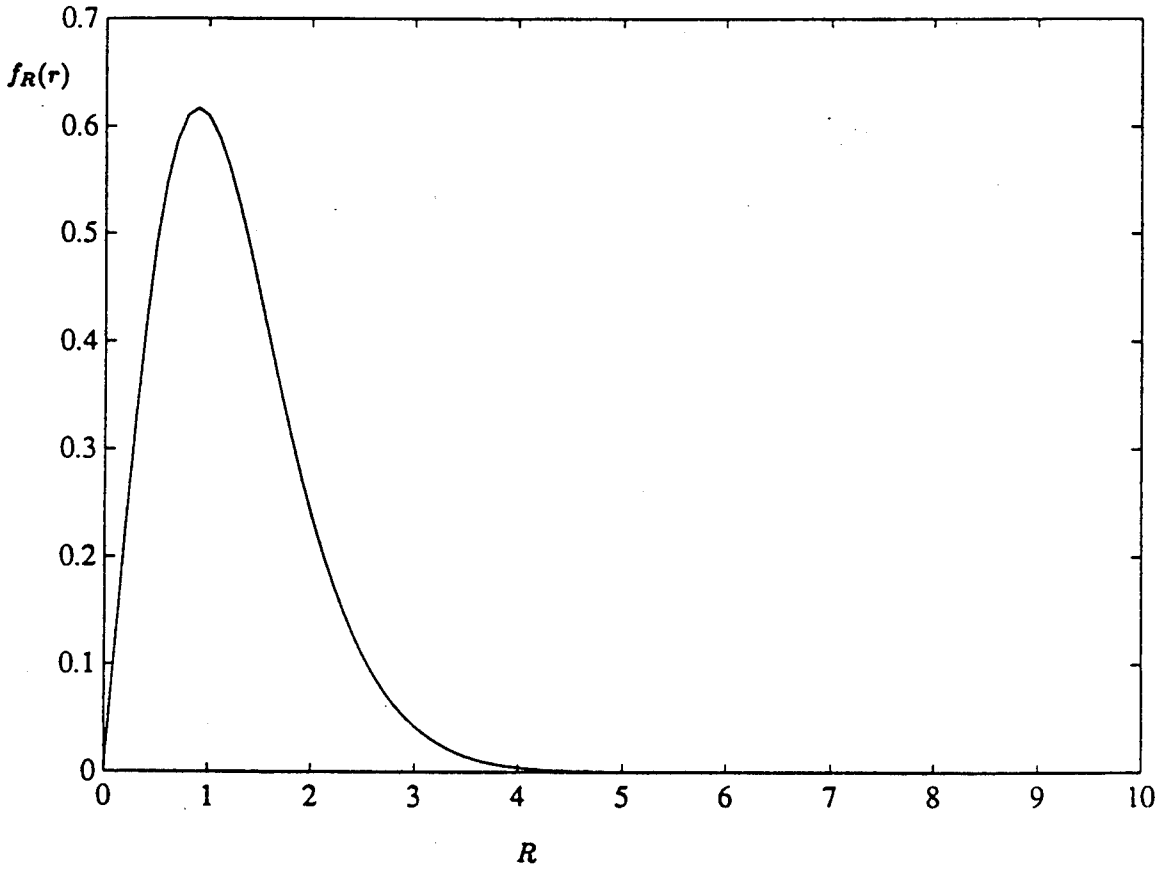

Figure 3.20: Rician Envelope PDF, $\rho = 0.5$

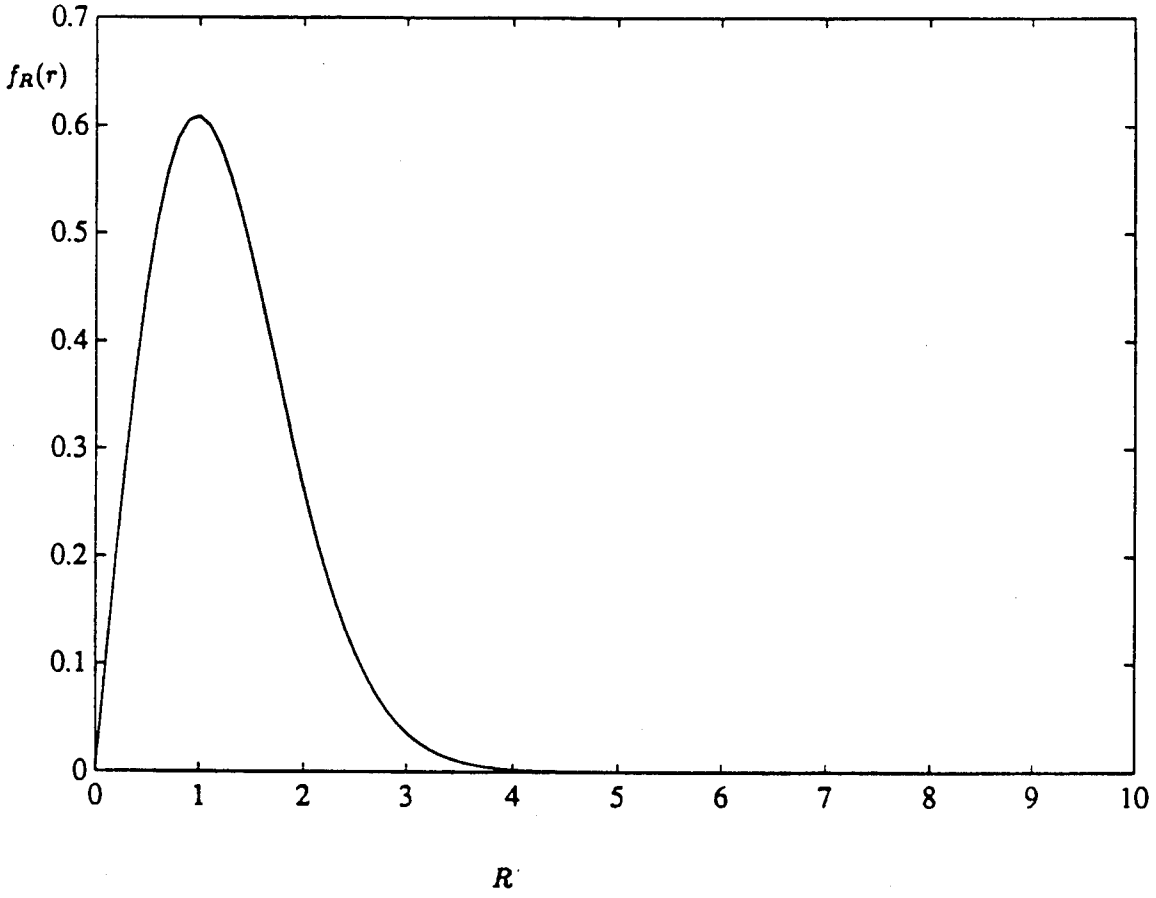

Figure 3.21: Rician Envelope PDF, $\rho = 0.9$

where

$$\xi_k = \sum_{m=0}^{k} \begin{pmatrix} k \\ m \end{pmatrix} I_{k-2m}(\rho A q). \tag{3.79}$$

For $\rho = 0$, note that the Rician envelope PDF corresponds to the Rayleigh envelope PDF.

3.4.2.5 Generalized Gamma Envelope PDF

In a recent effort [37] the Generalized Gamma envelope PDF has been proposed as a candidate for univariate non-Gaussian PDFs for modeling radar clutter. The Generalized Gamma envelope PDF is given by

$$\begin{gathered} f_R(r) = \frac{ac}{\Gamma(\alpha)}(ar)^{c\alpha-1}exp(-ar^c) \\ 0 \leq r \leq \infty, \;\; a, \; c, \; \alpha > 0 \end{gathered} \tag{3.80}$$

where a is the scale parameter and α and c are shape parameters of the PDF. Note that the Generalized Gamma envelope PDF reduces to:

1. the Weibull envelope PDF when $\alpha = 1$,
2. the Gamma envelope PDF when $c = 1$,
3. the Exponential envelope PDF when $c = \alpha = 1$,
4. the Chi envelope PDF when $c = 2$ and
5. the Rayleigh envelope PDF when $c = 2$ and $\alpha = 1$.

We show that this PDF is admissible as an SIRV. Using eq (3.14), we can write

$$h_2(q) = Aq^{\frac{c\alpha}{2}-1}exp(-Bq^{\frac{c}{2}}) \tag{3.81}$$

where $A = \frac{(a\sigma)^{c\alpha}c}{\Gamma(\alpha)}$ and $B = a\sigma^c$. Using eq(2.30), we have

$$\begin{gathered} h_{2N}(q) = (-2)^{N-1}\frac{d^{N-1}h_2(q)}{dq^{N-1}} \\ = (-2)^{N-1}A\frac{d^{N-1}}{dq^{N-1}}[q^{\frac{c\alpha}{2}-1}exp(-Bq^{\frac{c}{2}})]. \end{gathered} \tag{3.82}$$

Using eq (3.57) and eq (3.58), we can rewrite eq (3.82) as

$$h_{2N}(q) = (-2)^{N-1} A \sum_{k=0}^{N-1} \begin{pmatrix} N-1 \\ k \end{pmatrix} \frac{d^k}{dq^k}[exp(-Bq^{\frac{c}{2}})] \frac{\Gamma(\frac{c\alpha}{2})}{\Gamma(\frac{c\alpha}{2} - N + k + 1)} q^{\frac{c\alpha}{2} - N + k}. \tag{3.83}$$

The k^{th} derivative of the exponential term is readily obtained by using eqs (3.64-3.67). Hence, we have

$$h_{2N}(q) = \sum_{k=0}^{N-1} F_k q^{\frac{c\alpha}{2} - N} exp(-Bq^{\frac{c}{2}}) \tag{3.84}$$

where

$$F_k = (-2)^{N-1} A \begin{pmatrix} N-1 \\ k \end{pmatrix} \frac{\Gamma(\frac{c\alpha}{2})}{\Gamma(\frac{c\alpha}{2} - N + k + 1)} \sum_{m=1}^{k} \sum_{l=1}^{m} (-1)^{m+l-1} \frac{B^m}{m!} \frac{\Gamma(\frac{lc}{2} + 1)}{\Gamma(\frac{lc}{2} - k + 1)} w^{\frac{mc}{2}}. \tag{3.85}$$

The Generalized Gamma envelope PDF is admissible for characterization as an SIRV for values of $c\alpha$ less than or equal to 2. This is due to the fact that $h_2(q)$ and its derivatives fail to satisfy the monotonicity condition for other values of $c\alpha$. Interestingly enough, it is only these values of $c\alpha$ that give rise to extended tails for the PDF. Hence, the monotonicity conditions do not impose a serious restriction.

3.4.3 Examples Using the Marginal Characteristic Function

Successful use of the marginal characteristicfunction approach requires the knowledge of various Hankel transforms. For each example, the particular transform used is cited by equation and page number as it appears in [36]. To illustrate the procedure followed, a detailed derivation is presented in the first example. However, in the remaining examples, we simply list the univariate characteristic function of the quadrature components, the corresponding marginal PDF and the resulting $h_{2N}(q)$. Finally, $h_{2N}(p)$ is obtained by replacing q with p in the expressions for $h_{2N}(q)$.

3.4.3.1 Gaussian Distribution

First, we consider the characteristic function given by

$$\Psi(\omega) = exp(-\frac{\omega^2}{2}). \tag{3.86}$$

The corresponding marginal PDF of the quadrature components is

$$f_{Y_k}(y_k) = \frac{1}{\sqrt{(2\pi)}} exp(-\frac{y_k^2}{2}) \quad (-\infty \leq y_k \leq \infty). \tag{3.87}$$

Equation (3.87) is the PDF of a zero mean unit variance Gaussian random variable. Substitution of eq (3.86) in eq (3.30) yields

$$h_{2N}(q) = (\sqrt{q})^{1-N} \int_0^\infty \omega^N exp(-\frac{\omega^2}{2}) J_{N-1}(\omega\sqrt{q}) d\omega. \tag{3.88}$$

From [36], eq (10), p29, we have the Hankel transform

$$\int_0^\infty x^{v+\frac{1}{2}} exp(-ax^2) J_v(xy)\sqrt{xy}dx = \frac{y^{v+\frac{1}{2}}}{(2a)^{v+1}} exp(-\frac{y^2}{4a}). \tag{3.89}$$

By making the association that $a = 0.5$, $\nu = N-1$, $x = \omega$ and $y = \sqrt{q}$, the above result becomes

$$\int_0^\infty \omega^N exp(-\frac{\omega^2}{2}) J_{N-1}(\omega\sqrt{q})\sqrt{q}d\omega = \sqrt{q}^{N-1+\frac{1}{2}} exp(-\frac{q}{2}). \tag{3.90}$$

It follows that

$$h_{2N}(q) = exp(-\frac{q}{2}). \tag{3.91}$$

From eq (3.8), it is seen that the resulting SIRV PDF is the familiar multivariate Gaussian PDF, given by

$$f_{\mathbf{Y}}(y) = (2\pi)^{-N} |\Sigma|^{-\frac{1}{2}} exp(-\frac{p}{2}). \tag{3.92}$$

3.4.3.2 K-Distribution

The marginal characteristic function given by

$$\Psi(\omega) = (1 + \frac{\omega^2}{b^2})^{-\alpha} \tag{3.93}$$

corresponds to the K-distributed envelope whose PDF is

$$f_R(r) = \frac{2b}{\Gamma(\alpha)} (\frac{br}{2})^\alpha K_{\alpha-1}(br) u(r) \tag{3.94}$$

where α is the shape parameter of the distribution, b denotes its scale parameter, $K_N(t)$ is the N^{th} order modified Bessel function of the second kind and $u(r)$ is the unit step function. The pertinent Hankel transform for this example is found as [36] eq (20), p24:

$$\int_0^\infty x^{v+\frac{1}{2}}(x^2+a^2)^{-u-1}J_v(xy)\sqrt{xy}dx = \frac{a^{v-u}y^{u+\frac{1}{2}}K_{v-u}(ay)}{2^u\Gamma(u+1)} \tag{3.95}$$

The resulting $h_{2N}(q)$ is

$$h_{2N}(q) = \frac{b^{2N}}{\Gamma(\alpha)}\frac{(b\sqrt{q})^{\alpha-N}}{2^{\alpha-1}}K_{N-\alpha}(b\sqrt{q}). \tag{3.96}$$

As a special case, when α is equal to unity, eq (3.93) is the characteristic function of the Laplace distribution for the quadrature components whose PDF is given by

$$f_{Y_k}(y_k) = \frac{b}{2}exp(-b|y_k|) \ \ (-\infty \leq y_k \leq \infty) \tag{3.97}$$

where $|y_k|$ denotes the absolute value of y_k and b denotes the scale parameter. The corresponding $h_{2N}(q)$ is given by

$$h_{2N}(q) = b^{2N}(b\sqrt{q})^{1-N}K_{N-1}(b\sqrt{q}). \tag{3.98}$$

Another interesting case of the K-distribution arises when $\alpha = 0.5$. This corresponds to the exponential distribution for the marginal envelope PDF. Therefore, the K-distributed envelope PDF with $\alpha = 0.5$ is identical to the Weibull distributed envelope with $b = 1$. Although the characteristic PDF of the Weibull SIRV is unknown in general, the characteristic PDF of the Weibull SIRV for $b = 1$ is obtained when $\alpha = 0.5$ in eq (3.43). Finally, we point out that the K-distributed envelope reduces to the Rayleigh envelope PDF when α tends to ∞.

3.4.3.3 Student-t Distribution

The characteristic function for the Student-t distribution with scale parameter b and shape parameter ν is given by

$$\Psi(\omega) = \frac{K_\nu(b\omega)(b\omega)^\nu}{2^{\nu-1}\Gamma(\nu)}. \tag{3.99}$$

Note the functional similarity with the envelope PDF given by eq (3.94). The Student-t distribution is referred to as the generalized Cauchy distribution in [38] because the marginal PDF of the quadrature components is given by

$$f_{Y_k}(y_k) = \frac{\Gamma(\nu+\frac{1}{2})}{b\sqrt{\pi}\Gamma(\nu)}(1+\frac{y_k^2}{b^2})^{-\nu-\frac{1}{2}} \ (-\infty \leq x_k \leq \infty),\ \nu > 0 \tag{3.100}$$

where $\Gamma(\nu)$ is the Eulero-Gamma function. The relevant Hankel transform, [36] eq (3), p63 is

$$\int_0^\infty x^{u+v+\frac{1}{2}} K_u(ax) J_v(xy)\sqrt{xy}dx = \frac{2^{v+u}a^u\Gamma(u+v+1)y^{v+\frac{1}{2}}}{(y^2+a^2)^{u+v+1}}. \tag{3.101}$$

Using eq (3.30), $h_{2N}(q)$ is expressed as

$$h_{2N}(q) = \frac{2^N b^{2\nu}\Gamma(\nu+N)}{\Gamma(\nu)(b^2+q)^{N+\nu}}. \tag{3.102}$$

The Cauchy PDF for the quadrature components arises when ν is set equal to $\frac{1}{2}$ in eq (3.100) and is given by

$$f_{Y_k}(y_k) = \frac{b}{\pi(b^2+y_k^2)} \ (-\infty \leq x_k \leq \infty) \tag{3.103}$$

where b is the scale parameter. The corresponding $h_{2N}(q)$ is

$$h_{2N}(q) = \frac{2^N b\Gamma(\frac{1}{2}+N)}{\sqrt{\pi}(b^2+q)^{N+\frac{1}{2}}}. \tag{3.104}$$

Note that the Cauchy PDF does not have finite variance. However, this PDF is useful in modeling impulsive noise [39]. Finally, we point out that when $b = \sqrt{2\nu}$ and ν tends to ∞ in eq (3.100), the Student-t distribution reduces to the Gaussian distribution.

3.4.3.4 Rician Envelope PDF 2

We consider the Rician envelope PDF, arising from a non-zero mean complex Gaussian process, given by

$$f_R(r) = \frac{r}{\alpha^2} exp[-\frac{(r^2+a^2)}{2\alpha^2}] I_0(\frac{ar}{\alpha^2}). \tag{3.105}$$

Plots of the Rician envelope PDF are shown in Figures 3.20-3.22 for several values of a and $\alpha = 1$. Note that this PDF approaches the Rayleigh PDF as a tends to zero. For convenience, we assume that $\sigma^2 = \frac{1}{2}E(R^2) = 1$. Using eq (3.14), we have

$$h_2(r^2) = Aexp(-\frac{r^2}{2\alpha^2})I_0(\frac{ar}{\alpha^2}) \tag{3.106}$$

where $A = \frac{exp(-\frac{a^2}{2\alpha^2})}{\alpha^2}$. Noting that [35]

$$\int_0^\infty xexp(-\alpha x^2)I_\nu(\beta x)J_\nu(\gamma x)dx = \frac{1}{2\alpha}exp(\frac{\beta^2-\gamma^2}{4\alpha})J_\nu(\frac{\beta\gamma}{2\alpha}) \tag{3.107}$$
$$Re\{\alpha\} > 0, \quad Re\{\nu\} > -1,$$

eq (3.21) results in the characteristic function

$$\Psi(\omega) = exp(-\frac{\omega^2\alpha^2}{2})J_0(\frac{\omega a}{\alpha^2}). \tag{3.108}$$

Recognizing that [35]

$$\int_0^\infty x^{\lambda-1}exp(-\alpha x^2)J_\mu(\beta x)J_\nu(\gamma x)dx =$$
$$\frac{\beta^\mu\gamma^\nu\alpha^{-\frac{(\mu+\nu+\lambda+2)}{2}}}{2^{\mu+\nu+1}\Gamma(\nu+1)}\sum_{m=0}^\infty \frac{\Gamma(m+\frac{\nu}{2}+\frac{mu}{2}+\frac{\lambda}{2}+1)}{m!\Gamma(m+\mu+1)}(-\frac{\beta^2}{4\alpha})^m F(-m,\ -\mu-m;\ \nu+1;\ \frac{\gamma^2}{\beta^2}) \tag{3.109}$$
$$Re\{\alpha\} > 0,\ Re\{\mu+\nu+\lambda\} > -2,\ \beta > 0,\ \gamma > 0$$

where $F(.,\ .;\ .;\ .)$ is the four parameter hypergeometric function, it follows from eq (3.30) that

$$h_{2N}(q) = \frac{\alpha^{2N+2}}{2^{2N+1}\Gamma(N)}\sum_{m=0}^\infty \frac{\Gamma(m+N+1)}{m!\Gamma(m+1)}(\frac{-a^2}{2\alpha^6})^m F(-m,\ -m;\ N;\ \frac{q\alpha^4}{a^2}) \tag{3.110}$$

Since $h_{2N}(q)$ for this example involves an infinite series of hypergeometric functions, its form is mathematically intractable. Therefore, the corresponding multivariate SIRV PDF does not lend itself for use in practical applications.

We point out here that the log-normal envelope PDF and the Johnson (unbounded) distribution are not admissible for extension to SIRVs. This is due to the fact that $h_2(q)$ obtained for each of these distributions fails to satisfy the monotonicity conditions stated in Section 3.3. Table 3.1, presents a list of marginal PDFs suitable

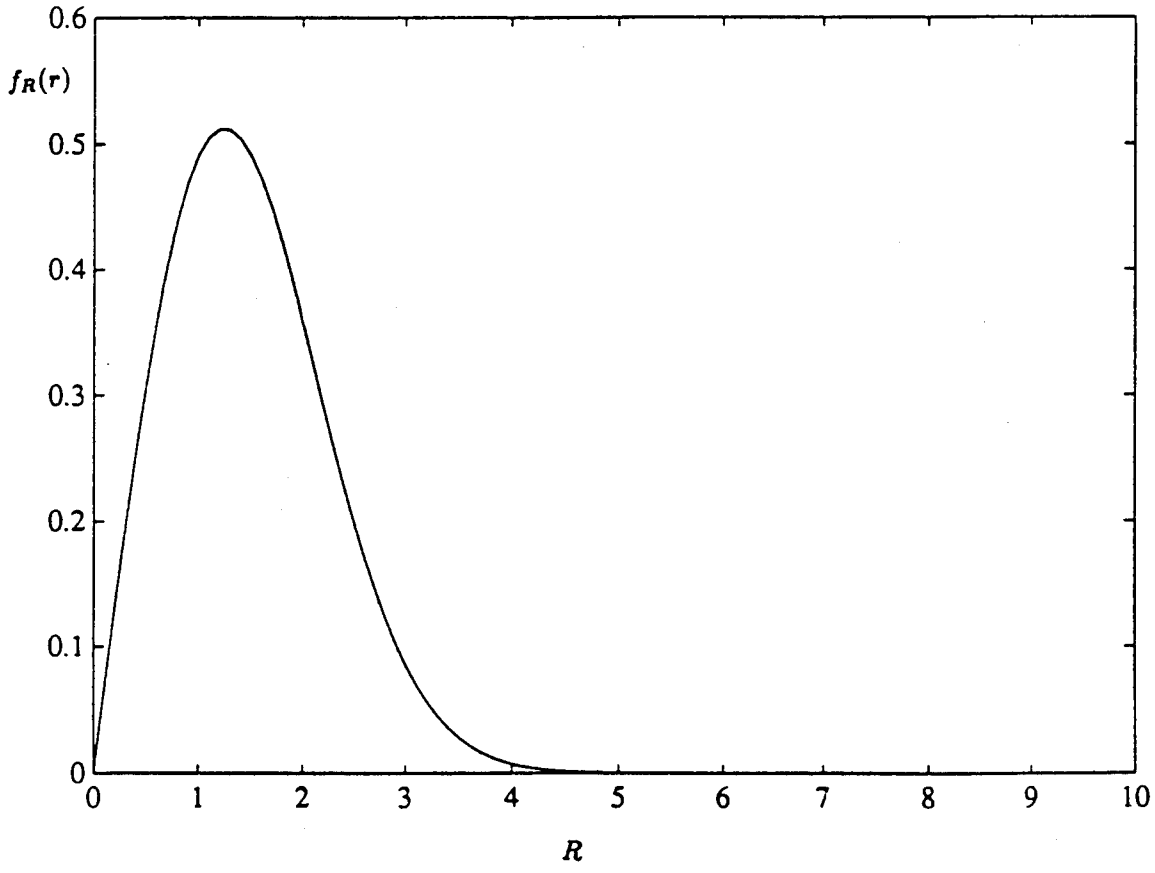

Figure 3.22: Rician Envelope PDF, $a = 0.25$, $\alpha = 1$

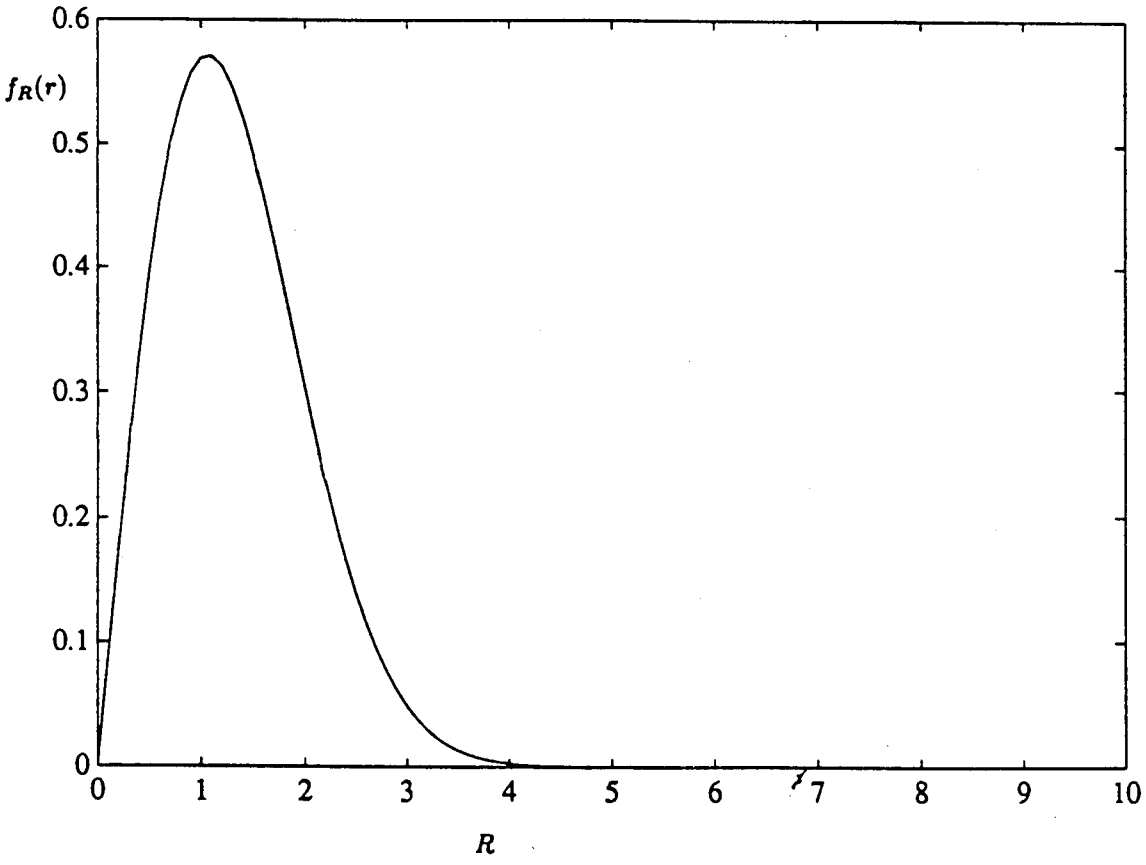

Figure 3.23: Rician Envelope PDF, $a = 0.5$, $\alpha = 1$

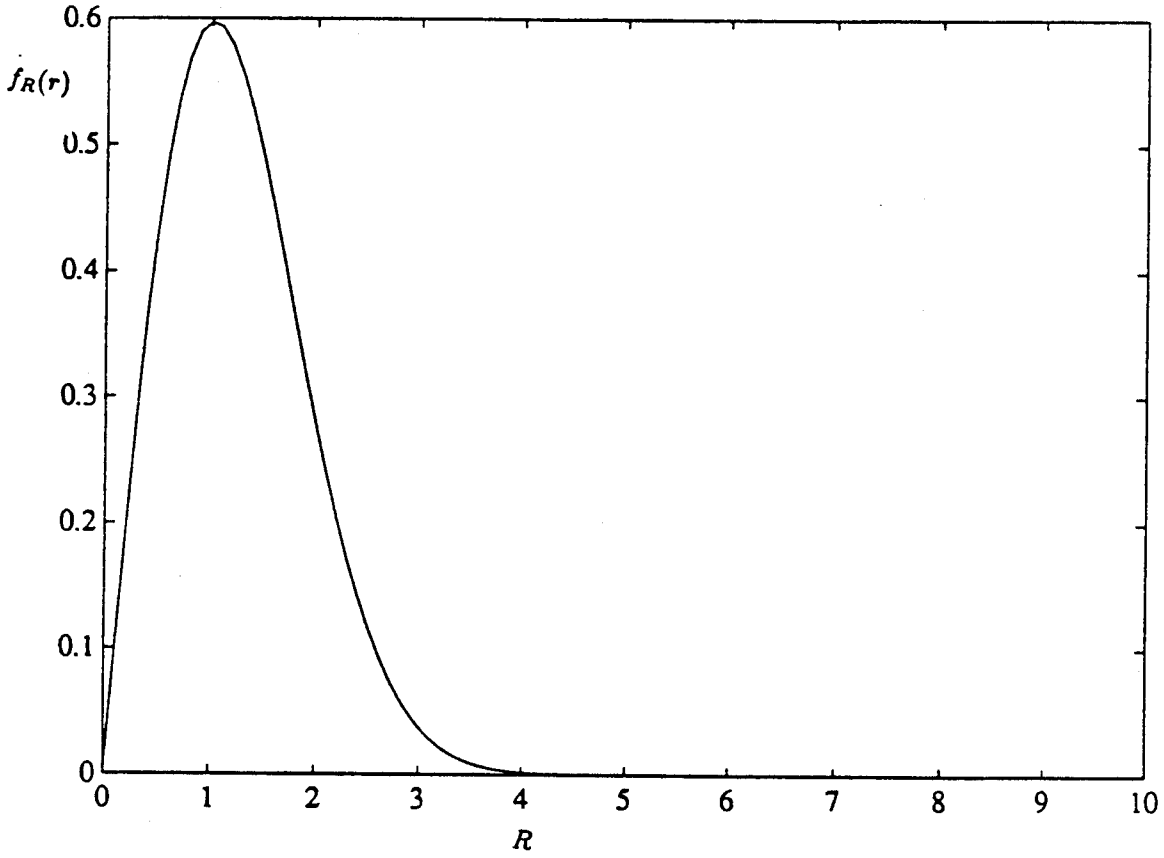

Figure 3.24: Rician Envelope PDF, $a = 0.9$, $\alpha = 1$

Table 3.1: Marginal PDFs Suitable for extension to SIRVs

Marginal PDF	$f_X(x)$
Chi	$\frac{2b}{\Gamma(\nu)}(bx)^{2\nu-1}exp(-b^2x^2)$
Weibull	$abx^{b-1}exp(-ax^b)$
Generalized Rayleigh	$\frac{\alpha x}{\beta^2\Gamma(\frac{2}{\alpha})}exp[-(\frac{x}{\beta})^\alpha]$
Generalized Gamma	$f_R(r) = \frac{ac}{\Gamma(\alpha)}(ar)^{c\alpha-1}exp(-ar^c)$
Rician	$\frac{x}{\sqrt{1-\rho^2}}exp[-\frac{x^2}{2(1-\rho^2)}]I_0[\frac{\rho x^2}{2(1-\rho^2)}]$
Gaussian	$\sqrt{2\pi}^{-1}exp(-\frac{x^2}{2})$
Laplace	$\frac{b}{2}exp(-b\lvert x_k\rvert)$
Cauchy	$\frac{b}{\pi(b^2+x_k^2)}$
K-distribution	$\frac{2b}{\Gamma(\alpha)}(\frac{bx}{2})^\alpha K_{\alpha-1}(bx)u(x)$
Student-t	$\frac{\Gamma(\nu+\frac{1}{2})}{b\sqrt{\pi}\Gamma(\nu)}(1+\frac{x_k^2}{b^2})^{-\nu-\frac{1}{2}}$

for extension to SIRVs. Table 3.2 tabulates $h_{2N}(p)$ for those marginal PDFs treated as envelope PDFs while Table 3.3 gives those $h_{2N}(p)$ obtained from the associated marginal characteristic function.

Plots of eq (3.8) with $N = 1$ for the various SIRV PDFs are shown in Figures 3.25-3.33. In all the plots, the covariance matrix used is given by

$$\mathbf{\Sigma} = \begin{bmatrix} 1 & 0.5 \\ 0.5 & 1 \end{bmatrix} \tag{3.111}$$

Observe that each PDF is unimodal. However, the width and height of the peak along with the behavior of the extreme values (i.e. the tails) differ significantly.

3.5 Significance of the Quadratic Form of the SIRV PDF

Thus far, our discussion has focussed on techniques that can be used to obtain the PDF of an SIRV starting from either the first order PDF or the first order characteristic function. Given random data, we are also interested in the problem of approximating the distribution of the underlying data. The problem of multivariate distribution identification is of interest in radar signal detection. Since the background clutter is not known a priori, there is a need to identify the underlying clutter PDF based on measurements obtained from a given environment. Since the radar processes N pulses at a time, knowledge of the joint PDF of the N samples is necessary in order to obtain the optimal radar signal processor for the given clutter background. We present an important theorem here which enables us to address the

Table 3.2: SIRVs obtained from the marginal envelope PDF

Marginal PDF	$h_{2N}(p)$
Chi	$(-2)^{N-1} A \sum_{k=1}^{N} G_k p^{\nu-k} exp(-Bp)$
	$G_k = \begin{pmatrix} N-1 \\ k-1 \end{pmatrix} (-1)^{N-k} B^{N-k} \frac{\Gamma(\nu)}{\Gamma(\nu-k+1)}$
	$A = \frac{2}{\Gamma(\nu)} (b\sigma)^{2\nu}$
	$B = b^2\sigma^2$
	$\nu \leq 1$
Weibull	$\sum_{k=1}^{N} C_k p^{\frac{kb}{2}-N} exp(-Ap^{\frac{b}{2}})$
	$A = a\sigma^b$
	$C_k = \sum_{m=1}^{k} (-1)^{m+N} 2^N \frac{A^k}{k!} \begin{pmatrix} k \\ m \end{pmatrix} \frac{\Gamma(1+\frac{mb}{2})}{\Gamma(1+\frac{mb}{2}-N)}$
	$b \leq 2$
Gen. Rayleigh	$\sum_{k=1}^{N-1} D_k p^{\frac{k\alpha}{2}-N+1} exp(-Bp^{\frac{\alpha}{2}})$
	$A = \frac{\sigma^2 \alpha}{\beta^2 \Gamma(\frac{2}{\alpha})}$
	$B = \beta^{-\alpha} \sigma^{\alpha}$
	$D_k = \sum_{m=1}^{k} (-1)^{m+N-1} 2^{N-1} \frac{B^k}{k!} \begin{pmatrix} k \\ m \end{pmatrix} \frac{\Gamma(1+\frac{m\alpha}{2})}{\Gamma(2+\frac{m\alpha}{2}-N)}$
	$\alpha \leq 2$
Generalized Gamma	$h_{2N}(p) = \sum_{k=0}^{N-1} F_k p^{\frac{c\alpha}{2}-N} exp(-Bp^{\frac{c}{2}})$
	$F_k = (-2)^{N-1} A \begin{pmatrix} N-1 \\ k \end{pmatrix} \frac{\Gamma(\frac{c\alpha}{2})}{\Gamma(\frac{c\alpha}{2}-N+k+1)} \sum_{m=1}^{k} \sum_{l=1}^{m} (-1)^{m+l-1} \frac{B^m}{m!} \frac{\Gamma(\frac{lc}{2}+1)}{\Gamma(\frac{lc}{2}-k+1)} p^{\frac{mc}{2}}$
	$c\alpha \leq 2$
Rician	$\frac{\sigma^{2N}}{(1-\rho^2)^{N-\frac{1}{2}}} \sum_{k=0}^{N-1} \begin{pmatrix} N-1 \\ k \end{pmatrix} (-1)^k (\frac{\rho}{2})^k \xi_k exp(-A)$
	$\xi_k = \sum_{m=0}^{k} \begin{pmatrix} k \\ m \end{pmatrix} I_{k-2m}(\rho A),\ A = \frac{p\sigma^2}{2(1-\rho^2)}$

Table 3.3: SIRVs obtained from the marginal characteristic function

Marginal PDF	$h_{2N}(p)$
Gaussian	$exp(-\frac{p}{2})$
Laplace	$b^{2N} (b\sqrt{p})^{1-N} K_{N-1}(b\sqrt{p})$
Cauchy	$\frac{2^N b \Gamma(\frac{1}{2}+N)}{\sqrt{\pi}(b^2+p)^{N+\frac{1}{2}}}$
K-distribution	$\frac{b^{2N}}{\Gamma(\alpha)} \frac{(b\sqrt{p})^{\alpha-N}}{2^{\alpha-1}} K_{N-\alpha}(b\sqrt{p})$
Student-t	$\frac{2^N b^{2\nu} \Gamma(\nu+N)}{\Gamma(\nu)(b^2+p)^{N+\nu}}$

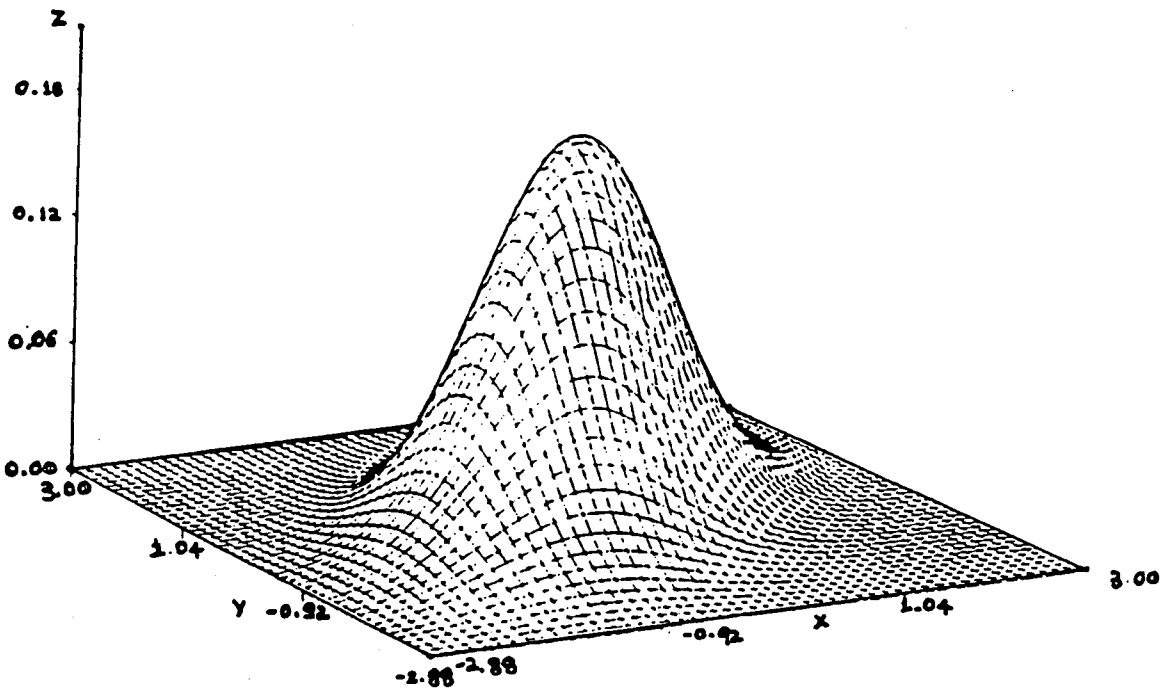

Figure 3.25: Gaussian distribution, zero mean, unit variance

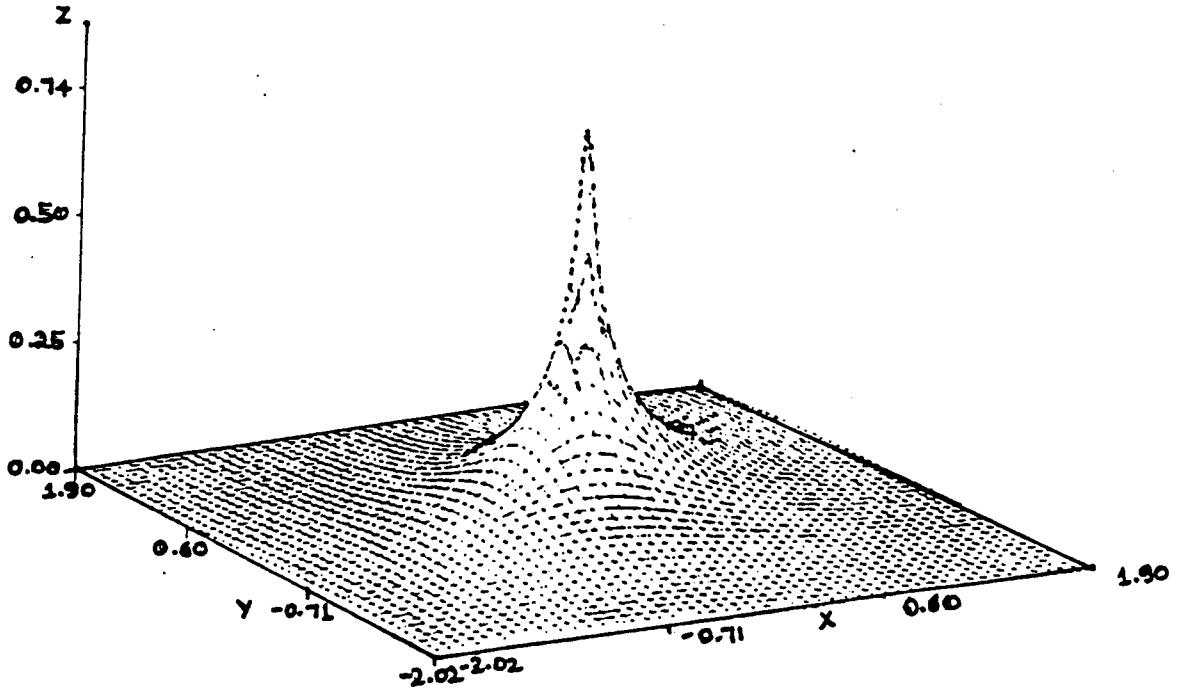

Figure 3.26: Laplace Distribution, $b = 1$

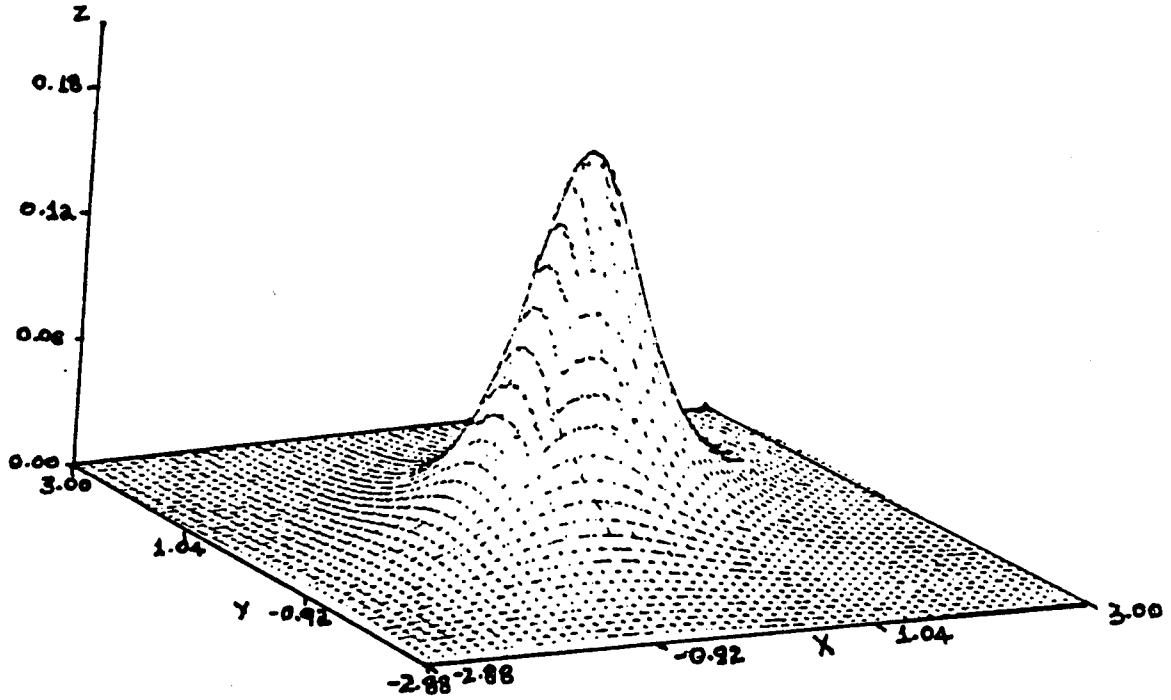

Figure 3.27: Cauchy Distribution, $b = 1$

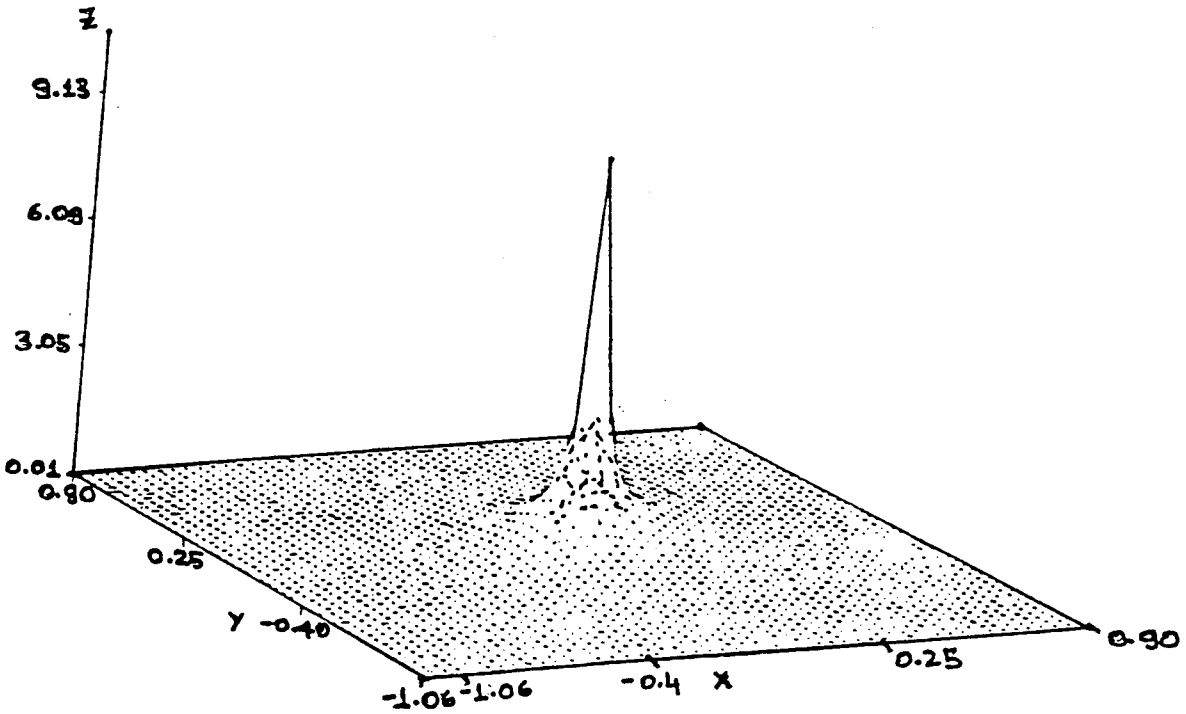

Figure 3.28: K-distribution, $b = 1$, $\alpha = 0.5$

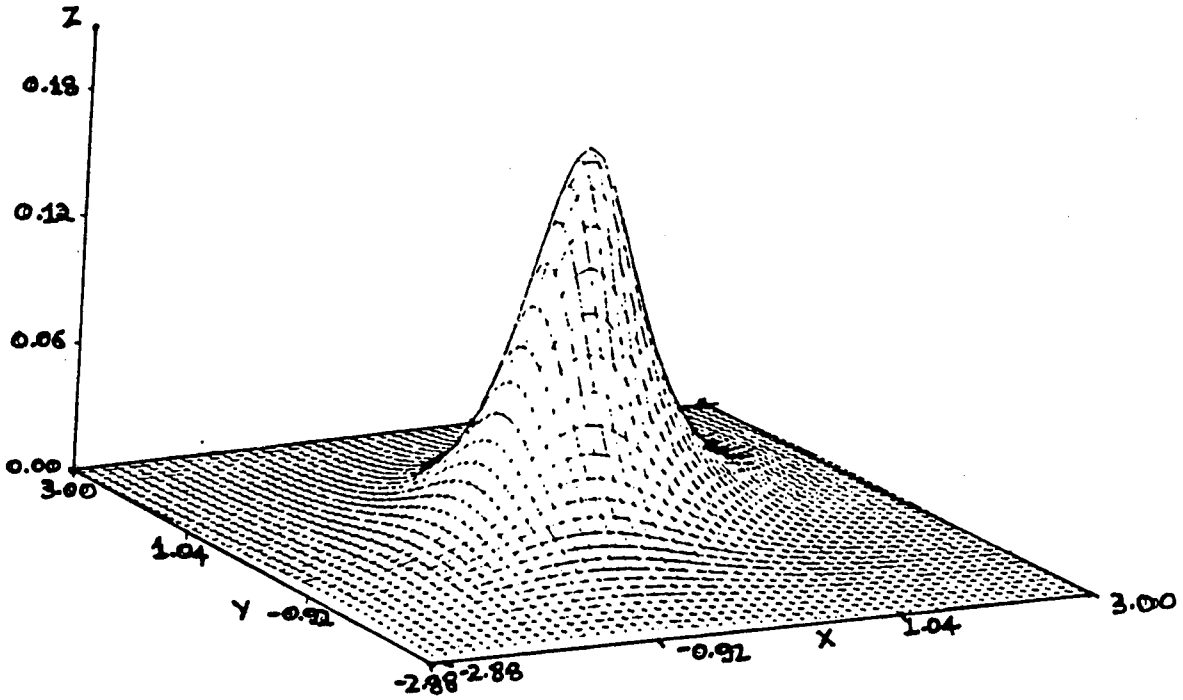

Figure 3.29: Student-t Distribution, $b = 1$, $\nu = 1.5$

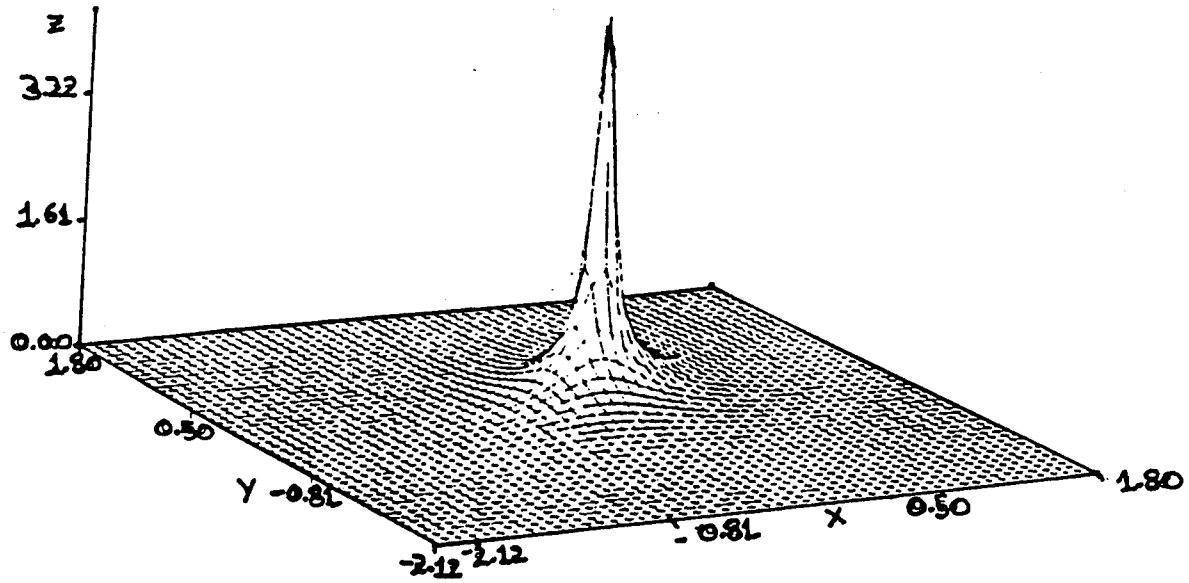

Figure 3.30: Chi-distribution, $b = 1$, $\nu = 1$

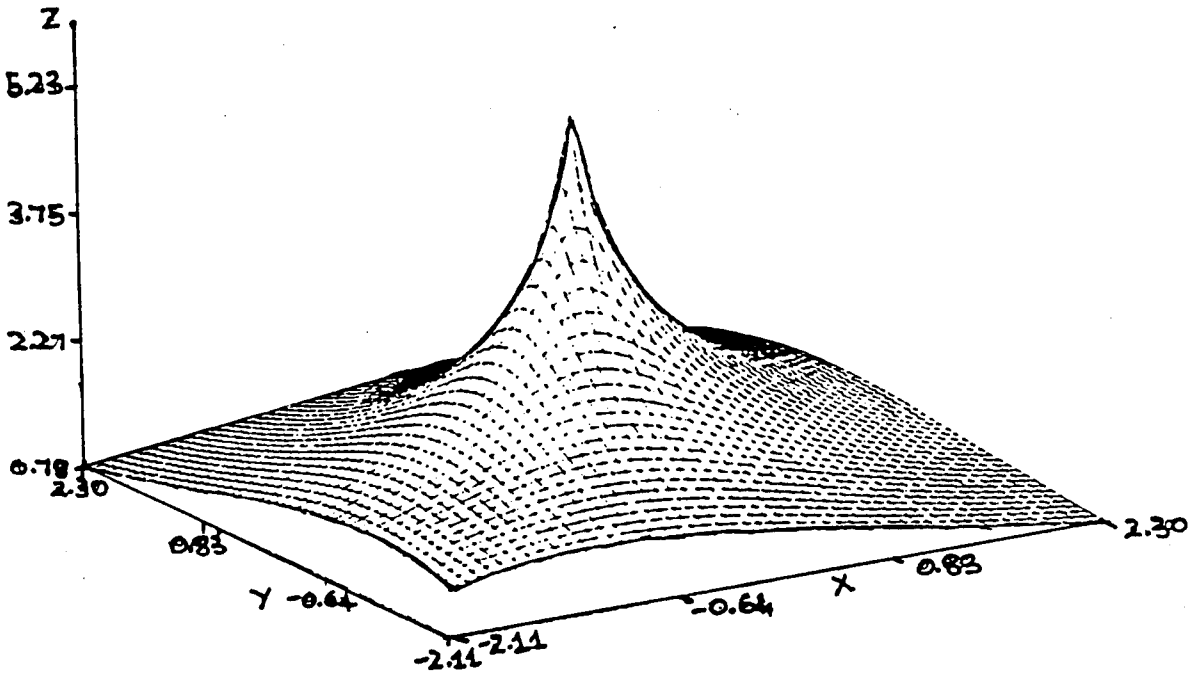

Figure 3.31: Generalized Rayleigh PDF, $\alpha = 0.5$, $\beta = 0.05$

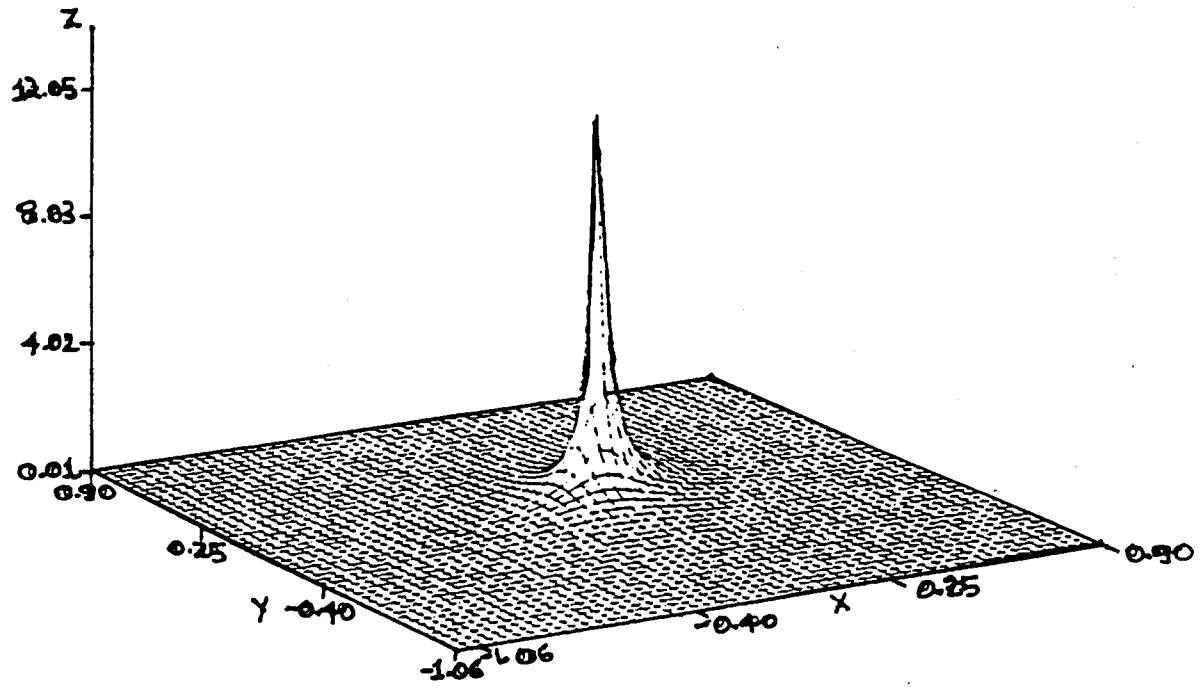

Figure 3.32: Weibull distribution, $a = 1$, $b = 1.0$

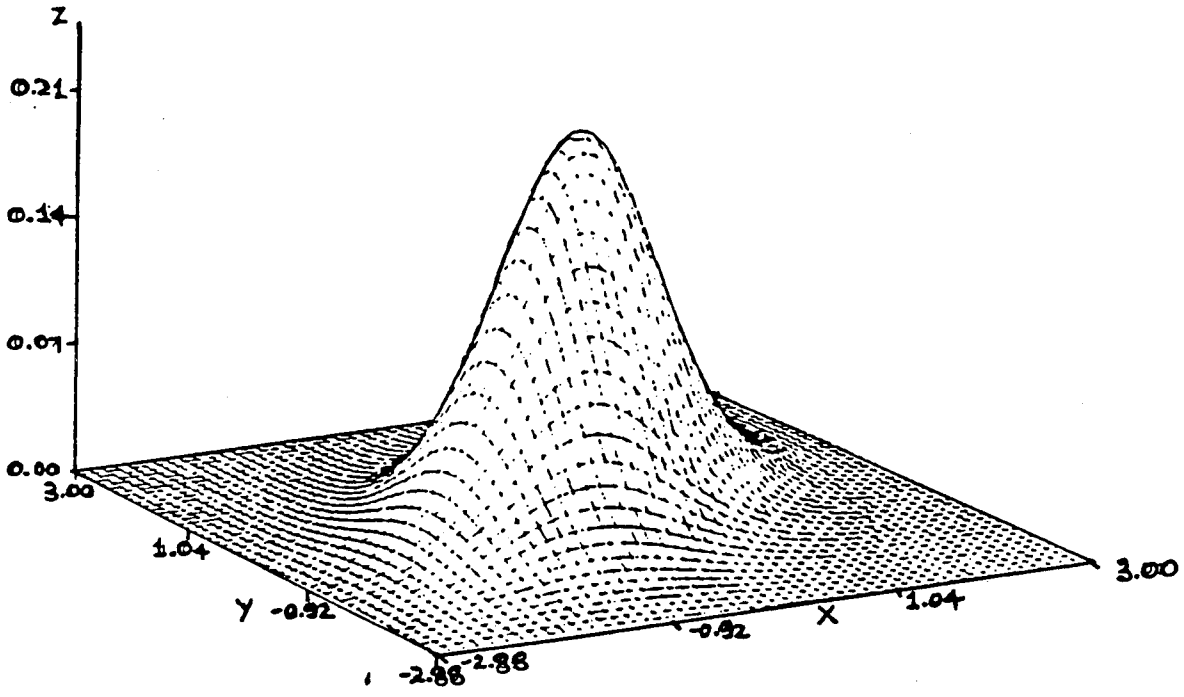

Figure 3.33: Rician PDF, $\rho = 0.5$

distribution identification of an SIRV.

Theorem 4 *The PDF of the quadratic form appearing in eq (2.20) is given by*

$$f_P(p) = \frac{1}{2^{\frac{N}{2}}\Gamma(\frac{N}{2})} p^{\frac{N}{2}-1} h_N(p) \quad (0 \leq p \leq \infty). \tag{3.112}$$

Proof: First, we consider a spherically symmetric random vector (SSRV) $\mathbf{X} = [X_1, X_2, \ldots, X_N]$ Because an SSRV is a special case of the SIRV, the representation theorem can be used to express $\mathbf{X}$ as

$$\mathbf{X} = \mathbf{Z}S \tag{3.113}$$

where $\mathbf{Z}$ is a Gaussian random vector having zero mean and identity covariance matrix and S is a non-negative random variable with PDF $f_S(s)$. Consider the random variable

$$P' = \mathbf{X}^T\mathbf{X}. \tag{3.114}$$

Using eq (3.113) in eq (3.114) gives

$$P' = \mathbf{Z}^T\mathbf{Z}S^2 \tag{3.115}$$

Since $\mathbf{Z}^T\mathbf{Z} = \sum_{i=1}^{N} Z_i^2$ is the sum of the squares of independent identically distributed Gaussian random variables having zero mean and unit variance, the PDF of $V = \mathbf{Z}^T\mathbf{Z}$ is a Chi square distribution with N degrees of freedom. Consequently,

$$f_V(v) = \frac{v^{\frac{N}{2}-1}}{2^{\frac{N}{2}}\Gamma(\frac{N}{2})} exp(-\frac{v}{2}) \quad ; v \geq 0. \tag{3.116}$$

The transformation $P' = VS^2$ then results in

$$f_{P'|S}(p'|s) = \frac{(p')^{\frac{N}{2}-1}}{2^{\frac{N}{2}}\Gamma(\frac{N}{2})} s^{-N} exp(-\frac{p'}{2s^2}). \tag{3.117}$$

From the theorem of total probability, we have

$$f_{P'}(p') = \int_0^\infty \frac{(p')^{\frac{N}{2}-1}}{2^{\frac{N}{2}}\Gamma(\frac{N}{2})} s^{-N} exp(-\frac{p'}{2s^2}) f_S(s) ds. \tag{3.118}$$

Recall that

$$h_N(p') = \int_0^\infty s^{-N} exp(-\frac{p'}{2s^2}) f_S(s) ds. \tag{3.119}$$

Consequently, the PDF of P' is expressed as

$$f_{P'}(p') = \frac{(p')^{\frac{N}{2}-1}}{2^{\frac{N}{2}}\Gamma(\frac{N}{2})} h_N(p'). \tag{3.120}$$

Recall that an SIRV $\mathbf{Y} = [Y_1, Y_2, \ldots, Y_N]^T$ having a mean vector $\mathbf{b}$ and covariance matrix $\mathbf{\Sigma}$ is related to the SSRV $\mathbf{X}$ by the linear transformation

$$\mathbf{Y} = \mathbf{AX} + \mathbf{b} \tag{3.121}$$

where $\mathbf{\Sigma} = \mathbf{AA}^T$. Then, the quadratic form appearing in eq (3.114) can be expressed as

$$P = (\mathbf{Y} - \mathbf{b})^T \mathbf{\Sigma}^{-1} (\mathbf{Y} - \mathbf{b}). \tag{3.122}$$

However, eq (3.122) is also the quadratic form appearing in eq (2.20) which is the PDF of $\mathbf{Y}$. Since $P = P'$, the PDF of the quadratic form P which is associated with $\mathbf{Y}$ is

$$f_P(p) = \frac{(p)^{\frac{N}{2}-1}}{2^{\frac{N}{2}}\Gamma(\frac{N}{2})} h_N(p). \tag{3.123}$$

This establishes the theorem. Thus, an SIRV is uniquely characterized by the quadratic form appearing in its PDF. Knowledge of the quadratic form PDF is sufficient to identify the SIRV PDF. This is an important result since it allows us to reduce the multivariate distribution identification problem to the equivalent problem of univariate distribution identification of the quadratic form. It is emphasized that the PDF of P is invariant to the choice of μ and $\mathbf{\Sigma}$. We point out that the invariance of the PDF of the quadratic form, arises from the fact that an SSRV arises from a uniform distribution over an N dimensional hypersphere of radius R. The radius of the hypersphere remains unchanged regardless of whether we consider an SIRV or an SSRV. Only the azimuthal angles and radial angle change depending on whether the random vector is a SSRV or an SIRV. In context of the radar problem, we are dealing with N complex samples or $2N$ quadrature components. The results presented in this section are applicable when N is replaced by $2N$.

3.6 Conclusion

In this chapter we have pointed out a method to obtain the PDF of correlated non-Gaussian random vectors arising in the problem of radar clutter modeling. The

theory of SIRPs has been used to develop the multivariate PDFs. Various techniques have been presented to obtain SIRV PDFs. Several examples are provided to illustrate these techniques. The admissibility of the Chi envelope PDF, Weibull envelope PDF, Generalized Rayleigh envelope PDF, Rician envelope PDF and Generalized Gamma envelope PDF as SIRVs has been pointed out for the first time. Finally, we have obtained the PDF of the quadratic form of a SIRV and we have shown that this PDF remains unchanged regardless of whether we are dealing with an SSRV or an SIRV. We have also established that the quadratic form contains all the information that is required in order to identify the SIRV PDF. As a consequence of this result, the problem of an SIRV (multivariate) distribution identification has been reduced to the equivalent identification of the univariate distribution of the non-negative quadratic form.

Chapter 4

Computer Generation of Simulated Radar Clutter Characterized as SIRPs

4.1 Introduction

This investigation is motivated by a desire to simulate correlated non-Gaussian radar clutter. Various investigators have reported experimental results where non-Gaussian marginal probability density functions (PDF) have been used to model the clutter. Usually, radars process N samples at a time. Statistical characterization of the clutter requires the specification of the joint PDF of the N samples. In addition, the clutter may be highly correlated. Hence, the joint PDF must take into account the correlation between samples. Statistical characterization of the clutter is necessary if an optimal radar signal processor is to be obtained. For use of the well known likelihood ratio test, it is necessary to have closed form expressions for the joint PDF of the N clutter samples in order to obtain the optimal radar signal processor. In most cases, it is difficult to evaluate the performance of the optimal radar signal processor analytically when the clutter samples are correlated and non-Gaussian. Then computer simulation may be necessary. Therefore, there is a need to develop efficient procedures that facilitate computer simulation of the clutter. A library of multivariate non-Gaussian PDFs has been developed in Chapter 3, using the theory of **Spherically Invariant Random Processes (SIRP)** and **Spherically Invariant Random Vectors (SIRV)**. In view of the large number of parameters that are free

to be specified, the library of multivariate non-Gaussian PDFs can be used to approximate many different radar clutter scenarios. In this chapter we concern ourselves with the development of computer simulation procedures for the library of non-Gaussian PDFs obtained in Chapter 3 so that the performance of any radar signal processor can be evaluated for a variety of different clutter scenarios. Another issue addressed in this chapter is performance assessment of the simulation procedures.

It has been pointed out in Chapter 3 that the quadratic form appearing in the PDF of the SIRV contains all the information necessary to identify the PDF of the underlying SIRV. We make use of this result in order to assess the performance of the simulation procedures. Some interesting simulation techniques have been proposed for SIRVs in [18] and [20]. The technique suggested in [18] makes use of Meijer's G-functions. These functions are generalizations of Hypergeometric functions which do not lend themselves to the development of simple and elegant simulation procedures. The technique suggested in [20] requires transformations from rectangular to spherical co-ordinates and then back again. Secondly, this simulation procedure involves the use of the inverse distribution function approach for a rather complicated distribution function. The approach developed in this chapter is simpler to implement than those proposed in [18] and [20]. In addition, a new approach is proposed for assessing the effectiveness of the simulation procedure.

The problem of computer generation of correlated non-Gaussian radar clutter is equivalent to the problem of generating random variables with a jointly specified marginal PDF and covariance matrix. While the problem of generating random sequences with either a specified PDF or prescribed covariance function has been well treated [34], the joint problem has received limited attention. In general, it has been possible to control either the PDF or the correlation function but not both simultaneously. Previous attempts [5, 12, 8, 10, 11] to address the problem of generating random sequences with jointly specified marginal PDF and covariance function have not been successful because the procedures proposed therein made use of zero memory nonlinear (ZMNL) transformations on a correlated Gaussian sequence to obtain the desired non-Gaussian sequence. Consequently, the covariance matrix of the non-Gaussian sequence was related to that of the Gaussian sequence in a rather complicated manner. Hence, given a certain covariance matrix for the non-Gaussian

sequence, it was not possible to determine the corresponding covariance matrix of the Gaussian sequence. Furthermore, not all nonlinear transformations gave rise to non-negative definite covariance matrices at their outputs [33, 34]. Thus, using ZMNL transformations on a correlated Gaussian sequence does not offer a practical solution to the joint problem. The techniques presented in this chapter successfully overcome the drawbacks of the previous efforts. This is due to the fact that SIRPs belong to the class of exogenous product models for radar clutter, which allows for independent control of the marginal PDF and correlation function.

In Section 4.2, we review some definitions and background information pertaining to the theory of spherically invariant random processes. Section 4.3 presents two canonical simulation proceduresfor generating SIRVs. Performance assessment of the simulation procedures is discussed in Section 4.4. Finally, conclusions are presented in Section 4.5.

4.2 Preliminaries

We begin by restating the definitions for a spherically invariant random vector and a spherically invariant random process. A spherically invariant random vector (SIRV) is a random vector (real or complex) whose PDF is uniquely determined by the specification of a mean vector, a covariance matrix and a characteristic first order PDF. Equivalently, the PDF of an SIRV can also be referred to as an elliptically contoured distribution. A spherically invariant random process (SIRP) is a random process (real or complex) such that every random vector obtained by sampling this process is an SIRV. The work of Yao [15] gave rise to a representation theorem which can be stated as follows (see Theorem 1):

If a random vector is a SIRV, then there exists a non-negative random variable S such that the PDF of the random vector conditioned on S is a multivariate Gaussian PDF.

We consider the product given by $\mathbf{X} = \mathbf{Z}S$, where $\mathbf{X} = [X_1 \dots X_N]^T$ denotes the SIRV, $\mathbf{Z} = [Z_1 \dots Z_N]^T$ is a Gaussian random vector with zero mean and covariance matrix $\mathbf{M}$ and S is a non-negative random variable with PDF $f_S(s)$. Since it is desirable to independently control the correlation properties and the non-Gaussian envelope PDF, $\mathbf{Z}$ and S are assumed to be statistically independent. The PDF of $\mathbf{X}$

conditioned on S is (see eq (2.14))

$$f_{\mathbf{X}|S}(\mathbf{x}|s) = (2\pi)^{-\frac{N}{2}}|\mathbf{M}|^{-\frac{1}{2}}s^{-N}exp(-\frac{p}{2s^2}) \tag{4.1}$$

where p is a non-negative quadratic form given by $p = \mathbf{x}^{\mathbf{T}}\mathbf{M}^{-1}\mathbf{x}$ and $|\mathbf{M}|$ denotes the determinant of the covariance matrix $\mathbf{M}$. The PDF of $\mathbf{X}$ is given by (see eqs (2.15) and (2.16))

$$f_{\mathbf{X}}(\mathbf{x}) = (2\pi)^{-\frac{N}{2}}|\mathbf{M}|^{-\frac{1}{2}}h_N(p) \tag{4.2}$$

where

$$h_N(p) = \int_0^\infty s^{-N}exp(-\frac{p}{2s^2})f_S(s)ds. \tag{4.3}$$

The PDF of the random variable S is called the characteristic PDF of the SIRV. Therefore, it is apparent that the PDF of a SIRV is completely determined by the specification of a mean vector, a covariance matrix and a characteristic first order PDF. In addition, the PDF of the SIRV is a function of a non-negative quadratic form. However, except for the Gaussian case, dependence on the quadratic form is more complicated than the simple exponential. Therefore, an SIRP can be regarded as a generalization of the familiar Gaussian random process. We point out that the covariance matrix of the SIRV is given by $\mathbf{\Sigma} = \mathbf{M}E(S^2)$ where $E(S^2)$ is the mean square value of the random variable S. It is seen that the covariance matrix of the SIRV normalized by the mean square value of S is the covariance matrix of the Gaussian random vector. Note that it is possible to set the covariance matrix of the SIRV equal to that of the Gaussian random vector by requiring that $E(S^2)$ be equal to unity. The desired non-Gaussian PDF can be obtained by chosing $f_S(s)$ appropriately. Thus, it is seen that the SIRV formulation for radar clutter modeling affords independent control over the non-Gaussian PDF of the clutter and its correlation properties. Several techniques are available in Chapter 3 for obtaining $h_N(p)$. Note that the Gaussian random vector is a special case of an SIRV and is obtained when $f_S(s) = \delta(s-1)$ where $\delta(t)$ is the unit impulse function. An interesting interpretation of the representation theorem is that every SIRV is the modulation of a Gaussian random vector by a non-negative random variable.

Many of the attractive properties of Gaussian random vectors also apply to SIRVs. The most relevant property of SIRVs for the purpose of computer simulation is the

closure property under linear transformation [15] stated below (see Theorem 2, Section 2.3):

If $\mathbf{X}$ *is an SIRV with characteristic PDF* $f_S(s)$*, then*

$$\mathbf{Y} = \mathbf{AX} + \mathbf{b} \tag{4.4}$$

is also an SIRV with the same characteristic PDF. It is assumed that $\mathbf{A}$ *is a nonsingular matrix and* $\mathbf{b}$ *is a known vector having the same dimension as* $\mathbf{X}$*.*

Theorem 2 provides us with a powerful technique for simulating SIRVs. A white SIRV is defined as one that has a diagonal covariance matrix. In other words, the components of the white SIRV are uncorrelated but not necessarily independent. We can start with a zero mean white SIRV $\mathbf{X}$ having identity covariance matrix and perform the linear transformation given by eq (4.4) to obtain an SIRV $\mathbf{Y}$ having a non-zero mean and desired covariance matrix $\mathbf{\Sigma}$. The matrix $\mathbf{A}$ and the vector $\mathbf{b}$ are given by

$$\begin{aligned} \mathbf{A} &= \mathbf{E}\mathbf{D}^{\frac{1}{2}} \\ \mathbf{b} &= \mu_{\mathbf{y}} \end{aligned} \tag{4.5}$$

where $\mathbf{E}$ is the matrix of normalized eigen-vectors of the covariance matrix $\mathbf{\Sigma}$, $\mathbf{D}$ is the diagonal matrix of eigen-values of $\mathbf{\Sigma}$ and $\mu_{\mathbf{y}}$ is the desired non-zero mean vector.

In many instances it is not possible to obtain $f_S(s)$ for an SIRV in closed form, even though its existence is guaranteed. In such cases, an alternate approach must be used in order to characterize the SIRV. The following theorem can be used to completely characterize a white SIRV having zero mean and identity covariance matrix (see Theorem 3, Section 2.3):

A random vector $\mathbf{X} = [X_1 \dots X_N]^T$ *is a zero mean white SIRV having identity covariance matrix if and only if there exist random variables* $R \in (0, \infty)$, $\Theta \in (0, 2\pi)$ *and* $\Phi_k \in (0, \pi)$, $(k = 1, \dots N-2)$ *such that when the components of* $\mathbf{X}$ *are expressed*

in the generalized spherical coordinates

$$
\begin{aligned}
X_1 &= R\cos(\Phi_1) \\
X_k &= R\cos(\Phi_k)\prod_{i=1}^{k-1}\sin(\Phi_i) \quad (1 < k \leq N-2) \\
X_{N-1} &= R\cos(\Theta)\prod_{i=1}^{N-2}\sin(\Phi_i) \\
X_N &= R\sin(\Theta)\prod_{i=1}^{N-2}\sin(\Phi_i)
\end{aligned}
\tag{4.6}
$$

then the random variables R, Θ and Φ_k are mutually statistically independent and have PDFs of the form

$$
\begin{aligned}
f_R(r) &= \frac{r^{N-1}}{2^{\frac{N}{2}-1}\Gamma(\frac{N}{2})}h_N(r^2)u(r) \\
f_{\Phi_k}(\phi_k) &= \frac{\Gamma(\frac{N-k+1}{2})}{\sqrt{\pi}\Gamma(\frac{N-k}{2})}sin^{N-1-k}(\phi_k)[u(\phi_k) - u(\phi_k - \pi)] \\
f_\Theta(\theta) &= (2\pi)^{-1}[u(\theta) - u(\theta - 2\pi)]
\end{aligned}
\tag{4.7}
$$

where $\Gamma(\nu)$ is the Eulero Gamma function and $u(t)$ is the unit step function.

As a consequence of Theorem 3, any SIRV with zero mean and identity covariance matrix can be represented in generalized spherical coordinates which are mutually and statistically independent regardless of the SIRV considered. Also, note that the PDFs of Θ and Φ_k, $(k = 1, \ldots N-2)$ are functionally independent of the white SIRV considered. Only the PDF of R changes from one white SIRV to another. Note that $R^2 = \sum_{k=1}^{N} X_k^2 = \mathbf{X^T X}$. Hence R is the norm of the SIRV.

Another important feature of the SIRV is that the quadratic form appearing in its PDF contains all the information necessary to identify the PDF. It follows that knowledge of the PDF of the quadratic form of the SIRV is sufficient to identify the PDF of the corresponding SIRV [21] (see Theorem 4):

The PDF of the quadratic form appearing in eq (4.2) is given by

$$
f_P(p) = \frac{1}{2^{\frac{N}{2}}\Gamma(\frac{N}{2})}p^{\frac{N}{2}-1}h_N(p) \quad (0 \leq p \leq \infty) \tag{4.8}
$$

and remains unchanged regardless of whether or not the SIRV is white.

The theorems reviewed in this section will be made use of in the proposed simulation approach, discussed in Section 4.3, and in assessing the performance of the simulation procedure, discussed in Section 4.4.

In the context of the problem of radar clutter modeling and simulation, the band-pass process $Y(t) = Re[\tilde{Y}(t)exp(j\omega_0 t)]$ can be expressed in terms of the corresponding complex, wide sense stationary random processes $\tilde{Y}(t)$. More precisely, we obtain N complex samples by sampling the complex random process $\tilde{Y}(t) = Y_c(t) + jY_s(t)$, where the subscripts c and s denote the in phase and out of phase quadrature components. This is equivalent to working with a real vector of $2N$ quadrature components which is the approach taken in this chapter. Therefore, the results presented in this section are applied to the problem of radar clutter modeling with N replaced by $2N$. For ease of reference, the library of non-Gaussian SIRV PDFs obtained in Chapter 3 is repeated here. However, $h_{2N}(p)$ for those SIRVs for which the characteristic PDF is known are listed in Table 4.1. The corresponding characteristic PDFs are listed in Table 4.2. Table 4.3 lists $h_{2N}(p)$ for those SIRVs whose characteristic PDF is unknown.

4.3 Two Canonical Simulation Procedures for Generating SIRVs

In this section, we concern ourselves with two simulation procedures for generating the SIRVs listed in Table 4.1 and Table 4.2. The first simulation procedure to be discussed is applicable when the characteristic PDF, $f_S(s)$, is known. For each of the PDFs listed in Table 4.1, the characteristic PDF $f_S(s)$ is tabulated in Table 4.3, where $E(S^2) = 1$. Since the representation theorem results in the covariance matrix of the SIRV being given by $\mathbf{\Sigma} = \mathbf{M}E(S^2)$, the choice of $E(S^2) = 1$ makes $\mathbf{\Sigma}$ identical to $\mathbf{M}$, the covariance matrix of the Gaussian random vector $\mathbf{Z}$. However, as shown in Table 4.4, the PDFs for the distributions in Table 4.1, as commonly expressed, do not have unit mean square value. In order to obtain the random variable S, with unit mean square value, and the corresponding PDF $f_S(s)$, we generate the random variable V having PDF $f_V(v)$ and mean square value $E(V^2) = a^2$, and perform the scaling $S = \frac{V}{a}$ to obtain the desired S. For each marginal PDF listed in Table 4.1, and Table 4.4, the scale parameters b are identical and so are the shape parameters

ν and $u(v)$ denotes the unit step function. The simulation procedure for these SIRV PDFs is fairly simple and is stated below:

(1) Generate a sample vector of a white zero mean Gaussian random vector $\mathbf{Z}$, having identity covariance matrix.

(2) Then generate a sample value of the random variable V from the PDF $f_V(v)$. Denote the mean square value of V by a^2.

(3) Normalize the sample value of the random variable V by a to obtain a sample value of the modulating random variable S. In other words generate $S = \frac{V}{a}$.

(4) Generate the product corresponding to $\mathbf{X} = \mathbf{Z}S$. At this step, we have a sample vector of a white SIRV having zero mean and identity covariance matrix.

(5) Finally, perform the linear transformation given by eq (4.5) to obtain a sample vector of the SIRV $\mathbf{Y}$ with desired mean and covariance matrix.

Fig 4.1 shows the simulation procedure presented above.

The subroutine RNNOR in IMSL was used for generating the sample vectors of the Gaussian random vector $\mathbf{Z}$. Interestingly enough, the PDFs listed in Table 4.4 can be related to the PDF of the Gamma distribution as discussed below. The PDF $f_V(v)$ for the K-distributed SIRV is a Chi PDF. We first address the random variable generation for the Chi PDF and then provide the transformations for obtaining the random variables for the other PDFs listed in Table 4.4.

Consider the standard Gamma distribution given by

$$f_T(t) = \frac{t^{\alpha-1}}{\Gamma(\alpha)} exp(-t) \quad t > 0 \tag{4.9}$$

where α denotes the shape parameter and $\Gamma(\alpha)$ is the Eulero- Gamma function. The random variable V for the Chi PDF is obtained by the transformation $V = \frac{\sqrt{2T}}{b}$. Samples of the random variable T are readily generated by using the IMSL subroutine RNGAM. The procedure for generating the Chi distributed random samples needed for the K-distributed SIRV is summarized below.

Table 4.1: $h_{2N}(p)$ for SIRVs with Known Characteristic PDF

Marginal PDF	$h_{2N}(p)$
Laplace	$b^{2N}(b\sqrt{p})^{1-N}K_{N-1}(b\sqrt{p})$
Cauchy	$\frac{2^N b\Gamma(\frac{1}{2}+N)}{\sqrt{\pi}(b^2+p)^{N+\frac{1}{2}}}$
K-distribution	$\frac{b^{2N}}{\Gamma(\alpha)}\frac{(b\sqrt{p})^{\alpha-N}}{2^{\alpha-1}}K_{N-\alpha}(b\sqrt{p})$
Student-t	$\frac{2^N b^{2\nu}\Gamma(\nu+N)}{\Gamma(\nu)(b^2+p)^{N+\nu}}$

1. Generate samples of the random variable T for the standard Gamma distribution of eq (4.9) by using the IMSL subroutine RNGAM.

2. Perform the transformation $V = \frac{\sqrt{2T}}{b}$.

The PDF $f_V(v)$ for the Laplace SIRV is a Rayleigh PDF and is obtained from that of the K-distributed SIRV by letting $\alpha = 1$. The random variable V for the PDF $f_v(v)$ listed in Table 4.4 for the Student-t SIRV is obtained from the standard Gamma PDF of eq (4.9) by the transformation $V = \frac{b}{\sqrt{2T}}$ and letting $\alpha = \nu$. Finally, the PDF $f_V(v)$ for the Cauchy SIRV is obtained from that of the Student-t SIRV by letting $\nu = 1$. The procedure for generating the random random samples needed for the Student-t SIRV is summarized below.

1. Generate samples of the random variable T for the standard Gamma distribution of eq (4.9) by using the IMSL subroutine RNGAM.

2. Perform the transformation $V = \frac{b}{\sqrt{2T}}$.

We now concern ourselves with the second simulation procedure which is applicable when the characteristic PDF is unknown, as is the case for SIRVs listed in Table 4.2. This alternate approach makes use of Theorem 3. In particular, this procedure requires the capability to generate the independent random variables R, Θ and Φ_k ($k = 1, 2, \ldots, N-2$). Generation of the random variables Θ and Φ_k ($k = 1, 2, \ldots, N-2$) is extremely difficult from a computational standpoint. This problem is overcome as follows.

Recall that the PDFs of Θ and Φ_k ($k = 1, 2, \ldots, N-2$) are remain unchanged regardless of the white SIRV considered. Only the PDF of R changes from one white SIRV to another. Furthermore, since a Gaussian random vector is a member of the family of SIRVs, a white Gaussian random vector having zero mean and identity

Table 4.2: $h_{2N}(p)$ for SIRVs with Unknown Characteristic PDFs

Marginal PDF	$h_{2N}(p)$
Chi	$(-2)^{N-1}A\sum_{k=1}^{N} G_k p^{\nu-k} exp(-Bp)$
	$G_k = \begin{pmatrix} N-1 \\ k-1 \end{pmatrix} (-1)^{k-1} B^{k-1} \frac{\Gamma(\nu)}{\Gamma(\nu-k+1)}$
	$A = \frac{2}{\Gamma(\nu)}(b\sigma)^{2\nu}$
	$B = b^2\sigma^2$
	$\nu \leq 1$
Weibull	$\sum_{k=1}^{N} C_k p^{\frac{kb}{2}-N} exp(-Ap^{\frac{b}{2}})$
	$A = a\sigma^b$
	$C_k = \sum_{m=1}^{k}(-1)^{m+N} 2^N \frac{A^k}{k!} \begin{pmatrix} k \\ m \end{pmatrix} \frac{\Gamma(1+\frac{mb}{2})}{\Gamma(1+\frac{mb}{2}-N)}$
	$b \leq 2$
Gen. Rayleigh	$\sum_{k=1}^{N-1} D_k p^{\frac{k\alpha}{2}-N+1} exp(-Bp^{\frac{\alpha}{2}})$
	$A = \frac{\sigma^2\alpha}{\beta^2\Gamma(\frac{2}{\alpha})}$
	$B = \beta^{-\alpha}\sigma^{\alpha}$
	$D_k = \sum_{m=1}^{k}(-1)^{m+N-1} 2^{N-1} \frac{B^k}{k!} \begin{pmatrix} k \\ m \end{pmatrix} \frac{\Gamma(1+\frac{m\alpha}{2})}{\Gamma(2+\frac{m\alpha}{2}-N)}$
	$\alpha \leq 2$
Rician	$\frac{\sigma^{2N}}{(1-\rho^2)^{N-\frac{1}{2}}} \sum_{k=0}^{N-1} \begin{pmatrix} N-1 \\ k \end{pmatrix} (-1)^k (\frac{\rho}{2})^k \xi_k exp(-A)$
	$\xi_k = \sum_{m=0}^{k} \begin{pmatrix} k \\ m \end{pmatrix} I_{k-2m}(\rho A),\ A = \frac{p\sigma^2}{2(1-\rho^2)}$

Table 4.3: Characteristic PDF for SIRVs listed in Table 4.1 $[E(S^2) = 1]$

Marginal PDF	$f_S(s)$
Laplace	$ab^2 s exp(-\frac{a^2b^2s^2}{2})u(s)$
Cauchy	$a^2b^2s^{-3}exp(-\frac{b^2}{2a^2s^2})u(s)$
K-distribution	$\frac{2ab}{\Gamma(\alpha)2^{\alpha}}(bas)^{2\alpha-1}exp(-\frac{b^2a^2s^2}{2})u(s)$
Student-t	$\frac{2ab}{\Gamma(\nu)2^{\nu}}b^{2\nu-1}(as)^{-(2\nu+1)}exp(-\frac{b^2}{2a^2s^2})u(s)$

Table 4.4: Related PDF $f_V(v)$

Marginal PDF	$f_V(v)$	$a^2 = E(V^2)$
Laplace	$b^2 v exp(-\frac{b^2v^2}{2})u(v)$	$\frac{2}{b^2}$
Cauchy	$b^2v^{-3}exp(-\frac{b^2}{2v^2})u(v)$	∞
K-distribution	$\frac{2b}{\Gamma(\alpha)2^{\alpha}}(bv)^{2\alpha-1}exp(-\frac{b^2v^2}{2})u(v)$	$\frac{2\alpha}{b^2}$
Student-t	$\frac{2b}{\Gamma(\nu)2^{\nu}}b^{2\nu-1}v^{-(2\nu+1)}exp(-\frac{b^2}{2v^2})u(v)$	$\frac{b^2}{2(\nu-1)}$

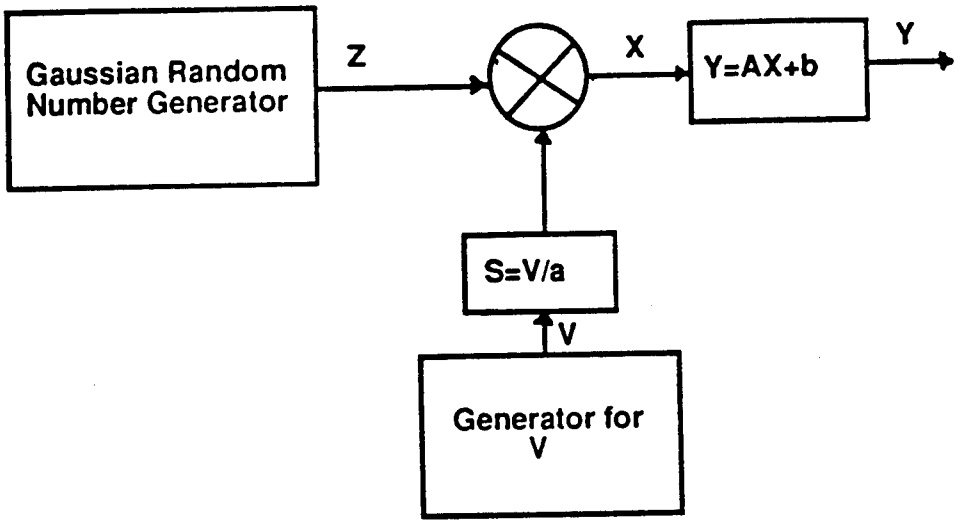

Figure 4.1: Simulation Scheme for SIRVs with Known Characteristic PDF

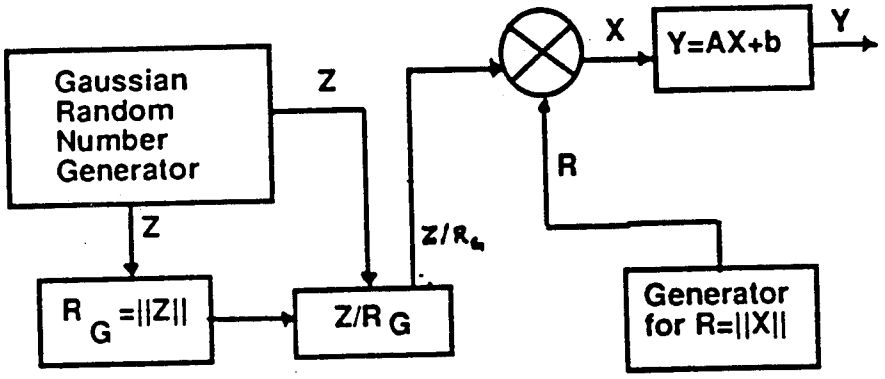

Figure 4.2: Simulation Scheme for SIRVs with Unknown Characteristic PDF

covariance matrix admits a representation of the form of eq (4.6). It follows that

$$\frac{X_k}{R} = \frac{Z_k}{R_G} \quad k = 1, 2, \ldots, N \tag{4.10}$$

where R is the norm of the desired white SIRV and R_G is the norm of the zero mean white Gaussian random vector. Consequently, the components of the desired white SIRV are obtained as

$$X_k = \frac{Z_k}{R_G} R \quad k = 1, 2, \ldots, N \tag{4.11}$$

The simulation procedure is stated below:

(1) Generate a sample vector of the white, zero mean Gaussian random vector $\mathbf{Z}$ having identity covariance matrix.

(2) Compute the norm $R_G = ||\mathbf{Z}|| = \sqrt{\mathbf{Z}^T\mathbf{Z}}$ of the sample vector $\mathbf{Z}$.

(3) Generate a sample of the norm $R = ||\mathbf{X}|| = \sqrt{\mathbf{X}^T\mathbf{X}}$ of the white SIRV from the PDF of R given by eq (4.7).

(4) Generate a sample vector of the white SIRV $\mathbf{X}$ by computing $\mathbf{X} = \frac{\mathbf{Z}}{\mathbf{R_G}} R$.

(5) Finally, perform the linear transformation given by eq (4.5) to obtain a sample of the SIRV $\mathbf{Y}$ with desired mean and covariance matrix.

The simulation procedure is shown schematically in Fig 4.2. Note that this simulation procedure avoids the explicit generation of the variables Θ and Φ_k $(k = 1, \ldots N - 2)$. The generation procedure for a white Gaussian random vector is well known. Therefore, we need to concern ourselves only with the development of a suitable generation scheme for samples of the norm R of the white SIRV $\mathbf{X}$. Generation of the samples of R is not trivial. This is due to the fact that the PDF of R is generally not in a simple functional form. Consequently, it may not be possible to conveniently evaluate analytically the distribution function and its inverse. Hence, generation methods based on the inverse distribution function do not offer a practical solution to this problem. Therefore, in this chapter we generate samples of R by making use of the approach called the 'Rejection Method'. The rejection method can be used to

generate samples of random variables whose cumulative distribution functions are not known, but whose PDFs are known explicitly [40]. The rejection procedure assumes knowledge of the maximum value of the PDF of R for a given SIRV PDF and an estimate for the finite range of the PDF of R so that the area under the PDF curve is close to unity. These quantities are denoted by c and b, respectively. We discuss the rejection procedure in detail in Appendix B. The Rejection method is summarized below:

(1) Generate a uniform random variate U_1 on the interval $(0, b)$.

(2) Generate another uniform variate U_2 on the interval $(0, c)$.

(3) If $U_2 \leq f_R(U_1)$, then $R = U_1$. Otherwise, reject U_1 and return to step 1.

Note that the simulation procedures of Fig 4.1 and Fig 4.2 are canonical in the sense that their forms remain unchanged from the simulation of one SIRV to another. Even though, the scheme of Fig 4.2 can be used even when $f_S(s)$ is known, the scheme of Fig 4.1 is preferred when S can be generated easily. The linear transformation of eq (4.5) is a filtering operation. In both schemes, pre-modulation filtering is equivalent to post-modulation filtering. This results from the fact that the representation theorem is valid whether or not the SIRV $\mathbf{X}$ and the Gaussian random vector $\mathbf{Z}$ are white.

4.4 Performance Assessment of the Simulation Schemes

In this section we concern ourselves with the performance assessment of the simulation procedures developed in section 4.3. We point out that the simulation procedures developed in section 4.3 are exact in the sense that they are derived without approximation from theory. Hence, departures from the exact SIRVs will depend for the most part on the nonideality of the uniform random number generators and on the number of samples used. Empirical assessment of the simulation procedures is necessary for practical applications.

One possible approach for assessing the distributional properties of the simulated data is to perform a hypothesis test on the marginal distributions of the components of the SIRV. More precisely, the problem is stated as follows.

H_0:The hypothesis that the simulated data is from the desired distribution

H_1:The hypothesis that the simulated data is not from the desired distribution.
For a fixed Type-1 error probability (i.e., the probability that H_1 is accepted given that H_0 is true) each marginal distribution can be checked by employing one of the commonly used goodness of fit procedures. Since the components of the random vectors are not statistically independent, we are now confronted with the problem of developing a goodness of fit test for the multivariate data. In general, it is very difficult to obtain the overall significance level of the test (i.e., the probability that H_0 is accepted given that H_0 is true) for the multivariate goodness of fit testing procedure.

However, an attractive feature of SIRVs is that the quadratic form p appearing in the SIRV PDF contains all the information necessary for identifying the PDF of the SIRV. In other words, knowledge of the PDF of the quadratic form is sufficient to determine the underlying SIRV PDF. Furthermore, the quadratic form PDF remains unchanged regardless of whether the SIRV is white or colored. The PDF of the quadratic form appearing in the SIRV PDF is given by eq (4.8). For the radar problem where we deal with N complex samples or $2N$ quadrature components, note that we make use of eq (4.8) with N replaced by $2N$. Hence, we base our goodness of fit test procedure for the generated SIRVs on the PDF of the quadratic form p. Note that we have now reduced the multivariate problem to an equivalent univariate problem involving the goodness of fit test for the PDF of the quadratic form.

In the examples presented in this section, we generated $m = 1000$ realizations of the random vector $\mathbf{Y}$ with $N = 2$ complex samples and from these computed one thousand samples of the quadratic form P for each of the non-Gaussian SIRVs whose PDFs are listed in Tables 4.1 and 4.3. In each case, we used the corresponding theoretical PDF of the quadratic form given by eq (4.8) to test for the distribution of the generated quadratic form. The frequency histograms for the generated data and the corresponding theoretical PDFs are shown in Figures 4.3-4.10. In addition, a Chi-Square test was performed on the generated data with the Type-1 error fixed at 0.05 and the null hypothesis was not rejected in each case. The frequency histograms provide a good idea about the true distributions for large sample sizes. Observe that the empirical PDFs are very close to the theoretical PDFs. Note that the procedure used in this section to assess the distributional assumptions of the random samples

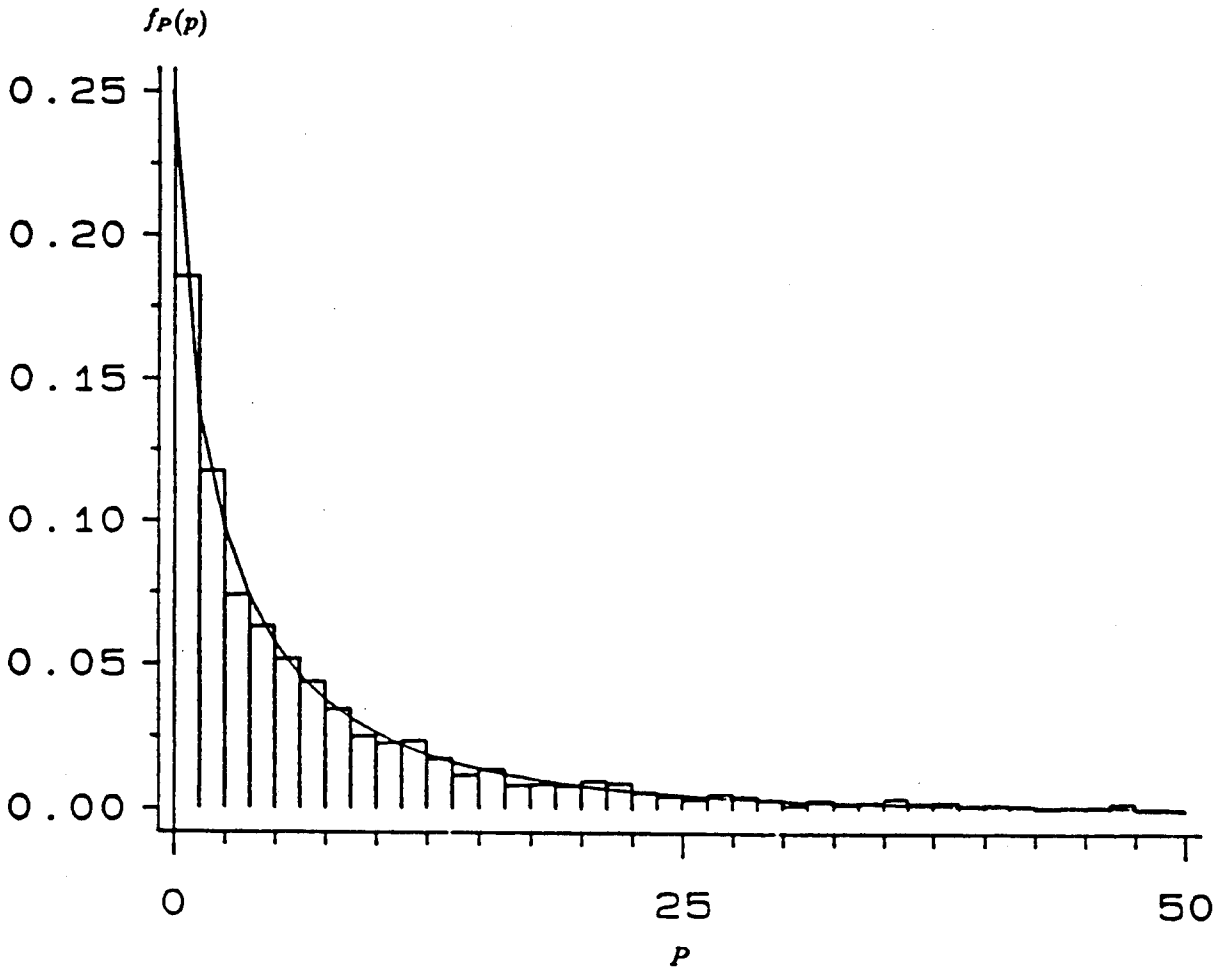

Figure 4.3: Theoretical and Empirical Quadratic form PDFs for Laplace SIRV

from the SIRV PDFs is a formal goodness of fit test. Similar procedures have been proposed to test for multivariate normality in [41, 42].

4.5 Conclusions

In this Chapter, we have presented two schemes that can be used in practice to simulate correlated non-gaussian radar clutter, when the clutter can be modeled as a spherically invariant random process. We pointed out that the simulation schemes developed are canonical schemes and do not change form from the simulation of one SIRV to another. A new approach, based on the PDF of the quadratic form appearing

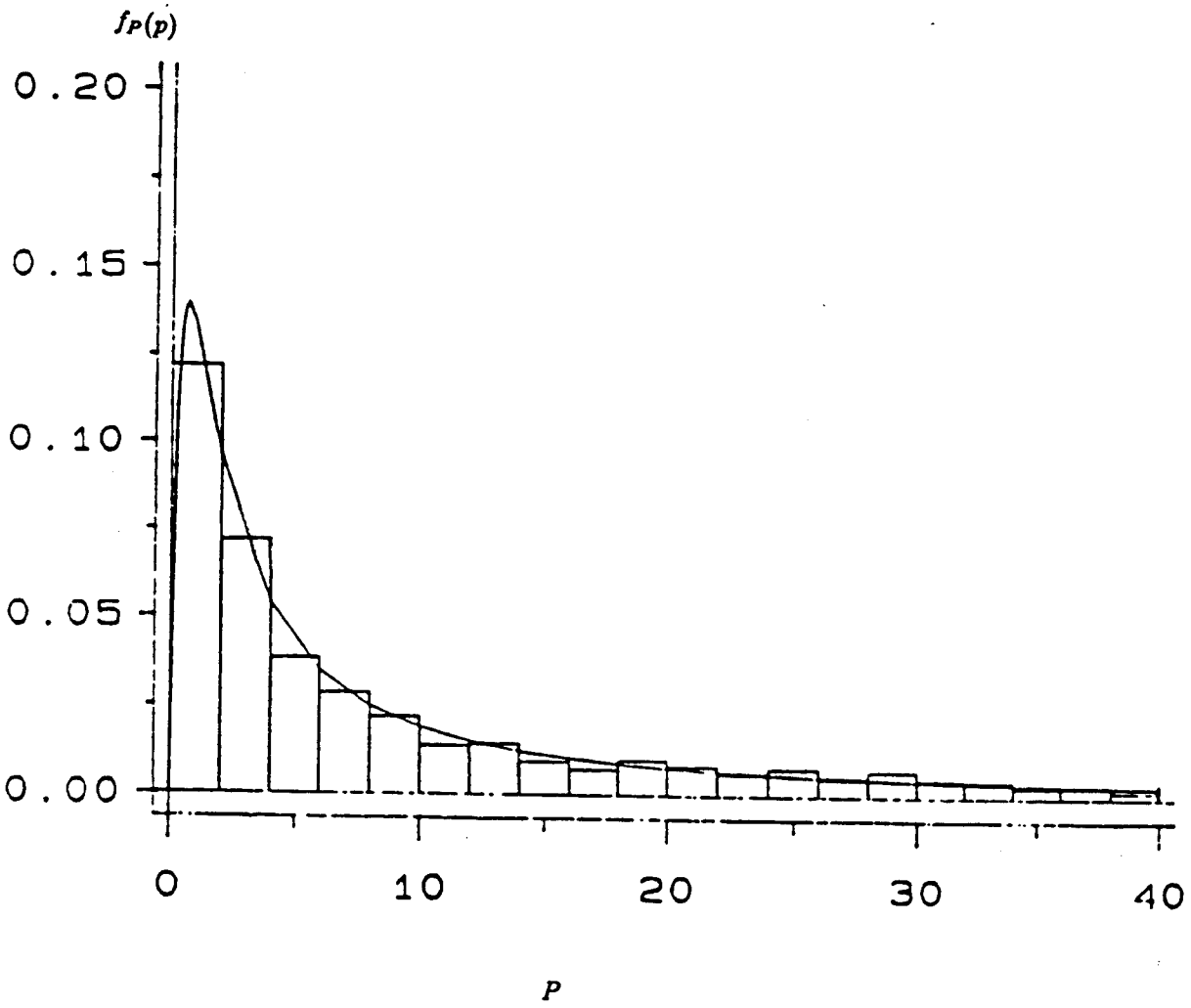

Figure 4.4: Theoretical and Empirical Quadratic form PDFs for Cauchy SIRV

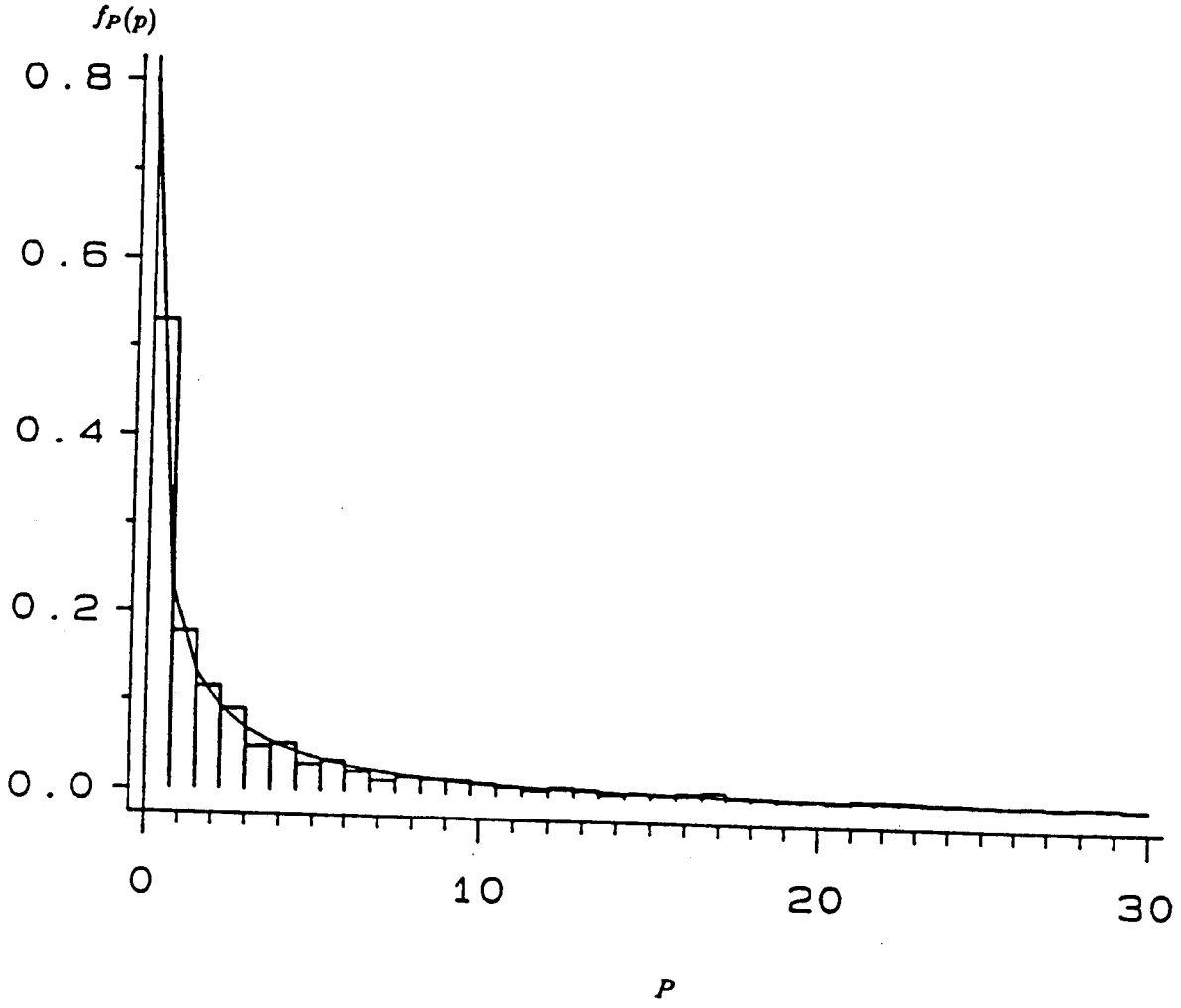

Figure 4.5: Theoretical and Empirical Quadratic form PDFs for K-distributed SIRV

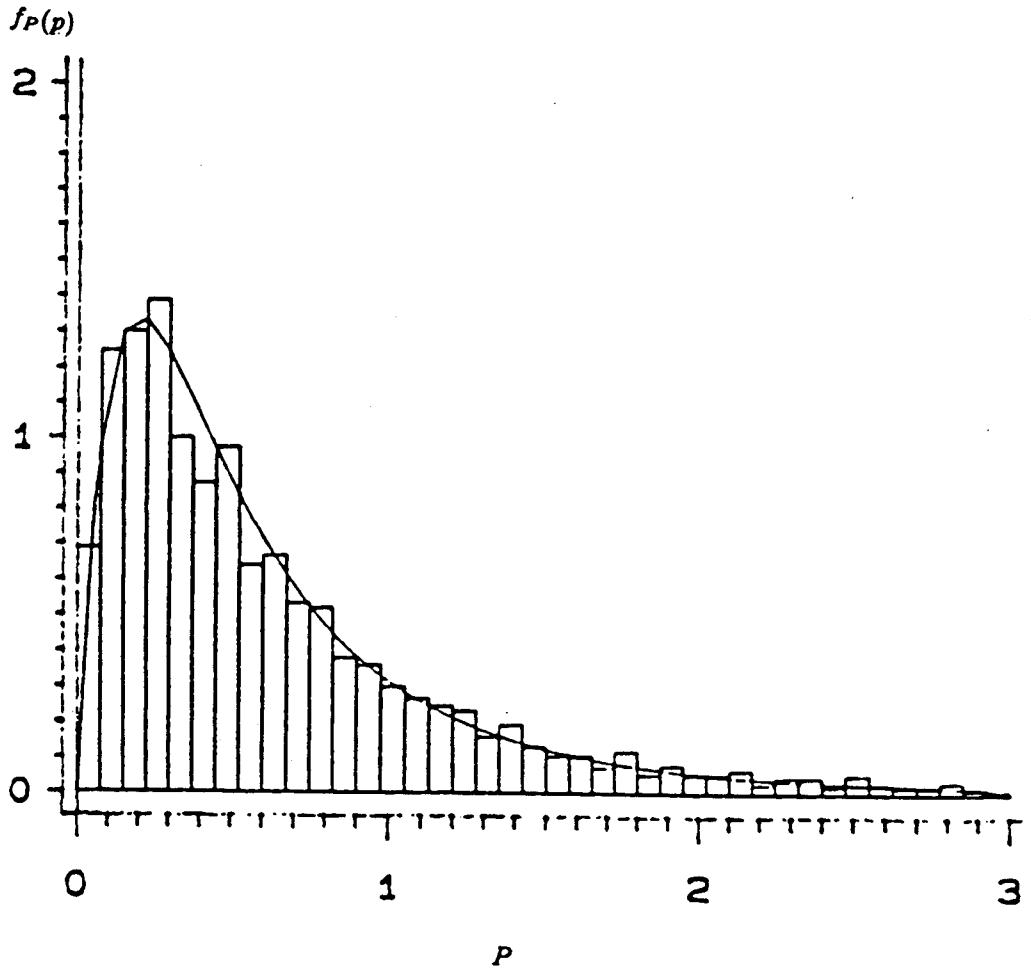

Figure 4.6: Theoretical and Empirical Quadratic form PDFs for Student-t SIRV

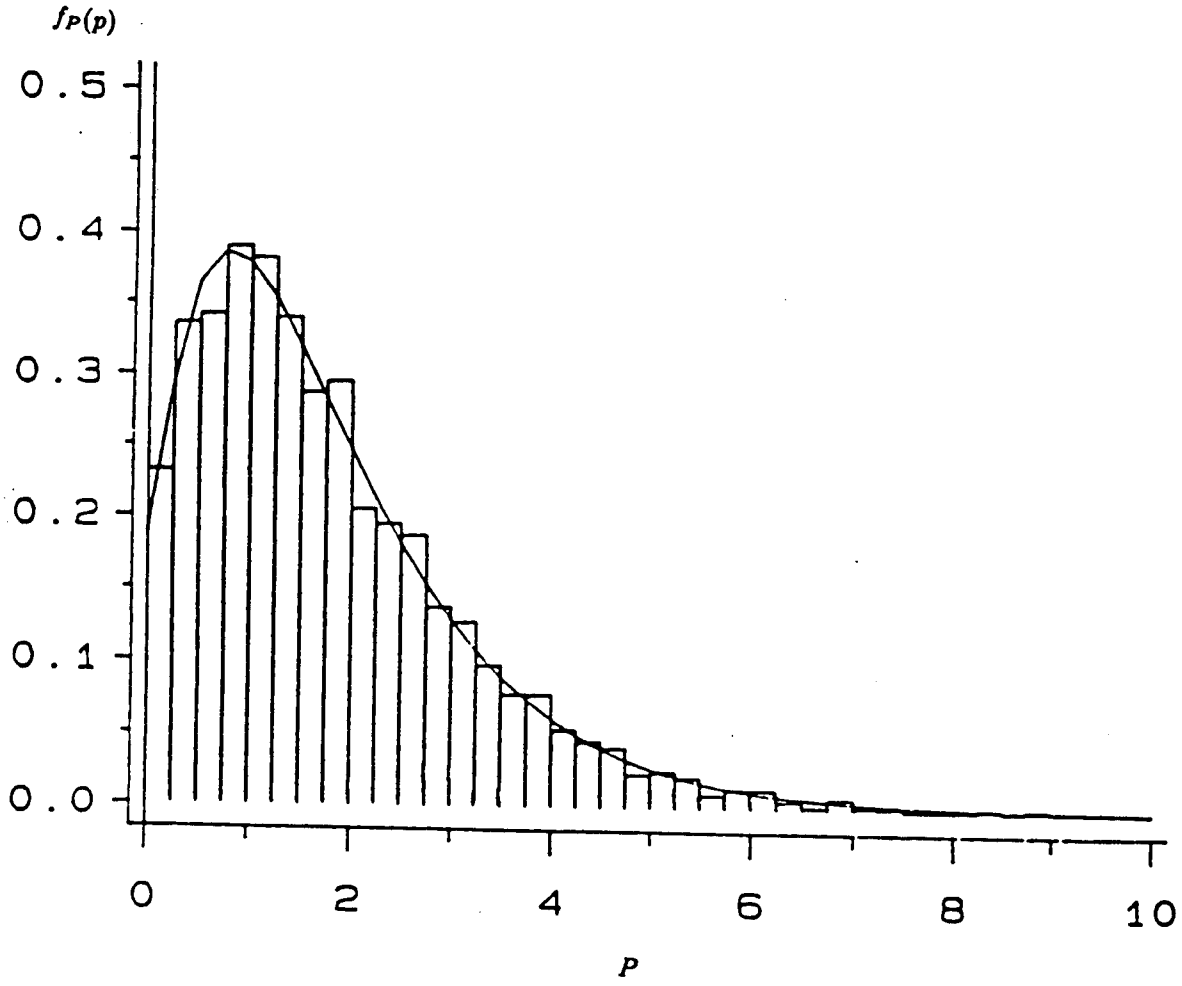

Figure 4.7: Theoretical and Empirical Quadratic form PDFs for Chi distributed SIRV

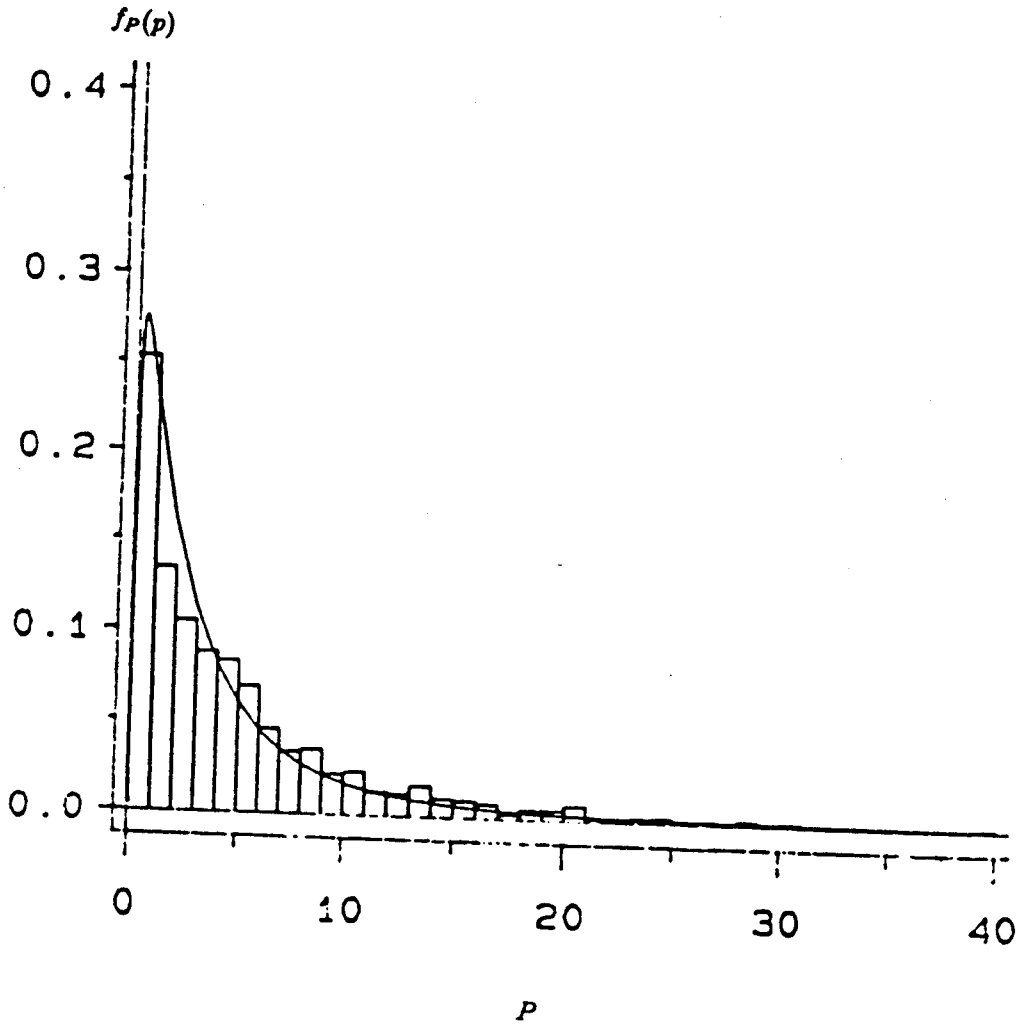

Figure 4.8: Theoretical and Empirical Quadratic form PDFs for Generalized Rayleigh SIRV

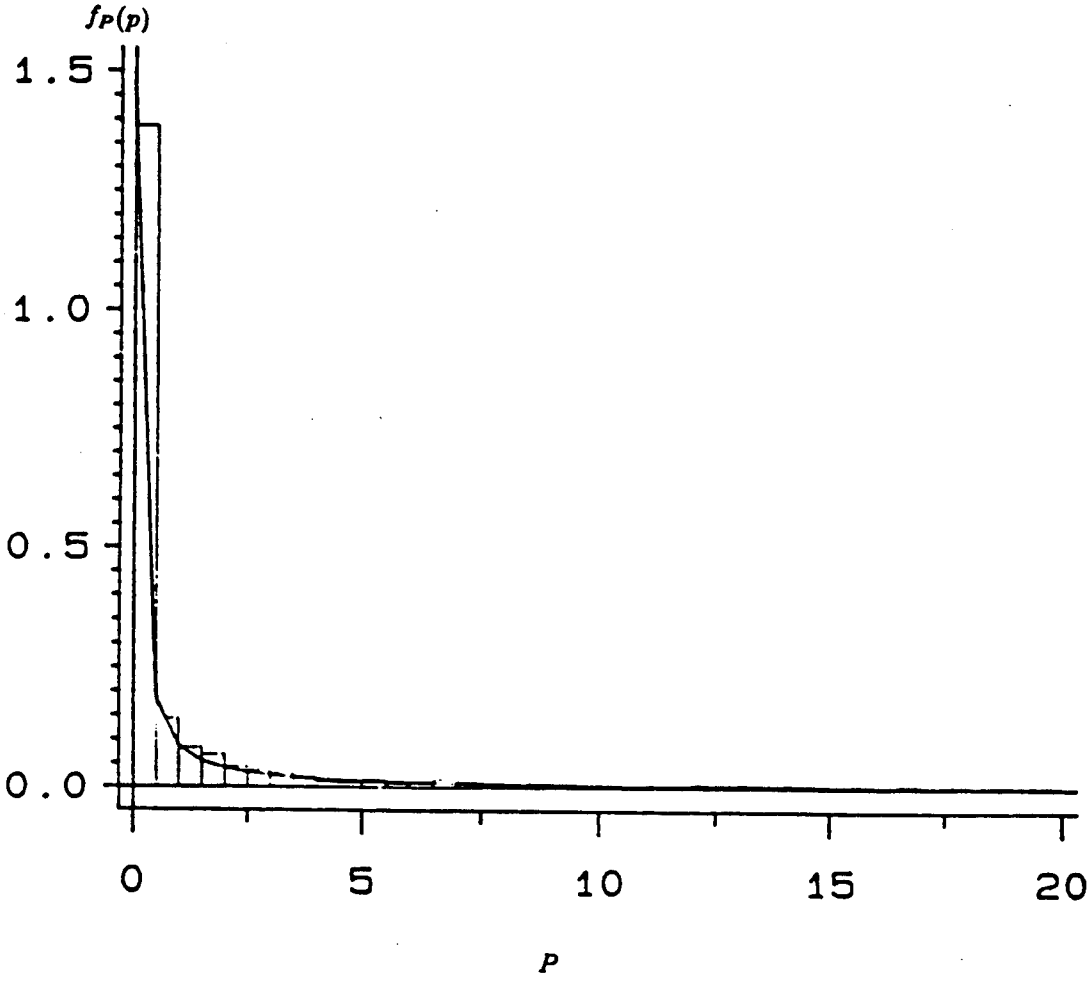

Figure 4.9: Theoretical and Empirical Quadratic form PDFs for Weibull SIRV

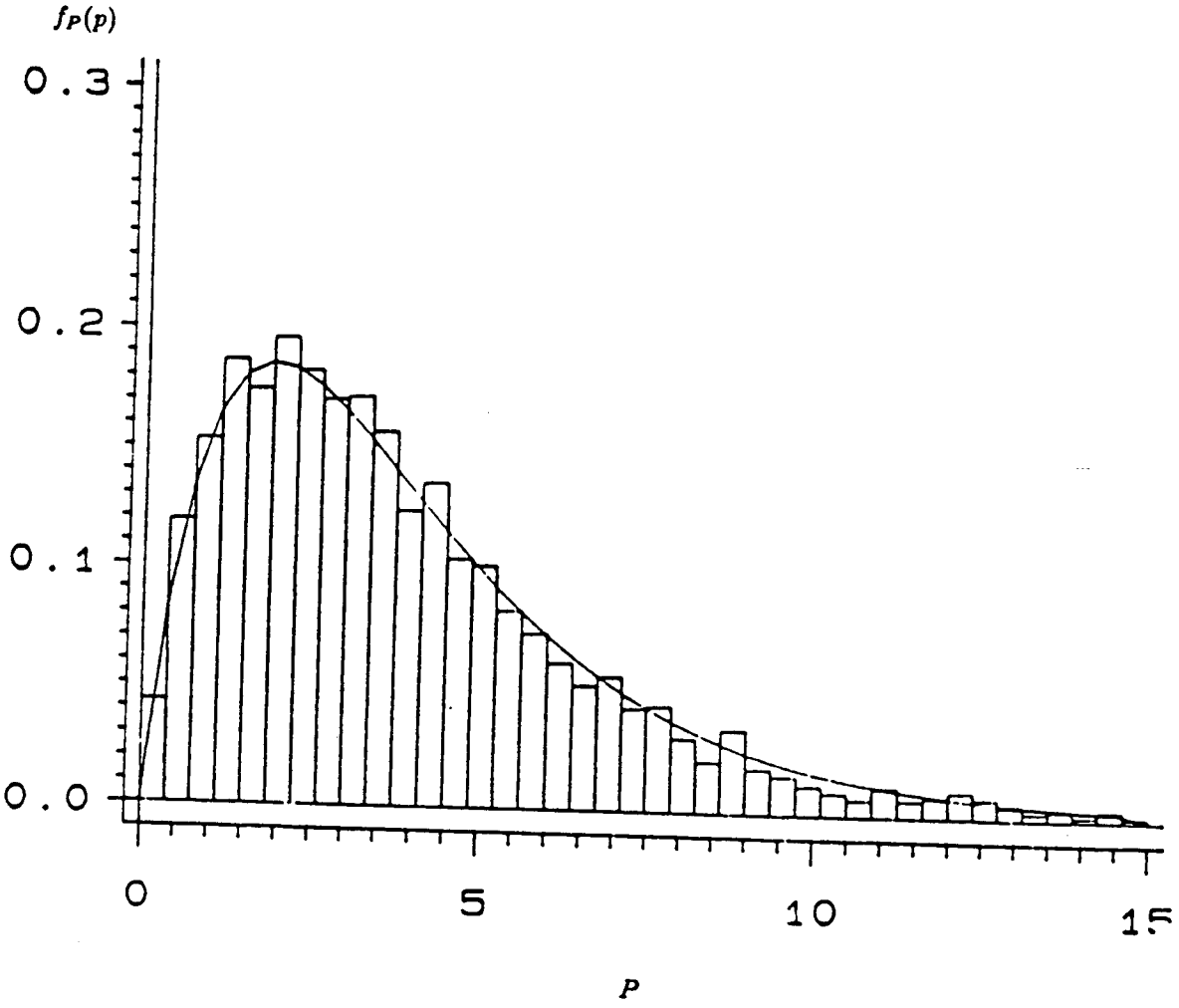

Figure 4.10: Theoretical and Empirical Quadratic form PDFs for Rician SIRV

in the SIRV PDF, was used to perform a goodness of fit test in order to assess performance of the proposed simulation schemes. Performance assessment based on this scheme showed excellent agreement between the theoretical and empirical PDFs of the quadratic form. Finally, it was pointed out that use of this technique reduced the goodness of fit test from a multivariate testing procedure to a univariate testing procedure resulting in tremendous processing simplicity. Therefore, this procedure lends itself very well to practical applications.

Chapter 5

Distribution Approximation to Radar Clutter Characterized by SIRPs

5.1 Introduction

This investigation is motivated by a desire to characterize correlated non-Gaussian radar clutter by approximating the underlying probability density function of the clutter. Various investigators have reported experimental results where non-Gaussian marginal probability density functions (PDF) have been used to model the clutter. Usually, radars process N samples at a time. Statistical characterization of the clutter requires the specification of the joint PDF of the N samples. In addition, the clutter may be highly correlated. Hence, the joint PDF must take into account the correlation between samples. Statistical characterization of the clutter is necessary if an optimal radar signal processor is to be obtained. For use of the well known likelihood ratio test, it is desirable to have a closed form expression for the joint PDF of the N clutter samples in order to obtain the optimal radar signal processor. The joint PDF of the N clutter samples can be easily specified when the clutter is Gaussian. However, when the clutter is non-Gaussian and is correlated, many different joint PDFs of the clutter samples can result in the same set of marginal (univariate) distributions having a specified non-Gaussian character. The multivariate non-Gaussian PDF is uniquely determined from the marginal distribution only when the samples are statistically independent.

Specification of the multivariate PDF is generally a non- trivial problem with no simple best solution [43]. The theory of Spherically Invariant Random Processes (SIRP) provides a powerful mechanism to obtain the joint PDF of the N correlated, non-Gaussian clutter samples. Many of the tractable properties of the Gaussian random process also apply to SIRPs. Typically, background clutter is not known a priori. Hence, while dealing with real world data, there is a need to approximate the clutter PDF from a set of measurements. In order to approximate the underlying clutter PDF, there is a need for a library of multivariate non-Gaussian PDFs. Such a library has been obtained in Chapter 3 based on the theory of SIRPs. The multivariate PDFs thus obtained are functions of non-negative quadratic forms. Therefore, these PDFs are sometimes referred to as elliptically symmetric distributions. The multivariate Gaussian PDF belongs to the family of SIRPs. The multivariate Pearson types II and VII are examples of elliptically symmetric multivariate non-Gaussian PDFs. SIRPs have received considerable attention over the past two decades since many of the elegant and mathematically tractable properties of the multivariate Gaussian distribution generalize to this class of distributions. Applications of SIRPs can be found in the random flight problem [14], signal detection [16], speech signal modeling [17] and radar clutter modeling [19, 21].

In practice, the clutter PDF encountered in radar signal processing is not known a priori. Consequently, a scheme that approximates the clutter PDF based on a set of measured data is necessary. Currently, available tests such as the Kolmogorov-Smirnov test and the Chi-Square test address the problem of goodness-of-fit for random data. In particular, these tests provide information about whether a set of random data is statistically consistent with a specified distribution, to within a certain confidence level. However, if the specified distribution is rejected, these tests cannot be used for approximating the underlying PDF of the random data. Moreover, these tests require large sample sizes for reliable results.

In practice, only a small number of samples may be available. Therefore, the scheme used should be efficient for small sample sizes. A new algorithm based on sample order statistics has been developed in [41] for univariate distribution identification. This algorithm has two modes of operation. In the first mode, the algorithm performs a goodness-of-fit test. Specifically, the test determines, to a desired con-

fidence level, whether random data is statistically consistent with a specified probability distribution. In the second mode of operation, the algorithm approximates the PDF underlying the random data. In particular, by analyzing the random data and without any a priori knowledge, the algorithm identifies from a stored library of PDFs that density function which best approximates the data. Estimates of the scale, location, and shape parameters of the PDF are provided by the algorithm. The algorithm typically works well with sample sizes which may be as small as 50 and 100 samples. An extension of this algorithm for the multivariate Gaussian PDF has been considered in [41, 44].

In this Chapter, using certain properties of SIRPs, we adopt the algorithm developed in [41] to identify the underlying distribution of a given set of data. In particular, we first show that the multivariate distribution approximation problem for SIRPs is reduced to an equivalent univariate distribution approximation problem. The new algorithm developed by Ozturk in [41] is used for the univariate approximation problem. Section 5.2 presents definitions. Sections 5.3-5.5 summarize the algorithm developed in [41] for approximating the univariate PDF of a set of random data. In Section 5.6 we present a procedure for the goodness of fit test for PDFs arising from SIRPs. The proposed distribution identification algorithm is discussed in Section 5.7. Section 5.8 proposes a method to estimate the shape parameter based on the procedure developed in Section 5.7. Finally, conclusions are presented in Section 5.9.

5.2 Definitions

Let $f_Y(y)$ denote the PDF of a random variable Y. Consider the linear transformation defined by

$$x = \beta y + \alpha \tag{5.1}$$

The PDF of X is given by

$$f_X(x) = \frac{1}{|\beta|} f_Y(\frac{x-\alpha}{\beta}) \tag{5.2}$$

where α and β are defined to be the location and scale parameters of $f_X(x)$, respectively. The mean μ_x and variance σ_x of the random variable X are given by

$$\begin{aligned} \mu_x &= E[X] \\ \sigma_x^2 &= E[(X-\mu_x)^2]. \end{aligned} \tag{5.3}$$

Although the mean and the variance are related to the location and scale parameters, note that the location parameter is not the mean value and the scale parameter is not the square root of the variance, in general. However, for a standardized Gaussian PDF $f_Y(y)$ for which the mean is zero and the variance is unity, the location parameter is the mean of X and the scale parameter is the standard deviation (square root of the variance) of X.

The coefficient of skewness, α_3, and the coefficient of kurtosis, α_4, of X, are defined to be

$$\begin{aligned} \alpha_3 &= \frac{E[(X-\mu_x)^3]}{\sigma_x^3} \\ \alpha_4 &= \frac{E[(X-\mu_x)^4]}{\sigma_x^4}. \end{aligned} \tag{5.4}$$

It is readily shown that α_3 and α_4 are invariant to the values of μ_x and σ_x. For any PDF that is symmetric about the mean, $\alpha_3 = 0$. For the case of the Gaussian distribution, $\alpha_3 = 0$ and $\alpha_4 = 3$.

5.3 Goodness of Fit Test

In this section, we introduce a general graphical method for testing whether a set of random data is statistically consistent with a specified univariate distribution. The proposed method not only yields a formal goodness-of-fit test but also a provides a graphical representation that gives insight into how well the random data is representative of the specified distribution (null hypothesis). Using the standard normal distribution with zero mean and unit variance as *a reference distribution*, the standardized sample order statistics are represented by a system of linked vectors. The terminal point of these linked vectors, as well as the shape of their trajectories, are used in determining whether or not to accept the null hypothesis.

In this section we first give a brief description of the corresponding test statistic and then explain the goodness of fit test procedure. For illustration purposes, we consider

the null distribution to be Gaussian. However, the proposed procedure works for any null hypothesis.

Let X_i; $i = 1, 2, \ldots n$ denote the i^{th} sample from a Gaussian distribution with mean μ and variance σ^2. Let $X_{1:n} \leq X_{2:n} \leq \ldots \leq X_{n:n}$ denote the ordered samples obtained by ordering X_i; $i = 1, 2, \ldots n$. We define

$$Y_i = \frac{|X_i - \overline{X}|}{S} \quad i = 1, 2, \ldots, n \tag{5.5}$$

where $\overline{X} = \Sigma X_i/n$ is the sample mean and $S = \{\Sigma(X_i - \overline{X})^2/(n-1)\}^{1/2}$ is the sample standard deviation. The standardized order statistics are denoted by $Y_{i:n}$ $i = 1, 2, \ldots n$ and are obtained by ordering the Y_i; $i = 1, 2, \ldots n$. It follows that

$$Y_{i:n} = \frac{|X_{i:n} - \overline{X}|}{S} \quad i = 1, 2, \ldots, n \tag{5.6}$$

The i^{th} linked vector is characterized by its length and orientation with respect to the horizontal axis. Let $G_{i:n}$denote the order statistics from the standard normal reference distribution. Also, let $m_{i:n} = E[G_{i:n}]$. The length of the i^{th} vector, a_i, is obtained from the magnitude of the i^{th} standardized sample order statistic, while its orientation θ_i is related to $m_{i:n}$. More specifically, by definition,

$$\begin{aligned} a_i &= \tfrac{Y_{i:n}}{n} \\ \theta_i &= \pi\Phi(m_{i:n}) \end{aligned} \tag{5.7}$$

where $\Phi(x) = (\sqrt{2\pi})^{-1} \int_{-\infty}^{x} exp(-\frac{t^2}{2})dt$ is the cumulative distribution function of the standard Gaussian distribution. We define the sample points Q_k in a two dimensional plane by

$$Q_k = (U_k, V_k) \quad k = 1, 2, \ldots n \tag{5.8}$$

where $U_0 = V_0 = 0$ and

$$\begin{aligned} U_k &= \tfrac{1}{k} \textstyle\sum_{i=1}^{k} \{Cos(\theta_i)\} Y_{i:n} \\ V_k &= \tfrac{1}{k} \textstyle\sum_{i=1}^{k} \{Sin(\theta_i)\} Y_{i:n} \\ k &= 1, 2, \ldots n. \end{aligned} \tag{5.9}$$

The sample linked vectors are obtained by joining the points Q_k. Note that $Q_0 = (0,0)$. It should also be noted that the statistic Q_n given in eq (5.8) represents the terminal point of the linked vectors defined above. Figure 5.1 shows the linked vectors obtained for the Gaussian distribution with $n = 6$. Since U_n and V_n are random variables for a given n, the corresponding linked vectors must be obtained by averaging the results of Monte-Carlo trials. In this case the linked vectors were obtained by averaging the results of 50,000 Monte Carlo trials. The solid curve in Figure 5.1 shows the linked vectors for the sample distribution while the dashed curve shows the ideal linked vectors for the null distribution. The magnitudes and angles of the linked vectors are obtained from eq (5.7). Note that the angles are independent of the data. Only the magnitudes of the linked vectors change from one trial to another.

For a typical set of ordered samples (i.e., ordered samples drawn from the null distribution) it is reasonable to expect that the sample linked vectors would follow the null pattern closely. If the ordered set of samples is not from the null distribution, the sample linked vectors are not expected to follow the null pattern closely. Hence, the procedure provides visual information about how well the ordered set of samples fit the null distribution.

An important property of the Q_n statistic is that it is invariant under linear transformation. In particular, we consider the standardization used in eq (5.5). Let $Z_i = cX_i + d$, where c and d are known constants. Let S' denote the sample standard deviation of the samples Z_i. Then, it is readily shown that $\frac{|X_i - \overline{X}|}{S} = \frac{|Z_i - \overline{Z}|}{S'}$. The invariance property follows as a consequence. The advantage of this property is that the PDF of $Q_n = (U_n,\ V_n)$, for a given sample and reference distribution depends only on the sample size n and is unaffected by the location and scale parameters. Since it is difficult to determine the joint PDF of U_n and V_n analytically, it is necessary to obtain empirical results.

Assuming that the conditions under the central limit theorem are satisfied, the marginal PDFs of U_n and V_n can be approximated as Gaussian, in the limit of large n. In addition, it is assumed that the joint PDF of U_n and V_n is approximately bivariate Gaussian. Consequently, all that is needed to determine the bivariate PDF is the specification of $E(U_n)$, $E(V_n)$, $E(U_nV_n)$, $Var(U_n)$ and $Var(V_n)$. Drawing samples from the Gaussian distribution, it has been shown empirically in [41] that for $3 \leq$

$n \leq 100$

$$E(U_n) = 0$$

$$E(V_n) = \mu_v \approx 0.326601 + \frac{0.412921}{n}$$

$$E(U_n V_n) = 0 \tag{5.10}$$

$$Var(U_n) = \sigma_u^2 \approx \frac{0.02123}{n} + \frac{0.01765}{n^2}$$

$$Var(V_n) = \sigma_v^2 \approx \frac{0.04427}{n} - \frac{0.0951}{n^2}.$$

Since U_n and V_n are approximately bivariate Gaussian for large or moderate sample sizes, their joint PDF can be written as

$$f_{U_n, V_n}(u_n,\ v_n) = (2\pi)^{-1}(\sigma_u\sigma_v)^{-1}exp(-\frac{t}{2}) \tag{5.11}$$

where

$$t = \frac{u_n^2}{\sigma_u^2} + \frac{(v_n - \mu_v)^2}{\sigma_v^2}. \tag{5.12}$$

Let $t = t_0$. Then the equation

$$t_0 = \frac{u_n^2}{\sigma_u^2} + \frac{(v_n - \mu_v)^2}{\sigma_v^2} \tag{5.13}$$

is that of an ellipse in the u_n, v_n plane for which

$$f_{U_n, V_n}(u_n,\ v_n) = (2\pi)^{-1}(\sigma_u\sigma_v)^{-1}exp(-\frac{t_0}{2}). \tag{5.14}$$

Points that fall within the ellipse correspond to those points in the u_n, v_n plane for which

$$f_{U_n, V_n}(u_n,\ v_n) > (2\pi)^{-1}(\sigma_u\sigma_v)^{-1}exp(-\frac{t_0}{2}). \tag{5.15}$$

Let

$$\alpha = P(T > t_0) = P(u_n,\ v_n\ \textit{fall outside the ellipse given by eq}\ (5.13)). \tag{5.16}$$

It is well known that the PDF of the random variable T defined by eq (5.12) has a Chi-Square distribution with two degrees of freedom [45] and is given by

$$f_T(t) = 0.5exp(-\frac{t}{2}). \tag{5.17}$$

Hence,

$$\alpha = 1 - exp(-\frac{t_0}{2}). \tag{5.18}$$

Consequently, $t_0 = -2ln(1-\alpha)$. Thus, eq (5.13) becomes

$$\frac{u_n^2}{\sigma_u^2} + \frac{(v_n - \mu_v)^2}{\sigma_v^2} = -2ln(1-\alpha). \tag{5.19}$$

α is known as the significance level of the test. It is the probability that Q_n falls outside the ellipse specified by eq (5.19) given that the data is coming from a Gaussian distribution. $1-\alpha$ is known as the confidence level and the corresponding ellipse is known as the confidence ellipse.

Eq (5.13) can be written in the standardized form

$$1 = \frac{u_n^2}{\sigma_u^2 t_0} + \frac{(v_n - \mu_v)^2}{\sigma_v^2 t_0} \tag{5.20}$$

where the lengths of the major and minor axes are given by $2max\ [\sigma_u\sqrt{t_0},\ \sigma_v\sqrt{t_0}]$ and

$2min\ [\sigma_u\sqrt{t_0},\ \sigma_v\sqrt{t_0}]$, respectively. From eq (5.18), observe that smaller values of α correspond to larger values of t_0. Consequently, the confidence ellipses become larger as the confidence level is increased.

For a given sample size n ($n \leq 100$) approximate values of μ_v, σ_u^2 and σ_v^2 can be obtained from eq (5.10). The confidence ellipse of eq (5.19) can then be used to make a visual as well as computational test of the null hypothesis. If the terminal sample point falls inside the ellipse, then the data is declared as being consistent with the Gaussian distribution with confidence level $1-\alpha$. Otherwise the null hypothesis is rejected with a significance level α.

A major difficulty in determining the joint PDF of U_n and V_n is that the coefficients of skewness and kurtosis of U_n and V_n (see Table 5.3) indicate that the Gaussian approximation for the bivariate PDF may not be satisfactory for $n < 10$. The empirical bivariate PDF of U and V were obtained by using 50,000 Monte-Carlo trials for n=3, 10, 20,30, 50 and 100. The corresponding constant probability contours of the joint PDF of U_n and V_n are shown in Figure 5.2. The same procedure is used even when the null distribution is different from the Gaussian distribution. However, note that the standard Gaussian distribution is always used as the reference distribution for

determining the angles of the linked vectors.

5.4 Distribution Approximation

In this section we present a graphical procedure for approximating the underlying PDF of a set of random data based on the goodness-of-fit test procedure discussed in section 5.3.

Following a similar approach to that outlined in section 5.3, random samples are generated from many different univariate probability distributions. For each specified distribution and for a given n, the statistic $Q_n = (U_n,\ V_n)$ given by eq (5.9) is obtained for various choices of the shape parameter. Thus, each distribution is represented by a trajectory in the two dimensional plane whose coordinates are U_n and V_n. Figure 5.3 shows an example of such a representation. Twelve distributions namely Gaussian (1), Uniform (2), Exponential (3), Laplace (4), Logistic (5), Cauchy (6), Extreme Value (7), Gumbel type-2 (8), Gamma (9), Pareto (10), Weibull (11) and Lognormal (12) are represented in this chart. Tables 5.1 and 5.2 show the standard form and the general form respectively, of the PDFs represented in the identification chart. The value of Q_n at each point of the trajectories is obtained by Monte-Carlo experiments using the standard Gaussian distribution as the reference distribution for determining the angles θ_i. The results are based on averaging 1000 trials of $n = 50$ samples from each distribution. The samples from each distribution are obtained by using the IMSL subroutines for specified values of the shape parameter. Since the procedure is location and scale invariant, the trajectory reduces to a single point for those PDFs which do not have shape parameters but are characterized only in terms of their location and scale parameters. By way of example, the Gaussian, Laplace, Exponential, Uniform and Cauchy PDFs are represented by single points in the $U_n - V_n$ plane. However, those PDFs which have shape parameters are represented by trajectories. For a given value of the shape parameter, a single point is obtained in the $U_n - V_n$ plane. By varying the shape parameter, isolated points are determined along the trajectory. The trajectory for the PDF is obtained by joining these points. In a sense the trajectory represents a family of PDFs having the same distribution but with different shape parameter values. For example, the trajectory corresponding to the Gamma distribution in Figure 5.3 is obtained by joining the points for which the shape parameters are 0.2, 0.3, 0.5, 0.7, 1.0, 2.0, 3.0, 4.0, 6.0, 10.0. As the shape

parameter increases, note that the Gamma distribution approaches the Gaussian distribution. The representation of Figure 5.3 is called an identification chart. Some distributions such as the β distribution and the SU-Johnson system of distributions, have two shape parameters. For these cases, the trajectories are obtained by holding one shape parameter fixed while the other is varied. For these distributions, several different trajectories are generated in order to cover as much of the $U_n - V_n$ plane as possible. For certain choices of the shape parameters, two or more PDFs become identical. When this occurs, their trajectories intersect on the identification chart.

It is apparent that the identification chart of Figure 5.3 provides a one to one graphical representation for each PDF for a given n. Therefore, every point in the identification chart corresponds to a specific distribution. Thus, if the null hypothesis in the goodness-of-fit test discussed in section 5.3 is rejected, then the distribution which approximates the underlying PDF of the set of random data can be obtained by comparing Q_n obtained for the samples with the existing trajectories in the chart. The closest point or trajectory to the sample Q_n is chosen as an approximation to the PDF underlying the random data. The closest point or trajectory to the sample point is determined by projecting the sample point Q_n to neighboring points or trajectories on the chart and considering that point or trajectory whose perpendicular distance from the sample point is the smallest. Consider the situation of Figure 5.4. Let $Q_n = (u', v')$ denote the coordinates of the sample point. Let x_1, y_1 and x_2, y_2 denote the coordinates of the points A and B on the trajectory shown in Figure 5.4. It is assumed that segment of the trajectory between the points A and B is linear. Let x_0, y_0 denote the coordinates of the point of intersection of the straight line between A and B and the projection of $Q_n = (u', v')$ onto this straight line. The equation of the straight line between the points A and B can be written as

$$y - y_1 = m(x - x_1) \tag{5.21}$$

where $m = \frac{y_2 - y_1}{(x_2 - x_1)}$. Also, the equation of the straight line joining x_0, y_0 and (u', v') is

$$y - v' = -\frac{1}{m}(x - u'). \tag{5.22}$$

The coordinates x_0, y_0 result from the solution of eqs (5.21) and (5.22) and are given

by

$$x_0 = \frac{1}{m^2+1}[m^2 x_1 - m y_1 + u' + m v'] \qquad (5.23)$$
$$y_0 = \frac{1}{m^2+1}[y_1 - m x_1 + m^2 v' + m u'].$$

Finally, the perpendicular distance from the sample point onto the trajectory between the points A and B is

$$D = \sqrt{\frac{1}{(m^2+1)}[m^2\zeta_1^2 - 2m\zeta_1\zeta_2 + \zeta_2^2]} \qquad (5.24)$$

where

$$\zeta_1 = u' - x_1 \qquad (5.25)$$
$$\zeta_2 = v' - y_1.$$

The complete approximation algorithm is summarized as follows.

1. Sort the samples $X_1, X_2, \ldots X_n$ in increasing order.
2. Obtain the standardized order statistic $Y_{i:n}$.
3. Compute U_n and V_n from eq (5.9).
4. Obtain an identification chart based on the sample size n and plot the sample point Q_n on this chart.
5. Compute D using the sample point Q_n and the existing distributions on the chart. Choose the PDF corresponding to the point or trajectory that results in the smallest value of D as an approximation to the PDF of the samples.

The approximation to the underlying PDF of the set of random data can be improved by including as many distributions as possible in the identification chart so as to fill as much of the space as possible with candidate distributions. However, it is emphasized that this procedure does not identify the underlying PDF. Rather it identifies a suitable approximation to the underlying PDF.

5.5 Parameter Estimation

Once the probability distribution of the samples is approximated, the next step is to estimate its parameters. The method discussed in section 5.4 lends itself for esti-

mating the parameters of the approximated distribution. We present the estimation procedure for the location, scale and shape parameters in this section.

5.5.1 Estimation of Location and Scale Parameters

Let $f(x;\alpha,\beta,)$ denote a known distribution which approximates the PDF of the set of random data, where α and β are the location parameter and scale parameter, respectively, of the approximating PDF. Let $X_{i:n}$ denote the ordered statistics of X from a sample of size n. A standardized ordered statistic is defined by

$$W_{i:n} = \frac{X_{i:n} - \alpha}{\beta}. \tag{5.26}$$

Let

$$\mu_{i:n} = E[W_{i:n}]. \tag{5.27}$$

Then

$$E[X_{i:n}] = \beta\mu_{i:n} + \alpha \tag{5.28}$$

We consider the following statistics

$$\begin{aligned} T_1 &= \textstyle\sum_i^n Cos(\theta_i)X_{i:n} \\ T_2 &= \textstyle\sum_i^n Sin(\theta_i)X_{i:n} \end{aligned} \tag{5.29}$$

where θ_i is the angle defined in eq (5.7). The expected values of T_1 and T_2 are

$$\begin{aligned} E[T_1] &= \textstyle\sum_i^n Cos(\theta_i)[\beta\mu_{i:n} + \alpha] \\ E[T_2] &= \textstyle\sum_i^n Sin(\theta_i)[\beta\mu_{i:n} + \alpha]. \end{aligned} \tag{5.30}$$

These can be written as

$$\begin{aligned} E(T_1) &= a\alpha + b\beta \\ E(T_2) &= c\alpha + d\beta \end{aligned} \tag{5.31}$$

where

$$\begin{aligned} a &= \sum_i^n Cos(\theta_i) \\ b &= \sum_i^n \mu_{i:n} Cos(\theta_i) \\ c &= \sum_i^n Sin(\theta_i) \\ d &= \sum_i^n \mu_{i:n} Sin(\theta_i). \end{aligned} \tag{5.32}$$

Because the standardized Gaussian distribution is used as the refernce distribution for θ_i, it follows that $a = 0$ [41]. The estimates for β and α are then given by

$$\begin{aligned} \hat{\beta} &= \frac{\hat{E}[T_1]}{\hat{b}} \\ \hat{\alpha} &= \frac{\hat{E}[T_2] - \hat{d}\hat{\beta}}{c} \end{aligned} \tag{5.33}$$

where the symbol $\wedge$ is used to denote an estimate. For n sufficiently large (i.e., $n > 50$), suitable estimates for $E[T_1]$ and $E[T_2]$ are

$$\begin{aligned} \hat{E}[T_1] &= T_1 \\ \hat{E}[T_2] &= T_2. \end{aligned} \tag{5.34}$$

Estimates for b and d rely upon an estimate of $\mu_{i:n}$. $\hat{\mu}_{i:n}$ is obtained from a Monte Carlo simulation of $W_{i:n}$ where $W_{i:n}$ is generated from the known approximating distribution $f(x; 0, 1)$ having zero location and unity scale parameters. $\hat{\mu}_{i:n}$ is the sample mean of $W_{i:n}$ based upon 1000 Monte Carlo trials. Having $\hat{\mu}_{i:n}$, the estimates for b and d are given by

$$\begin{aligned} \hat{b} &= \sum_i^n \hat{\mu}_{i:n} Cos(\theta_i) \\ \hat{d} &= \sum_i^n \hat{\mu}_{i:n} Sin(\theta_i). \end{aligned} \tag{5.35}$$

The scale and location parameters are then estimated by application of eq (5.33).

5.5.2 Shape Parameter Estimation

In this section we present an approximate method for estimating the shape parameter of the approximating PDF. This procedure can be used only when the approximating PDF has a single shape parameter to be determined. Let γ denote the shape parameter of the approximating PDF. Since U_n and V_n are location and scale

invariant, the point Q_n depends only on the sample size n and the shape parameter γ.

Recall that the trajectories on the identification chart are obtained by averaging the results of a large number of trials for U_n and V_n. Consequently, for a given value of n, the coordinates of the points along the trajectory for a specified distribution and can be characterized by

$$\begin{aligned} E(U_n) &= \varphi_1(n,\gamma) \\ E(V_n) &= \varphi_2(n,\gamma) \end{aligned} \tag{5.36}$$

where the complete trajectory is obtained by repeating the large number of trials over a suitable range of γ. On a given trial involving the random data it is likely that the coordinates U_n and V_n for the samples will not coincide with any of the trajectories on the chart. The random data is approximated by that distribution which falls closest to the sample point Q_n. The situation is illustrated in Figure 5.7. $Tr1$ and $Tr2$ denote the trajectories for two different candidate distributions denoted by PDF1 and PDF2, respectively. Let x_0 denote the point on $Tr1$ closest to Q_n. Assume that the linear segment of $Tr1$ on which x_0 falls was drawn between the points (u_1, v_1) and (u_2, v_2). Let the shape parameter values corresponding to these points be denoted by γ_1 and γ_2, respectively. Then the value of the shape parameter corresponding to the sample point Q_n is obtained by linear interpolation and is given by

$$\hat{\gamma} \approx \gamma_1 + \frac{(\gamma_2 - \gamma_1)(x_0 - u_1)}{(u_2 - u_1)} \tag{5.37}$$

where

$$\begin{aligned} x_0 &= \frac{\{A(V_n - v_1) + A^2 u_1 + U_n\}}{(A^2+1)} \\ A &= \frac{(v_2 - v_1)}{(u_2 - u_1)}. \end{aligned} \tag{5.38}$$

The accuracy of the procedure can be improved by employing a non-linear interpolation method. It must be emphasized that the location, scale and shape parameter estimation procedures presented in this section are approximate procedures.

5.6 Assessing the Distributional Properties of SIRVs

A random vector $\mathbf{Y} = [Y_1, Y_2, \ldots Y_N]^T$ is a spherically invariant random vector (SIRV) if its PDF has the form

$$f_{\mathbf{Y}}(\mathbf{y}) = (2\pi)^{-\frac{N}{2}} |\mathbf{\Sigma}|^{-\frac{1}{2}} h_N(p) \tag{5.39}$$

where $p = (\mathbf{y} - \mu)^{\mathbf{T}} \mathbf{\Sigma}^{-1} (\mathbf{y} - \mu)$ is a non-negative quadratic form, μ and $\mathbf{\Sigma}$ are the mean vector and covariance matrix, respectively of $\mathbf{Y}$ and $h_N(p)$ is a non-negative, monotonically decreasing, real valued function for all N.

Recall from Chapter 3 that the PDF of the quadratic form appearing in eq (5.39) is given by

$$f_P(p) = \frac{p^{\frac{N}{2}} - 1}{2^{\frac{N}{2}} \Gamma(\frac{N}{2})} h_N(p) u(p) \tag{5.40}$$

where $\Gamma(\alpha)$ is the Eulero-Gamma function and $u(p)$ is the unit step function. It was also pointed out in Chapter 3 that the PDF of the quadratic form is invariant to the choice of μ and $\mathbf{\Sigma}$. For example, in the multivariate Gaussian case, the PDF of the quadratic form is the well known Chi-square distribution with N degrees of freedom. Therefore, for a given N, the SIRV is uniquely characterized by the quadratic form. In order to identify the PDF of the underlying SIRV it is sufficient to identify the PDF of the quadratic form. This attractive property of SIRVs enables us to study various distributional aspects of the corresponding multivariate samples. When a radar uses coherent processing, the joint PDF of the $2N$ quadrature components is of interest. Eqs (5.39) and (5.40) are then applicable with N replaced by $2N$.

In modeling real world data, the first step is to determine the most appropriate PDF that approximates the data. In the univariate case, the fit and assessment of the goodness of fit for various distributions has been studied extensively and several methods are available for this purpose. However, limited success has been achieved for the multivariate situation. Although a number of multivariate distributions have been developed, the multivariate Gaussian distribution has been the focus of much of the techniques for multivariate analysis [46].

Assessment of the distributional assumptions for multivariate data is a non trivial problem. Several techniques have been proposed to assess multivariate Gaussianity. In a recent paper Ozturk and Romeu [44] give a review of the methods for testing

multivariate Gaussianity. Many of these methods can be modified or generalized to develop goodness of fit methods for SIRVs. If a random vector $\mathbf{Y}$ is an SIRV, then the corresponding marginal distributions must be identical (up to location and scale parameters). Based on this property, one can use the the standard univariate goodness of fit testing procedures to assess the degree of similarity of the marginal distributions of the multivariate data. However, such an approach does not provide a way to assess the joint distribution of the components of the multivariate sample.

Since SIRVs can be uniquely characterized in terms of the quadratic form P, eq (5.40) provides an important property for developing goodness of fit test procedures for SIRVs. Specifically, if the PDF of P can be identified, then the corresponding PDF of the SIRV can also be identified. In fact, many tests for assessment of multivariate Gaussianity are based on the use of this quadratic form [47]. By use of this technique, note that the multivariate distribution approximation problem is reduced to a corresponding univariate distribution approximation of the quadratic form. Any of the classical goodness of fit testing procedures like the Kolmogorov-Smirnov and Chi-Square tests can be used to address the problem of distribution identification of the quadratic form. However, the requirement of large sample sizes for specifying the parameters of the distribution and low power of the test necessitate use of alternate procedures that are more efficient.

A general algorithm was developed in [41] to test for univariate and multivariate normality and has been summarized in sections 5.3-5.5. In this section we propose the use of this algorithm for performing the goodness of fit test for SIRVs. The procedure is summarized here for completeness. Let $\mathbf{Y} = [Y_1, Y_2 \ldots Y_N]^T$ denote a vector of observations. For each observation vector of size N, we compute the corresponding quadratic form $\hat{P}_i$, $(i = 1, 2, \ldots n)$ where the maximum likelihood (ML) estimates of the mean vector of $\mathbf{Y}$ and its covariance matrix are used. For the Gaussian case, it is well known that these ML estimates are the sample mean and the sample covariance matrix, respectively [48]. In Appendix C, it is shown that the same results hold for SIRVs [49]. Our goal is to test whether $\hat{P}_i$, $(i = 1, 2, \ldots n)$ are samples from a certain distribution $F(p; \alpha, \beta, \gamma)$ where α, β are the location and scale parameters, respectively and γ is the shape parameter.

Let $\hat{P_{1:n}} \leq \hat{P_{2:n}} \leq \ldots \leq \hat{P_{n:n}}$ denote the ordered observations of the quadratic

form $\hat{P}_i$ $(i = 1, 2, \ldots n)$. We define the standardized i^{th} sample order statistic as

$$R_{i:n} = \frac{(\hat{P_{i:n}} - \overline{P})}{S_P} \tag{5.41}$$

where $\overline{P}$ and S_P are the sample mean and sample standard deviation, respectively. Corresponding to the i^{th} sample order statistics $R_{1:n}$ through $R_{i:n}$, the point $Q_i = (U_i, V_i)$ is defined where

$$\begin{aligned} U_i &= \tfrac{1}{i}\textstyle\sum_{j=1}^{i} cos\{\pi\Phi(m_{j:n})\}|R_{j:n}| \\ V_i &= \tfrac{1}{i}\textstyle\sum_{j=1}^{i} sin\{\pi\Phi(m_{j:n})\}|R_{j:n}| \end{aligned} \tag{5.42}$$

where $\Phi(.)$ and $m_{j:n}$ were defined in Section 5.3.

For a given set of n multivariate samples, the points Q_i $(i = 1, 2, \ldots n)$ are plotted and joined to obtain a linked vector chart. The linked vectors under the null hypothesis are obtained by averaging the results of 50,000 Monte Carlo trials from the PDF of the quadratic form given by eq (5.40). The proposed test is based on comparing the sample and the null linked vectors. If the null hypothesis is true, then we expect that the sample linked vectors will follow the null linked vectors closely.

Finally, a formal goodness of fit test is performed using the terminal point of the null linked vectors (i.e $Q_n = (U_n, V_n)$). Using the central limit theorem, as outlined in section 5.3, confidence ellipses centered at Q_n for the null linked vectors are obtained. If the terminal point of the sample linked vectors does not fall inside the $100(1-\alpha)\%$ confidence ellipse, then the corresponding null hypothesis is rejected at the α level of significance. Note that the Q_n test provides an interesting graphical representation of the data. An example of such a graphical representation is given in Fig 5.5 for testing a multivariate Gaussian distribution with $n = 50$ and $N = 4$.

It should be noted that the Q_n statistic is location and scale invariant. In other words it is independent of the location and scale parameters. However, it depends on the shape parameter of the null distribution. Assessment of the distributional assumptions of distributions that have shape parameters is conceptually different from those that do not. In the former case, we test whether the sample comes from a family of distributions while in the latter case, we test for a simple distribution. One possibility for dealing with this problem is to specify the value of the shape parameter

and perform the test in the usual way. If the shape parameter cannot be specified, then an adaptive approach which uses a sample estimate of the shape parameter must be employed.

Advantages of using the Q_n procedure are explained in [41]. Usually the classical goodness of fit tests end up with either rejecting or accepting the null hypothesis. An attractive property of the Q_n procedure is that it provides some information about the true distributions if the null hypothesis is rejected. Using this property an algorithm for characterizing and identifying the distributions can be developed. The next section explains these ideas.

5.7 Distribution Identification of SIRVs

Following the same procedure described in Section 5.4, where the reference distribution was Gaussian, an identification chart can be generated for each of quadratic form PDFs of the SIRVs listed in Tables 5.3 and 5.4. Recall from Chapter 3 that the PDF of the quadratic form is invariant to the choice of μ and $\mathbf{\Sigma}$. Hence, for simplicity, the trajectories for the PDFs of the quadratic forms of the SIRVs listed in Tables 5.1 and 5.2 are obtained by generating the SIRVs having zero mean and identity covariance matrix. Each point on a trajectory is obtained by averaging the results of 2000 Monte Carlo trials of size $n = 100$. As before, PDFs which do not have shape parameters are represented by a single point in the U-V plane while those which have shape parameters generate a trajectory in the U-V plane by changing the shape parameter.

Assuming coherent radar processing, Table 5.3 and Table 5.4 provide a library of $h_{2N}(p)$ for various multivariate SIRV PDFs. An example of the identification chart is given in Fig 5.6 for $N = 4$ and $n = 50$ where the expected values of $Q_n = (U_n, V_n)$ is plotted for various distributions. The Gaussian distribution was used as the reference distribution. The SIRVs listed in Table 5.1 and Table 5.2 are included in the chart and labeled by number. It is noted that the multivariate Gaussian (1), Laplace (2) and Cauchy (3) distributions are represented by single points on the chart while the multivariate K-distribution (8), Chi (9), Generalized Rayleigh (10) Weibull (11) and Rician (12) are represented by trajectories. The Student-t distribution (4, 5, 6, 7) with degrees of freedom 3, 5, 10 and 15, respectively, is also shown in the chart. The trajectories for each distribution were obtained by joining 10 points resulting from the

use of the distributions with parameter values listed in Table 5.3. Each point in the chart is obtained by simulating 2000 samples from the corresponding distributions. The methods developed by Rangaswamy et al. [22, 50] were used to generate the multivariate samples.

The identification chart provides an interesting display for identifying and characterizing the distributions. Also, relationships between the various distributions are clearly seen. For example, as their parameters are varied, certain distributions approach the multivariate Gaussian distribution. Also, for appropriately chosen parameters, the multivariate Weibull distribution and the Generalized Rayleigh distribution can be seen to coincide. For a given N-variate sample of size n, the statistic Q_n based on the sample quadratic forms can be computed and plotted on the identification chart. Then the nearest distribution to the sample point is identified to be the best candidate for the underlying true distribution of the data. An example of such an identification is shown in Figure 5.6 where a well known data set (i.e. Iris Setosa [51]) is used to obtain a value for Q_n and is denoted by the point S. The Iris Setosa data consists of four measurements taken from 50 plants. It is seen from Figure 5.6 that the best candidate for approximating the data is the multivariate Chi(9) distribution.

We point out that there are other methods which can be used for the distribution identification problem. A commonly used technique is the $Q - Q$ plot. To identify the underlying distribution the sample quantiles are plotted against the expected quantiles of a reference distribution. Then the resulting shape of the plotted curve is taken as a basis for identifying the corresponding candidate for the true distributions. However, the identification is made on a subjective basis. Even then the procedure is not very easy. Another well known approach for distinguishing between distribution is to characterize them via their skewness (α_3) and kurtosis (α_4) coefficients. In this case, all the distributions are represented by points on the α_3- α_4 plane and the sample data point is compared with the points representing the theoretical distributions in the same way as in the Q_n procedure. However, estimates of α_3 and α_4 are known to be highly sensitive to extreme observations and therefore, large sample sizes are necessary to perform the identification for a given degree of accuracy.

5.8 Parameter Estimation

It is well known that the maximum likelihood estimate of the covariance matrix of a Gaussian random vector is the sample covariance matrix. Interestingly enough, it has been shown in [49]that the maximum likelihood estimate of the covariance matrix $\mathbf{\Sigma}$ for SIRVs is the same sample covariance matrix used in the Gaussian case. From eq (5.40), it is clear that the expected value of the quadratic form can be expressed as

$$E[P] = \varphi(N, \gamma) \tag{5.43}$$

where γ is the shape parameter of the distribution. For those SIRVs where $\varphi(.)$ can be evaluated in closed form and is invertible, the sample mean of P, denoted by $\overline{P}$ can be used to estimate the shape parameter according to

$$\hat{\gamma} = \varphi^{-1}\{\overline{P}, N\}. \tag{5.44}$$

where $\overline{P} = \frac{1}{n}\sum_{i=1}^{n} P_i$. For example, in case of the K-distribution, we have $E[P] = 2\alpha N$ where α is the shape parameter of the K-distribution. Clearly, the shape parameter is given by $\hat{\alpha} = \frac{\overline{P}}{2N}$. Unfortunately, it is not always possible to obtain an invertible closed form expression for $\varphi(.,.)$. The shape parameter estimation procedure suggested here is not suitable in such a case. An alternate method for the parameter estimation problem is then needed.

In this section we propose to use the Q_n statistic to obtain an approximate estimator for the shape parameter. The underlying procedure is explained in [41] and is summarized here. Let the points (U_1, V_1) and (U_2, V_2) denote the coordinates of Q_n corresponding to parameters γ_1 and γ_2 respectively, of a given SIRV. Suppose these points are the nearest points, on the trajectory for the identified distribution to the sample point $Q_n = (U_n, V_n)$ corresponding to the data. Then by using linear interpolation, an approximate estimator of γ is given by

$$\hat{\gamma} \approx \gamma_1 + \frac{(\gamma_2 - \gamma_1)(x_0 - U_1)}{(U_2 - U_1)} \tag{5.45}$$

Table 5.1: Table of Standard Forms of Univariate PDFs Used For Identification Chart of Figure 5.3

Distribution	Standard Form $f_Y(y)$
Gaussian	$(\sqrt{2\pi})^{-1}exp(-\frac{y^2}{2})$ $-\infty < y < \infty$
Uniform	1 $0 < y < 1$
Exponential	$exp(-y)$ $(0 < y < \infty)$
Laplace	$0.5exp(-\|y\|)$ $-\infty < y < \infty$
Logistic	$exp(-y)[1+exp(-y)]^{-2}$ $-\infty < y < \infty$
Cauchy	$\frac{1}{\pi(1+y^2)}$ $-\infty < y < \infty$
Extreme Value (Type 1)	$exp(-y)exp[-exp(-y)]$ $-\infty < y < \infty$
Gumbel (Type 2)	$\gamma y exp(-\gamma-1)exp(-y^{-\gamma})$ $-\infty < y < \infty$
Gamma	$\frac{1}{\Gamma(\alpha)}exp(-y)y^{\gamma-1}$ $0 < y < \infty$
Pareto	$\frac{\gamma}{y^{\gamma+1}}$ $y > 1$, $\gamma > 0$
Weibull	$\gamma y^{\gamma-1}exp(-y^{\gamma})$ $y > 0$
Lognormal	$\frac{\gamma}{\sqrt{2\pi}y}exp[-\frac{\{\gamma log(y)\}^2}{2}$ $y > 0$

where

$$x_0 = \frac{\{A(V_n - V_1) + A^2U_1 + U_n\}}{(A^2+1)}$$
$$A = \frac{(V_2 - V_1)}{(U_2 - U_1)} \tag{5.46}$$

The accuracy of the proposed estimator for γ depends on the distance between the sample point Q_n and the corresponding curve. If necessary, the approximation can be improved by using non-linear interpolation methods.

5.9 Conclusions

In this Chapter we have addressed the problem of distribution identification of radar clutter under the assumption that the clutter can be characterized as a SIRP. First and foremost, we have shown that the multivariate distribution identification problem for SIRPs can be reduced to an equivalent univariate distribution identification problem of a non-negative quadratic form, resulting in considerable processing simplicity. A new algorithm which provides a graphical representation for the goodness of fit test and the distribution identification has been used. This algorithm, while conceptually simple, is extremely efficient while dealing with small sample sizes. Therefore, it is suitable for use in a variety of practical applications. Finally, based on this algorithm, a new approach has been proposed for estimating the shape parameter of SIRPs.

Table 5.2: Table of General Form of Univariate PDFs Used For Identification Chart of Figure 5.3

Distribution	General Form $f_X(x)$
Gaussian	$(\sqrt{2\pi}\beta)^{-1}exp(-\frac{(x-\alpha)^2}{2\beta^2})$ $-\infty < x < \infty$
Uniform	$\frac{1}{\beta}$ $\alpha < x < \alpha+\beta$
Exponential	$\frac{1}{\beta}exp(-\frac{(x-\alpha)}{\beta})$ $\alpha < x < \infty$
Laplace	$\frac{0.5}{\beta}exp[-\lvert\frac{(x-\alpha)}{\beta}\rvert]$ $-\infty < x < \infty$
Logistic	$\frac{1}{\beta}exp[-\frac{(x-\alpha)}{\beta}][1+exp(-\frac{(x-\alpha)}{\beta})]^{-2}$ $-\infty < x < \infty$
Cauchy	$\frac{1}{\pi\beta[1+\frac{(x-\alpha)^2}{\beta^2}]}$ $-\infty < x < \infty$
Extreme Value (Type 1)	$\frac{1}{\beta}exp[-\frac{(x-\alpha)}{\beta}]exp[-exp\{-\frac{(x-\alpha)}{\beta}\}]$ $-\infty < x < \infty$
Gumbel (Type 2)	$\frac{\gamma}{\beta}\frac{(x-\alpha)}{\beta}exp(-\gamma-1)exp[-\frac{(x-\alpha)^{-\gamma}}{\beta^\gamma}]$ $-\infty < x < \infty$
Gamma	$\frac{1}{\beta\Gamma(\alpha)}exp[-\frac{(x-\alpha)}{\beta}](\frac{x-\alpha}{\beta})^{\gamma-1}$ $\alpha < x < \infty$
Pareto	$\frac{\gamma}{\beta}\frac{1}{(\frac{x-\alpha}{\beta})^{\gamma+1}}$ $x > \alpha+\beta,\ \gamma > 0$
Weibull	$\frac{\gamma}{\beta}(\frac{x-\alpha}{\beta})^{\gamma-1}exp[-(\frac{x-\alpha}{\beta})^\gamma]$ $x > \alpha$
Lognormal	$\frac{\gamma}{\sqrt{2\pi}\beta(\frac{x-\alpha}{\beta})}exp[-\frac{\{\gamma log(\frac{x-\alpha}{\beta})\}^2}{2}$ $x > \alpha$

Table 5.4: SIRVs obtained from the marginal envelope PDF

Marginal PDF	$h_{2N}(p)$
Chi	$(-2)^{N-1}A\sum_{k=1}^{N}G_k p^{\nu-k}exp(-Bp)$
	$G_k = \begin{pmatrix} N-1 \\ k-1 \end{pmatrix}(-1)^{k-1}B^{k-1}\frac{\Gamma(\nu)}{\Gamma(\nu-k+1)}$
	$A = \frac{2}{\Gamma(\nu)}(b\sigma)^{2\nu}$
	$B = b^2\sigma^2$
	$\nu \leq 1$
Weibull	$\sum_{k=1}^{N}C_k p^{\frac{kb}{2}-N}exp(-Ap^{\frac{b}{2}})$
	$A = a\sigma^b$
	$C_k = \sum_{m=1}^{k}(-1)^{m+N}2^N\frac{A^k}{k!}\begin{pmatrix} k \\ m \end{pmatrix}\frac{\Gamma(1+\frac{mb}{2})}{\Gamma(1+\frac{mb}{2}-N)}$
	$b \leq 2$
Gen. Rayleigh	$\sum_{k=1}^{N-1}D_k p^{\frac{k\alpha}{2}-N+1}exp(-Bp^{\frac{\alpha}{2}})$
	$A = \frac{\alpha^2\alpha}{\beta^2\Gamma(\frac{2}{\alpha})}$
	$B = \beta^{-\alpha}\sigma^\alpha$
	$D_k = \sum_{m=1}^{k}(-1)^{m+N-1}2^{N-1}\frac{B^k}{k!}\begin{pmatrix} k \\ m \end{pmatrix}\frac{\Gamma(1+\frac{m\alpha}{2})}{\Gamma(2+\frac{m\alpha}{2}-N)}$
	$\alpha \leq 2$
Rician	$\frac{\sigma^{2N}}{(1-\rho^2)^{N-\frac{1}{2}}}\sum_{k=0}^{N-1}\begin{pmatrix} N-1 \\ k \end{pmatrix}(-1)^k(\frac{\rho}{2})^k\xi_k exp(-A)$
	$\xi_k = \sum_{m=0}^{k}\begin{pmatrix} k \\ m \end{pmatrix}I_{k-2m}(\rho A),\ A = \frac{p\sigma^2}{2(1-\rho^2)}$

Table 5.3:

Some Monte Carlo moments of U and V

N	U				V			
	MEAN	VARIANCE	SKEW.	CURTOS.	MEAN	VARIANCE	SKEW.	CURTOS.
3	0.00037	0.00846	-0.0036	1.7594	0.47067	0.00168	-0.3174	1.8720
4	0.00052	0.00585	-0.0157	3.1854	0.43458	0.00448	0.3599	2.5413
5	-0.00030	0.00472	0.0186	2.6987	0.41276	0.00475	0.0141	2.2890
6	0.00007	0.00391	-0.0055	2.8623	0.39793	0.00459	-0.0243	2.5650
7	0.00021	0.00333	-0.0033	2.9035	0.38763	0.00426	-0.0552	2.6668
8	-0.00025	0.00290	-0.0025	2.9141	0.38000	0.00399	-0.0694	2.7219
9	0.00008	0.00257	0.0050	2.9201	0.37362	0.00369	-0.0551	2.7671
10	-0.00051	0.00229	0.0041	2.9428	0.36865	0.00349	-0.0528	2.7722
11	0.00032	0.00206	0.0110	2.9936	0.36516	0.00322	-0.0384	2.7936
12	0.00012	0.00189	-0.0213	2.9812	0.36154	0.00302	-0.0496	2.8342
13	0.00005	0.00174	0.0088	2.9905	0.35858	0.00286	-0.0362	2.8251
14	-0.00012	0.00160	-0.0023	3.0230	0.35633	0.00266	-0.0466	2.8730
15	0.00003	0.00151	-0.0133	3.0185	0.35457	0.00253	-0.0370	2.8489
16	0.00008	0.00139	-0.0193	3.0052	0.35271	0.00242	-0.0297	2.8659
17	-0.00005	0.00132	0.0073	3.0413	0.35108	0.00227	-0.0304	2.8528
18	0.00004	0.00124	-0.0018	3.0004	0.34973	0.00218	-0.0088	2.8815
19	0.00041	0.00117	-0.0070	3.0683	0.34829	0.00207	-0.0297	2.8922
20	0.00012	0.00110	0.0065	3.0402	0.34728	0.00197	-0.0344	2.9201
21	-0.00011	0.00105	-0.0013	2.9875	0.34632	0.00189	-0.0368	2.9358
22	0.00008	0.00101	-0.0043	3.0316	0.34525	0.00183	-0.0097	2.8972
23	0.00000	0.00097	-0.0122	2.9970	0.34431	0.00176	-0.0111	2.9226
24	-0.00009	0.00091	-0.0141	3.0537	0.34360	0.00170	-0.0114	2.8925
25	-0.00006	0.00088	-0.0112	3.0061	0.34273	0.00161	-0.0260	2.9097
26	0.00013	0.00084	-0.0153	3.0136	0.34225	0.00156	-0.0387	2.9512
27	0.00003	0.00081	0.0056	3.0316	0.34167	0.00150	-0.0165	2.9120
28	0.00010	0.00078	-0.0030	3.0137	0.34120	0.00146	-0.0155	2.9277
29	-0.00016	0.00076	0.0052	3.0226	0.34056	0.00143	-0.0282	2.9290
30	-0.00006	0.00073	0.0016	3.0383	0.34009	0.00138	-0.0131	2.9298
31	-0.00007	0.00070	-0.0157	3.0120	0.33980	0.00132	-0.0308	2.9065
32	0.00000	0.00069	-0.0055	3.0323	0.33904	0.00129	-0.0083	2.9174
33	0.00009	0.00066	-0.0051	3.0171	0.33901	0.00126	-0.0215	2.9402
34	-0.00012	0.00064	-0.0050	3.0454	0.33827	0.00122	-0.0056	2.9411
35	0.00002	0.00062	0.0023	2.9721	0.33815	0.00119	-0.0126	2.9340
36	0.00000	0.00060	-0.0048	2.9961	0.33789	0.00115	-0.0139	2.9395
37	0.00003	0.00059	-0.0144	3.0520	0.33752	0.00114	0.0082	2.9454
38	-0.00007	0.00057	-0.0002	3.0222	0.33739	0.00111	-0.0187	2.9512
39	0.00000	0.00056	0.0191	3.0391	0.33712	0.00107	-0.0130	2.9595
40	-0.00007	0.00055	0.0161	3.0269	0.33682	0.00104	-0.0267	2.9823
41	-0.00001	0.00052	-0.0189	3.0157	0.33649	0.00103	-0.0085	2.9511
42	0.00010	0.00052	0.0076	2.9818	0.33602	0.00100	-0.0074	2.9569
43	-0.00006	0.00050	0.0036	3.0233	0.33578	0.00098	-0.0099	2.9548
44	0.00001	0.00050	0.0044	3.0025	0.33583	0.00096	-0.0161	2.9515
45	-0.00022	0.00048	0.0025	3.0340	0.33568	0.00093	-0.0128	2.9680
46	0.00004	0.00047	0.0058	3.0439	0.33548	0.00092	-0.0241	2.9734
47	0.00011	0.00045	-0.0072	2.9621	0.33532	0.00089	-0.0068	2.9415
48	0.00004	0.00045	0.0015	3.0596	0.33520	0.00087	-0.0077	2.9795
49	-0.00005	0.00044	-0.0015	3.0063	0.33491	0.00086	-0.0270	2.9255
50	0.00006	0.00044	0.0104	2.9943	0.33473	0.00084	-0.0322	2.9442
51	-0.00007	0.00042	-0.0014	3.0078	0.33448	0.00083	0.0030	2.9332
52	-0.00011	0.00041	0.0086	2.9636	0.33420	0.00081	-0.0207	3.0032
53	0.00000	0.00041	0.0046	3.0510	0.33435	0.00080	-0.0141	2.9716
54	-0.00008	0.00040	-0.0050	2.9991	0.33417	0.00079	0.0080	2.9615
55	0.00006	0.00040	0.0117	3.0644	0.33415	0.00078	0.0028	2.9750
56	-0.00003	0.00038	-0.0100	3.0360	0.33404	0.00076	-0.0178	2.9792
57	-0.00017	0.00038	0.0024	3.0245	0.33380	0.00075	-0.0012	2.9731
58	0.00003	0.00037	0.0091	2.9809	0.33353	0.00073	-0.0038	2.9540
59	0.00006	0.00037	-0.0080	3.0141	0.33371	0.00072	-0.0128	2.9767
60	0.00006	0.00036	0.0189	2.9986	0.33362	0.00071	-0.0061	2.9756
61	-0.00004	0.00035	0.0015	2.9801	0.33339	0.00070	0.0001	2.9630
62	-0.00011	0.00035	0.0092	2.9575	0.33332	0.00069	-0.0189	2.9607
63	-0.00004	0.00034	-0.0160	3.0105	0.33315	0.00069	-0.0124	2.9839
64	0.00007	0.00033	-0.0101	3.0385	0.33300	0.00068	-0.0098	2.9753
65	-0.00001	0.00033	0.0030	3.0394	0.33277	0.00066	0.0018	2.9691
66	0.00013	0.00033	0.0282	3.0242	0.33273	0.00065	-0.0206	2.9699
67	0.00005	0.00032	0.0199	3.0353	0.33273	0.00064	-0.0151	2.9870
68	0.00007	0.00032	0.0138	3.0174	0.33265	0.00063	-0.0028	2.9478
69	0.00001	0.00031	0.0091	3.0329	0.33263	0.00062	-0.0022	2.9994
70	-0.00001	0.00030	-0.0072	3.0419	0.33230	0.00062	0.0111	2.9338
71	0.00018	0.00030	0.0129	3.0295	0.33248	0.00061	-0.0105	2.9810
72	-0.00004	0.00030	0.0067	3.0035	0.33231	0.00060	-0.0231	2.9837
73	-0.00010	0.00030	-0.0108	3.0114	0.33204	0.00059	-0.0071	2.9928
74	0.00002	0.00029	0.0082	3.0396	0.33210	0.00058	-0.0096	2.9811
75	-0.00001	0.00028	-0.0138	3.0576	0.33221	0.00058	-0.0013	2.9766
76	0.00001	0.00028	0.0150	2.9840	0.33202	0.00056	0.0057	2.9676
77	0.00002	0.00028	-0.0006	3.0450	0.33204	0.00055	0.0064	2.9976
78	0.00001	0.00028	0.0187	2.9942	0.33183	0.00056	-0.0099	2.9492
79	-0.00001	0.00027	0.0142	3.0058	0.33195	0.00054	-0.0021	2.9621
80	0.00009	0.00027	-0.0015	2.9686	0.33184	0.00054	-0.0041	2.9766
81	0.00000	0.00027	0.0094	3.0087	0.33175	0.00053	-0.0045	2.9790
82	-0.00002	0.00026	-0.0045	3.0379	0.33182	0.00052	-0.0199	2.9482
83	0.00012	0.00026	0.0130	2.9860	0.33164	0.00052	-0.0102	2.9827
84	0.00004	0.00026	0.0038	3.0150	0.33167	0.00051	-0.0053	2.9966
85	0.00001	0.00025	-0.0090	3.0179	0.33158	0.00051	0.0110	2.9789
86	-0.00012	0.00025	-0.0082	2.9790	0.33144	0.00050	-0.0045	2.9701
87	-0.00001	0.00025	-0.0125	3.0148	0.33136	0.00049	0.0042	2.9658
88	0.00001	0.00024	-0.0044	2.9644	0.33126	0.00049	0.0028	2.9725
89	0.00003	0.00024	-0.0060	3.0055	0.33123	0.00048	-0.0245	2.9970
90	-0.00004	0.00024	-0.0149	2.9977	0.33110	0.00048	-0.0047	2.9775
91	-0.00011	0.00023	-0.0031	2.9945	0.33113	0.00047	0.0022	2.9718
92	0.00003	0.00023	0.0052	3.0332	0.33115	0.00047	0.0019	2.9709
93	-0.00001	0.00023	-0.0034	2.9954	0.33136	0.00047	0.0138	2.9993
94	0.00016	0.00023	0.0202	3.0274	0.33115	0.00046	-0.0221	3.0140
95	0.00004	0.00022	-0.0046	3.0133	0.33100	0.00046	-0.0097	2.9855
96	-0.00002	0.00023	-0.0026	3.0332	0.33086	0.00045	-0.0102	2.9731
97	0.00014	0.00022	0.0147	2.9938	0.33083	0.00045	-0.0136	2.9586
98	-0.00002	0.00022	-0.0049	3.0553	0.33081	0.00044	-0.0041	2.9902
99	0.00002	0.00022	0.0138	3.0012	0.33091	0.00044	0.0032	2.9974
100	0.00002	0.00021	0.0132	3.0208	0.33086	0.00043	0.0007	2.9950

Table 5.5: SIRVs obtained from the marginal characteristic function

Marginal PDF	$h_{2N}(p)$
Gaussian	$exp(-\frac{p}{2})$
Laplace	$b^{2N}(b\sqrt{p})^{1-N}K_{N-1}(b\sqrt{p})$
Cauchy	$\frac{2^N b\Gamma(\frac{1}{2}+N)}{\sqrt{\pi}(b^2+p)^{N+\frac{1}{2}}}$
K-distribution	$\frac{b^{2N}}{\Gamma(\alpha)}\frac{(b\sqrt{p})^{\alpha-N}}{2^{\alpha-1}}K_{N-\alpha}(b\sqrt{p})$
Student-t	$\frac{2^N b^{2\nu}\Gamma(\nu+N)}{\Gamma(\nu)(b^2+p)^{N+\nu}}$

Table 5.6: Shape Parameters of the SIRVs Used for the Identification Chart

K-Distribution	0.1, 0.2, 0.3, 0.4, 0.5, 0.7, 0.9, 1.1, 1.5, 1.9
Chi	0.15, 0.2, 0.25, 0.3, 0.35, 0.4, 0.5, 0.6, 0.75, 0.95
Gen. Rayleigh	0.2, 0.3, 0.4, 0.5, 0.6, 0.7, 0.8, 1.0, 1.5, 2.0
Weibull	0.3, 0.4, 0.6, 0.8, 1.0, 1.2, 1.4, 1.6, 1.8, 2.0
Rician	0.15, 0.2, 0.3, 0.4, 0.5, 0.6, 0.7, 0.8, 0.85, 0.9

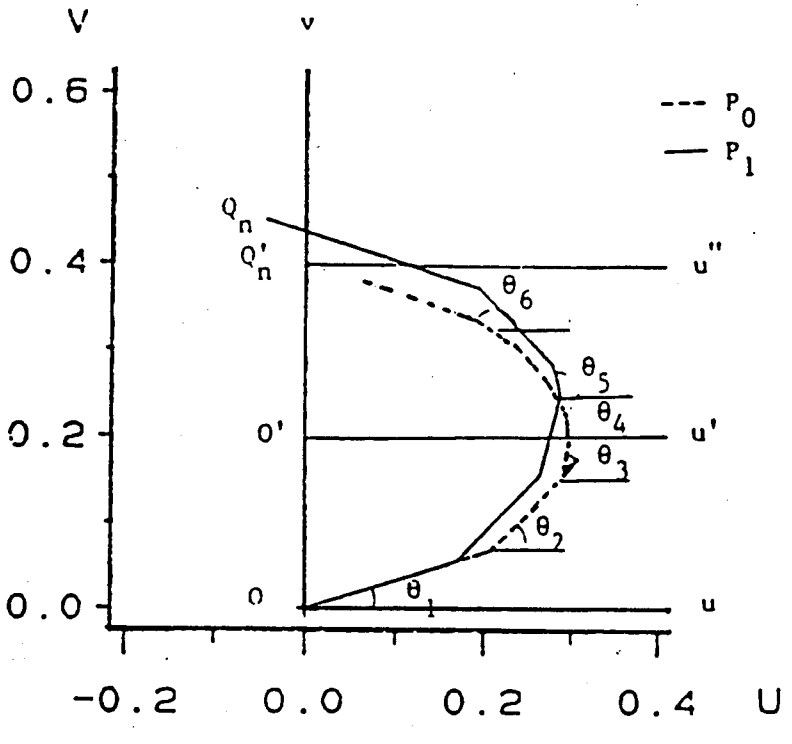

Figure 5.1: Linked Vector Chart:Dashed lines P_0= Null Linked Vectors, Solid Lines P_1= Sample Linked Vectors

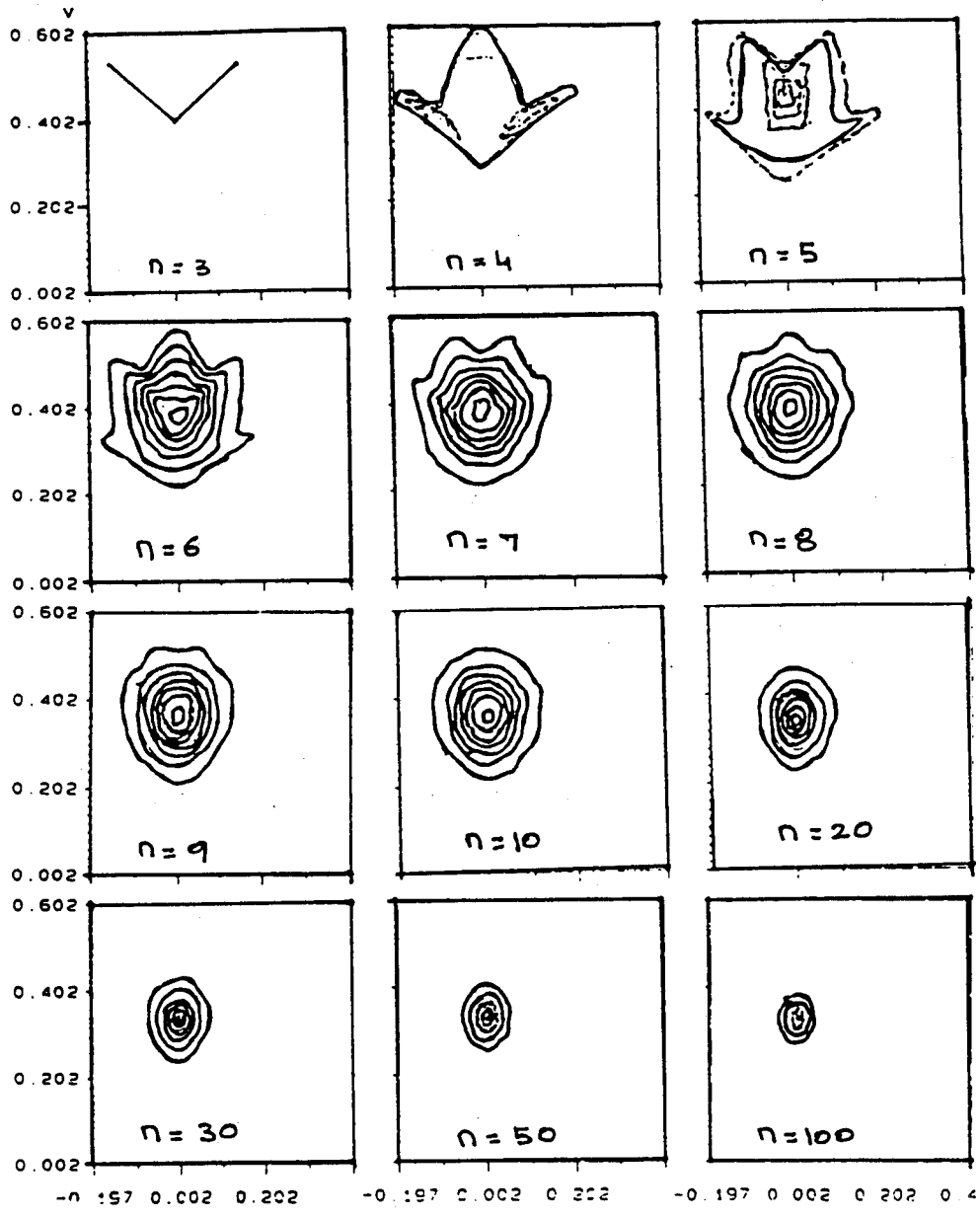

Figure 5.2: Empirical Distribution of Q_n for several values of n

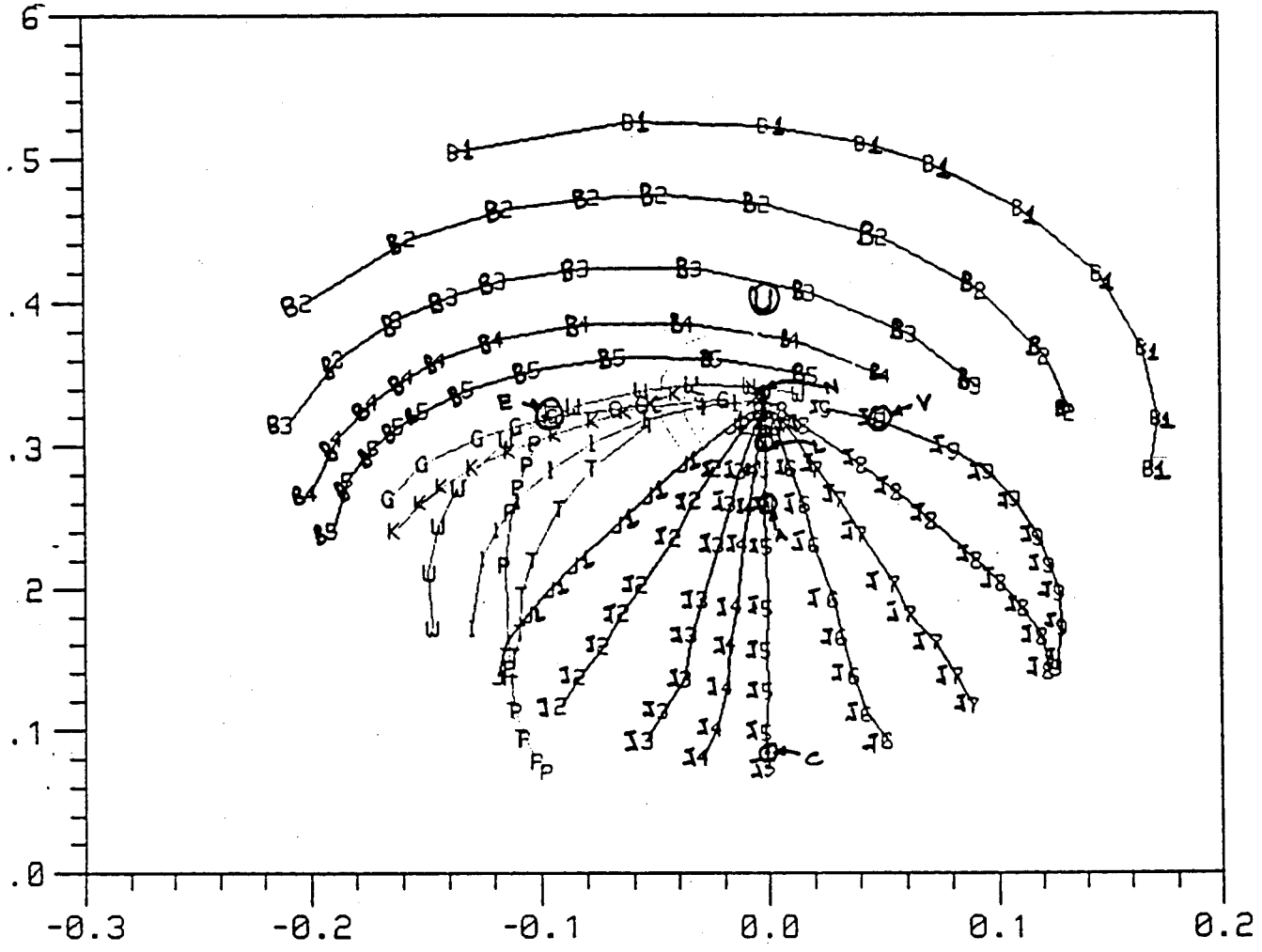

Figure 5.3: Identification Chart for Univariate Distributions Based on 1000 samples (n=50); B1-B5=Beta, J1-J9=SU Johnson, G=Gamma, W=Weibull, K=K-distribution, P=Pareto, l=Log-normal, T=Gumbel, E=Exponential, V=Extreme Value, A=Laplace, L=Logistic, U=Uniform, N=Normal, C=Cauchy

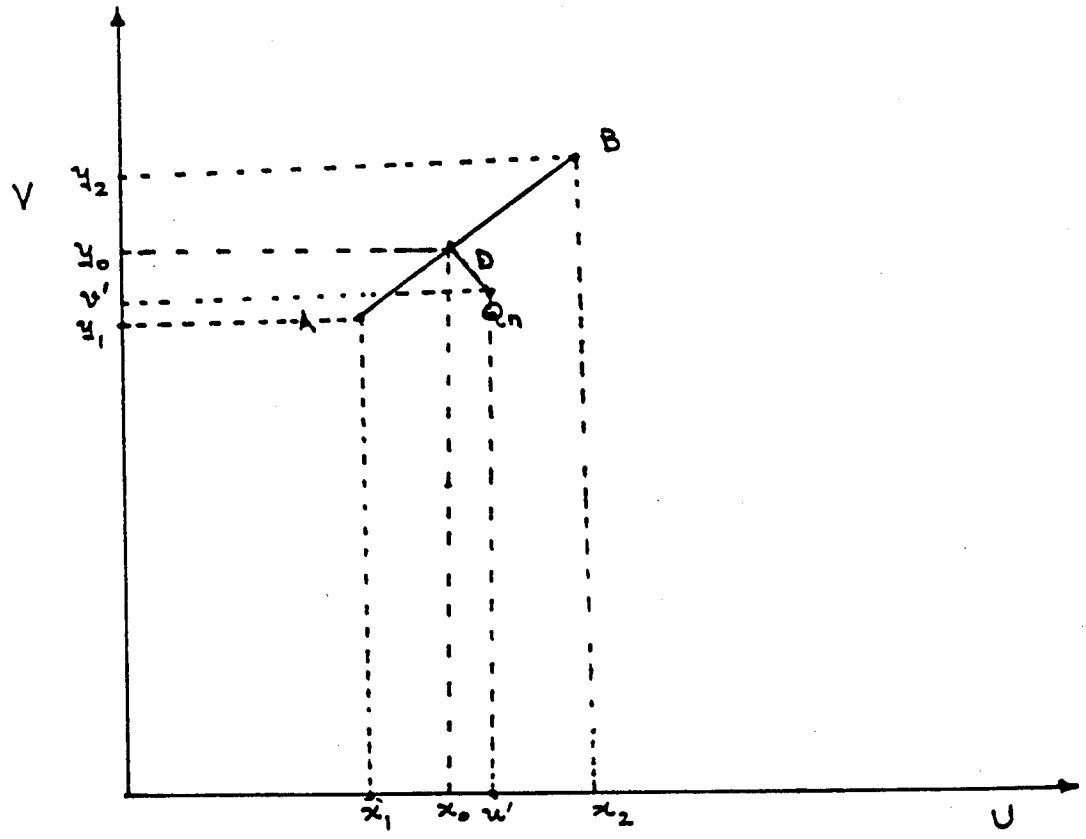

Figure 5.4: Distance Computation

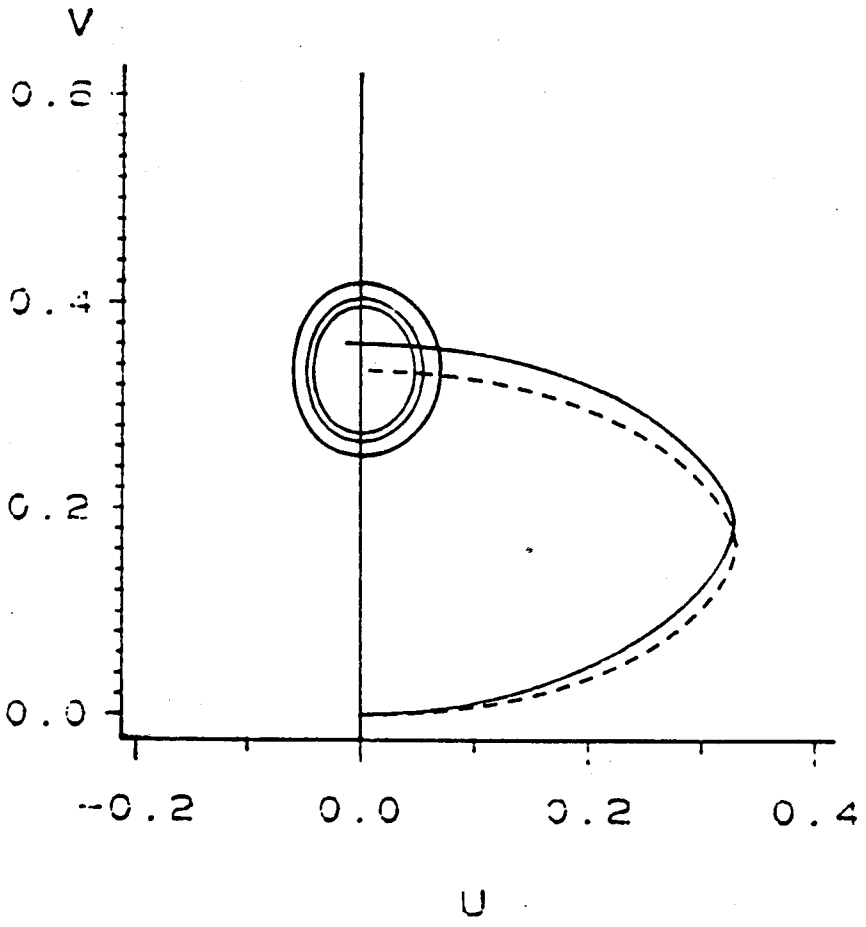

Figure 5.5: Goodness of Fit Test for SIRVs using the Q_n Procedure. 90, 95 and 99% contours for the Gaussian distribution. Broken Line = Null distribution Pattern

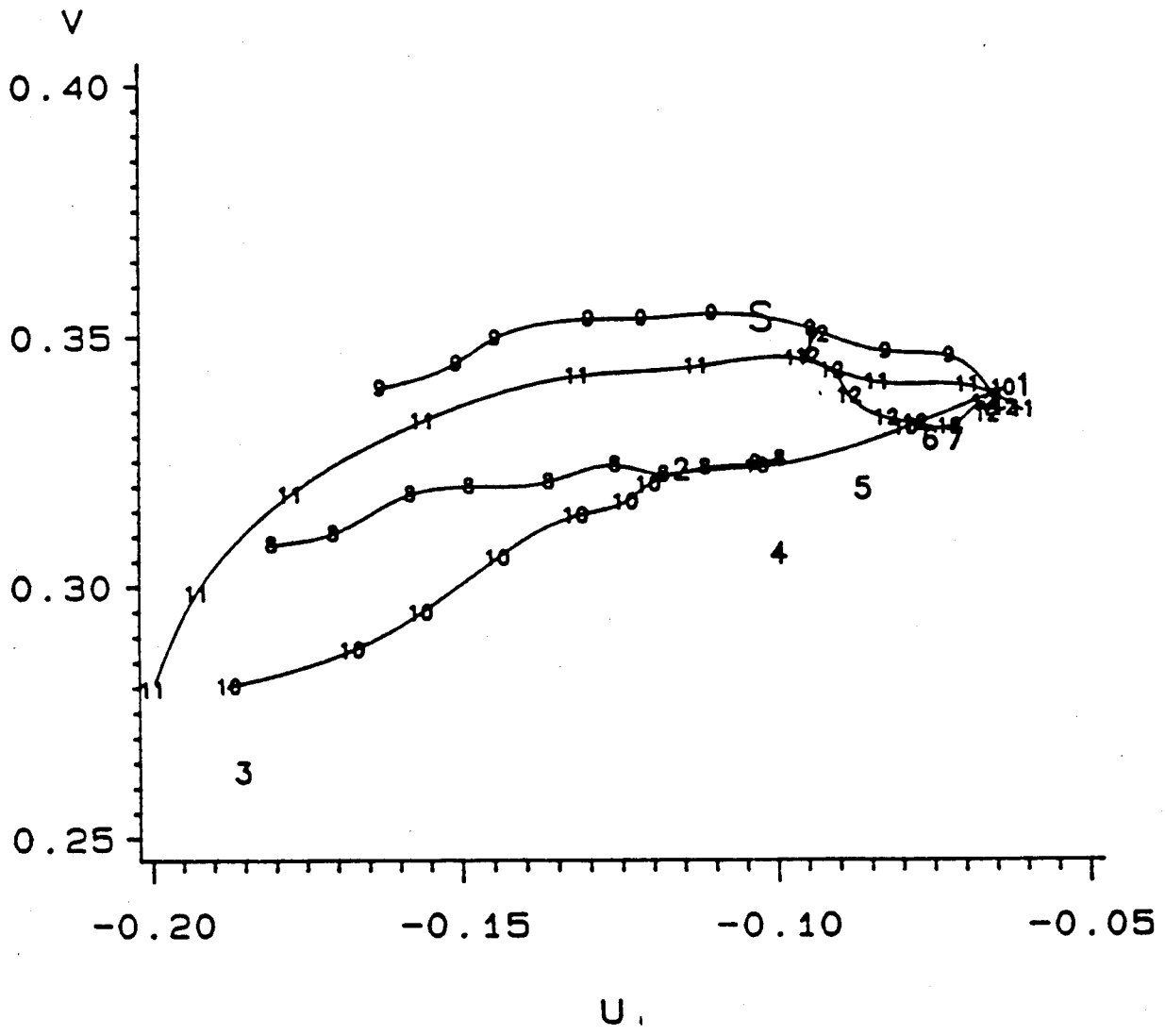

Figure 5.6: Identification Chart for SIRVs (n=2000, N=4) 1 = Gaussian, 2 = Laplace, 3 = Cauchy, 4, 5, 6, 7 = Student-t, 8 = K-distribution, 9 = Chi, 10 = Generalized Rayleigh, 11 = Weibull, 12 = Rician

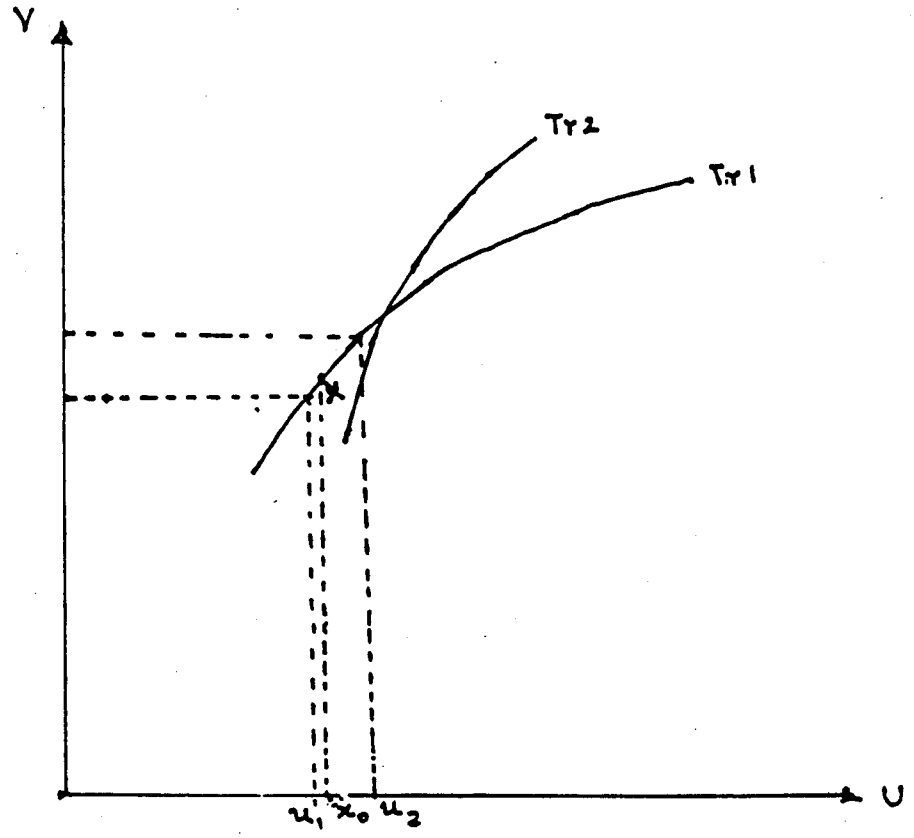

Figure 5.7: Shape Parameter Estimation

Chapter 6

Conclusions

6.1 General Remarks

We present conclusions and suggestions for future work in this Chapter. We have addressed the problem of modeling, simulation and distribution identification (multivariate) of correlated non-Gaussian radar clutter that can be characterized as a spherically invariant random process (SIRP). The SIRP model for the clutter belongs to the class of exogenous product models, where the clutter process can be decomposed as a product of two independent random processes. One of the processes is Gaussian while the other is a highly correlated non-Gaussian process, which modulates the Gaussian process. The SIRP model arises as a special case when the modulating process is a non-negative random variable. This in turn, imposes the requirement that the modulating random process have a decorrelation time much larger than that of the Gaussian process, so that the modulating process is approximately constant in a given time observation interval.

For example, consider a high resolution airborne radar operating in a maritime environment at low grazing angles. The overall sea clutter return is composed of returns from the capillary waves and the gravity waves. The capillary waves correspond to a rapidly time variant process. It has been pointed out in [19] that the returns from the capillary waves can be approximated as being jointly Gaussian. Therefore, the returns from the the capillary waves can be modeled by a Gaussian random process. The gravity waves correspond to a slowly time variant phenomenon. Furthermore, it has been shown in [19, 3, 7] that the decorrelation time of the slowly time variant process is much larger than that of the Gaussian process. Consequently, the

slowly time variant process can be approximated by a non-negative random variable. Hence, the SIRP model is applicable in this case. In fact, if the non-negative random variable has a Chi-distribution, the overall sea clutter returns are characterized by a K-distribution. We have pointed out that the K-distribution is a member of the family of SIRPs. Therefore, for this case, the SIRP characterization enables us to determine the optimal radar signal processor. The validity of other SIRPs as models for radar clutter must be determined through an experimental effort.

This dissertation has made the following significant original contributions.

1. Application of the theory of SIRP to obtain a library of multivariate PDFs of correlated non-Gaussian random vectors.

2. Derivation of the result that an SIRV is uniquely characterized through the knowledge of the PDF of a quadratic form.

3. Development of elegant and powerful simulation procedures for computer generation of SIRVs.

4. Reduction of the distribution identification for SIRVs from a multivariate problem to an equivalent univariate distribution identification problem.

As a result of these contributions, the problem of modeling, simulation and distribution identification for SIRVs has resulted in tremendous computational simplicity. Consequently, the schemes developed here are suitable for use in several practical applications.

6.2 Suggestions for Future Research

It has been pointed out in this work that many of the attractive properties of Gaussian random processes also apply to SIRPs. Consequently, the use of SIRPs provides a convenient vehicle for solving several signal detection and estimation problems involving correlated non-Gaussian processes. In particular, the following issues may be addressed as extensions of this work.

1. Use of experimental data to determine the applicability of the SIRP model for modeling clutter in radar, sonar and image processing.

2. Application of the Kalman filter for SIRPs.

3. Use of SIRPs for radar ambiguity function analysis.

4. Application of SIRPs for canceling interference in digital communications.

5. Use of SIRPs in innovations based multichannel detection and estimation.

6. Use of SIRPs in linear predictive coding for speech processing.

7. Use of neural networks for identifying SIRPs.

8. Information theoretic considerations, such as channel capacity and rate distortion theory, for SIRPs.

9. Use of SIRPs in parameter estimation involving the log likelihood function.

Appendix A

Properties of SIRVs

In this appendix we present some original proofs for properties of SIRPs stated in the literature.

A.1 Statistical Independence

An SSRV $\mathbf{X} = [X_1, X_2, \ldots, X_N]^T$ has statistically independent components X_i $i = 1, 2, \ldots, N$ if and only if the SSRV is Gaussian.

Proof: Recall that the PDF of $\mathbf{X}$ can be expressed as

$$f_{\mathbf{X}}(\mathbf{x}) = k h_N[(x_1^2 + x_2^2 + \ldots + x_N^2)^{\frac{1}{2}}] = (2\pi)^{-\frac{N}{2}} h_N(\sqrt{\mathbf{x}^T\mathbf{x}}). \tag{A.1}$$

If the components of $\mathbf{X}$ are statistically independent, then the PDF given by eq (A.1) must factor into the product of the marginal PDFs of the components of $\mathbf{X}$. It then follows that

$$h_N[(x_1^2 + x_2^2 + \ldots + x_N^2)^{\frac{1}{2}}] = \prod_{i=1}^{N} g(x_i). \tag{A.2}$$

Letting $r = (x_1^2 + x_2^2 + \ldots + x_N^2)^{\frac{1}{2}}$ and differentiating both sides of eq (A.2) with respect to x_i, results in

$$\frac{x_i}{r} h_N'(r) = \prod_{\substack{j=1 \\ j \neq i}}^{N} g(x_j) g'(x_i). \tag{A.3}$$

Dividing both sides of eq (A.3) by $x_i h_N(r)$ results in

$$\frac{h_N'(r)}{r h_N(r)} = \frac{g'(x_i)}{x_i g(x_i)}. \tag{A.4}$$

Equality holds in eq (A.4) if and only if the left and right sides of eq (A.4) are equal to the same constant. Denoting this constant by $-\lambda$, we have

$$\frac{h_N'(r)}{r h_N(r)} = -\lambda. \tag{A.5}$$

Integrating both sides of eq (A.5) with respect to r gives

$$h_N(r) = a exp(-\frac{\lambda r^2}{2}) \tag{A.6}$$

where a is the constant of integration. Hence,

$$h_N[(x_1^2 + x_2^2 + \ldots + x_N^2)^{\frac{1}{2}}] = a exp[-\frac{\lambda}{2}(x_1^2 + x_2^2 + \ldots + x_N^2)] \tag{A.7}$$

Substitution of eq (A.7) in eq (A.1)clearly results in the Gaussian PDF. The constraint of unity volume under the PDF results in $a = \lambda^{\frac{N}{2}}$.

In order to prove the sufficient part of the property, we start with the PDF of a Gaussian SSRV $\mathbf{X}$ given by

$$f_{\mathbf{X}}(\mathbf{x}) = (\frac{2\pi}{\lambda})^{-\frac{N}{2}} exp(-\frac{\lambda}{2}\sum_{i=1}^{N} x_i^2). \tag{A.8}$$

Clearly the PDF given by eq (A.8) can be expressed as

$$f_{\mathbf{X}}(\mathbf{x}) = \prod_{i=1}^{N} f_{X_i}(x_i) \tag{A.9}$$

where

$$f_{X_i}(x_i) = (\frac{2\pi}{\lambda})^{-\frac{1}{2}} exp(-\frac{\lambda x_i^2}{2}). \tag{A.10}$$

Hence, the sufficient part of the property follows.

An alternate proof of this property can be obtained by using the representation theorem. The representation theorem allows us to express the SSRV $\mathbf{X}$ as a product of a Gaussian random vector $\mathbf{Z}$ having zero mean and identity covariance matrix and

a non-negative random variable S. More precisely, we can write

$$\mathbf{X} = \mathbf{Z}S. \tag{A.11}$$

The components of $\mathbf{X}$ can be statistically independent if and only if S is a constant. When S is a constant, $\mathbf{X}$ is a Gaussian SSRV. As is often the case, the representation theorem provides a simplified approach for determining properties of SIRVs.

A.2 Spherically Symmetric Characteristic function

In this section, we prove that the characteristic function of an SSRV is spherically symmetric.

Proof: We consider the SSRV $\mathbf{X} = [X_1, X_2, \ldots, X_N]^T$. From the representation theorem, we can write $\mathbf{X} = \mathbf{Z}S$ where $\mathbf{Z}$ is a Gaussian random vector having zero mean and identity covariance matrix and S is a non-negative random variable with PDF $f_S(s)$. The characteristic function of $\mathbf{X}$ given by

$$\Phi_{\mathbf{X}}(\omega) = E[exp(j\omega^T\mathbf{X})] \tag{A.12}$$

where $\omega = [\omega_1, \omega_2, \ldots, \omega_N]^T$, can be expressed as

$$\Phi_{\mathbf{X}}(\omega) = E_S[\Phi_{\mathbf{X}|S=s}(\omega)] \tag{A.13}$$

where $\Phi_{\mathbf{X}|S=s}(\omega) = E[exp(j\omega^T\mathbf{Z}s)]$. However,

$$E[exp(j\omega^T\mathbf{Z}s)] = exp(-\frac{s^2}{2}\sum_{i=1}^{N}\omega_i^2). \tag{A.14}$$

Using eq (A.14) in eq (A.13) results in

$$\Phi_{\mathbf{X}}(\omega) = \int_0^\infty exp(-\frac{s^2}{2}\sum_{i=1}^{N}\omega_i^2) f_S(s) ds. \tag{A.15}$$

The characteristic function given by eq (A.15) can be expressed as a function of $\sqrt{\omega^T\omega}$. Hence it is spherically symmetric.

A.3 Relationship Between Higher Order and Lower Order SIRV PDFs

In this section we examine the relationship between the higher order and lower order SIRV PDFs. More precisely we consider an SIRV $\mathbf{Y} = [Y_1, Y_2, \ldots, Y_N]^T$ having mean vector μ, covariance matrix $\mathbf{\Sigma}$ and characteristic PDF $f_S(s)$. The PDF of $\mathbf{Y}$ is given by

$$f_{\mathbf{Y}}(\mathbf{y}) = (2\pi)^{-\frac{N}{2}} |\mathbf{\Sigma}|^{-\frac{1}{2}} h_N(p) \tag{A.16}$$

where $p = (\mathbf{y} - \mu)^{\mathbf{T}} \mathbf{\Sigma}^{-1} (\mathbf{y} - \mu)$ and

$$h_N(p) = \int_0^\infty s^{-N} exp(-\frac{p}{2s^2}) f_S(s) ds. \tag{A.17}$$

The vector $\mathbf{Y}$ can be partitioned as $\mathbf{Y} = [\mathbf{Y_1}^T \mathbf{Y_2}^T]^T$ where $\mathbf{Y_1} = [Y_1, Y_2, \ldots Y_m]^T$ and $\mathbf{Y_2} = [Y_{m+1}, Y_{m+2}, \ldots Y_N]^T$. Let μ_1 and μ_2 denote the mean vectors of $\mathbf{Y_1}$ and $\mathbf{Y_2}$ respectively, and $\mathbf{\Sigma_1}$ and $\mathbf{\Sigma_2}$ denote the corresponding covariance matrices. We wish to obtain the PDF of $\mathbf{Y_1}$ from the PDF of $\mathbf{Y}$ by integrating out over the $N - m$ random variables (i.e., the components of $\mathbf{Y_2}$). Let $p_1 = (\mathbf{y_1} - \mu_1)^{\mathbf{T}} \mathbf{\Sigma_1^{-1}} (\mathbf{y_1} - \mu_1)$ and $p_2 = (\mathbf{y_2} - \mu_2)^{\mathbf{T}} \mathbf{\Sigma_2^{-1}} (\mathbf{y_2} - \mu_2)$. The PDF of $\mathbf{Y_1}$ is given by

$$f_{\mathbf{Y_1}}(\mathbf{y_1}) = (2\pi)^{-\frac{N}{2}} |\mathbf{\Sigma}|^{-\frac{1}{2}} \int_{-\infty}^\infty \int_0^\infty s^{-N} exp(-\frac{p}{2s^2}) f_S(s) ds d\mathbf{y_2}. \tag{A.18}$$

From [26] (p17 eq.8, p18 eq.11) we have

$$(2\pi)^{-\frac{N}{2}} |\mathbf{\Sigma}|^{-\frac{1}{2}} \int_{-\infty}^\infty exp(-\frac{p}{2s^2}) d\mathbf{y_2} = (2\pi)^{-\frac{m}{2}} |\mathbf{\Sigma_1}|^{-\frac{1}{2}} s^{N-m} exp(-\frac{p_1}{2s^2}). \tag{A.19}$$

Using eq (A.19) in eq (A.18) gives

$$f_{\mathbf{Y_1}}(\mathbf{y_1}) = (2\pi)^{-\frac{m}{2}} |\mathbf{\Sigma_1}|^{-\frac{1}{2}} \int_0^\infty s^{-m} exp(-\frac{p_1}{2s^2}) f_S(s) ds. \tag{A.20}$$

The PDF of $\mathbf{Y_1}$ can be expressed as

$$f_{\mathbf{Y_1}}(\mathbf{y_1}) = (2\pi)^{-\frac{m}{2}} |\mathbf{\Sigma_1}|^{-\frac{1}{2}} h_m(p_1) \tag{A.21}$$

where

$$h_m(p_1) = \int_0^\infty s^{-m} exp(-\frac{p_1}{2s^2}) f_S(s) ds. \tag{A.22}$$

Clearly, $h_m(p_1)$ given by eq (A.22) can be obtained from eq (A.17) by simply replacing N by m and p by p_1. To determine the PDF of $\mathbf{Y_1}$, all that is needed is the specification of its mean vector and covariance matrix. As a special case, when $m = 1$, eq (A.20) gives us the first order SIRV PDF. Therefore, to obtain the first order SIRV PDF of the i^{th} component of $\mathbf{Y}$ starting from the N^{th} order SIRV PDF, we simply use eq (A.20) with $m = 1$, $\mathbf{\Sigma_1} = \sigma_i$ and $p_1 = \frac{(y_i - \mu_i)^2}{\sigma_i^2}$.

Appendix B

Computer Generation of SIRVs Using the Rejection Method

B.1 Rejection Method

We present a proof of the rejection procedure [30] used for generating the norm R of the white SIRV $\mathbf{X}$ in Chapter 4. In many instances, it is likely that the PDF of a random variable is known explicitly, but its cumulative distribution function is either unknown or has a complicated functional form. Consequently, the cumulative distribution function cannot be inverted easily. Therefore, the use of the inverse distribution function for generating the random variable does not offer a practical solution for this problem. Hence, it is necessary to use a different scheme for generating the random variable. We consider the problem of generating a sequence of random numbers with PDF $f_R(r)$ of a random variable R, in terms of a random number sequence with PDF $f_{U_1}(u_1)$ of a random variable U_1. The underlying assumption is that the random number sequence from the PDF of U_1 can be readily generated.

The rejection method used in Chapter 4 is based on the relative frequency interpretation of the conditional PDF

$$f_{U_1}(u_1|\mathcal{M})du_1 = \frac{P\{u_1 < U_1 \leq u_1 + du_1, \mathcal{M}\}}{P(\mathcal{M})} \tag{B.1}$$

of a random variable U_1 given the event $\mathcal{M}$. $\mathcal{M}$ is expressed in terms of the random variable U_1 and another random variable U_2 and is chosen so that the resulting conditional PDF $f_{U_1}(u_1|\mathcal{M})$ equals $f_R(r)$. The desired sequence is generated by setting $R = U_1$ given that the event $\mathcal{M}$ has occurred and rejecting U_1 otherwise. The

problem has a solution only if the domains of r and u_1 are such that $f_R(r) = 0$ in every interval for which $f_{U_1}(u_1) = 0$. Therefore, we can assume that the ratio $\frac{f_{U_1}(u_1)}{f_R(u_1)}$ is bounded from below by some positive constant a:

$$\frac{f_{U_1}(u_1)}{f_R(u_1)} \geq a > 0 \quad for \ \ every \ \ u_1 \tag{B.2}$$

B.2 Rejection Theorem

It is desired to generate a random variable R with PDF $f_R(r)$. Let U_1 be any random variable with PDF $f_{U_1}(u_1)$ such that $f_{U_1}(u_1) = 0$ whenever $f_R(r) = 0$. Let U_2 be a uniformly distributed random variable on the interval $(0, 1)$. If the random variables U_1 and U_2 are statistically independent and

$$\mathcal{M} = \{U_2 \leq g(U_1)\} \tag{B.3}$$

where

$$g(u_1) = a\frac{f_R(u_1)}{f_{U_1}(u_1)} \leq 1, \tag{B.4}$$

then

$$f_{U_1}(u_1|\mathcal{M}) = f_R(u_1). \tag{B.5}$$

Proof: The joint PDF of the random variables U_1 and U_2 can be written as $f_{U_1,U_2}(u_1, u_2) = f_{U_1}(u_1)f_{U_2}(u_2)$, since U_1 and U_2 are statistically independent. Hence, we have

$$P(\mathcal{M}) = \int_{-\infty}^{\infty}\int_{0}^{g(u_1)} f_{U_1}(u_1)f_{U_2}(u_2)du_1du_2. \tag{B.6}$$

However, since U_2 is uniformly distributed in the interval $(0, 1)$ and $g(u_1) \leq 1$,

$$\int_{0}^{g(u_1)} f_{U_2}(u_2)du_2 = g(u_1). \tag{B.7}$$

Using eq (B.7) in eq (B.6) gives

$$P(\mathcal{M}) = \int_{-\infty}^{\infty} g(u_1)f_{U_1}(u_1)du_1. \tag{B.8}$$

However, $g(u_1) = a\frac{f_R(u_1)}{f_{U_1}(u_1)}$. Therefore, we have

$$P(\mathcal{M}) = a\int_{-\infty}^{\infty} f_R(u_1)du_1 = a. \tag{B.9}$$

We can express the numerator of eq (B.1) as

$$P\{u_1 < U_1 \leq u_1+du_1, \mathcal{M}\} = \int_0^{g(u_1)} f_{U_1}(u_1) f_{U_2}(u_2) du_1 du_2 = g(u_1) f_{U_1}(u_1) du_1 = a f_R(u_1) du_1. \tag{B.10}$$

Using eqs (B.9) and (B.10) in eq (B.1) results in eq (B.5).

Thus, we have the following algorithm for generating the sequence of random numbers from the PDF of R.

1. Generate U_1 and U_2.
2. If $U_2 \leq a\frac{f_R(u_1)}{f_{U_1}(u_1)}$, then $U_1 = R$
3. Otherwise reject U_1.

Refering now to the generation of saples of the norm R in Chapter 4, note that U_1 and U_2 were uniformly distributed random variables. Let c denote the maximum value of the PDF of R and b denote a finite range for the PDF of R such that the area under the curve of the PDF is close to unity. U_1 is assumed to be uniformly distributed in the interval $(0, b)$. Clearly, $\frac{f_{U_1}(u_1)}{f_R(u_1)} \geq \frac{1}{bc}$. Hence, $\frac{f_R(u_1)}{bcf_{U_1}(u_1)} \leq 1$. Therefore, $a = \frac{1}{bc}$. Step 2 above becomes: *If* $U_2 \leq \frac{f_R(u_1)}{bcf_{U_1}(u_1)} = \frac{f_R(u_1)}{c}$, *then* $U_1 = R$. This can be rewritten as: *If* $cU_2 \leq f_R(u_1)$, *then* $U_1 = R$. For ease of implementation, this latter form is used in conjunction with a uniform random variable U_2' that is uniformly distributed over the interval $(0,\ c)$. This is the procedure followed in Chapter 4.

The method used in Chapter 4 becomes inefficient if U_1 is rejected frequently in step 3, resulting in the necessity to generate the two uniformly distributed random variables of step 1 an inordinate number of times. This problem can be overcome by using for U_1 a PDF which bounds the PDF of R and satisfies the conditions stated in section B.1 and in the rejection theorem. Then a random variable from this PDF is used in step 1 instead of the uniform random variable U_1.

A second drawback of using a uniformly distributed random variable U_1 is that it may not be possible to efficiently generate SIRVs of length greater than 8. This is due to the fact that the PDF of R depends on N. Consequently, the uniform distribution for U_1 may not satisfactorily bound the PDF of the norm R for all N. This drawback can be overcome by choosing a different PDF for U_1 for each choice of N, such that the conditions stated in section B.1 and in the rejection theorem are satisfied. This

method would require the use of an exhaustive table which tabulates the appropriate PDF of U_1 for each desired value of N.

Finally, it is pointed out that by using a composite function for the PDF of U_1, it is possible to improve the simulation procedure by making it possible to generate random numbers from the body and the tail of the PDF of R. These issues are suitable topics for future investigation as an extension of this work.

Appendix C

Maximum Likelihood Estimation Involving SIRVs

The objective of this appendix is to determine maximum likelihood estimates for the mean vector and covariance matrix of an N dimensional SIRV obtained by sampling a wide sense stationary (WSS) SIRP. Ideally, n independent data vectors $\mathbf{Y}_i$, $i = 1, 2, \ldots, n$ should be processed corresponding to n independent trials of the basic experiment. This corresponds to the sample space given by the product

$$\int = \int_1 \times \int_2 \times \ldots \times \int_n \tag{C.1}$$

where $\int_i$, $i = 1, 2, \ldots, n$ denotes the i^{th} ensemble of the SIRP and $\mathbf{Y}_i$ is obtained from $\int_i$. This is shown in Figure C.1.

However, the approach becomes unwieldy from a practical point of view because n ensembles are required. An alternate approach [49] makes use of a single ensemble as shown in Figure C.2, where $\mathbf{Y} = [\mathbf{Y}_1^T, \mathbf{Y}_2^T, \ldots, \mathbf{Y}_n^T]^T$ is obtained by sampling a WSS SIRP at nN time instants, such that

$$\begin{aligned} t_{mN+j} - t_{mN+k} &= t_j - t_k \\ j,\ \ k &= 1, 2, \ldots, N \\ m &= 1, 2, \ldots n-1 \end{aligned} \tag{C.2}$$

and the $\mathbf{Y}_i$, $i = 1, 2, \ldots, n$, are obtained from n different sample functions of the same

ensemble. Due to this, the mean of $\mathbf{Y}$ is

$$\alpha = [\mathbf{b}^T, \mathbf{b}^T, \ldots, \mathbf{b}^T]^T \tag{C.3}$$

and

$$E[(\mathbf{Y}_i - \mathbf{b})(\mathbf{Y}_i - \mathbf{b})^T] = \mathbf{\Sigma}\delta_{jk} \tag{C.4}$$

where δ_{jk} is the Kronecker delta function, so that the covariance matrix of $\mathbf{Y}$ is

$$\mathbf{C} = \begin{bmatrix} \mathbf{\Sigma} & 0 & \ldots & 0 \\ 0 & \mathbf{\Sigma} & \ldots & 0 \\ 0 & 0 & \mathbf{\Sigma} & 0 \\ \ldots & \ldots & \ldots & \ldots \\ 0 & 0 & 0 & \mathbf{\Sigma} \end{bmatrix}. \tag{C.5}$$

In the context of the radar problem, we consider a surveillance volume that represents a single ensemble for the SIRP. Each cell within the volume generates a sample function of the SIRP. The i^{th} data vector $\mathbf{Y}_i$ is obtained from the i^{th} cell of the volume by sampling at the time instants $t_{(i-1)N+k}$ as shown in FigureC.2. In terms of the representation theorem, each cell corresponds to a different value of the random variable S whose density function is the characteristic PDF $f_S(s)$.

The PDF of $\mathbf{Y}$ given $\mathbf{b}$ and $\mathbf{\Sigma}$ is

$$f_{\mathbf{Y}|\mathbf{b},\mathbf{\Sigma}}(\mathbf{y}|\mathbf{b},\mathbf{\Sigma}) = (2\pi)^{-\frac{nN}{2}}|\mathbf{\Sigma}|^{-\frac{n}{2}}h_{nN}(p) \tag{C.6}$$

where $p = (\mathbf{Y}_i - \alpha)^T\mathbf{C}^{-1}(\mathbf{Y}_i - \alpha) = \sum_{j=1}^{n}(\mathbf{y}_j - \mathbf{b})^T\mathbf{\Sigma}^{-1}(\mathbf{y}_j - \mathbf{b})$ and

$$h_{nN}(p) = \int_0^\infty s^{-nN} exp(-\frac{p}{2s^2}) f_S(s) ds. \tag{C.7}$$

Note that $h_{nN}(.)$ is a monotonically decreasing function for all n and N.

Since p is a scalar, we have

$$\begin{aligned} p &= \sum_{j=1}^{n}(\mathbf{y}_j - \mathbf{b})^T\boldsymbol{\Sigma}^{-1}(\mathbf{y}_j - \mathbf{b}) \\ &= tr\sum_{j=1}^{n}(\mathbf{y}_j - \mathbf{b})^T\boldsymbol{\Sigma}^{-1}(\mathbf{y}_j - \mathbf{b}) \end{aligned} \tag{C.8}$$

where $tr(.)$ denotes the trace of the matrix (.). However, for any two square matrices $\mathbf{A}$ and $\mathbf{B}$,

$$tr(\mathbf{AB}) = tr(\mathbf{BA}). \tag{C.9}$$

Consequently,

$$p = tr(\boldsymbol{\Sigma}^{-1}\mathbf{G}) \tag{C.10}$$

where

$$\mathbf{G} = \sum_{j=1}^{n}(\mathbf{y}_j - \mathbf{b})(\mathbf{y}_j - \mathbf{b})^T. \tag{C.11}$$

Thus, we have

$$f_{\mathbf{Y}|\mathbf{b},\boldsymbol{\Sigma}}(\mathbf{y}|\mathbf{b},\boldsymbol{\Sigma}) = (2\pi)^{-\frac{nN}{2}}|\boldsymbol{\Sigma}|^{-\frac{n}{2}}h_{nN}[tr(\boldsymbol{\Sigma}^{-1}\mathbf{G})]. \tag{C.12}$$

Let

$$\mathbf{W} = \sum_{j=1}^{n}(\mathbf{y}_j - \overline{\mathbf{y}})(\mathbf{y}_j - \overline{\mathbf{y}})^T. \tag{C.13}$$

where

$$\overline{\mathbf{y}} = \frac{1}{n}\sum_{j=1}^{n}\mathbf{y}_j. \tag{C.14}$$

Then, we can express p as

$$\begin{aligned} p &= \sum_{j=1}^{n}(\mathbf{y}_j - \mathbf{b})^T\boldsymbol{\Sigma}^{-1}(\mathbf{y}_j - \mathbf{b}) \\ &= \sum_{j=1}^{n}(\mathbf{y}_j - \overline{\mathbf{y}} + \overline{\mathbf{y}} - \mathbf{b})^T\boldsymbol{\Sigma}^{-1}(\mathbf{y}_j - \overline{\mathbf{y}} + \overline{\mathbf{y}} - \mathbf{b}) \\ &= \sum_{j=1}^{n}(\mathbf{y}_j - \overline{\mathbf{y}})^T\boldsymbol{\Sigma}^{-1}(\mathbf{Y}_j - \overline{\mathbf{y}}) \\ &\quad + \sum_{j=1}^{n}(\mathbf{y}_j - \overline{\mathbf{y}})^T\boldsymbol{\Sigma}^{-1}(\overline{\mathbf{y}} - \mathbf{b}) \\ &\quad + \sum_{j=1}^{n}(\overline{\mathbf{y}} - \mathbf{b})^T\boldsymbol{\Sigma}^{-1}(\mathbf{y}_j - \overline{\mathbf{y}}) \\ &\quad + \sum_{j=1}^{n}(\overline{\mathbf{y}} - \mathbf{b})^T\boldsymbol{\Sigma}^{-1}(\overline{\mathbf{y}} - \mathbf{b}) \end{aligned} \tag{C.15}$$

However, from eq (C.14),

$$\begin{aligned} \textstyle\sum_{j=1}^{n}(\mathbf{y}_j - \overline{\mathbf{y}})^T\boldsymbol{\Sigma}^{-1}(\overline{\mathbf{y}} - \mathbf{b}) = 0 \\ \textstyle\sum_{j=1}^{n}(\overline{\mathbf{y}} - \mathbf{b})^T\boldsymbol{\Sigma}^{-1}(\mathbf{y}_j - \overline{\mathbf{y}}) = 0. \end{aligned} \tag{C.16}$$

Therefore,

$$p = \sum_{j=1}^{n}(\mathbf{y}_j - \overline{\mathbf{y}})^T\boldsymbol{\Sigma}^{-1}(\mathbf{y}_j - \overline{\mathbf{y}}) + n(\overline{\mathbf{y}} - \mathbf{b})^T\boldsymbol{\Sigma}^{-1}(\overline{\mathbf{y}} - \mathbf{b}). \tag{C.17}$$

Using eq (C.9), we have

$$p = tr(\boldsymbol{\Sigma}^{-1}\mathbf{W}) + n(\overline{\mathbf{y}} - \mathbf{b})^T\boldsymbol{\Sigma}^{-1}(\overline{\mathbf{y}} - \mathbf{b}). \tag{C.18}$$

Thus, the likelihood function for $\mathbf{b}$ and $\boldsymbol{\Sigma}$ can be expressed as

$$L(\mathbf{b},\ \boldsymbol{\Sigma}) = f_{\mathbf{Y}|\mathbf{b},\boldsymbol{\Sigma}}(\mathbf{y}|\mathbf{b},\boldsymbol{\Sigma}) = (2\pi)^{-\frac{nN}{2}}|\boldsymbol{\Sigma}|^{-\frac{n}{2}}h_{nN}(p) \tag{C.19}$$

where p is given by eq (C.18). We first prove that $\mathbf{W}$ is positive definite with probability one. We can express $\mathbf{W}$ as

$$\mathbf{W} = \sum_{i=1}^{n}\mathbf{W}_i \tag{C.20}$$

where $\mathbf{W}_i = (\mathbf{y}_i - \overline{\mathbf{y}_i})(\mathbf{y}_i - \overline{\mathbf{y}_i})^T$. $\mathbf{W}$ is positive definite if $\mathbf{W}_i$, $i = 1, 2, \ldots, n$ are positive definite. We consider a vector $\mathbf{a} = [a_1,\ a_2\ \ldots a_N]^T$ such that $a_i \neq 0$, $i = 1, 2, \ldots, n$. Then $\mathbf{W}_i$ is positive definite if and only if

$$\mathbf{a}^T\mathbf{W}_i\mathbf{a} > 0. \tag{C.21}$$

We have

$$\begin{aligned} q_i &= \mathbf{a}^T\mathbf{W}_i\mathbf{a} \\ &= \textstyle\sum_{j=1}^{N}\sum_{k=1}^{N} a_j a_k (y_{ij} - \overline{y_{ij}})(y_{ik} - \overline{y_{ik}}) \\ &= [\textstyle\sum_{j=1}^{N} a_j (y_{ij} - \overline{y_{ij}})]^2 \geq 0. \end{aligned} \tag{C.22}$$

However, the probability of $Q_i = 0$ is zero. Therefore, $\mathbf{W}_i$ is positive definite with probability one. It follows that $\mathbf{W}$ is positive definite with probability one.

Before proceeding with the maximum likelihood estimate of $\mathbf{b}$ and $\boldsymbol{\Sigma}$, we present

an important lemma [49] which is useful for the maximization problem.

Lemma: *Let $g(.)$ be a monotonically decreasing differentiable function such that $cg(x_1^2 + x_2^2 + \ldots + x_K^2)$ is a PDF of $\mathbf{X} = [X_1,\ X_2\ \ldots X_K]^T$, where c is a non-zero constant. Then the function $h(x) = x^{\frac{K}{2}} g(x)$ for $x > 0$ has a maximum at some finite x_0 and is a solution of*

$$g'(x) + \frac{K}{2x} g(x) = 0. \tag{C.23}$$

Proof: Since $cg(.)$ is a PDF,

$$\int_{-\infty}^{\infty} \cdots \int_{-\infty}^{\infty} g(\sum_{i=1}^{K} x_i^2) dx_1 \ldots dx_K = \frac{1}{c} < \infty. \tag{C.24}$$

Also, using the transformation to generalized spherical coordinates of eq (2.22) and integrating over θ and Φ_k, $k = 1, 2, \ldots K-2$, it follows that

$$\int_{-\infty}^{\infty} \cdots \int_{-\infty}^{\infty} g(\sum_{i=1}^{K} x_i^2) dx_1 \ldots dx_K = \frac{\pi^{\frac{K}{2}}}{\Gamma(\frac{K}{2})} \int_0^{\infty} 2r^{K-1} g(r^2) dr. \tag{C.25}$$

Making the change of variable $r^2 = \alpha$, we have

$$\int_{-\infty}^{\infty} \cdots \int_{-\infty}^{\infty} g(\sum_{i=1}^{K} x_i^2) dx_1 \ldots dx_K = \frac{\pi^{\frac{K}{2}}}{\Gamma(\frac{K}{2})} \int_0^{\infty} \alpha^{\frac{K}{2}-1} g(\alpha) d\alpha. \tag{C.26}$$

Since $g(.)$ is a monotonically decreasing function,

$$g(2x)[2x - x] = x g(2x) \leq \int_x^{2x} g(t) dt. \tag{C.27}$$

Hence,

$$2^{-\frac{K}{2}} (2x)^{\frac{K}{2}} g(2x) = x^{\frac{K}{2}} g(2x) \leq x^{\frac{K}{2}-1} \int_x^{2x} g(t) dt. \tag{C.28}$$

Since $g(.)$ is a monotonically decreasing function,

$$x^{\frac{K}{2}} g(2x) \leq x^{\frac{K}{2}-1} \int_x^{2x} g(t) dt \leq \int_x^{2x} t^{\frac{K}{2}-1} g(t) dt. \tag{C.29}$$

Since $t^{\frac{K}{2}-1} g(t)$ is the PDF of $t = \sum_{i=1}^{K} x_i^2$, to within a multiplicative constant, and

since the PDF of $t \rightarrow 0$ as $t \rightarrow \infty$ (see Chapter 3 for details), it follows that

$$\int_x^{2x} t^{\frac{K}{2}-1} g(t)dt \rightarrow 0 \ as \ x \rightarrow \infty. \tag{C.30}$$

Also, $h(0) = 0$ and $h(x) \geq 0 \ \forall x > 0$. Therefore, $h(x)$ has a maximum at some finite $x_0 > 0$. The first assertion of the lemma follows. Differentiating $h(x)$ with respect to x, we have

$$h'(x) = \frac{K}{2} x^{\frac{K}{2}-1} g(x) + x^{\frac{K}{2}} g'(x). \tag{C.31}$$

Since $h(x)$ has a maximum at some finite $x_0 > 0$, it follows that x_0 is a solution to the equation

$$\frac{K}{2x_0} g(x_0) + g'(x_0) = 0. \tag{C.32}$$

Letting $K = nN$ and $x = \frac{N}{\lambda}$, we have $h(\frac{N}{\lambda}) = (\frac{N}{\lambda})^{\frac{nN}{2}} g(\frac{N}{\lambda})$. It follows from the above lemma that the function

$$f(\lambda) \equiv \lambda^{-\frac{nN}{2}} g(\frac{N}{\lambda}) \tag{C.33}$$

arrives at its maximum at some finite positive λ_0 and arises as a solution of

$$\frac{n\lambda_0}{2} g(\frac{N}{\lambda}) + g'(\frac{N}{\lambda}) = 0 \tag{C.34}$$

We now return to the problem of maximization of $L(\mathbf{b}, \ \mathbf{\Sigma})$. Since $h_{nN}(.)$ is a monotonically decreasing function and $\mathbf{\Sigma}$ is positive definite with probability one, $L(\mathbf{b}, \ \mathbf{\Sigma})$ arrives at its maximum when $\hat{\mathbf{b}} = \overline{\mathbf{y}}$. We then focus on the concentrated likelihood function

$$L(\mathbf{b}, \ \mathbf{\Sigma}) = (2\pi)^{-\frac{nN}{2}} |\mathbf{\Sigma}|^{-\frac{n}{2}} h_{nN}[tr(\mathbf{\Sigma}^{-1}\mathbf{W})]. \tag{C.35}$$

Since $\mathbf{W}$ is a positive definite matrix, it can be represented as $\mathbf{W} = \mathbf{C}\mathbf{C}^{\mathbf{T}}$ where $\mathbf{C}$ is a nonsingular matrix. We define the matrix $\tilde{\mathbf{\Sigma}} = \mathbf{C}^{-1}\mathbf{\Sigma}(\mathbf{C}^{\mathbf{T}})^{-1}$, so that $\mathbf{\Sigma} = \mathbf{C}\tilde{\mathbf{\Sigma}}\mathbf{C}^{\mathbf{T}}$. Also, it follows that

$$\begin{gathered} tr(\mathbf{\Sigma}^{-1}\mathbf{W}) = tr[(\mathbf{C}\tilde{\mathbf{\Sigma}}\mathbf{C}^{\mathbf{T}})^{-1}\mathbf{W}] = tr(\tilde{\mathbf{\Sigma}}^{-1}[\mathbf{C}\mathbf{C}^{\mathbf{T}}]^{-1}\mathbf{W}) = tr(\tilde{\mathbf{\Sigma}}^{-1}) \\ |\mathbf{\Sigma}| = |\mathbf{C}\tilde{\mathbf{\Sigma}}\mathbf{C}^{\mathbf{T}}| = |\tilde{\mathbf{\Sigma}}||\mathbf{W}| \end{gathered} \tag{C.36}$$

Hence, the likelihood function can be rewritten as

$$L(\mathbf{b},\ \mathbf{\Sigma}) = (2\pi)^{-\frac{nN}{2}}|\mathbf{W}|^{-\frac{n}{2}}|\tilde{\mathbf{\Sigma}}|^{-\frac{n}{2}}h_{nN}[tr(\tilde{\mathbf{\Sigma}}^{-1})]. \tag{C.37}$$

Let $\lambda_i > 0,\ i = 1, 2, \ldots N$ denote the eigen values of $\tilde{\mathbf{\Sigma}}$. Then,

$$\begin{aligned} L(\mathbf{b},\ \mathbf{\Sigma}) &= (2\pi)^{-\frac{nN}{2}}|\mathbf{W}|^{-\frac{n}{2}}(\textstyle\prod_{i=1}^{N}\lambda_i^{-1})^{-\frac{n}{2}}h_{nN}(\sum_{i=1}^{N}\lambda_i^{-1}) \\ &= (2\pi)^{-\frac{nN}{2}}|\mathbf{W}|^{-\frac{n}{2}}(\textstyle\prod_{i=1}^{N}\lambda_i^{-\frac{1}{N}})^{-\frac{Nn}{2}}h_{nN}(\sum_{i=1}^{N}\lambda_i^{-1}) \end{aligned} \tag{C.38}$$

Since the arithmetic mean is always greater than or equal to the geometric mean, it follows that

$$L(\mathbf{b},\ \mathbf{\Sigma}) \leq (2\pi)^{-\frac{nN}{2}}|\mathbf{W}|^{-\frac{n}{2}}(\overline{\lambda})^{\frac{nN}{2}}h_{nN}(N\overline{\lambda}) \tag{C.39}$$

where $\overline{\lambda} = \frac{1}{N}\sum_{i=1}^{N}\lambda_i^{-1}$. Equality between the arithmetic and geometric mean holds only if $\lambda_1 = \lambda_2 = \ldots = \lambda_N = \lambda$. Therefore, $L(\mathbf{b},\ \mathbf{\Sigma})$ arrives at its maximum when the eigen values of $\tilde{\mathbf{\Sigma}}$ are equal. Consequently,

$$\begin{aligned} max L(\mathbf{b},\ \mathbf{\Sigma}) &= max(2\pi)^{-\frac{nN}{2}}|\mathbf{W}|^{-\frac{n}{2}}\lambda^{-\frac{nN}{2}}h_{nN}(\tfrac{N}{\lambda}) \\ &= max(2\pi)^{-\frac{nN}{2}}|\lambda\mathbf{W}|^{-\frac{n}{2}}h_{nN}(\tfrac{N}{\lambda}) \\ &= max(2\pi)^{-\frac{nN}{2}}|\mathbf{W}|^{-\frac{n}{2}}f(\lambda). \end{aligned} \tag{C.40}$$

where $f(\lambda)$ is given by eq (C.33) with $g(.)$ replaced by $h_{nN}(.)$. Note that $h_{nN}(.)$ satisfies all the conditions of the lemma dealing with the maximization of $h(.)$. Let the value of λ resulting in the maximum be denoted by λ_0. Comparing eq (C.40) with eq (C.33), it follows that the maximum likelihood estimate of $\mathbf{\Sigma}$ is

$$\hat{\mathbf{\Sigma}} = \lambda_0\mathbf{W}. \tag{C.41}$$

In summary, the maximum likelihood estimates of $\mathbf{b}$ and $\mathbf{\Sigma}$ are:

$$\begin{aligned} \hat{\mathbf{b}} &= \overline{\mathbf{y}} \\ \hat{\mathbf{\Sigma}} &= \lambda_0\mathbf{W} \end{aligned} \tag{C.42}$$

In order to guarantee the non-negative definite property of $\hat{\mathbf{\Sigma}}$, it is required that

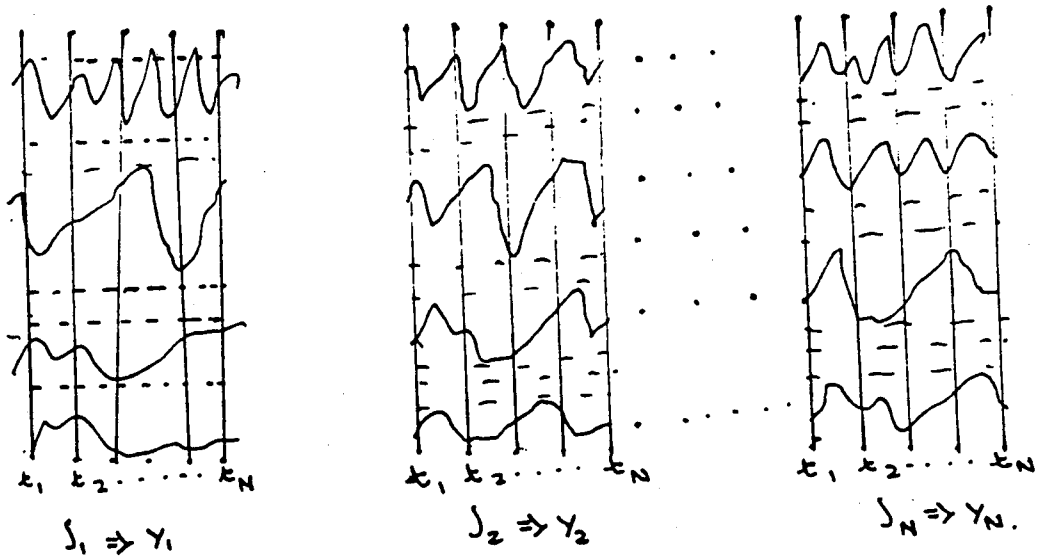

Figure C.1: Independent Sampling

$n > N$. It has been pointed out in [52, 53] that a rule of thumb for obtaining a reasonably good estimate of Σ is that $n \geq 2N - 3$.

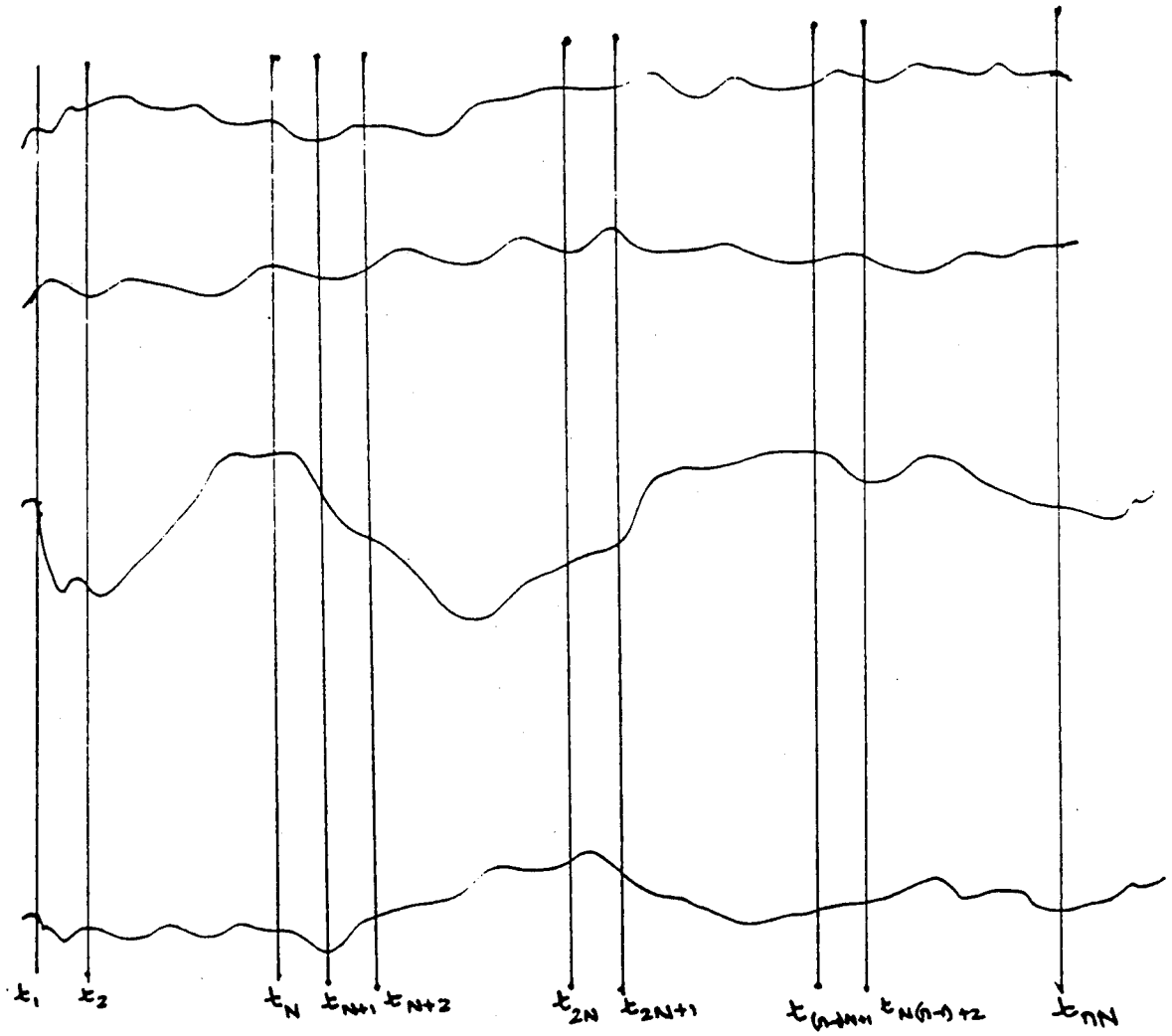

Figure C.2: Sampling From a Single Ensemble

Bibliography

[1] M. Sekine, T. Musha, Y. Tomita, T. Hagisawa, T. Irabu, and E. Kiuchi, "On Weibull distributed weather clutter," *IEEE Trans. on Aerospace and Electronic Systems*, vol. **AES-15**, pp. 824–828, 1979.

[2] E. Jakeman and P. Pusey, "A model for non-Rayleigh sea echo," *IEEE Trans. on Antennas and Propagation*, vol. **AP-24**, pp. 806–814, 1976.

[3] S. Watts and K. Ward, "Spatial correlation in K-distributed sea clutter," *IEE Proc.F, Commun., Radar, & Signal Process.*, vol. **134**, (6), pp. 526–532, 1987.

[4] C. Hawkes and S. Haykin, "Modeling of clutter for coherent pulsed radar," *IEEE Trans. on Information Theory*, vol. **IT-21**, pp. 703–707, 1975.

[5] A. Farina, A. Russo, and F. Studer, "Coherent radar detection in log-normal clutter," *IEE Proc.F, Commun., Radar, & Signal Process.*, vol. **133**, (1), pp. 39–54, 1986.

[6] E. Conte and M. Longo, "On a coherent model for log-normal clutter," *IEE Proc.F, Commun., Radar, & Signal Process.*, vol. **134**, (2), pp. 198–201, 1987.

[7] S. Watts, "Radar detection prediction in K-distributed sea clutter and thermal noise," *IEEE Trans. on Aerospace and Electronic Systems*, vol. **AES-23**, pp. 40–45, 1987.

[8] G. Li and K.-B. Yu, "Modeling and simulation of coherent Weibull clutter," *IEE Proc.F, Commun., Radar, & Signal Process.*, vol. **136**, (1), pp. 2–12, 1989.

[9] E. Jakeman, "On the statistics of K-distributed noise," *J. Phys. A.*, vol. **13**, pp. 31–48, 1980.

[10] W. Szajnowski, "The generation of correlated Weibull clutter for signal detection problems," *IEEE Trans. on Aerospace and Electronic Systems*, vol. **AES-13**, pp. 536–540, 1977.

[11] P. Peebles, "The generation of correlated lognormal clutter for radar simulation," *IEEE Trans. on Aerospace and Electronic Systems*, vol. **AES-7**, pp. 1215–1217, 1971.

[12] A. Farina, A. Russo, F. Scannapieco, and S. Barbarossa, "Theory of radar detection in coherent Weibull clutter," *IEE Proc.F, Commun., Radar, & Signal Process.*, vol. **134**, (2), pp. 174–190, 1987.

[13] E. Conte, G. Galati, and M. Longo, "Exogenous modeling of non-Gaussian clutter," *J. IERE*, vol. **57**, (4), pp. 151–155, 1987.

[14] J. Kingman, "Random walks with spherical symmetry," *Acta Math.*, vol. 109, pp. 11–53, 1963.

[15] K. Yao, "A representation theorem and its applications to spherically invariant random processes," *IEEE Trans. on Information Theory*, vol. **IT-19**, pp. 600–608, 1973.

[16] J. Goldman, "Detection in the presence of spherically symmetric random vectors," *IEEE Trans. on Information Theory*, vol. **IT-22**, pp. 52–58, 1976.

[17] H. Brehm, "Description of spherically invariant random processes by means of G-functions," *Springer Lecture Notes*, vol. **969**, pp. 39–73, 1982.

[18] H. Brehm and W. Stammler, "Description and generation of spherically invariant speech-model signals," *Signal Process.*, vol. **12**, (2), pp. 119–141, 1987.

[19] E. Conte and M. Longo, "Characterization of radar clutter as a spherically invariant random process," *IEE Proc.F, Commun., Radar, & Signal Process.*, vol. **134**, (2), pp. 191–197, 1987.

[20] E. Conte, M. Longo, and M. Lops, "Modelling and simulation of non-Rayleigh radar clutter," *IEE Proc.F, Commun., Radar, & Signal Process.*, vol. **138**, (2), pp. 121–130, 1991.

[21] M. Rangaswamy, D. Weiner, and A. Ozturk, "Spherically invariant random processes for modeling and distribution identification of non-Gaussian random vectors." Accepted for publication in **IEEE-AES** trans.

[22] M. Rangaswamy, D. Weiner, and A. Ozturk, "Computer generation of correlated non-Gaussian clutter for radar signal detection." Accepted for publication in **IEEE-AES** trans.

[23] J. Kingman, "On random sequences with spherical symmetry," *Biometrika*, vol. 59, pp. 492–494, 1972.

[24] G. Wise and N. Gallagher, "On spherically invariant random processes," *IEEE Trans. on Information Theory*, vol. **IT-24**, pp. 118–120, 1978.

[25] M. Johnson, *Multivariate Statistical Simulation.* New York: John Wiley and sons, 1987.

[26] K. Miller, *Multidimensional Gaussian Distributions.* New York: Wiley, 1964.

[27] I. Blake and J. Thomas, "On a class of processes arising in linear estimation theory," *IEEE Trans. on Information Theory*, vol. **IT-14**, pp. 12–16, 1968.

[28] M. Abramowitz and I. Stegun, *Handbook of Mathematical Functions.* New York: Dover Publications Inc., 1972.

[29] K. Chu, "Estimation and decision for linear systems with elliptical random processes," *IEEE Trans. on Automatic Control*, vol. **AC-18, pp. 499–505, 1973.**

[30] A. Papoulis, *Probability, Random Variables and Stochastic Processes.* **New York: McGraw-Hill, 1984.**

[31] J. Frame, "Matrix functions and applications part-1-matrix operations and generalized inverses," *IEEE Spectrum*, **vol. 3, p. 212, 1964.**

[32] B. Picinbono, "Spherically invariant and compound Gaussian stochastic processes," *IEEE Trans. on Information Theory*, **vol. IT-16, pp. 77–79, 1970.**

[33] G. Wise, A. Traganitis, and J. Thomas, "The effect of a memoryless nonlinearity on the spectrum of a random process," *IEEE Trans. on Information Theory*, **vol. IT-23, pp. 84–89, 1977.**

[34] B. Liu and D. Munson, "Generation of a random sequence having a jointly specified marginal distribution and autocovariance function," *IEEE Trans. on Acoust., Speech, Signal Processing*, **vol. ASSP-6, pp. 973–983, 1982.**

[35] I. Gradshteyn and I. Ryzhik, *Table of Integrals, Series and Products.* **New York: Academic Press Inc., 1980.**

[36] A. Erdelyi, W. Magnus, and F. Oberhettinger, *Tables of Integral Transforms.* **New York: McGraw-Hill, 1954.**

[37] J. Ritcey and P. Tran, "Tail behavior of compound clutter models," in *Proceedings of Twentysixth Annual Conference on Information Sciences and Systems*, **(Princeton, NJ), 1992.**

[38] J. Modestino and A. Ningo, "Detection of weak signals in narrowband non-Gaussian noise," *IEEE Trans. on Information Theory*, vol. IT-25, pp. 592–600, 1979.

[39] S. Kassam, *Signal Detection in Non-Gaussian Noise.* New York: Springer-Verlag, 1988.

[40] P. Bratley, B. Fox, and L. Schrage, *A Guide to Simulation.* New York: Springer-Verlag, 1987.

[41] A. Ozturk, "A new method for univariate and multivariate distribution identification." Submitted for publication to JASA.

[42] J. Koziol, "A class of invariant procedures for assessing multivariate normality," *Biometrika*, vol. 69, pp. 423–427, 1982.

[43] A. Martinez, P. Swaszek, and J. Thomas, "Locally optimal detection in multivariate non-Gaussian noise," *IEEE Trans. on Information Theory*, vol. IT-30, pp. 815–822, 1984.

[44] A. Ozturk and J. Romeu, "A new method for assessing multivariate normality with graphical applications." Accepted for Publication in Commun. in Statistics.

[45] N. Johnson and S. Kotz, *Distributions in Statistics:Continuous Multivariate Distributions.* New York: John Wiley and sons, 1976.

[46] R. Gnanadesikan, *Methods of Statistical Data Analysis of Multivariate Observations.* New York: John Wiley and sons, 1977.

[47] K. Mardia, "Test of univariate and multivariate normality," *Handbook of Statistics*, vol. 1, pp. 279–320, 1980.

[48] N. Goodman, "Statistical analysis based on a certain multivariate complex distribution," *Ann. Math. Statistics*, vol. 34, pp. 152–177, 1963.

[49] K. Fang and T. Anderson, *Statistical Inference in Elliptically Contoured and Related Distributions.* New York: Allerton Press inc., 1990.

[50] M. Rangaswamy, D. Weiner, and A. Ozturk, "Simulation of correlated non-Gaussian interference for radar signal detection," in *Proceedings of twentyfifth Asilomar Conference on Signals, Systems and Computers*, (Pacific Grove, CA), 1991.

[51] R. Fisher, "The use of multiple measurements in taxonomic problems," *Ann.Eugenics*, vol. 7, pp. 179–188, 1936.

[52] I. Reed, J. Mallett, and L. Brennan, "Rapid convergence rate in adaptive arrays," *IEEE Trans. on Aerospace and Electronic Systems*, vol. AES-10, pp. 853–863, 1974.

[53] C. Khatri and C. Rao, "Effects of estimated noise covariance matrix in optimum signal detection," *IEEE Trans. on Acoust., Speech, Signal Processing*, vol. ASSP-35, pp. 671–679, 1987.

Acknowledgements

This work was supported by the Rome Laboratory, U.S. Air Force, under contract numbers SCEE-DACS-P35498-2, and UM 91S025/28140, which I gratefully acknowledge. I would like to thank my mother for her patience and support, during the course of this effort. I would like to thank Dr. Donald.D. Weiner for his patience, encouragement and thought provoking suggestions which contributed significantly to this effort. Thanks are also due to Dr. Rajan Srinivasan, Dr. Aydin Ozturk, Lisa Slaski, Russell Brown, Michael Wicks, Dr. James H. Michels and Prakash Chakravarthi for the many interesting and stimulating discussions. I would like to thank Dr. Tapan Sarkar for allowing me to use the resources of the Microwave Laboratory while typing the manuscript and Academic Computing Services of Syracuse University for the excellent computational resources that made this effort possible. I am extremely grateful to Dr. Harry Schwarzlander for his careful and thorough reading of the manuscript.

Rome Laboratory

Customer Satisfaction Survey

RL-TR-_____

Please complete this survey, and mail to RL/IMPS, 26 Electronic Pky, Griffiss AFB NY 13441-4514. Your assessment and feedback regarding this technical report will allow Rome Laboratory to have a vehicle to continuously improve our methods of research, publication, and customer satisfaction. Your assistance is greatly appreciated.
Thank You

_____

_____

Organization Name:_____(Optional)

Organization POC: _____(Optional)

Address:_____

1. On a scale of 1 to 5 how would you rate the technology developed under this research?

5-Extremely Useful 1-Not Useful/Wasteful

Rating_____

Please use the space below to comment on your rating. Please suggest improvements. Use the back of this sheet if necessary.

2. Do any specific areas of the report stand out as exceptional?

Yes___ No_____

If yes, please identify the area(s), and comment on what aspects make them "stand out."

3. Do any specific areas of the report stand out as inferior?

Yes___ No___

If yes, please identify the area(s), and comment on what aspects make them "stand out."

4. Please utilize the space below to comment on any other aspects of the report. Comments on both technical content and reporting format are desired.

*U.S. GOVERNMENT PRINTING OFFICE: 1995-610-126-20052

MISSION

OF

ROME LABORATORY

Mission. The mission of Rome Laboratory is to advance the science and technologies of command, control, communications and intelligence and to transition them into systems to meet customer needs. To achieve this, Rome Lab:

a. Conducts vigorous research, development and test programs in all applicable technologies;

b. Transitions technology to current and future systems to improve operational capability, readiness, and supportability;

c. Provides a full range of technical support to Air Force Materiel Command product centers and other Air Force organizations;

d. Promotes transfer of technology to the private sector;

e. Maintains leading edge technological expertise in the areas of surveillance, communications, command and control, intelligence, reliability science, electro-magnetic technology, photonics, signal processing, and computational science.

The thrust areas of technical competence include: Surveillance, Communications, Command and Control, Intelligence, Signal Processing, Computer Science and Technology, Electromagnetic Technology, Photonics and Reliability Sciences.